Podocyte-specific glucocorticoid effects in childhood nephrotic syndrome

A thesis submitted to The University of Manchester for the degree of Doctor of Philosophy in the Faculty of Medical and Human Sciences

2015

James C. McCaffrey

School of Medicine

Institute of Human Development

Table of Contents

Word Count: 64,678

Table of Figures

Table of tables

Key abbreviations

11β-HSD 11 beta-hydroxysteroid dehydrogenase

ChIP-Seq Chromatin immunoprecipitation followed by high-throughput DNA sequencing

CKD Chronic kidney disease

CNS Congenital nephrotic syndrome

ECIS Electric cell-substrate impedance sensing

ECM Extracellular matrix

ESL Endothelial surface layer

ESRD End-stage renal disease

FPs Foot processes

FSGS Focal segmental glomerulosclerosis

GAP GTPase Activation Protein

GBM Glomerular basement membrane

GBS Glucocorticoid receptor binding site

Gc Glucocorticoid

GDI Guanosine nucleotide dissociation inhibitors

GECs Glomerular endothelial cells

GEF Guanine nucleotide-exchange factor

GFB Glomerular filtration barrier

GR Glucocorticoid receptor

HPA Hypothalamic-pituitary-adrenal

INS Idiopathic nephrotic syndrome

IPA® Ingenuity pathway analysis

kDa Kilodalton

LC-MS/MS Liquid chromatography-tandem mass spectrometry

LPS Lipopolysaccharide

MCD Minimal change disease

MR Mineralocorticoid receptor

mRNA messenger ribonucleic acid

MS Mass spectrometry

NPHS1 Nephrin

NPHS2 Podocin

NRSF Nuclear receptor super-family

NS Nephrotic syndrome

PAN Puromycin aminonucleoside

PBS Phosphate buffered saline

Rac1 Ras-related C3 botulinum toxin substrate 1

RhoA Ras homolog gene family, member A

SD Slit diaphragm

SDS-PAGE sodium dodecyl sulfate polyacrylamide gel electrophoresis

SRNS Steroid resistant nephrotic syndrome

SSNS Steroid sensitive nephrotic syndrome

TED Thromboembolic disease

UUO Unilateral ureteral obstruction

WT1 Wilms'Tumour 1

Abstract

University of Manchester

Candidate name: James C. McCaffrey

Degree title: Doctor of Philosophy

Thesis Title: Podocyte-specific glucocorticoid effects in childhood nephrotic syndrome

Date: 2015

BACKGROUND: Nephrotic syndrome (NS) occurs when the glomerular filtration barrier becomes abnormally permeable, leading to the clinical triad of proteinuria, massive oedema, and hypoalbuminaemia. Historically, NS has been thought to result from dysregulation of the immune system, although recent evidence suggests the glomerular podocyte plays a central role in disease pathogenesis. Children with NS are generally treated with an empiric course of glucocorticoid (Gc) therapy; a class of steroids which are activating ligands for the glucocorticoid receptor (GR) transcription factor. A major factor limiting the clinical utility of these agents is the marked variation observed in response to treatment. Although Gc-therapy has been the cornerstone of NS management for several decades, the mechanism of action, and target cell, remain poorly understood.

HYPOTHESIS AND AIMS: The central hypothesis for this thesis states that glucocorticoids act directly on the podocyte to produce clinically useful effects without involvement of the immune system.

FINDINGS: Using a wild-type human podocyte cell line, I demonstrated that the basic GR-signalling mechanism is intact in the podocyte, and that glucocorticoids produce a direct, protective effect on the podocyte without immune cell involvement, by using electrical resistance across a podocyte monolayer as a surrogate marker for barrier integrity. To understand potential mechanisms underpinning this direct effect I defined the podocyte GR cistrome (using a combination of chromatin immunoprecipitation followed by massively parallel DNA sequencing and transcriptomic analysis) as well as total cell proteomics. Subsequent gene ontology analysis revealed that Gc treatment had prominent effects on podocyte motility, and these findings were validated with live-cell imaging. To gain mechanistic insight, I investigated the role of the pro-migratory small GTPase regulator Rac1, and demonstrated that treatment with Gc reduced Rac1 activity. Furthermore, the Rac1 inhibitor EHT 1864 had a direct, protective effect on the podocyte. To create a model to study the role of podocyte GR *in vivo* I generated a mouse line with a podocyte-specific GR deletion.

IMPACT: Gc exposure produces potentially clinically-relevant effects directly on the podocyte, and Gc-induced podocyte hypomobility may underlie the clinical efficacy of these agents. Future animal studies investigating the consequences of GR deletion in the podocyte and the anti-proteinuric effects of Rac1 inhibition are warranted.

Declaration

No portion of the work referred to in the thesis has been submitted in support of an application for another degree or qualification of this or any other university or other institute of learning.

Copyright Statement

Acknowledgements

Firtsly, I would like to thank my primary supervisor, Dr. Rachel Lennon for the opportunity to work in such an excellent and friendly group, and for her inspiring enthusiasm for all things residing inside the glomerulus. Also thanks to Prof. David Ray for his valuable guidance at critical times of the project, and to Prof. Webb for the fantastic tuition he provided in preparing important presentations.

When I arrived in the lab, I did not know one end of a Gilson pipette from the other; I thank Hellyeh Hamidi for remedying this and for her endless patience. Thanks to all members of the Lennon lab for their humour and making my PhD such an enjoyable experience. Special thanks go to Mikey for providing solutions to I.T. and lab problems with remarkable consistency, and his willingness to always find time to help. I would like to thank all members of the Humphries and Caswell groups for showing me how science should be done, and to Toryn and Shona for all the help in the torturous and tortuous ChIP-Seq method development. Also, thanks to Cressie for sharing in the mind-numbing repetitiveness of manual cell tracking.

Finally, I'd like to thank my wonderful wife Lotte and my parents. This thesis is dedicated to them.

1 Introduction

1.1 General

Nephrotic syndrome (NS) is one of the commonest causes of chronic kidney disease in the paediatric population. The cardinal clinical features are proteinuria (urinary loss of plasma proteins) leading to hypoalbuminaemia (low blood levels of the plasma protein albumin) and oedema (massive body swelling). Historically the disease had a dismal prognosis, with five-year mortality rates of 67% being recorded in the period 1929-1936.[1] Although the introduction of glucocorticoid (Gc) and antibiotic therapy in the modern era has reduced mortality rates to approximately 3%,[2] NS remains a significant clinical burden due to the side effects of Gc treatment, the ongoing threat of NS-related sepsis, thromboemobolic disease, and the high rates of chronic kidney disease among patients resistant to Gc-therapy.

1.2 The Kidney

The kidneys perform a wide range of essential regulatory functions in mammals including water and electrolyte homeostasis, excretion of toxic metabolites, acid-base balance, and regulation of blood pressure. Additionally, they play roles in vitamin D metabolism and produce erythropoietin which is a regulator of red blood cell production.

A key step necessary for the kidneys to maintain physiological homeostasis is the filtering of blood to produce an initial ultrafiltrate of primary urine. This primary urine then enters the renal tubular system where regulated specific reabsorption and excretion events finally lead to the production of urine for excretion. Normally, water and small solutes (eg, urea, glucose, amino acids) freely cross the kidney filtration barrier, while circulating cells (eg, erythrocytes) and high-molecular weight proteins (eg, albumin) are retained in blood. This filter selects for both size and charge: the glomerular permeability of negatively charged proteins such as albumin is exceeded by those of neutral dextrans of comparable or even larger sizes. [3]

In health, the normal rate of urinary protein excretion throughout childhood in both boys and girls is <100 mg/m^2/day.[4] For a typical 5 year old boy weighing 20 kg with a body surface area of 0.79 m^2, this would equate to 79 mg urinary protein loss/day. Approximately 50% of this small urinary protein loss consists of a glycoprotein secreted into the renal tubular system called Tamm-Horsfall protein, with the remainder consisting of plasma proteins such as albumin, immunoglobulins and β_2-microglobulin. Albumin comprises <30% of the total urinary protein in normal individuals.[4] NS occurs when the renal filtration barrier becomes hyperpermeable to plasma proteins, leading to urinary protein losses >2 mg protein/mg creatinine (with normal levels in a healthy individual being <0.2 mg protein/mg creatinine).[4, 5] In a hospital setting, urinary protein:creatinine ratios are often reported as mg protein/mmol creatinine, and values ≥200 are considered to be in the nephrotic range.[6]

The major functions of the kidney are performed by a repeating functional unit called the nephron. The filtering sub-unit of the nephron is the glomerulus; each human adult kidney contains approximately 1.4 million glomeruli.[7] (see **Figure 1.1**) Filtration at

the glomerulus is dependent on several components, which collectively form the ‘glomerular filtration barrier’ (GFB).

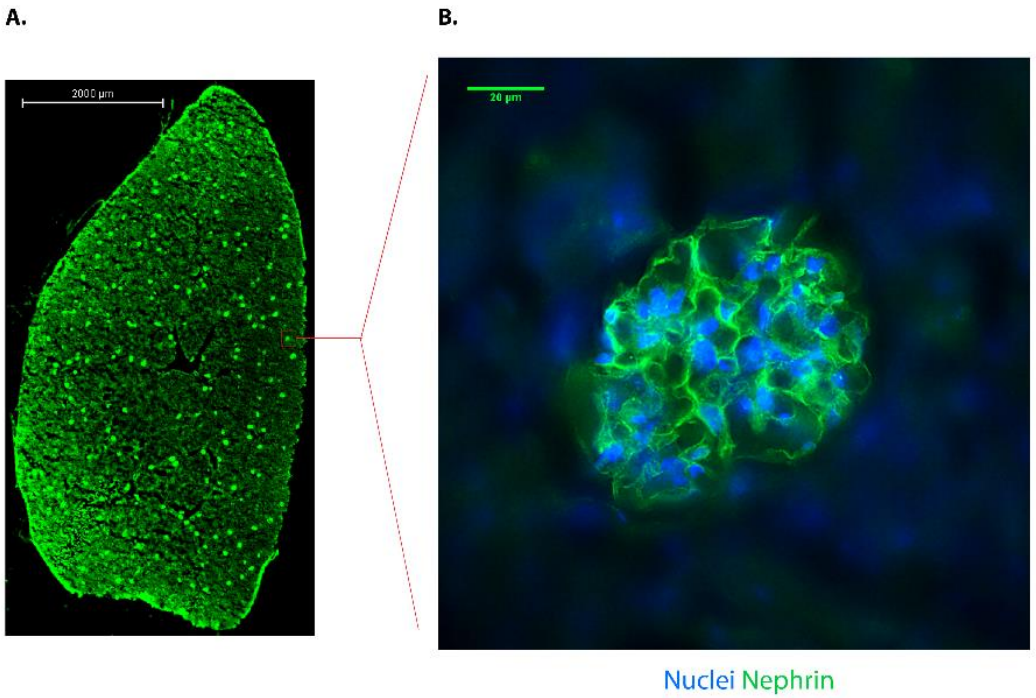

Figure 1.1 The glomerulus

The glomerulus is the filtering sub-unit of the kidney and each glomerulus consists of a tuft of capillaries surrounded by the glomerular filtration barrier (GFB). Glomerular epithelial cells called podocytes have a key role in maintaining GFB integrity. Images show immunofluorescence staining for a podocyte-specific marker nephrin using kidney cryosections from a C57BL/6 mouse. **(A)** shows the location of glomeruli visualised using a 3D Histech Pannoramic 250 Flash II slide scanner (2X magnification); **(B)** shows a high-magnification image (40X) of a single glomerulus imaged using a DeltaVision microscope.

1.2.1 The five layers of the glomerular filtration barrier

The GFB is a highly specialised structure, responsible for the selective ultrafiltration of blood, ensuring minimal urinary protein loss in health.[8] Proteinuria occurs when the GFB becomes abnormally permeable.[9]

Traditionally, the GFB has been viewed as consisting of three layers: endothelial cells of the glomerular capillaries, the glomerular basement membrane (GBM), and visceral epithelial cells lining the outside of glomerular capillaries called podocytes. However, more recent data has also highlighted the importance of the endothelial surface layer, and the sub-podocyte space (see **Figure 1.2**).[10] In the following section, I will describe each of the GFB layers in turn.

1.2.1.1 Endothelial surface layer

The endothelial surface layer (ESL) is a carbohydrate-rich barrier lying at the interface of blood and glomerular endothelial cells. The ESL can be sub-divided into two layers: membrane-bound secreted proteoglycans comprising a protein core (including perlecan and syndecan) with covalently associated glycosaminoglycan side-chains (eg, heparan sulphate and hyaluronic acid), and an adsorbed layer of plasma proteins including albumin.[11-14] A role for the ESL in regulating glomerular permeability came initially from Singh *et al*., who demonstrated that removal of a significant portion of the ESL from glomerular endothelial cells *in vitro* with neuraminidase altered both transendothelial albumin passage and electrical resistance, and selective removal of heparan sulphate proteoglycans with heparanase increased transendothelial monolayer albumin passage only.[15] Additionally, an increase in the fractional clearance of albumin in isolated perfused murine kidneys was seen following treatment with the glycosaminoglycan-degrading enzyme hyaluronidase.[16]

1.2.1.2 Glomerular Endothelial Cells

Glomerular endothelial cells (GECs) differ from endothelial cells found in many other areas of the body due to their abnormally large fenestrated area, constituting 20-50% of the entire endothelial surface.[17, 18] The fenestrae are approximately 60 nm in diameter, while the dimensions of albumin (whose passage across the GFB occurs only at very low levels in health), are 5.97 x 9.70 x 5.97 nm.[18, 19] Additionally, endothelial fenestrae in other organs (eg, salivary gland) are bridged by diaphragms that express plasmalemmal vesicle associated protein (PV-1), but these diaphragms seem to

be absent from GEC fenestrae. [20] Thus, although GECs are suited to the role the glomeruli performs as a high-capacity filtering unit due to their large fenestrations, the diameter of these diaphragm-free fenestrations suggests their direct contribution to preventing the passage of plasma proteins such as albumin is limited.

1.2.1.3 Glomerular Basement Membrane

The GBM is a dense network of secreted extracellular matrix (ECM) components supporting GECs on the inner capillary wall and podocytes on the outer layer of the GFB.[21] The GBM arises from the fusion of two membranes: one derived from podocytes and the second derived from endothelial cells,[22] and openings of the GBM protein mesh of variable dimensions (10-20nm in radius) have been identified.[23]

The main structural support of the GBM is provided by two major networks of laminin and collagen IV. Laminins are heterotrimeric glycoproteins consisting of α, β, and γ chains, and are an absolute requirement for basement membrane formation.[24] The mature GBM is predominantly composed of laminin α5β2γ1, and the importance of laminin is underscored by the observation that mutations in *LAMB2* (the gene encoding the laminin β2 chain) causes Pierson syndrome, a disease characterised by congenital NS and ocular abnormalities.[21]

Collagen IV consists of heterotrimers comprising three α chain combinations (α1α1α2, α3α4α5, or α5α5α6), with the mature GBM principally containing α3α4α5. Although the collagen IV network is not an absolute requirement for basement membrane formation, mutations leading to reduced or absent α3α4α5 cause Alport Syndrome, characterised by progressive renal failure, sensorineural hearing loss and ocular defects.[21, 25]

Although the collagen/laminin network forms the core of the GBM, a recent proteomics analysis of the human glomerular ECM has shown the matrix to be a complex system of structural and regulatory proteins: 144 glomerular ECM proteins were identified, with >50% expressed in the GBM.[26]

1.2.1.4 Podocytes

Podocytes are highly differentiated epithelial cells located on the outside of glomerular capillaries, consisting of a large cell body in the urinary space, connecting to the underlying GBM via cell protrusions (‘major processes’) which terminate in smaller

foot processes (FPs). FPs from one podocyte interdigitate with FPs from neighbouring podocytes creating a signature structural motif.[18] In addition to FPs arising from major processes, FPs that arise directly from the podocyte cell body to connect the cell body to the GBM ('anchoring processes') have also been described.[27]

Both podocyte-podocyte and podocyte-GBM interactions are critical for the maintenance of GFB function. The most important adhesion receptor responsible for binding the podocyte to underlying matrix is integrin α3β1,[28] and homozygous mutations in *ITGA3* (the gene encoding integrin α3) leads to congenital NS, as well as lung and skin disease.[29]

The junction between adjacent podocyte FPs is termed the slit diaphragm and is approximately 40 nm wide. In parallel view, the slit diaphragm is a continuous band between FPs with a zipper-like structure consisting of cross-bridges extending from the walls of the FPs to a longitudinal central filament, thus forming rectangular pores in the diaphragm. In one early study, the pore sizes were found to be variable and robust quantitative analysis was not possible; however superimposing albumin molecules from x-ray crystallographic data onto the electron tomography slit-diaphragm data showed that the pore sizes of the larger pores was similar to, or smaller than, albumin molecules. Additionally, the slit diaphragm pores form convoluted interconnected channels with varying diameter, rather than simple straight holes of regular size. These observations suggest the slit diaphragm contributes significantly to the retention of macromolecules such as albumin within the circulation.[30, 31]

More recent transmission electron microscopy in rat glomeruli identified ellipsoidal pores in slit diaphragms with a minor and major radius of 9.8 and 14.7 nm, respectively (the dimensions of albumin are 5.97 x 9.70 x 5.97nm), with a higher frequency of larger pores in proteinuric rats compared to healthy controls. This observation may help to provide an explanation for the increased permeability of the GFB in proteinuric conditions. [32]

The podocyte is thought to play a critical role in maintaining GFB integrity, and this will be discussed in detail in later sections. However, the importance of this cell in the pathogenesis of NS is highlighted by the observation that in NS presenting before the age of 1 year, two-thirds of cases can be explained by mutations in just four genes: i) *NPHS1* – encoding nephrin, a critical component of the podocyte slit diaphragm; ii)

NPHS2-encoding podocin, a close interactor of nephrin in the podocyte slit diaphragm; iii) *WT1*- encoding Wilms tumor suppressor gene 1, a transcriptional regulator of several podocyte genes such as *NPHS1, NPHS2, MAGI2, PLCE1* and *NCK2*[33-35] and; iv) *LAMB2*- encoding laminin β2, which as a GBM component is critical for maintaining podocyte architecture and stability.[36]

1.2.1.5 Subpodocyte space

Until recently, it was assumed that there was no significant resistance to solute and fluid flux downstream of the podocyte FPs. However, it has now been shown that anchoring processes directly connecting the podocyte cell body to the GBM form a subpodocyte space (SPS) that is restrictive to fluid flow. This SPS is on the urinary side of the GBM and is bound by the GBM and FPs on one side and the underside of the podocyte cell body on the other, with 61% of the filtration area of the GBM (ie, excluding mesangium) filtering into an SPS. [27]

Fluid that enters the SPS follows a tortuous pathway before reaching a constriction between the SPS and a larger fluid channel between neighbouring podocytes, termed the interpodocyte space (IPS). This constriction is termed the SPS exit pore (SEP), and is a significant barrier to fluid flow: filtrate that crosses the GBM needs to pass through an SEP area that is 4% of the filtration area to reach the peripheral, pre-tubular urinary space termed Bowman's space (BS). [10, 27] Further evidence of the functional importance of the SPS was provided by multiphoton microscopy in *ex vivo* perfused rat glomeruli, which demonstrated that Lucifer yellow flux (a surrogate marker of fluid flux) in SPS regions was 66-75% of that occurring through regions of GFB that were not covered by SPS.[37]

Mathematical modelling suggests the resistance of the SEP is 2.47 times that of the remainder of the GFB and exquisitely sensitive to changes in the dimensions of the SEP, suggesting an important role for the podocyte in the regulation of fluid flux across the GFB.[38] Additionally, it has been proposed that the SPS may be important in preventing clogging of the GFB with solutes, through transient back flux of fluid.[10]

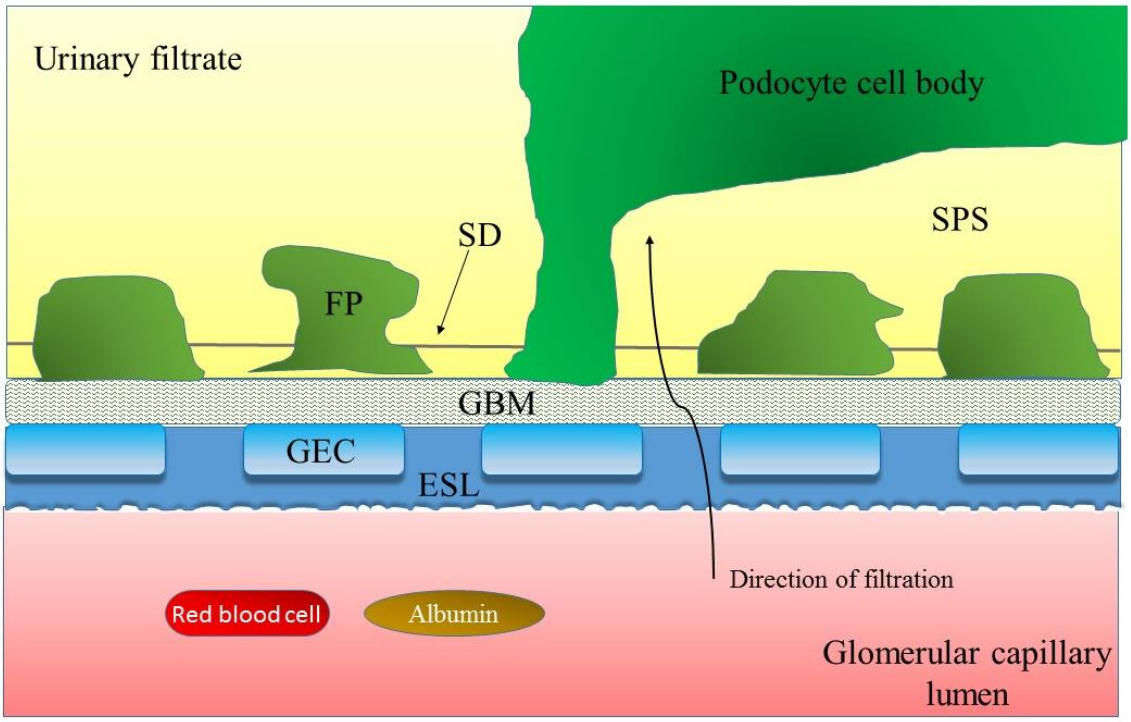

Figure 1.2 The layers of the glomerular filtration barrier (GFB).

The GFB is reponsible for the selective ultrafiltration of blood, ensuring minimal passage of proteins such as albumin into the primary urinary filtrate in health. The GFB consists of five layers: the endothelial surface layer (ESL); glomerular endothelial cells (GECs); the glomerular basement membrane (GBM); podocytes, which are specialised epithelial cells whose foot process (FP) protrusions are linked by the slit diaphragm (SD); and the sub-podocyte space (SPS).

1.2.2 Models of filtration

An appreciation of the mechanism underpinning normal glomerular filtration is a prerequisite to understanding the development of proteinuria, which is the key feature of NS. In the following section, I will explain the main hypotheses of filtration and address the strengths and weaknesses of each model.

1.2.2.1 The albumin retrieval hypothesis

An ongoing area of debate is the degree to which albumin traverses the GFB under normal conditions. The term used to quantify this is the 'sieving coefficient' (SC): the ratio of the concentration of albumin (or other high-molecular weight proteins) in primary filtrate compared to plasma. Micropuncture of rat proximal tubules gives a SC of $6x10^{-4}$,[39] while a SC of $8x10^{-5}$ was found in patients with Fanconi syndrome (dysfunction of proximal tubule reabsorption).[40] Values of $3x10^{-4}$ were obtained in rats in which tubular reabsorption was inhibited with lysine, [18] and a SC of $5x10^{-5}$ was found in mice with reduced capacity for tubular albumin reabsorption due to tubular-cell-specific cubulin/megalin double knock-out.[41] However, use of fluorescent labelled albumin coupled with intravital two photon microscopy in rats by Russo *et al.*, suggest a SC of 0.034, [42] which, if true, would mean approximately 8% instead of 0.02-0.06% of albumin would cross the renal filter.[43]

The proposal that the GFB is more permeable to albumin than previously thought gave rise to the 'albumin retrieval hypothesis' whereby relatively large amounts of albumin pass through the GFB and are subsequently retrieved by downstream tubular cells. In addition to the vast majority of published evidence suggesting the SC is much smaller than 0.034, mathematical modelling suggests that the high rates of tubular albumin reabsorption required by this burden would be impossible, even if every albumin molecule that reaches an epithelial cell were internalised immediately.[44, 45] When the two photon microscopy technique applied by Russo et al., (described above), was used by two independent groups, they found the SC of albumin and 70-kD dextran were much lower than values obtained by Russo (~0.002 Vs ~0.03). [46, 47] Explanations put forward to explain Russo's data include the use of external (instead of internal) photodetectors that were responsible for the collection of significant out-of-focus fluorescence (background noise potentially erroneously recorded as an albumin reading). With further developments in intravital imaging allowing highly precise measurements of fluorophore intensity in the glomerulus, a sieving coefficient of 70-kD

dextran was found to be approximately 0.001, suggesting the GFB is a strong barrier to protein flux.[48]

Further problems with this hypothesis involve the tubular reabsorption of albumin. Although it is known that albumin is taken up by the megalin-cubulin complex, a significant proportion of this would subsequently undergo degradation in lysosomal vesicles.[49] The 'albumin retrieval hypothesis' of filtration remains controversial and is not widely accepted.[18, 43]

1.2.2.2 The pore model

The observation that there is increasing restriction to the passage of macromolecules from the capillaries into the primary filtrate as molecular diameter increases led to the idea that the glomerulus is essentially a passive mechanical sieve consisting of a series of pores: the GBM acting as a coarse filter for large proteins, while podocyte slit diaphragms restricting the passage of smaller proteins such as albumin. This theoretical scheme was the basis of the 'pore model' of filtration.[50]

The first data suggesting filtration may be a more dynamic process came from Ryan *et al.*, who examined haemodynamic effects on filtration in the rat glomerulus. It was found that during periods of normal blood flow, plasma albumin does not significantly penetrate beyond the endothelial layer of the glomerular capillary wall. When renal blood flow was interrupted via occlusion of the renal pedicle, albumin was found in large amounts in the urinary space and the GBM, with glomerular structural architecture being preserved. Interestingly, this seemed to be a reversible process: if the blood flow was restored following a five minute period of ligation, the distribution of albumin in the glomerulus returned to normal (within minutes). These data suggest that GFB function cannot be attributed solely to structural elements, and haemodynamic features play a role. [50, 51]

The model was subsequently developed to include two major forces dictating albumin flux across the filter: convection and diffusion. Convective flux is driven by the drag of the flow of water across the GFB and is proportional to the hydraulic pressure difference across the layer. Diffusion is driven by the concentration difference within the capillary lumen and the primary filtrate. The flux of albumin across the GFB in the absence of blood flow/convection identified by Ryan *et al.*, was ascribed to diffusion.[43, 51]

However, the most problematic aspect of this model is its failure to explain why the filter does not clog with macromolecules. An analogous example of the 'pore model' of filtration used in clinical practice is continuous venovenous filtration (CVVH), which produces a protein-free ultrafiltrate from plasma using a semi-permeable membrane (as does the glomerulus), but typically clogs after three days use.[43] Additionally, it seems that under normal conditions albumin does not penetrate further than the GBM, despite the pores in the GBM being much larger than albumin. [23, 51] A more refined model incorporating an anti-clogging mechanism, and explaining why albumin does not significantly penetrate the GBM despite limited structural resistance has been proposed, as described below.

1.2.2.3 The electrokinetic model

The electrokinetic model of glomerular filtration assumes that, in addition to convection and diffusion, an electrical field is generated across the barrier by the physical phenomenon of a 'streaming potential,' which in turn prevents the negatively charged plasma proteins from entering or passing the filter.[52, 53]

The most likely mechanism by which a charge is generated across the GFB is by a streaming potential. When a filtration pressure is applied to a porous membrane separating two spaces, cations (eg, sodium, potassium) and anions (eg, chloride, bicarbonate) will be differentially separated. This streaming potential across the filtration layer is proportional to the effective filtration pressure.[52]

This model has supportive *in vivo* data. It is technically challenging to perform micropuncture experiments in mammalian glomerular capillaries due to their small size (4-5μm). However, in the amphibian *Necturus maculosus* (with a capillary diameter of 50μm), a potential difference was measured across the GFB that was proportional to the filtration pressure (-0.045 mV/ 10cm H_2O), and negative within Bowman's (urinary) space.[54] The authors postulate that the electrokinetic model may provide an explanation for orthostatic proteinuria (proteinuria in the upright position, but not in the supine position, as a consequence of a drop in renal perfusion and glomerular filtration rate when upright). As the filtration pressure is a vital factor in generating the streaming potential, when the filtration pressure is reduced in the upright position, the streaming potential across the GFB is diminished and proteinuria results.

The electrokinetic model may also explain the link between the podocyte cytoskeletal changes associated with NS, and the development of proteinuria. In health, the filtering surface is covered with interdigitating podocyte foot processes, allowing filtration to occur homogeneously across the filtering surface (the main podocyte cell bodies, which would act as barriers to filtration, are not in contact with the filtering surface, but are submerged in primary urine). During periods of proteinuria, podocyte foot processes are effaced so that they cover almost the entire filtering surface: some filtration (and therefore charge separation) will still occur between cells, but the anions will immediately fall back across the non-filtering (but still electrically conductive) areas underneath the effaced podocyte, so short-circuiting the streaming potential throughout the glomerulus.[54]

In summary, the electrokinetic model of filtration describes the GFB as a barrier with electrical effects, not simply as a passive filter. The GFB produces streaming potentials, generated whenever an ionic fluid passes through an electrically charged barrier, and is sufficient to repel negatively charged plasma proteins from entering the GFB.[55] This explains the observation that most of the albumin in the mammalian kidneys never reaches the podocyte slit diaphragm, even though the fenestrations in the endothelial cells, and pores in the GBM are unlikely to offer sufficient mechanical resistance to albumin flux.[50, 56] The negative charge on the urinary side of the GFB also provides an explanation for why anionic proteins are preferentially retained in the blood compared to other (non-anionic) molecules of comparable size. [3, 54] When podocyte foot process effacement occurs in NS, larger parts of the GFB will block filtration because they are covered by flattened podocytes, the electrical field decays, plasma proteins are incompletely repelled, and this results in proteinuria.[55]

1.3 The podocyte

1.3.1 The podocyte cytoskeleton

A complex system of cytoskeletal and signalling molecules is responsible for ensuring podocyte structural integrity is maintained and efficient renal filtration can occur. Podocyte cytoarchitecture is characterised by an arborised cell body with multiple major projections, which subdivide into secondary processes and eventually into finer terminal foot processes (see **Figure 1.3**). The cytoskeleton consists of three distinct sets of structural elements: microfilaments (7-9 nm in diameter), intermediate filaments (10 nm), and microtubules (24 nm). Podocyte cell bodies, major processes and secondary processes are supported by microtubules (polymers of α-tubulin and β-tubulin) and intermediate filaments (eg, vimentin and desmin), while foot processes are rich in parallel bundles of F-actin microfilaments, myosin, and the actin-bundling protein, α-actinin-4. [57-59]

Foot processes of neighbouring podocytes are connected with one another via the slit diaphragm (SD) in a characteristic interdigitating pattern. The SD bridges the 30-50nm space between neighbouring foot processes and is classified as a 'modified adherens junction' composed of P-cadherin, α-, β-, and γ-catenin, and zonula occludens-1 (ZO-1), unique podocyte proteins such as nephrin, but lacking the characteristic adherens junction protein vinculin. [60] Transmission electron microscopy studies suggest the SD consists of rodlike units, connected in the centre to a linear bar, forming a 'zipperlike' pattern.[31, 57] Proteins that have been localised to the SD are listed in **Table 1.1**.

A protein of critical importance for maintaining SD function is nephrin, and mutations in the nephrin gene *NPHS1* are the cause of congenital nephrotic syndrome of the Finnish type.[61] Nephrin is a member of the immunoglobulin (Ig) superfamily, and interacts with other nephrin molecules in the SD via its extracellular domain. [62] The intracellular cytoplasmic tail of nephrin indirectly links to the cytoskeleton via modulators of actin dynamics including CD2-associated protein (CD2AP) and podocin.[63, 64] CD2AP, in turn, interacts with actin,[65] as well as the actin-binding proteins CapZ,[66] cortactin,[67] and the α–actinin-modulating protein synaptopodin.[68] Nephrin also plays a central role in the transduction of extracellular signals via phosphorylation-dependent mechanisms to the internal podocyte cytoskeleton, and this will be discussed in the following section.

Table 1.1 Proteins located at the slit diaphragm

Protein	Reference(s)
α-, β-, γ- catenin	[60]
aPKC/Par3/Par6 complex	[69]
CASK	[70]
CD2AP	[64, 71]
Cingulin	[70]
CLIC5	[72]
Cx43	[73]
Dendrin	[74]
Ephrin-B1	[75]
FAT1	[76]
Galectin-1	[77]
JAM-A	[70]
MAGI-1, -2	[78, 79]
Neph-1, -2	[80, 81]
Nephrin	[30, 82, 83]
Occludin	[70]
P-cadherin	[60]
Podocin	[63, 84]
Spectrin (αII, βII)	[79]
Zonula occludens-1	[85, 86]

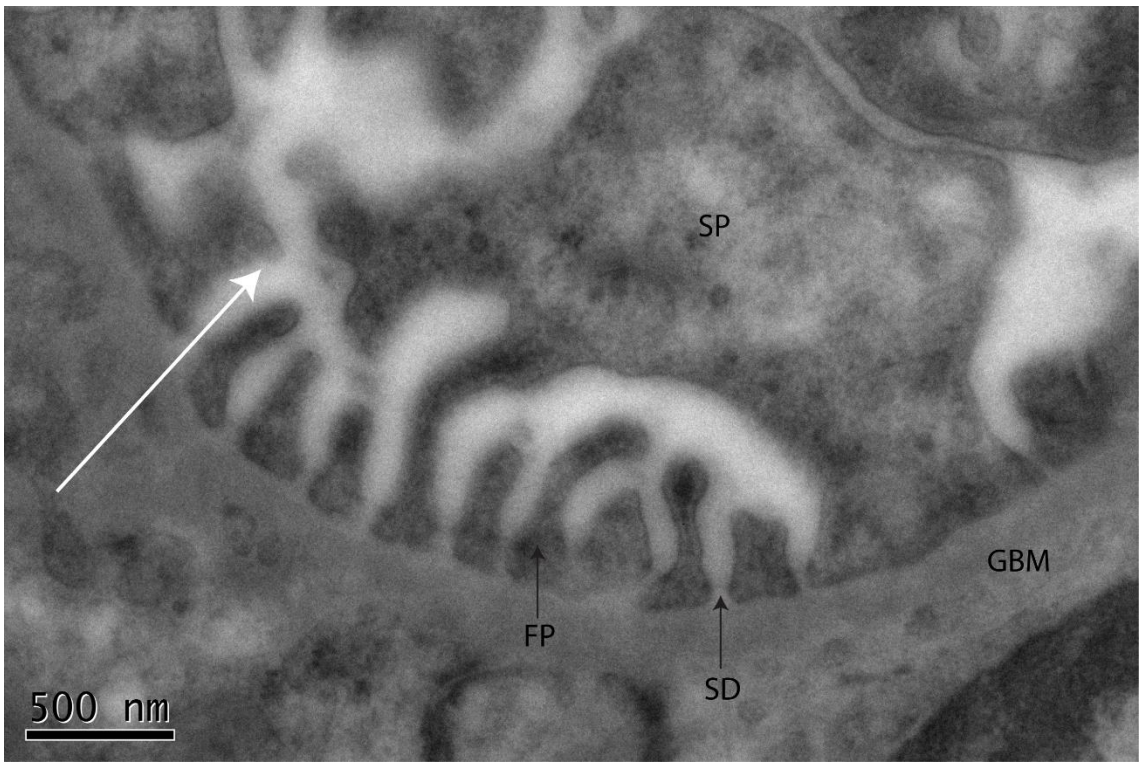

Figure 1.3 Podocyte ultrastructure
Podocytes form an important part of the glomerular filtration barrier. These cells have an arborized structure, whereby actin-rich major processes extended from the cell body, to form major processes, which sub-divide further into secondary processes (SP) and eventually foot processes (FP). FPs are connected by a complex modified adherens junction called the slit diaphragm (SD). The white arrow shows the direction of filtration across the glomerular filtration barrier. GBM=glomerular basement membrane. Transmission electron microscopy images taken by Dr Aleksandr Mironov (University of Manchester), using samples from a female, 4 month old C57BL/6 mouse.

1.3.2 Signalling at the slit diaphragm

The SD functions as a complex signalling hub, playing a critical role in the transduction of a variety of extracellular signals to the podocyte cytoskeleton (see **Figure 1.4**).[59, 87] A key step in initiating this signalling cascade is the tyrosine-phosphorylation of nephrin by the Src family kinase Fyn.[88] Phosphorylation of nephrin leads to the recruitment of several proteins including the adaptor proteins Nck1/2[89], Crk1/2[90], CrkL [91], Grb2[92], as well as PI3-kinase.[93, 94] Additionally, Neph1 forms a protein complex with Nephrin, and Fyn-dependent tyrosine phosphorylation of Neph1 leads to recruitment of Grb2.[95]

After Nck1/2 has bound phosphorylated nephrin, Nck1/2 binds to neuronal Wiskott-Aldrich syndrome protein (N-WASP), which in turn activates the Arp2/3 complex, and leads to cytoskeletal reorganization.[59, 96] In contrast to the role nephrin plays in promoting actin polymerisation, signalling via the podocyte Robo2 receptor inhibits nephrin-induced actin polymerisation.[97]

1.3.3 The role of the podocyte in nephrotic syndrome

Shortly after the podocyte SD was first identified in healthy glomeruli using electron microscopy,[31] it was observed that the flattening of podocyte foot processes with loss of the SD (‘effacement’) was a characteristic morphological feature of proteinuria. Additionally, it was discovered that the SD reforms after administration of Gc therapy and regression of proteinuria.[98] These observations gave rise to the concept that NS results from functional and structural alterations to the podocyte and SD.[87]

Further evidence implicating the podocyte in the development of proteinuria came with the discovery that mutations in *NPHS1* (coding for the podocyte-specific protein nephrin) cause congenital nephrotic syndrome of the Finnish type.[61] Additionally, mutations in genes encoding other SD proteins such as podocin,[99] Neph1,[80] protocadherin Fat1,[100] the ion channel TRPC6,[101] and the adaptor protein CD2AP,[71] result in proteinuria in mice and humans. For a more complete list of gene mutations implicated in NS, see **Table 1.3**.

Over the previous decades, an immunological basis for NS has been postulated, partly due to the presumption that medications known to be effective in INS (eg, Gc, calcineurin inhibitors) are potent immunosuppressive agents.[102] However, more recent data has shown that many of these therapeutic agents have direct effects on the

podocyte, underlining the role of this cell as a key player in the pathogenesis of INS. For example, the calcineurin inhibitor ciclosporin A is used to treat children with steroid dependent- or steroid resistant NS (definitions provided in **Table 1.2**) and exerts an immunosuppressive effect through inhibition of nuclear factor of activated T-cells (NFAT) signalling in T-cells. However, Faul *et al.*, showed the therapeutic efficacy of ciclosporin A in INS is not dependent on NFAT inhibition in T cells, but directly via stabilisation of the actin cytoskeleton in podocytes by protecting the actin-regulating protein synaptopodin from degradation by cathepsin L.[103] I will now discuss direct effects of Gc on the podocyte.

1.3.3.1 Direct effects of Gc on the podocyte

As will be discussed in later sections, the canonical mechanism of action of Gc is through binding to the cytosolic glucocorticoid receptor (GR). GR is a ligand-activated transcription factor. Upon ligand binding, GR translocates into the nucleus and directs the expression of target genes. Yan *et al.*, provided the first data in adult human histology specimens that podocytes express GR, and GR could be identified in transcriptionally-active nuclear euchromatin, but not in the heterochromatic nuclear areas which typically exhibit lower transcriptional activity.[104] It was subsequently shown that exposure of an immortalised murine podocyte cell line to the Gc dexamethasone causes cytosolic GR to translocate into the nucleus, induces upregulation of protein and messenger ribonucleic acid (mRNA) of known Gc-targets, and reduces GR expression in a negative feedback loop. These data confirm the key components of the Gc signalling pathway are intact in the mouse podocyte.[105]

Building on these data, several studies have characterised Gc-effects on the podocytes. Ransom *et al.*, compared the total proteomic output of murine podocytes with and without Gc treatment using a mass spectrometry approach, and identified 7 Gc-regulated proteins (ATPase, H^+ transport, lysosomal; annexin 5; ciliary neurotrophic factor; αB-crystallin; gelosin; purine nucleotide phosphorylase; and heat shock protein 27).[106]

A microarray approach has been utilised to understand how Gc exposure affects podocyte differentiation at the transcriptomic level.[107] The immortalised human podocyte cell line used in the study takes 10-14 days to fully differentiate.[108] The authors allowed 2 days of differentiation before treating with either vehicle or dexamethasone for a further 3 days. Dexamethasone altered the expression of several

genes involved in inflammation, cell migration, angiogenesis, as well as the nuclear factor kappa-light-chain-enhancer of activated B cells (NF-κB) and transforming growth factor β (TGF-β) pathways.

Other studies have investigated Gc effects on the podocytes using disease-models. It has been demonstrated that treatment of a murine podocyte cell line with dexamethasone protected, and enhanced recovery, from the puromycin aminonucleoside (PAN) model of podocyte injury (quantified using a cell viability assay and total polymerised cell actin content).[109] Activity of the actin-regulating GTPase Ras homolog gene family, member A (RhoA) was also increased when cells were treated with dexamethasone for 30 minutes, followed by culture for a further 3 days in fresh (non-dexamethasone containing) medium.

Wada *et al.*, have shown that dexamethasone significantly reduced podocyte apoptosis in a PAN cell culture model. [110] This protective effect was associated with decreased expression of the pro-apoptosis protein cellular tumour antigen p53 (p53), and increased expression of anti-apoptotic protein B-cell lymphoma-extra large (Bcl-xL). Of potential functional benefit was the observation that Gc upregulated expression of nephrin and α-tubulin in an immortalised human podocyte cell line.[102]

Gc treatment also has potentially clinically-relevant effects on the expression of vascular endothelial growth factor (VEGF). The VEGF-A isoform regulates SD-signalling and podocyte cytoskeletal dynamics via nephrin-nck-actin interactions, and VEGF-A overexpression causes proteinuria and FP effacement in mice.[111, 112] Podocytes are the major source of VEGF-A in glomeruli [113, 114] and higher expression levels are observed in NS.[115] Gc has been shown to reduce VEGF-A expression in podocytes *in vitro*.[102]

The possible immunological basis for INS will be discussed in Section 1.5.2. Podocytes express a number of chemokine receptors (CCR4, CCR8, CCR9, CCR10, CXCR1, CXCR3, CXCR4, and CXCR5)[116] and dexamethasone treatment supresses podocyte expression of interleukin-6 (but not interleukin-8).[102]

Some data exist that Gc may be exerting a direct, potentially clinically-relevant effect on podocytes through altering intracellular trafficking and post-translational modifications of nephrin. Fuji *et al.*, have shown in human embryonic kidney-293 (HEK 293) cells that endoplasmic reticulum (ER) stress led to the formation of

underglycosylated nephrin that remained in the ER.[117] Dexamethasone exposure restored the synthesis of fully glycosylated nephrin via stimulation of adenosine triphosphate production (ATP) and restored normal trafficking of nephrin to the plasma membrane. On the basis of these observations, the authors speculate that Gc may exert protective effects by affecting intracellular levels of ATP. Building on data demonstrating that nephrin is phosphorylated under normal conditions, and phosphorylation is decreased in rodent PAN and human NS,[118] Ohashi *et al.*, showed that Gc (dexamethasone) exposure increased the phosphorylation of nephrin via serum/glucocorticoid-induced kinase 1 (SGK1).[119]

Using an *in vivo* rodent model of adriamycin-induced NS,[120] Gc (prednisone) reduced proteinuria, possibly through stabilising the abnormal subcellular localisation of nephrin, podocin, CD2AP, and α-actinin observed after adriamycin exposure.[120]

A report from 2014 suggests Gc may be exerting protective effects on podocytes through altering expression of microRNA (miRNA) molecules, specifically the miR-30 family.[121] All members of miR-30 were found to be downregulated in patients with NS, as well as in rats treated with PAN. Moreover, transfer of exogenous miR-30a to podocytes of PAN-treated rats using an *in vivo* gene delivery system ameliorated proteinuria and podocyte injury and reduced Notch1 activation. Gc exposure sustained miR-30 expression and reduced Notch1 activation, leading to the possibility that miR-30a expression may be a novel mechanism underlying the therapeutic effectiveness of Gc in INS.

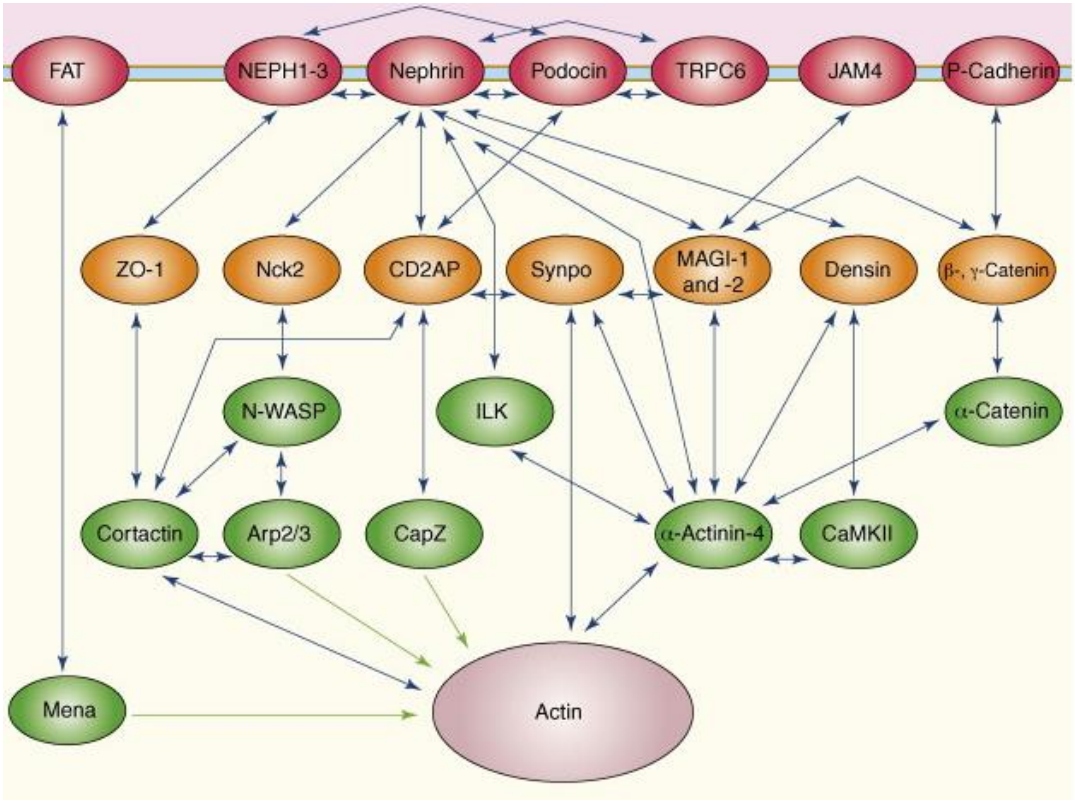

Figure 1.4 Schematic diagram of the linkage between slit-diaphragm (SD) proteins and the actin cytoskeleton.
The SD is a multiprotein, complex signalling hub connecting adjacent podocyte foot processes (FPs). Membrane proteins are shown in red, adaptor proteins in orange, and effector proteins in green. Biochemical protein-protein interactions are shown by blue double arrows, and the effector pathways are indicated by green arrows. Taken from [59].

1.3.4 Podocyte contractility and motility

As described above, podocytes contain a complex cytoskeletal network. It has been proposed that these distinct architectural features are necessary to withstand, and possibly react to, the highly dynamic conditions existing in the urinary space: varying filtration flow rates; the mechanical stress imposed by the shear stress from primary filtrate; and the hydraulic pressure from capillaries.[59, 122, 123] Indeed, the requirement for podocytes to withstand such stresses is underscored by the observation that they exhibit several characteristics of smooth muscle cells, including rapid insulin-sensitive glucose uptake, expression of smooth muscle markers smoothelin and calponin,[124, 125] and spontaneous contraction *in vitro*.[124] Additionally, fluid shear stress induces a reorganisation of the actin cytoskeleton including enhancement of podocyte cell protrusion formation and redistribution of the actin nucleation protein cortactin to the cell periphery.[126]

Mechanistically, stretch- and calcium-sensitive potassium channels have been identified in podocytes,[127] and the podocyte cytoskeletal reorganisation elicited by mechanical force involves the (calcium-sensitive) calmodulin-dependent kinase and activation of the small GTPase ras homolog gene family, member A (RhoA). It has also been shown that the TRPC5 and TRPC6 ion channels mediate calcium influx into podocytes in response to angiotensin II, eliciting reorganisation of the actin cytoskeleton via RhoA and Ras-related C3 botulinum toxin substrate 1 (Rac1).[128]

Thus, the podocyte cytoskeleton is sensitive to the mechanical stimuli it experiences within the glomerulus. Additionally, the concept of podocyte motility as a determinant of GFB function is an emerging theme in renal biology.[129, 130] This originated from the observation that treating primary rodent podocytes with puromycin aminonucleoside (PAN) (used to induce proteinuria in the rodent model of puromycin aminonucleoside nephrosis) promoted podocyte migration *ex vivo*.[131] PAN treatment also upregulated expression of the cysteine protease cathepsin L (CatL) in podocytes *in vivo*, and isolated rodent podocytes lacking CatL were protected from PAN-induced cell detachment. Additionally, PAN-induced cell migration was slowed in CatL-deficient podocytes. From these data, the authors postulated that the onset of proteinuria represents a migratory event in podocytes, possibly mediated via CatL.

Recent developments in serial multiphoton imaging have also allowed direct visualisation of the kidney at a cellular level *in vivo* and shown that podocytes are

motile along the basement membrane.[48, 132] Using serial multiphoton microscopy of the same glomeruli over several days in mice expressing green fluorescent protein under the control of the podocyte-specific podocin promoter *in vivo*, it was possible to observe podocytes migrate within the glomerulus.[132] Higher rates of podocyte migration were observed in mice after renal injury was induced through unilateral ureteral obstruction (UUO) and via the adriamycin nephropathy model compared to healthy control mice. Cell bridges of podocyte origin also formed between the visceral and parietal glomerular cell layers in mice post-injury. These observations have altered the view of the GFB from a static to a highly dynamic structure, with podocytes capable of rapidly reorganising their actin-based cytoskeleton in response to external stimuli.[130] It has been proposed that under normal conditions, podocyte motility is necessary to ensure the GFB remains clear of proteins, which may otherwise become trapped under the SD. However, a hypermotile podocyte phenotype signals the onset of proteinuria.[123]

Insight into potential mechanisms underlying disease-associated podocyte hypermotility came from Ma *et al.*, who demonstrated a role for focal adhesion kinase (FAK). The group demonstrated that in murine models, glomerular injury led to podocyte FAK activation associated with FP effacement and proteinuria, and glomerular damage was reduced by FAK inhibition. Furthermore, *in vitro*, podocytes isolated from FAK knockout mice demonstrated reduced motility, suggesting pharmacological inhibition of FAK may have therapeutic potential in NS.[133] In a more recent study, Harris *et al.*, demonstrated that proteases present in serum from patients with active FSGS can activate the protease activated receptor 1 (PAR1), which leads to the podocin-dependent phosphorylation of actin-associated protein vasodilator stimulated phosphoprotein (VASP), and enhanced podocyte motility.[134]

1.4 Clinical aspects of nephrotic syndrome

NS is characterised by heavy proteinuria and resultant hypoalbuminaemia, leading to a fall in plasma oncotic pressure and generalised oedema. These features are typically associated with hyperlipidaemia.[135] Children with NS are at risk of a wide range of complications associated with significant morbidity and experience mortality rates of up to 2.7%.[2]

1.4.1 Classification of NS

Several schemes have been used to classify NS including: i) histopathological criteria; ii) time of disease onset (congenital/infantile NS or idiopathic NS); and iii) response to pharmacological therapy.

1.4.1.1 Classification by histopathological criteria

The introduction of percutaneous needle renal biopsy in the 1950's led to a recognition of the range of histopathological abnormalities that can underlie NS. [136] In childhood NS, the three most common histopathological patterns seen are: minimal change disease (MCD), focal segmental glomerulosclerosis (FSGS), and mesangial proliferative (mesangiocapillary) glomerulonephritis (MPGN). Analysis of renal biopsy findings in 127 new-onset, untreated cases of paediatric NS revealed MCD accounted for 79% of cases, FSGS for 9% of cases, and MPGN for 5% of cases.[137]

In MCD, glomeruli appear normal by light microscopy.[138] However, electron microscopy reveals podocyte FP effacement. Although MCD is the most common histological diagnosis among NS paediatric patients, it displays a distinctive age-related distribution: MCD accounts for 90% of cases in patients under 10 years old, falling to 50% of cases in children older than 10 years, and 10% of adults.[138, 139]

FSGS is characterised by a segmental scarring of the glomerular tuft, affecting only some glomeruli,[140] and is the most common glomerular histological pattern of paediatric end stage renal disease (ESRD).[141] For unclear reasons, the incidence of FSGS seems to have approximately doubled over a number of decades (1978-1997), and may even have surpassed MCD as the most frequent diagnosis in the paediatric African American population. [142]

There is considerable debate focussed on whether MCD and FSGS are actually distinct clinical entities. Hoyer *et al.* reported 3 children suffering from NS refractory to

pharmacological management, who were undergoing kidney transplantation. All 3 children suffered disease-recurrence post-transplantation. Two of the children showed histological progression from MCD early in the disease to FSGS after transplantation (the third child showed features of FSGS at presentation).[143] Some authors suggest MCD and FSGS are parts of a single spectrum of disease, with MCD resulting from minor glomerular injury and rapidly corrected by pharmacological therapy, with FSGS an 'irreversible' form of MCD, frequently progressing to ESRD.[144]

1.4.1.2 Classification by age of disease onset

NS can also be divided into congenital NS (presentation before 3 months of age), infantile NS (presentation between 3 months-1 year of age) and idiopathic NS (INS) (NS presenting after the age of 1 year). Congenital and infantile NS are extremely rare, while the incidence of INS from a study in northern England using data collected over a 12 year period was found to be 2.3/ 100,000 patient years (pyrs). The authors found a marked difference in incidence according to ethnic background: 7.4/100,000 pyrs in South Asian children, compared with 1.6/100,000 in non-South Asian children.[145] Asian children with INS also had an earlier mean age of onset of 3.4 years compared to European children who typically present at 4.2 years.[146]

Although the majority of congenital and infantile NS have an underlying genetic basis (and will be discussed subsequently), other rarer causes include: infection (eg, congenital cytomegalovirus, heptatitis B and C, congenital rubella), malignancy (eg, nephroblastoma), and drug reactions. The underlying cause(s), and treatment of INS will be discussed in detail in section 1.5.

Unlike the treatment for INS, pharmacological management does not produce disease-remission in congenital NS.[147, 148] The mainstay of treatment involves controlling oedema with albumin infusions, preventing malnutrition with high-energy and high-protein feeds, and reducing proteinuria by nephrectomy. Kidney transplantation is the only curative option.[147]

1.4.1.3 Classification by response to pharmacological therapy

Arneil in 1956 was the first investigator to publish evidence supporting the use of the synthetic glucocorticoid prednisolone as effective therapy for childhood INS.[149] This landmark discovery led to the International Study of Kidney Disease in Children (ISKDC)[137, 139] and later work by the Arbeitsgemeinschaft für Pädiatrische

Nephrologie (APN),[150, 151] which forms the basis of modern management. Consensus definitions for terms used to describe clinical stages of nephrotic syndrome are summarised in **Table 1.2**.

Table 1.2 Consensus definitions for clinical aspects of nephrotic syndrome

Remission	*Albustix*-negative or trace for 3 days.*
Relapse	*After remission, Albustix reading of ≥2 for 3 of 5 consecutive days*
Frequently relapsing nephrotic syndrome (FRNS)	*2 or more relapses within 6 months after initial therapy or ≥4 relapses in any 12-month period*
Steroid dependent nephrotic syndrome (SDNS)	*Relapse during tapering section of Gc treatment protocol or within 2 weeks of discontinuation of Gc therapy*
Steroid resistant nephrotic syndrome (SRNS)	*Inability to induce a remission with 4 weeks of daily Gc therapy*

Above definitions taken from childhood NS management guidelines issued by the American Academy of Pediatrics.[152]

*'Albustix' is a urinalysis strip used to quantify proteinuria into the following categories of increasing severity: Negative, Trace, +1, +2, +3, and +4.

Current initial standard management includes a minimum eight week course of oral Gc (prednisolone in the UK) at a dose of 60mg/m^2 (maximum dose 80mg) once a day for the first month, followed by 40mg/m^2 (maximum dose 60mg) on alternate days for the second month, without renal biopsy at presentation. This established regimen is currently being compared to an extended (sixteen week) tapering prednisolone regimen in a UK multicentre randomised double blind trial called the PREDnisolone in NephrOtic Syndrome (PREDNOS) study.

Approximately 92% of children with INS will go into remission during the initial course of Gc therapy, and are classified as having steroid-sensitive nephrotic syndrome (SSNS), while 8% of children fail to enter remission during this initial treatment period and are classified as having steroid resistant nephrotic syndrome (SRNS).[153] Of SSNS patients, 44% will go into long-term remission, 22% have an infrequently relapsing course (relapsing but not satisfying criteria for FRNS), 31% have a frequently relapsing course, and 3% subsequently develop SRNS.

Pharmacological management of FRNS, SDNS and SRNS may involve the anthelmintic drug levamisole, alkylating agents (eg, cyclophosphamide), calcineurin inhibitors (eg, ciclosporin), antiproliferative agents (eg, mycophenolate mofetil) and an anti-CD20 antibody (rituximab).

1.4.2 Prognosis

Children with SSNS generally have a good long-term outcome. However, significant morbidity is associated with a disease course refractory to pharmacological management. Acute problems include infection and thromboembolic events, while long-term risks include medication toxicity and the risk of developing end-stage renal disease (ESRD) necessitating a period of dialysis and ultimately kidney transplantation.

The leading cause of mortality in the childhood INS population is infection, and the annual incidence of invasive bacterial infection is approximately 1-2%.[2, 154] The ISKDC followed up 373 children with INS for 5-10years and reported 10 deaths, 6 due to infection.[2] Potential reasons for the increased rates of infection in INS include urinary loss of immunoglobulin, disturbances of the complement system, [155] defective opsonisation and altered T-cell function.[5] The importance of infection in INS is underscored by the observation that the first significant reductions in mortality attributed to INS came with the introduction of antimicrobial agents: in the pre-

antibiotic era INS mortality was 67% (1929-1936), falling to 42% after the introduction of sulphonamide antibiotics in 1939, and still further to 35% in 1944 following wide-spread use of penicillin.[1]

The second leading cause of mortality in nephrotic children is thromboembolic disease (TED).[2] A study involving 326 children with INS with a median follow-up time of 3.7 years reported that 9.2% of the patient cohort experienced at least one episode of TED. In addition to these acute complications, children with INS face several long-term complications, and these will be addressed below.

1.4.2.1 Prognosis for children with SSNS

Although the majority of children with SSNS achieve long-term disease remission without further relapses by the early-mid teenage years,[156] recent studies indicate a significant relapse rate after 18 years of age between 27-42%.[157-159] Many of the complications faced by children with SSNS are attributable to medication side effects. Indeed, one of the major challenges facing clinicians is to effectively treat the acute complications associated with the proteinuric state, whilst minimising risk to long-term health outcomes.

Repeated courses of Gc therapy during childhood have a number of significant adverse effects, including short stature, obesity and osteoporosis.[160] Gc administration is also associated with ophthalmological complications: in a study including 45 Japanese children with SSNS, 20% had elevated intraocular pressure, while one-third had posterior subcapsular cataracts. The severity of cataract was related to total duration of Gc therapy.[161] It has been shown that children with INS receiving long-term alternate day Gc therapy are at risk of developing suppression of the hypothalamic-pituitary-adrenal axis (HPA), and those with evidence of HPA suppression are at greater risk of disease relapse.[162] Children with INS on prolonged Gc remain at risk of adrenal insufficiency until at least 9 months after Gc-discontinuation.[163]

Children with SSNS may be at risk from Gc-induced osteoporosis and osteomalacia due to decreased 25-hydroxy-vitamin D levels secondary to urinary loss of vitamin D binding protein.[164] Some evidence suggests that children with INS receiving Gc therapy do suffer from Gc-induced osteoporosis defined by radiological criteria [quantitatively expressed as a bone mineral density (BMD) value evaluated by dual-energy X-linked absorptiometry of the lumbar spine],[165] although it has not been

shown that reduced BMD in paediatric nephrotic patients results in an increased fracture rate. However, adults taking a prednisolone dose ≥7.5 mg/day for either treatment of asthma or rheumatoid arthritis double their risk of experiencing a fracture.[166] Some studies report a loss of growth (height) velocity with high cumulative Gc doses,[167, 168] although significant catch-up growth seems to compensate for pubertal growth retardation and children with SSNS attain normal final adult heights (as defined by estimated target height).[158]

It must be emphasised that even though some Gc-induced side effects may be transitory, they may still significantly impact patient outcome. Leonard *et al.*, examined 60 children and adolescents with SSNS who had received Gc-therapy within 1 year of recruitment. It was found that they were shorter ($p=0.008$) and had a greater body-mass index ($p<0.001$) than controls.[169] Side-effects are thought to be a key cause of non-adherence to medication, especially in the adolescent population. Data for INS patients specifically is lacking, but non-compliance has been identified as the aetiology of graft failure in 13% of adolescent kidney transplant recipients,[170] and the World Health Organization has identified cosmetic side effects (eg, Gc-induced acne) and chronicity of medication prescription as influencing factors on medication adherence.[171]

1.4.2.2 Prognosis for children with SRNS

In contrast to the generally favourable outcome of SSNS, patients with SRNS have a much more guarded prognosis, with 53% of children progressing to ESRD within 15 years.[172] In a European study involving 78 children with SRNS with a median follow-up period of 7.7 years, twenty patients (26%) received kidney transplants. Following transplant, ten children showed recurrence of NS. Deep venous thrombosis confirmed by imaging occurred in 6 patients (8%), and infections requiring hospitalisation occurred in 24 patients (31%). Two (2.6%) children died: one from sepsis and one from renal and haemodynamic failure.[172]

Additionally, the PodoNet consortium has recently reported data from a heterogeneous population of 1655 children with SRNS [defined as either congenital NS (6%), infantile NS (7%), adolescent-onset NS (13%), or childhood onset NS (74%)], with a median follow-up time of 3.7 years. At time of the last follow-up, 11.7% required dialysis, 14.2% of the children had received kidney allografts, and 2.3% of the patients were deceased.[173]

1.4.2.3 Significance of histology for prognosis

Children with a histopathological diagnosis of FSGS, MPGN or diffuse mesangial sclerosis are less likely to respond to Gc therapy and more likely to relapse than those with MCD.[137, 174] Conversely, the most common histopathological diagnosis in children with clinically more aggressive SRNS is FSGS (56% of SRNS children),[173] compared to MCD in children with SSNS (children with SSNS no longer undergo kidney biopsy, but older data shows 98/99 children with SSNS had MCD at presentation).[137]

However, Webb *et al.*, examined renal biopsy specimens from 51 children with SSNS (FRNS or SDNS) prior to the start of cyclophosphamide treatment and found that prebiopsy clinical course did not predict for histologic diagnosis and histology had little value in predicting future disease course. [175] Indeed, it is now well recognised that initial response to Gc therapy has a superior prognostic value than histology findings. In a study of 103 children with INS, a significant association was found between the interval from onset of treatment to remission and future risk of relapse. Patients with non-relapsing and infrequent relapsing NS had a median time to remission of <7 days; patients with frequently relapsing and SDNS had a median time to remission of >7 days.[176]

1.4.3 The genetics of NS

Known disease-causing mutations are only responsible for NS in a minority of children. However, recognition of the affected genes has led to a greater understanding of the pathophysiology underlying NS, and increased the likelihood of targeted therapies being developed for those children for whom current management is suboptimal.[177] As will be discussed below, detecting causative genetic mutations can also guide current management of children with NS by helping the clinician to decide whether immunosuppressive therapy (with the associated side-effects) is in the best interests of the patient prior to kidney transplantation, and for some very rare mutations involving mitochondrial genes, specific therapy to delay or avoid renal failure may be instigated. [178] **Table 1.3** lists genes mutated in NS.

Table 1.3 Genetic mutations identified in NS

Gene	Protein	Syndrome
Slit-diaphragm proteins		
NPHS1	Nephrin	CNS/SRNS
NPHS2	Podocin	CNS/SRNS
PLCE1	Phospholipase Cε1	SRNS
CD2AP	CD2 associated protein	SRNS
TRPC6	Transient receptor potential cation channel, subfamily C, member 6	Adult-onset SRNS
Cytoskeletal components and regulators		
ACTN4	α-actinin-4	Late-onset SRNS
MYH9	Nonmuscle myosin heavy chain-A	Increased propensity to FSGS in African-Americans
MYO1E	Nonmuscle class I myosin 1e	SRNS
INF2	Inverted formin 2	SRNS
ARHGAP24	Rho GTPase activating protein 24	SRNS
Nuclear proteins		
LMX1B	LIM/homeobox protein LMX1B	Nail-patella syndrome: NS in 40% of cases.
SMARCAL1	SMARCA-like protein	Schimmke immune-osseous dysplasia
WT1	Wilms' tumour 1	Denys-Drash syndrome, Frasier syndrome

Glomerular basement membrane proteins		
LAMB2	Laminin-β2	Pierson syndrome
ITGA3	Integrin-α3	CNS
Mitochondrial proteins		
PDSS2	Decaprenyl diphosphate synthase-2	Leigh syndrome and SRNS
COQ2	Para-hydroxybenzoate-polyprenyl-transferase	CoQ10 deficieny, SRNS
COQ6	Coenzyme Q6 monooxygenase	SRNS and sensorineural deafness

List of genes mutated in nephrotic syndromes. Table modified from [177]and [179]. Abbreviations: CNS-Congenital nephrotic syndrome; FSGS-Focal segmental glomeruloscelrosis; SRNS-Steroid resistant nephrotic syndrome; NS-Nephrotic syndrome.

1.4.3.1 Genetics of congenital and infantile NS

In a large cohort of 89 children from 80 families of non-Scandinavian European decent, 66.3% of patients presenting with NS within the first year of life were found to carry a mutation in one of four genes: *NPHS1*, *NPHS2*, *WT1*, and *LAMB2*. *NPHS2* mutations (coding for the protein podocin) were the most common cause of both congenital and infantile NS. Mutations in *NPHS1* (coding for the protein nephrin), accounted for 23% of cases of congenital NS (CNS), but did not appear to cause infantile NS. Of the 45/89 children who were treated with Gc, only one child achieved a remission. This child did not carry a disease-causing mutation in one of the four genes included in the study. None of the children who carried a disease-causing mutation was responsive to Gc therapy.[36]

Although congenital NS is found in infants of many ethnic backgrounds,[36, 180] the disease has a particularly high incidence in Finland of 1:10,000 [181] CNS of the Finnish type is characterised by autosomal recessive inheritance and is caused by mutations in *NPHS1*.[61] Two *NPHS1* mutations, Fin-major and Fin-minor, account for more than 90% of mutations found in infants with Finnish type CNS, while these mutations are rare in non-Finns.[182] In non-Finns, more than 60 different *NPHS1* mutations have been reported. Although the majority of these *NPHS1* mutations cause medication-refractory proteinuria and rapid progression to ESRD typical of CNS, some result in a relatively mild phenotype. For example, two siblings with compound heterozygous *NPHS1* mutations (L130F and C623F) mutation have been reported who experienced persistent NS since birth, but had not progressed to ESRD at 20 and 24 years of age.[183] Also, female Maltese children with the homozygous R1160X *NPHS1* mutation have a particularly mild phenotype with only mild proteinuria, although boys with the same mutation follow a more typical CNS clinical course. The reason for the marked difference between males and females is currently unclear.[184]

1.4.3.2 Genetics of SSNS

Unlike congenital, infantile and steroid resistant nephrotic syndrome, SSNS is only very rarely found in familial form.[185] Fuchshuber *et al.*, investigated 15 families with 32 individuals with autosomal recessive SSNS from Europe. The clinical course was found to be similar to the more common sporadic form of SSNS, and linkage to the *NPHS2* locus (the most common mutation found in congenital, infantile and steroid resistant NS) was excluded, which led the authors to conclude that familial SSNS is genetically

distinct from other familial variants of NS.[186] Ruf *et al.*, later examined a family from Germany including three children with SSNS and identified a disease-causing locus on chromosome 2p12-p13.2.[187] Landau *et al.*, compared rates of familial SSNS in Jewish (low consanguineous marriage rates) and Bedouin (high consanguineous marriage rates of approximately 65%) families in Southern Israel, and found higher familial SSNS rates among the Bedouin community than the Jewish community (28% compared to 4%, $p<0.05$). The authors suggested a role for susceptibility gene enrichment resulting in highly consanguineous populations experiencing an increased incidence of SSNS. However, they were unable to identify linkage to a chromosomal locus or find causative mutations in 80 NS-associated genes analysed.[185]

1.4.3.3 Genetics of SRNS

The predominant mutation found in childhood-onset SRNS is in *NPHS2*, with a significantly smaller proportion having *WT1* or *NPHS1* mutations.[177] In a cohort of 338 patients with SRNS (mean age of presentation approximately 5 years old), a mutation in NPHS2 was found in 43% of familial SRNS compared to 10.5% of sporadic SRNS.[188]

As described above, PodoNet have recently reported data from a heterogenous SRNS cohort. Mutation analysis was performed in 1174/1655 patients, and a genetic cause was identified in 23.6% of the screened patients. The most commonly observed mutations were in *NPHS2* (n=138), *WT1* (n=48) and *NPHS1* (n=41). The proportion of children with an underlying genetic cause of SRNS inversely correlated with the age of disease manifestation: 66% in congenital NS to 15-16% in schoolchildren and adolescents. Marked differences in rates of disease recurrence post-transplantation were also noted: recurrence occurred in 28.5% of patients without a genetic diagnosis, compared to 4.5% of those with a genetic diagnosis.[173]

A retrospective study investigated 91 patients with SRNS or CNS and found 68% of patients without an identified genetic defect responded to immunosuppression, while none of those with genetic-based NS experienced a complete remission and only 17% achieved a partial response.[189] These data are useful to clinicians: children with SRNS and a genetic mutation in one of the five genes detailed above are unlikely to respond to immunosuppressive therapy, but have low-rates of disease recurrence post-transplant, and so planning for a live related kidney transplant could begin at an early

stage, pre-emptively avoiding a prolonged period of dialysis and futile immunosuppressive therapy.[177]

However, it should be noted that children with certain genetic mutations can respond to immunosuppressive therapy. Hinkes *et al.*, reported truncating mutations in the phospholipase C epsilon gene causing early onset NS in twelve children. Two of these twelve children responded to pharmacotherapy: one boy presented with NS at the age of 2 months but following a 2.5 year course of ciclosporin A, remains free of proteinuria at the last follow-up at the age of 13yrs, while another boy presented with NS at the age of 8 months, subsequently received an 8 week course of Gc therapy, and was symptom free at the last recorded follow up at age 6 years.[190] Additionally, for the rare patient for whom a mutation affecting the mitochondrial COQ10 biosynthesis pathway is discovered, supplemental enzyme therapy to delay or avoid renal failure could be instigated.[177, 178] Two children with SRNS and sensorineural deafness due to a *COQ6* mutation were treated with oral COQ10 supplementation: both children experienced lower levels of proteinuria, and one additionally experienced an improvement in hearing.[178] There is also a case report of the early administration of COQ10 restoring renal function in an infant with a *COQ2* mutation.[191]

1.5 Aetiology of INS

The cause of idiopathic nephrotic syndrome (INS) is unclear. Various hypotheses have been proposed to explain the underlying basis for disease including an (as yet, unknown) circulating serum factor, immune system dysregulation, and enzymatic cleavage of key podocyte cytoskeletal components by cathespsin L.[5, 129] Some overlap exists between these hypotheses, and I will discuss the main possibilities below.

1.5.1 Circulating glomerular permeability factor

Hoyer *et al.*, proposed the existence of a circulating serum factor as a causative agent for INS to explain the observation that patients are at risk of recurrence of INS post-kidney transplantation (frequently occurring within hours).[143] For children with FSGS undergoing kidney transplantation, the risk of disease recurrence in a first graft is 14–50%.[192] Interestingly, the incidence of recurrence after transplantation is reduced in patients with SRNS due to mongenic disorders, and initial Gc-sensitivity at the onset of NS is highly predictive of post-transplant disease. These data clearly support a role for a circulating factor in the pathogenesis of SSNS, but not in forms of NS with a genetic basis.[193]

The idea of INS as a systemic disease was further strengthened by the report of a patient with MCD who died following an intracranial haemorrhage.[194] Although he was suffering from active MCD at the time of death, each of his kidneys were transplanted into different individuals. Proteinuria initially persisted in the transplant recipients, but subsequently resolved in both patients. Post-transplantation biopsies revealed a normal podocyte FP architecture. It appears transferring a kidney from an ‘INS environment’ to a ‘non-INS environment’ leads to reversal of the signature podocyte cytoskeletal disturbances usually associated with MCD.

Alternative evidence in support of a circulating factor include the observation that plasmapheresis (extracorporeal filtration of plasma) can reduce proteinuria in FSGS,[195] and reports of transient proteinuria transmission from a mother to her babies; possibly through a permeability factor crossing the placenta.[196] Zimmerman *et al.*, demonstrated that transferring serum from a patient with recurrent INS into a rat produced proteinuria in the recipient.[197] Savin *et al.*, produced similar data with an assay involving isolated rat glomeruli incubated with serum from 100 patients with FSGS. The group found that the serum from patients with recurrent FSGS after renal

transplantation had a higher mean value for permeability to albumin than normal subjects, or those FSGS patients who did not suffer disease recurrence.[198]

1.5.1.1 Permeability factors in MCD and FSGS

Although a circulating factor(s) does seem to have some role in the development of INS, a definitive understanding of the factor(s) identity and the pathological mechanisms involved has proved elusive. Savin *et al.*, partially characterised the permeability factor found in the study described in the previous paragraph: using ammonium sulphate precipitation, only the serum precipitate obtained at 70-80% saturation was active, and the estimated molecular mass of the protein was approximately 50kDa.[198]

A study on SSNS in human MCD and the puromycin aminonucleoside nephrosis (PAN) rat model found that expression of angiopoietin-like-4 (Angptl4), a glycoprotein, is Gc-sensitive, and highly upregulated in serum and in podocytes during the disease process.[199] The group also found that podocyte-specific transgenic overexpression of Angptl4 (using a *NPHS2-Angptl4* construct) in rats induced nephrotic-range proteinuria, loss of charge across the GBM, and FP effacement, while transgenic overexpression specifically in adipose tissue resulted in increased circulating Angptl4, but no proteinuria. This could be explained by the observation that Angptl4 secreted from podocytes lack normal sialylation. Indeed, it was found that feeding the sialic acid precursor *N*-acetyl-D-mannosamine (ManNAc) to *NPHS2-Angptl4* transgenic rats increased sialyation of Angptl4 and decreased albuminuria by more than 40%.

Another candidate for a permeability factor in MCD is hemopexin (Hx). Hx is a heme-scavenging protein with serine protease activity when activated. Hx has enhanced protease activity (although lower absolute concentration) in MCD patients in relapse compared with patients with MCD in remission, patients with FSGS and healthy controls.[200] It increases the permeability of a monolayer of endothelial cells to albumin and induces nephrin-dependent reorganisation of the podocyte actin cytoskeleton *in vitro*.[201] Interestingly, this Hx-induced actin reorganisation was partially blocked when cells were preincubated with culture medium containing 10% normal human plasma, raising the possibility that the systemic component of INS arises from the loss of a protective factor(s), rather than an accumulation of a harmful factor(s).

In (typically steroid resistant) FSGS, a role for the podocyte urokinase receptor (uPAR; encoded by *PLAUR*) has been demonstrated by Wei *et al*.[202] uPAR is a glycosylphosphatidylinisotol (GPI)-anchored three-domain protein, which can be released from the plasma membrane as a soluble marker (suPAR) by cleavage of the GPI anchor. suPAR ranges in size from 20-50kDa depending on the degree of glycosylation and proteolytic cleavage, thus approximating the size of the partially-characterised serum factor identified by Savin *et al*.[198] It was found that suPAR serum concentrations were raised in 45/63 (71.4%) subjects with FSGS, but only 4/11 (36.4%) of subjects with membranous nephropathy, 1/7 subjects with preeclampsia (14.3%), and 0/25 (0.0%) subjects with SSNS/MCD. The authors also reported that a higher serum concentration of suPAR in pre-transplant FSGS patients who subsequently went on to develop recurrent disease. Mechanistically, it was demonstrated that suPAR binds to and activates podocyte β_3 integrin, and in human graft tissue obtained 2 hours post-reperfusion, β_3 integrin activity was increased in patients with recurrent FSGS, but not patients with nonrecurrent FSGS (using the activation epitope-recognizing antibody for β_3 integrin AP5). This study identified suPAR as a circulating factor that may cause FSGS; therefore, removal of this protein from patients with high serum levels may have therapeutic benefit.

However, since publication of the data by Wei *et al*. in 2011,[202] several concerns have been raised regarding the identification of suPAR as the soluble proteinuric factor that causes FSGS. Initial criticism focussed on the specificity of suPAR as a biomarker for FSGS, as it was already known that suPAR is massively elevated in patients suffering from a range of primarily non-renal diseases including lung cancer, sepsis and systemic lupus erythematosus.[203-205] Subsequently it was noted that in the western blotting of Wei et al.,[202] the molecular weight of the predominant suPAR fragment in FSGS serum was 21 kDa: proteins of this size pass through the GFB into the urine.[206] Wei *et al*, had not adjusted for estimated glomerular filtration rate (eGFR) in their study, leading to the possibility that the raised suPAR levels may simply be a marker for poorer renal filtration in the FSGS patient cohort. Indeed, numerous studies subsequently confirmed an inverse relationship between serum levels of suPAR and eGFR in a variety of renal diseases.[207-209] One study examining Japanese adult patients did find serum suPAR levels were significantly higher in patients with FSGS than healthy controls, but no significant difference was found between patients with FSGS and other renal diseases (MCD, membranous nephropathy, and immunoglobulin

A nephropathy).[208] Additionally, no significant difference was observed in serum suPAR levels in patients with nephrotic-range proteinuria and non-nephrotic range proteinuria (of any aetiology).

Of direct relevance to the paediatric INS population was the study by Sinha *et al.*, in which serum suPAR levels were prospectively measured in healthy controls and children with various forms of NS.[209] Serum suPAR levels in INS were similar to controls and did not distinguish between the various aetiologies of INS. Similar proportions of patients in each group had suPAR levels over 3000 pg/mL (the cut-off suPAR level used by Wei *et al.* to identify patients with FSGS). Mean levels of suPAR were 3021 pg/mL in healthy controls (n=83), 3316 pg/mL in steroid resistant FSGS (n=99), 3253 pg/mL in biopsy-proven MCD (n=117) and 3150 pg/mL in SSNS (n=138; no biopsy performed). There were no changes in serum suPAR levels following therapy or remission. Additionally, no correlation was found between urinary and serum suPAR levels, but urinary suPAR levels were inversely correlated with age, weight, height and directly correlated to the degree to proteinuria. Although the possibility remains that different forms of suPAR may differentially contribute to the development of proteinuria, no data are yet available to substantiate this, and the discrepancies between various studies is difficult to explain, especially as all the results were obtained with the same commercially available suPAR ELISA kit.[210]

1.5.2 Possible immunological basis for INS

In 1974 Shalhoub proposed that the source of the causative circulating factor in INS is an abnormal clone of T cells.[211] There are multiple lines of evidence in support of an immunological basis for INS: measles infection often result in remission of INS, possibly through T-cell immunosuppression;[212] INS onset and recurrence can coincide with viral infection;[213] MCD is associated with Hodgkin lymphoma (HL);[214] and the therapeutic benefit of medications known to exert immunosuppressive effects such as Gc and cyclophosphamide in INS.[5] Also, T-cell culture supernatants from patients with MCD produced significant proteinuria and a change in charge of the GBM when infused into rats, and these differences were not produced by healthy donors.[215]

Some groups have attempted to refine the source of a potential immunological circulating permeability factor further. The association of INS with atopy led to the proposal that INS had a predominantly T helper 2 (Th2)-mediated aetiology.[216]

Although the cardinal Th2 cytokine interleukin-4 does not induce INS, a rat model of MCD with similar histological findings has been produced through over-expression of the Th2-cytokine interleukin-13.[217]

Further support for an immune-cell source of a circulating factor came from immunodeficient mice reconstituted with cells from patients with SSNS or FSGS.[218] Mice reconstituted with human cells expressing the marker of myeloid and lymphoid progenitors CD34 developed proteinuria and characteristic podocyte morphological changes. When CD34+ cells were excluded from the population of injected cells, these changes did not arise, suggesting a potential role for immature differentiating cells in the pathogenesis of INS.

Sahali *et al.*, hypothesised a role for the transcription factor nuclear factor kappa-light-chain-enhancer of activated B cells (NF-κB) in MCD because of its central role in the regulation of cytokine expression.[219] Using an electrophoretic mobility shift assay, they showed nuclear extracts from peripheral blood mononuclear cells from adults and children with MCD displayed higher levels of NF-κB-DNA binding during relapse than remission. The authors postulated that abnormalities of the NF-κB pathway may contribute to the pathophysiological process of MCD.

1.5.2.1 Links between immune dysregulation and podocyte cytoskeletal changes

T-cells of patients with MCD express higher levels of c-maf inducing protein (c-mip) in relapse compared with remission.[220] It was subsequently found that c-mip is found in the podocytes of adult patients with MCD but not in control specimens (obtained from patients undergoing renal biopsy due to a polar kidney tumour). Mice overexpressing c-mip in podocytes developed proteinuria. c-mip was found to block interaction of nephrin with Fyn, thereby decreasing phosphorylation of nephrin *in vitro* and *in vivo*. Additionally, c-mip inhibited interactions between Fyn and N-WASP, and between Nck and nephrin, potentially explaining the cytoskeletal dysregulation characteristic of INS. Finally, injection of small interfering RNA targeting c-mip prevented lipopolysaccharide-induced proteinuria in mice. These data suggest c-mip may be a key component in the molecular pathogenesis of INS. The authors postulate that as c-mip is found in low abundance under physiological conditions but induced in T-cells and podocytes in patholphysiological situations, it may form a possible bridge between immune alterations and podocyte dysfunction.

Another possible mechanism whereby dysregulated immune signalling leads to proteinuria is through persistent overexpression of CD80 (B7-1). CD80 is a T-cell costimulatory molecule expressed on antigen-presenting dendritic cells, natural killer cells, and activated B lymphocytes. Binding of CD80 to the T-cell receptor CD28 has a key role in T-cell activation, as well as termination of the T-cell response [the latter partly through binding of CD80 by cytotoxic T-lymphocyte-associated (CTLA)-4 on the membrane of FOXp3+ regulatory T-cells (Tregs)]. [221] Resier and Mundel were the first to propose that glomerular CD80 expression may have a role in MCD,[222] based on observations that proteinuria-inducing lipopolysaccharide (LPS) signalling through toll-like receptor-4 (TLR-4) reorganised the podocyte actin cytoskeleton *in vitro*, and LPS upregulated CD80 expression on podocytes in wild-type mice, causing heavy proteinuria.[223] Furthermore, mice lacking CD80 were protected from LPS-induced proteinuria, while SCID (severe combined immunodeficiency) mice were still susceptible to LPS-induced proteinuria. These data suggest direct activation of podocytes, independent of T-cell involvement, can induce CD80 expression, podocyte cytoskeletal changes and proteinuria.

More recently, the potential therapeutic role of a CD80 inhibitor called cytotoxic T-lymphocyte–associated antigen 4–immunoglobulin fusion protein (CTLA-4–Ig)/Abatacept has been investigated. Abatacept blocked LPS- or CD80 (stable transfection)- induced podocyte hypermotility *in vitro* and in five patients (4 with rituximab-resistant recurrent FSGS after transplantation and 1 patient with Gc-resistant FSGS) aged 7-28 years, with positive podocyte staining for CD80 on biopsy specimens, abatacept induced partial or complete remission of proteinuria (no controls were included in the study).[224] A larger-scale, adequately controlled, successful study would be required before abatacept could potentially be considered for use in a sub-group of INS patients with podocyte CD80 expression [225]

The identification of circulating permeability factors can be of immediate clinical benefit. This has been shown by Delville *et al.*, who constructed a panel of seven antibodies (*CD40, PTPRO, CGB5, FAS, P2RY11, SNRPB2,* and *APOL2*) by comparing sera from FSGS patients experiencing post-transplant relapse, from those not experiencing post-transplant disease relapse. This panel was shown to predict post-transplant FSGS recurrence with 92% accuracy, with the single most powerful predictor being pre-transplant elevation of CD40 (78% accuracy).[226]

1.5.3 Protease dysregulation leading to a hypermotile podocyte phenotype

As described previously, CatL is a member of the cathepsin family of cysteine proteases.[129] Building on the observation that CatL inhibitors reduced proteinuria in a rat model of glomerulonephritis,[227] Reiser *et al.*, subsequently demonstrated that PAN treatment upregulates CatL expression in podocytes *in vivo*, and primary podocytes from mice lacking CatL are protected from PAN-induced cell detachment *ex vivo*. [131] PAN-induced podocyte migration was also slowed in CatL-deficient podocytes. CatL expression is also increased in podocytes in human renal disease (membranous nepropathy, FSGS, and diabetic nephropathy) and murine LPS-induced nephropathy.[228] Two podocyte targets of CatL-mediated proteolysis are synaptopodin and dynamin.

Synaptopodin is highly expressed in podocytes and is a key regulator of cytoskeletal dynamics. Mechanistically, synaptopodin induces stress fibre formation by blocking the ubiquitin-mediated targeting of RhoA for proteasomal degradation.[68] Synaptopodin also blocks pro-migratory filopodial cell protrusions by disrupting cell division control protein 42 homolog (Cdc42) - insulin receptor tyrosine kinase substrate of 53 kDa (IRSp53)-Mena complexes.[229] Synaptopodin is therefore an antagonistic regulator of RhoA and Cdc42 signalling that blocks the reorganisation of the podocyte into a migratory phenotype.[129] Faul *et al.*, demonstrated that the antiproteinuric effect was mediated through preventing the CatL-induced proteolysis of synaptopodin.[103]

The GTPase dynamin also has a key role in maintaining normal glomerular function. In human FSGS (but not MCD) and murine LPS-induced nephropathy, induction of CatL in podocytes leads to cleavage of dynamin, associated with cytoskeletal dysregulation and proteinuria.[228] When dynamin mutants that lack the CatL cleavage site are delivered into mice, these mutants were resistant to LPS-induced proteinuria.

Together, these data suggest CatL-mediated proteolysis may have a role in the development of proteinuria in INS.[129]

1.6 Glucocorticoids

Glucocorticoids are a class of steroid hormone synthesised in the adrenal cortex under control of the hypothalamic-pituitary-adrenal (HPA) axis. Glucocorticoids regulate a vast array of biological processes including carbohydrate-, protein-, and lipid-metabolism, maintenance of vascular tone, apoptosis, lung development, regulation of the inflammatory and immune response, and exert effects on the central nervous system affecting cognition, arousal, and mood. [230] The human adrenal gland synthesises and secretes two main glucocorticoids: cortisol and corticosterone, but the latter is synthesised at a rate of approximately $1/10^{th}$ that of cortisol.[231] Synthetic glucocorticoids such as prednisolone, prednisone and dexamethasone are amongst the most prescribed medicines in clinical use today, producing beneficial responses in diseases as diverse as lymphoma, asthma, and rheumatoid arthritis, as well as NS.[232]

Cortisol is the major physiological ligand in humans for the glucocorticoid receptor (GR), which is a member of the nuclear receptor super-family (NRSF). The steroid receptor subgroup of the NRSF includes the androgen receptor, estrogen receptors (ERα, ERβ), the progesterone receptor, the 1,25-dihydroxyvitamin D3 receptor, GR, and the mineralocorticoid receptor (MR).[233] The importance of GR is underscored by the observation that global knock-out of GR in mice by inserting a neomycin phosphotransferase gene cassette into exon 2 of the mouse GR gene, leads to death within a few hours of birth due to respiratory failure. This effect was partially dependent on the genetic background of the mice: 7.1% of mutant mice born with a C57BL/6 background were alive 4 hours after birth, compared to no mice born with a 129/J background.[234] Further studies suggested this discrepancy in mortality may be due in part to production of a Gc-binding GR fragment.[235]

1.6.1 Gc bioavailability *in vivo*

Ligand-free GR is located mostly in the cytoplasm of human cells; after binding to Gc-ligand, GR dimerizes and translocates to the nucleus to regulate transcription.[236] Regulation of bioavailability of Gc-ligand is controlled both at the systemic and tissue level. The majority of Gc circulating in blood is bound to plasma proteins, which controls Gc systemic distribution, the fraction of total Gc available for GR-binding, and the rate of release of Gc to surrounding tissues during periods of inflammation.[237] Another pre-receptor regulatory mechanism involves 11 beta-hydroxysteroid

dehydrogenase (11β-HSD), which metabolises Gc and contributes to whether GR- or MR- effects predominate, in a tissue-specific manner.

1.6.1.1 Gc binding to plasma proteins

In human subjects, cortisol is the most abundant circulating Gc. 90-95% of total serum cortisol circulates bound to proteins. Corticosteroid-binding globulin (CBG, also known as transcortin) binds >80% of serum cortisol, and albumin binds 10-15%.[236] It is generally assumed that carrier proteins are required for cortisol to circulate in blood because cortisol is hydrophobic. However, Moisan has challenged this assumption with 3 pieces of evidence: i) in CBG-deficient patients, cortisol circulates normally; ii) CBG is not present in many species, such as teleost fish, in which cortisol circulates; and iii) circulating aldosterone is equally hydrophobic and does not have a specific binding protein.[238] CBG deficiency in mice results in markedly reduced total circulating corticosterone at rest and in response to stress.[239] Also, free corticosterone concentrations are normal at rest but reduced after stress in CBG-deficient mice. This suggests that CBG functions as a reservoir of Gc for times of physiological stress. Bound and unbound forms of cortisol in serum are in a dynamic equilibrium, which can be affected by several factors including temperature and pH.[240] Additionally, the local release of cortisol during inflammation involves cleavage of CBG by neutrophil elastase.[241]

The prevailing view is that the biological activity of Gc is defined by the levels of circulating unbound hormone rather than the bound fraction because only free cortisol is able to cross the capillary boundary, enter tissues and passively diffuse into cells ('free-hormone' hypothesis).[236] This is supported by data showing that the rate of dissociation of cortisol from binding proteins defines and is always higher than tissue uptake rate,[242] and intracellular cortisol concentrations in rat liver are proportional to circulating free cortisol levels.[243] No evidence currently exists for the internalisation of bound cortisol or CBG.[236]

Of relevance to the current project is that circulating proteins the size of albumin (66 kDa) and CBG (52 kDa) are excreted into the urine during periods of impaired GFB function in INS. Prednisolone (the standard Gc used clinically in the UK for INS) binds to CBG, but most other synthetic glucocorticoids bind with very low affinity. For example, in a study analysing the ability of synthetic compounds to displace labelled cortisol from CBG absorbed onto a solid phase matrix, the relative binding activities

(RBA-relative to cortisol) and association constants (K, 10^6 M^{-1}) were found to be as follows: cortisol RBA=1, K=76; prednisolone RBA=0.59, K=41, dexamethasone RBA=<0.001, K=<0.1.[244] The authors also used a computer model to predict the *in vivo* effect of administration of synthetic Gc on circulating cortisol levels, and found the presence of maximal therapeutic levels of prednisolone decreased the concentration of cortisol bound to CBG by 32%. However, the displacement of cortisol from CBG by administration of exogenous prednisolone is unlikely to be of any clinical relevance as total plasma cortisol concentrations are decreased to undetectable levels within 4 hours of administration of exogenous Gc due to suppression of the hypothalamic-pituitary-adrenal (HPA) axis.[245]

Frey *et al.*, showed that total prednisolone serum concentrations in a group of adults with INS were lower than in healthy volunteers, with a higher unbound fraction of prednisolone.[246] The authors postulated that this was due to the lower concentrations of CBG and albumin observed in the INS group. Prednisone is the inactive pre-cursor of prednisolone, which is converted to prednisolone by first-pass hepatic metabolism by 11β-HSD 1 [247, 248]. A study involving thirteen children treated with the Gc prednisone during a relapse of INS found that the elimination of prednisolone was increased when serum albumin was decreased.[245] No statistically significant difference was found for prednisolone pharmacokinetic properties between children with SSNS, SRNS and SDNS.

Another study examined the pharmacokinetics of intravenous prednisolone and oral prednisone administration in six children with INS during active disease and in remission.[249] Results were compared to existing values previously obtained from asthmatic children who had received similar intravenous doses. The results showed that the area under the curve for prednisolone (the area under the curve is a value proportional to the total amount of drug that reached the circulation) was higher after oral doses of prednisone when compared to the intravenous prednisolone doses, indicating that INS relapse does not produce impaired absorption and conversion of prednisone to prednisolone. A larger steady-state volume of distribution was observed in active disease than in remission, suggesting greater availability of the steroid to tissues. Additionally, apparent prednisolone clearance in both stages of nephrotic syndrome were greater than those obtained in asthmatic children, possibly due to decreased protein binding of prednisolone in INS.

1.6.1.2 Metabolism of Gc by 11β-HSD

Gc bioavailability at the tissue level is also affected by the interconversion of biologically active cortisol and inactive cortisone by 11β-HSD, which has two subtypes.[236] 11β-HSD 1 is a predominant reductase enzyme under most conditions, generally amplifying Gc-action by converting cortisone to cortisol, and transgenic overexpression of 11β-HSD 1 in either adipose tissue or the liver in mice causes components of the metabolic syndrome (type 2 diabetes mellitus, hypertension and dyslipidaemia.), which typically occurs in people with primary Gc-excess.[250] Cortisol, and the synthetic glucocorticoids prednisolone and prednisone are substrates for 11β-HSD 1, while no reductase activity was observed with dexamethasone as the substrate.[251] 11β-HSD1 is widely distributed in adult mammals, with highest expression found in the liver.[252] Other tissues with 11β-HSD1 expression include ovary, testis, brain, uterus, skeletal muscle and kidney (distribution is mostly in the proximal tubules and medulla; glomerular expression has not specifically been investigated).[253, 254]

As will be discussed in section 1.6.1.3 Gc ligands can also activate MR in a similar manner to the classical MR-ligand aldosterone. 11β-HSD 2 converts cortisol to inactive cortisone. The tissue-specific expression of 11β-HSD2 is an important pre-receptor regulatory mechanism 'protecting' MR from cortisol-activation, ensuring aldosterone is the predominant MR-activating ligand.[254] Data supporting the view of 11β-HSD2 as a determinant of MR-receptor occupancy includes a study demonstrating co-localisation of 11β-HSD2 and MR in the same cells in the distal convoluted tubule, Henle's loop and collecting ducts of the kidney, and the absorptive epithelia of the gastrointestinal tract.[255] Additionally, mutations of the 11β-HSD 2 gene in humans are a rare monogenic cause of hypertension due to 'apparent mineralocorticoid excess,' whereby overstimulation of the MR by cortisol in sodium-transporting epithelia such as the tubular system of the kidney leads to sodium retention, hypokalaemia, low plasma renin and aldosterone concentrations, and hypertension.[256] 11β-HSD2 expression is largely restricted to classical aldosterone/MR-target tissues such as the distal nephron of the kidney, sweat and salivary glands and colonic epithelium.[254] 11β-HSD2 expression has also been found in the glomerulus.[254] Interestingly, while 11β-HSD2 shows exclusive oxidative activity (converting cortisol to cortisone) with endogenous glucocorticoids, it reduces 9-fluorinated glucocorticoids (such as dexamethasone),

regenerating 11-dehydrodexamethasone to dexamethasone, thus *potentiating* dexamethasone action (no reduction data are provided for prednisolone). [254, 257]

1.6.1.3 Glucocorticoid ligand potency at the GR and MR

As described above, regulatory mechanisms exist to control the access of physiological and synthetic Gc-ligands to the GR in a tissue-specific manner. In addition to their ability to bind GR, glucocorticoids also bind the MR to varying degrees; this is most likely due to the close structural relationship between GR and MR. The physiological human ligands for GR and MR are cortisol and aldosterone respectively. In a similar manner to GR, MR is located mostly in the cytoplasm of the cell in the ligand-free state; subsequent ligand-binding activates MR, causing dissociation from chaperone molecules and the translocation of MR to the cell nucleus where it directs the transcription of target genes.[258]

GR is expressed almost ubiquitously (with the notable exception of the suprachiasmatic nucleus of the hypothalamus which has a key role in regulating circadian rhythm[259]), whereas MR shows a much more restricted tissue distribution, with high-expression confined to the sodium-transporting epithelia of the distal colon and distal nephron, the salivary glands, in certain regions of the central nervous system (eg, hippocampus), and at lower abundance in a variety of other tissues.[254, 260] All subsets of human glomerular cells express GR,[104] while several studies have demonstrated that MR is not present in the human,[255, 261] and rabbit glomerulus.[261]

In vitro, MR has a high and very similar affinity for cortisol and aldosterone, whereas synthetic glucocorticoids such as dexamethasone only activate MR at high concentrations. In contrast, GR has low affinity for physiological glucocorticoids and aldosterone, but a higher affinity for synthetic glucocorticoids. Therefore, under basal conditions, the GR is occupied to only a small extent by ligand, but becomes progressively activated as Gc levels rise during ultradian pulses, a stress response or pharmacotherapy.[254] The relative ligand binding affinities also highlight the need for the pre-receptor gating mechanisms discussed previously: plasma cortisol concentrations are 100- to 1000-fold higher than that of aldosterone and without the regulation provided by the 11β-HSD system, most of MR would be bound by Gc, severely reducing the ability of aldosterone to exert physiological responses.[258] In addition, Lombes *et al.*, demonstrated that the off-rate of aldosterone from human MR

was five times lower than that of cortisol, suggesting an intrinsic discriminatory property of MR.[262]

Grossmann *et al.*, compared the mineralocorticoid- and glucocorticoid- properties of different steroids in a luciferase transactivation assay in CV-1 cells (African green monkey kidney cells) transfected with either human MR or human GR vectors.[263] Drug responses were quantified by a variety of parameters including EC_{50} (the half maximal effective concentration of a drug which induces a response halfway between the baseline and maximum after a specified exposure time) and relative potencies [for GR, relative to cortisol (GCP); for MR, relative to aldosterone (MCP)]. The results for GR were as follows: Cortisol (EC_{50} $1.2x10^{-8}$ M, GCP=1.0), aldosterone (EC_{50} $1.7x10^{-7}$ M, GCP=0.07), dexamethasone (EC_{50} $5.6x10^{-10}$ M, GCP=21), prednisolone (EC_{50} $6.9x10^{-9}$ M, GCP=1.7). The results for MR were as follows: Aldosterone (EC_{50} $4.8x10^{-11}$ M, MCP=1.0), cortisol (EC_{50} $9.0x10^{-10}$ M, MCP=0.054), dexamethasone (EC_{50} $5.09x10^{-9}$ M, MCP=0.0094), prednisolone (EC_{50} $3.78x10^{-9}$, MCP=0.013). Therefore, at GR the synthetic glucocorticoids dexamethasone and prednisolone have a higher potency than either cortisol or aldosterone, while at MR, dexamethasone and prednisolone have a very low potency.

1.6.2 GR structure

1.6.2.1 GR gene structure

Human GR is encoded by the *NR3C1* (nuclear receptor subfamily 3, group C, member 1) gene on chromosome 5q31-32 and contains ten exons.[264] The protein-coding region is formed by exons 2-9, whereas exon 1 represents the 5'-untranslated region. Exon 1 contains three transcription-initiation sites, each of which produces an alternative first exon that is fused to a common exon 2 after splicing. This array of binding sites on *NR3C1* promoters could account for the observation that *NR3C1* is constitutively expressed under a variety of physiological conditions. Exon 2 contains the coding sequence for the transactivation domain 1 (AF1), exon 3 and exon 4 each contain the sequence for a zinc finger motif, and constitute the DNA binding domain (DBD); and the region encompassing exons 5-9 encodes for the transactivation domain 2 (AF2), the ligand binding domain (LBD), and the 3'-untranslated region.[230]

Alternative splicing of exon 9α and exon 9β on the pro-mRNA transcript produces two distinct mRNAs: GRα and GRβ. The two isoforms are identical up to amino acid 727,

but diverge beyond this position. The classical GR (GRα) consists of 777 amino acids. In GRβ the 50 carboxy terminal amino acids of GRα have been replaced by 15 non-homologous amino acids encoded by exon 9β resulting in a protein of 742 amino acids.[230]

GRα is expressed in almost all human tissues, while GRβ is expressed in a variety of human tissues, but usually at a lower concentration that GRα.[230] Pujols *et al.*, investigated the expression levels of both these isoforms in human tissue and cells and found GRα mRNA abundance (x10^6 cDNA copies/µg total RNA) as follows: brain (3.83) > skeletal muscle > macrophages > lung > kidney > liver > heart > eosinophils > peripheral blood mononuclear cells (PBMCs) > nasal mucosa > neutrophils > colon (0.33). GRβ mRNA levels were much lower than GRα levels, with the following abundances (x10^3 cDNA copies/µg total RNA): eosinophils (1.55) > PBMCs > liver ≥ skeletal muscle > kidney > macrophages > lung > neutrophils > brain ≥ nasal mucosa > heart (0.15). GRβ mRNA was not found in colon. GRα protein was detected in all cells and tissues, while GRβ was not detected in any specimen.[265]

In contrast to GRα, GRβ does not appear to bind Gc and is transcriptionally inactive. In cell culture, overexpressed GRβ acts as a dominant negative inhibitor on GRα-mediated transcription and may contribute to tissue-specific sensitivity to Gc.[266]

An additional GR splice variant, GRγ, has been detected in childhood acute lymphoblastic leukaemia. The functional relevance of GRγ is unknown but GRγ expression was observed to be lower in leukaemic blast cells from patients with a good response to Gc therapy, compared to patients who had a poor response to Gc therapy.[267]

1.6.2.2 GR protein structure

GRα mRNA is translated from at least eight alternative initiation sites into multiple GRα isoforms termed GRα-A to D (A, B, C1, C2, C3, D1, D2, and D3). GRα-A has a molecular weight of 94kDa, while GRα-B has a molecular weight of 91 kDa.[230, 268] Additionally, some data suggests that multiple isoforms may exist for GRβ.[230]

Lu *et al.*, found that levels of various GRα isoforms differ among tissues, and they investigated whether the relative amounts of the different GR isoforms could alter tissue Gc-sensitivity. [268]They co-transfected COS-1 cells with a constant amount of the GRα-A isoform and an increasing amount of the GRα-C3 or GRα-D3 isoform and

measured glucocorticoid responsiveness in a luciferase assay. Increasing the amount of the GRα-C isoform enhanced GRα-A transcriptional activity whereas increasing the amount of the GRα-D3 isoform did not. These data suggest that the ratios of various GRα in a tissue may alter the Gc-sensitivity. The group also examined whether each GRα isoform could regulate a different set of genes within the same cell. Comparing the transcriptional output of U-2 OS cells treated with either vehicle or Gc using a cDNA microarray revealed that 189 genes were regulated commonly by all GRα isoforms. However, the total number of genes regulated by individual isoforms varies: 1318, 1054, 664, 1077, or 626 for the GRα-A, -B, -C3, or -D3 isoforms, respectively, indicating that each GRα isoform also regulated a unique set of genes.

Although different GRα isoforms vary at their N-terminal domain, their overall general structures are similar to each other, and to other steroid receptors. GR is a modular protein organised into 3 major functional domains: the N-terminal domain (NTD), the central DNA-binding domain (DBD), and the C-terminal ligand-binding domain (LBD).[230] The NTD varies in both size and amino-acid sequence between GR isoforms, and contains the transactivation domain AF-1 capable of activating target genes in a ligand-dependent manner,[269] and also contains the sites of GR-phosphorylation.[270]

The DBD is highly conserved between GR isoforms and contains two zinc finger motifs which interact with DNA, as well as a dimerization and nuclear localisation domain (NLS1).[271] The C-terminal LBD is responsible for the recognition and binding of Gc.[230] A weaker activation function (AF-2) and a second nuclear localisation signal (NLS2) are also embedded within this region. The C-terminus also contains sequences important for interaction with heat shock proteins (hsps), nuclear transcription factors, nuclear translocation and receptor dimerisation.[272, 273]

1.6.3 Mode of action of GR

1.6.3.1 Genomic actions

In the absence of ligand, GR resides predominantly in the cytoplasm of cells in a large multi-protein complex consisting of several proteins including hsp90, hsp70, immunophilins, tyrosine protein kinase Src (c-Src), and p23.[274] The interaction of GR with two hsp90 molecules keeps the ligand-binding pocket of the receptor in a high affinity conformation. Upon ligand binding, GR undergoes conformational changes,[230] leading to its dissociation from the cytoplasmic chaperones, exposing the two nuclear localisation signals, and GR is rapidly translocated into the nucleus through nuclear pores.[275] GR can both positively and negatively regulate gene expression through three main mechanisms (direct, tethering and composite) which will be discussed in turn.

In the 'direct' mechanism of GR-mediated regulation of gene expression, the activated receptor binds as a homodimer to target DNA sequences called glucocorticoid response elements (GREs). The consensus GRE sequence is the palindromic 15 base pair motif AGAACAAnnnTGTTCT (where n is any nucleotide).[237] Binding of GR to a GRE promotes the recruitment of co-activators to the GR-DNA complex, such as cyclic AMP response element binding binding protein (CBP), p300, p-300-CBP.[276] These co-activators contain histone acetylase (HAT) activity, which results in nucleosomal rearrangement and DNA unwinding which allows the basal transcription machinery to access the promoter. Gc-mediated synthesis of several anti-inflammatory proteins including glucocorticoid-induced leucine zipper protein (GILZ), IL-1 receptor antagonist, IL-10, and lipocortin-1 are thought to be mediated via direct binding of GR to GREs.[276-278]

GR can also repress genes by binding directly to a negative GRE (nGRE), which are more variable in sequence than positive GREs. One example of this mechanism is GR binding to the ostocalcin nGRE, which prevents binding of the transcription factor, TATA box binding protein (TBP) whose binding site overlaps with the nGRE.[279]

The second mechanism of GR-mediated regulation of gene expression is independent of DNA-binding and involves direct protein-protein interaction between GR and other transcription factors ('tethering' or 'transrepression'). Many of the transcription factors bound by GR in this manner normally upregulate a variety of pro-inflammatory

proteins, and this direct tethering by GR is thought to be a major mechanism whereby GR exerts its potent anti-inflammatory effects.[276] Pro-inflammatory transcription factors shown to physically interact with GR, leading to a reduction in expression of target genes, includes nuclear factor-κβ (NF-κβ) and activator protein-1 (AP-1).[278] Tethering of GR to AP-1 or NF-κβ alters the assembly of coactivator complexes that are required for gene activation, eg, at the *Il8* promoter.[280] Interestingly, the repressive effect of GR on NF-κβ seems to be mutual, since NF-κβ has also been shown to negatively regulate GR-mediated transcription.[281] Interaction of GR with some transcription factors [eg, signal transduction and activator of transcription (STAT)], without GR-DNA binding, can also enhance the transcription of target genes.[282]

A central characteristic of tethering is that GR-DNA binding is not required for GR to exert is effects on gene transcription. However, in the 'composite' mechanism of GR-mediated regulation of gene expression, GR binds directly to a GRE before physically interacting with AP-1 or NF-κβ bound on a neighbouring site on the DNA. Recruitment of the GR corepressor glucocorticoid receptor-interacting protein 1 (GRIP1) plays a central role in this mechanism.[283]

Genome-wide data examining the characteristics of GR-upregulated compared to GR-repressed genes was provided by Uhlenhaut *et al*. who identified 918 GR-bound regulatory elements linked to positive gene expression and 729 elements that served repressed gene expression in LPS-treated macrophages.[284] Surprisingly, they found that a majority of both negative and positive GR enhancers are composed of canonical GREs in combination with NF-κβ and AP-1 sites. Additionally, while up to 20% of GR-dependent gene repression is found at nGREs and tethered sites, approximately 20% of GR-induced genes also harbour these same motifs. It therefore appears that cistromic motif classification is insufficient to predict whether a particular GR-binding event will lead to gene upregulation or downregulation. The group also found that GR recruits GRIP1 in a comparable fashion to both up- and down-regulated genes, where it may act as a coactivator or corepressor, as determined by the presence of interferon regulatory factor 3/IRF3 (in the case of repressive enhancers) and other, currently unknown, factors.

The development of chromatin immunoprecipitation combined with next-generation sequencing (ChIP-seq) has allowed the characterisation of GR-binding patterns on a genome-wide scale. A surprising finding from these studies is that the majority of GR

binding sequences (GBSs) are located outside of the promoter of Gc-responsive genes in intergenic or intragenic regions, often far removed from the transcription start site.[237] For example, John *et al.*, found that 93% of GBSs were 2.5 kb distal to the nearest transcriptional start site, and there was no clear relationship between GR occupancy patterns and transcriptional activation of nearby genes.[285] Explanations for this include that GR acts through long-range mechanisms (the 'chromosome folding' mechanism) or many GR-binding events are opportunistic and do not lead to changes in transcriptional activity.

Another surprising finding is that different cell types display a low degree of overlap in GBSs. The data provided by John *et al.*, highlighted the importance of cell-specific chromatin accessibility as a determinant of GR-binding. By comparing GBSs in mammary (3134) and pituitary (AtT-20) cell lines, they found that the majority of GR binding events occurred in areas of accessible chromatin (as determined by DNAse 1 sensitivity) before Gc-exposure (71% and 95% for 3134 and AtT-20 cells respectively).[285] However, only 11% of GBSs were shared between the two cell lines.

Recent data has also highlighted the highly dynamic interaction between GR and DNA. A study involving GR labelled with a green fluorescent protein revealed GR-DNA interactions on a time-scale of seconds; a mechanism described as 'hit and run.'[286] Voss e*t al.*, also investigated the GR steady-state occupancy at a given GBS.[287, 288] The group used a cell line containing a tandem array of gene copies harbouring GREs. In the cells, they co-expressed fluorescently tagged GR and a mutated form of the estrogen receptor (ER). They then monitored the association of these receptors to the array by fluorescence microscopy, in the presence of dexamethasone alone (which activates GR), estradiol alone (which activates ER), or both ligands together. It was found that steady-state levels of DNA-bound GR are virtually unchanged in cells treated with dexamethasone alone compared to both ligands together, suggesting the receptors are not competing for binding to the GREs. Even more surprisingly, the ER-DNA associations were even enhanced in cells exposed to both agonists; a phenomenon the authors refer to as 'assisted loading.' The authors conclude that GREs are largely unsaturated during hormone-induced transcriptional activation, and they also confirm the previous observations that GR-DNA interactions are in the timescale of seconds.

1.6.3.2 Non-genomic actions

Although the principal effects of glucocorticoids are mediated by changes in transcriptional response that occur in minutes to hours, accumulating evidence suggests GR can also act through rapid mechanisms (taking seconds to minutes), which do not require changes in gene transcription.[289] These non-genomic effects of glucocorticoids can be mediated by proteins that dissociate from the cytoplasmic GR-chaperone complex following ligand binding. For example, dissociation of c-Src from the chaperone complex leads to the phosphorylation of annexin 1, inhibition of cytosolic phospholipase A2 activity, and impaired release of arachidonic acid which is a pro-inflammatory mediator.[290, 291]

Non-genomic actions also underlie Gc-mediated effects on neural progenitor cells (NPCs). Gc activation of GR localised at the plasma membrane leads to MAPK-dependent phosphorylation of connexin-43 and c-Src activity limits proliferation of NPCs and alters gap junction intercellular communication.[292] It has also been proposed that glucocorticoids affect cellular permeability, eg, altering the synchrony of spontaneous calcium transient currents across the plasma membrane.[292]

1.6.4 Post-translational modifications of GR

As described above, tissue-specific GR action is controlled by several layers of regulatory mechanisms including pre-receptor bioavailability, differential expression of GR isoforms, and accessibility of DNA for GR-binding as dictated by the chromatin landscape. In addition, GR function can also be affected by post-translational modifications such as phosphorylation, sumoylation and ubiquitination.

Human GRα is phosphorylated on at least seven serine residues (Ser-113, Ser-134, Ser-141, Ser-203, Ser-211, Ser-226, and Ser-404), all of which are located in the NTD of the receptor. These sites can be phosphorylated by mitogen protein kinases (MAPK), cyclin-dependent kinase (CDK), glycogen synthase kinase-3 (GSK-3) and c-Jun N-terminal kinases. [230, 293, 294] One of the major effects of GR-phosphorylation is to alter the transcriptional activity of the receptor, but this is highly context dependent. This is shown by a study which compared the activity of wild-type GR and GR with mutated serine phosphorylation sites in two different chloramphenicol acetyltransferase (CAT) reporter genes after transient transfection into COS-1 cells.[270] One CAT

reporter had a mouse mammary tumour virus long terminal repeat (MMTV-LTR) promoter, the other a promoter with two copies of the GRE from the aminotransferase gene linked to a TATA sequence. Activities of the mutants did not differ significantly from that of wild-type GR with the first reporter, but almost all the mutants had activities that were 50-75% lower than that of wild type GR with the second reporter.

The majority of data suggests that the phosphorylation of GR is induced by ligand-binding,[295] and accumulating data suggests phosphorylation at particular residues have specific effects. For example, one group found that transcriptional activity of GR correlated with the amount of phosphorylation at Ser 211, suggesting Ser 211 is a marker for activated GR.[296] In the same study, it was found that the Ser 203-phorphorylated form of the receptor was predominantly cytoplasmic, whereas Ser 211-phosphorylated GR was found in the nucleus. Furthermore, GR has the greatest transcriptional activity when Ser 211 phosphorylation exceeds that of Ser 226 phosphorylation, and blocking Ser 226 phosphorylation has been found to enhance the transcriptional response of GR.[297] Another example is phosphorylation of Ser 404 causes a conformational change within GR, leading to altered co-factor recruitment and attenuated GR-signalling.[298]

Phosphorylation also alters other properties of GR including protein stability: this is shown by data demonstrating that phosphorylation-deficient mutant GR is stabilised in the presence of Gc, suggesting degradation of the GR protein is enhanced by Gc-dependent phosphorylation of GR.[299]

Other post-translational modifications of GR include ubiquitination. Ubiquitin is a 76 amino acid protein that, when attached to specific lysine residues, marks proteins for proteasomal degradation.[237] Ubiquitination of GR at Lys-419 targets the receptor for the proteasome, and mutant receptors that cannot be ubiquitinated at this residue are resistant to Gc-dependent downregulation and exhibit potentiated transcriptional activity on Gc-responsive reporter genes.[300, 301]

GR is also post-translationally modified by sumoylation, whereby SUMO (small ubiquitin-related modifier) peptides are covalently attached to specific lysine residues (eg, Lys-277 and Lys-293, Lys-703) on GR. SUMO peptides are attached in the absence of ligand, but attachment is increased following Gc-exposure. Transcriptional activity of

GR can either be enhanced or repressed depending on the site of sumoylation.[237, 302, 303]

Acetylation of GR on lysine residues (Lys-494 and Lys-495) has been shown to limit the inhibitory actions of Gc on NF-κβ signalling.[237] It has also been shown that GR acetylation is higher in the morning than in the evening in peripheral blood mononuclear cells from humans, and GR acetylation may form part of a counter regulatory mechanism to the actions of diurnally fluctuating cortisol, effectively decreasing tissue sensitivity to glucocorticoids in the morning and increasing it at night.[304]

1.6.5 Gc resistance

In addition to NS, Gc therapy is also used to treat many other clinical conditions including asthma, rheumatoid arthritis, inflammatory bowel disease and autoimmune diseases.[305, 306] In a similar fashion to NS, a proportion of patients with these conditions show a poor or absent response to Gc treatment (eg, about 30% of patients with rheumatoid arthritis have a poor clinical response to glucocorticoids).[307] In the following section, I will discuss potential reasons for this resistance to Gc therapy. Most glucocorticoid resistance studies have focussed on inflammatory conditions such as asthma, but I will highlight data relating directly to NS whenever possible.

1.6.5.1 Genetic basis for Gc-resistance

A study from 1981 describing Gc-resistant asthma found that sufferers had a family history of asthma more commonly than Gc-sensitive patients. This led the authors to postulate that Gc-resistance may have a genetic basis.[308] Additionally, although SRNS usually occurs as a sporadic disease, familial cases have frequently been reported.[309] Transcriptomic profiling using peripheral blood mononuclear cells (PBMCs) from Gc-sensitive and Gc-resistant asthma patients identified 11 genes which discriminate between these groups.[310] Thus, it may be possible to predict response to Gc-therapy, avoiding exposing patients to unnecessary courses of glucocorticoids. Additionally, Donn *et al.*, stratified healthy subjects according to Gc-responsiveness using a low dose dexamethasone suppression test.[311] The group compared the transcriptome of primary lymphocytes from the 10% with the greatest and least Gc-responsiveness and identified 24 genes that were differentially regulated. The most discriminate differentially-expressed gene between the two groups was bone

morphogenetic protein receptor type II, and overexpression of this protein *in vitro* resulted in enhancement of Gc-mediated activation of a reporter gene.

Further data suggesting a genetic basis for Gc-resistance comes from a genome-wide association study in patients with asthma which identified a single-nucleotide polymorphism (SNP) mapping to the glucocorticoid-induced transcript 1 gene (*GLCCI1*) associated with a poor response to Gc therapy. Following reports that *GLCCI1* is expressed in podocytes, Cheong *et al.*, genotyped 211 Korean children with INS and 102 controls but did not identify SNPs correlating with Gc-responsiveness (or any other factor).[312] The relevance of *GLCCI1* in INS is therefore questionable.

1.6.5.2 Familial glucocorticoid resistance

Insight into potential molecular mechanisms underlying Gc-resistance came from studies examining the extremely rare inherited syndrome familial glucocorticoid resistance (FGR), which is characterised by high circulating cortisol concentration without signs or symptoms of hypercortisolism.[305, 306] Clinical manifestations (which may be absent) are due to an excess of non-Gc adrenal steroids stimulated by high adrenocorticotrophin (ACTH) levels, and may include hypertension with hypokalaemia and/or signs of androgen excess (eg, hirsutism and menstrual abnormalities in females). Inheritance seems to be dominant with variable expression, and since its first description in 1976 only about 30 patients with mostly asymptomatic family members have been described in the literature.[313] Several causative *NR3C1* mutations have been identified in FGR patients leading to defective binding of ligand to GR, reduced binding of GR to DNA, and reduced GR expression.

1.6.5.3 Defects in GR

These findings do not appear to be generalisable to other disease processes as a study comparing GR complementary DNA (cDNA) from asthmatic patients with differential response to Gc-therapy did not detect any base-pair mismatches between groups, suggesting the defect in Gc-resistant asthma does not seem to be related to the structure of GR.[314] Some data from the INS population suggests overall GR expression levels may be a factor in Gc-resistance: lower GR expression levels in the glomeruli of adults with INS correlated with a longer time to respond to Gc therapy,[315] and lower GR expression levels were found in the lymphocytes and monocytes of children with SRNS compared to children with SSNS.[316]

Further work examining a role for *NR3C1* mutations in Gc-resistance comes from Koper *et al.,* who examined the prevalence of *NR3C1* mutations responsible for insensitivity to glucocorticoids.[317] The group analysed the *NR3C1* genotype in a group of 20, otherwise healthy, people with a reduced response to a dexamethasone suppression test and in 20 controls, and found no mutations or polymorphisms associated with a reduced sensitivity to glucocorticoids. However, they did identify five novel mutations in *NR3C1*; one of which (ER22\23EK in exon 2) was subsequently shown to result in reduced transactivation capacity of GR *in vitro* when transfected in COS-1 cells.[318] The E22\23EK polymorphism has also been shown to be associated with an increased survival rate associated with lower levels of an inflammatory markers (C-reactive protein) in a general population of elderly men.[319] The mechanism for this Gc-insensitivity *in vitro* and reduced inflammatory profile *in vivo* may involve a shift from GRα to GRβ expression leading to a decrease in transactivation activity.[320]

As described in section 1.6.2.1, GRβ acts as a dominant negative inhibitor of GRα by binding DNA, but not binding ligand. A SNP of GRβ (GR-9β) was found to be associated with a reduced trans-repression, but normal transactivation, response in an elderly cohort of patients recruited as part of a larger prospective study determining factors underlying the development of illnesses in old age.[321] Some studies have reported increased expression of GRβ in Gc-resistant patients in several diseases including asthma, rheumatoid arthritis, and inflammatory bowel disease, and children with INS.[322-325] However, other studies have not been able to replicate these findings,[326] and the clinical relevance of altered GRβ remains uncertain.[327]

1.6.5.4 Abnormalities of GR chaperones

Some groups have focussed attention on molecular chaperones of GR including hsp90. The expression of hsp90 in peripheral blood mononuclear cells (PBMCs) from adult INS patients resistant to Gc therapy was found to be higher than those with SSNS.[328] Additionally, the distribution of hsp90 in the SRNS group was greater in the nuclei than that of SSNS patients. Further work in the adult INS population demonstrated increased nuclear hsp90 binding to GR, and decreased GR–GRE binding activity in PBMCs from Gc-resistant patients, leading to the possibility that nuclear hsp90 may hinder GR activity and contribute to Gc-resistance.[329] A recent study has shown that Gc-insensitivity in Cushing disease (a neuroendocrine condition caused by a partially Gc-resistant corticotroph adenoma that excessively secretes ACTH, leading to

hypercortisolism) may be caused by overexpression of hsp90, and pharmacological inhibition of hsp90 can lead to restoration of Gc-sensitivity.[330]

1.6.5.5 Abnormalities in inflammatory mediators

As described in section 1.5.2, some evidence suggests INS may have an immunological basis. Based on this, Jafar *et al.*, investigated 150 children with INS and 569 healthy controls, and found the following polymorphisms were more prevalent in children with SRNS compared to children with SSNS: IL-6 (G174C); IL-4 (C590T); and tumour necrosis factor α (G308A).[331]

IL-2 and IL-4 are highly expressed in the airways of patients with Gc-resistant asthma, and *ex vivo*, this combination of cytokines reduced GR nuclear translocation in T-cells and reduced ligand-binding affinity of GR.[332] The mechanism underlying this defect may involve p38 mitogen-activated kinase (MAPK) inhibitor, as inhibition of this kinase blocks the effects triggered by IL-2 and IL-4.[333] Defective GR nuclear translocation in Gc-resistant asthmatic patients has also been identified in another study.[334]

Another cytokine with a potential role in Gc-resistance is the pro-inflammatory mediator macrophage migration inhibitory factor (MIF). MIF is produced mainly by T lymphocytes, but also by epithelial and endothelial cells.[335] Unlike many other pro-inflammatory cyctokines, MIF expression is *increased* following Gc exposure, but in parallel leads to inhibition of Gc-efficacy.[336] Indeed, MIF-inhibition has been shown to be therapeutically useful in a range of rodent models of inflammatory diseases.[337] Interestingly, Berdeli *et al.*, examined the MIF -173G/C polymorphism in 214 children with INS and 103 healthy controls and found that a significant increase in GC genotype and C allele frequency in INS.[338] The group also identified a 20-fold higher expression of the CC-genotype in the SRNS group compared to children with SSNS, and CC-genotype were at increased risk of developing ESRD. The authors conclude that MIF antagonists may be useful therapeutic agents for children with SRNS, but no human clinical data is currently available.

1.6.5.6 Histone deacetylation

Epigenetic factors may also play a role in Gc-resistance. For example, histone deacetylase (HDAC) 2 deacetylates lysine residues at the N-terminal regions of core histone proteins, and low HDAC2 expression has been found in PBMCs and alveolar

macrophages from patients with Gc-resistant asthma,[339] and in surgically-resected lung tissue from patients with (typically Gc-resistant) chronic obstructive pulmonary disease (COPD).[340] Additionally, HDAC2 overexpression in broncho-alveolar macrophages from patients with Gc-resistant chronic obstructive pulmonary disease *ex vivo* restored Gc-sensitivity to the level seen in healthy control subjects.[341]

1.6.5.7 Vitamin D

Some data linking vitamin D deficiency to Gc-resistance comes from a study demonstrating that T-helper cells from patients with Gc-resistant asthma did not secrete the Gc-induced anti-inflammatory cytokine IL-10, but this was restored after addition of vitamin D3.[342] Additionally, an enhanced Gc-induced IL-10 response was found in 3 patients with Gc-resistant asthma following oral ingestion of vitamin D3, suggesting this intervention may be of some therapeutic relevance.

1.6.5.8 Pharmacokinetics

Another potential mechanism underlying Gc-resistance may involve membrane transporter systems. For example, P-glycoprotein 170 (P-gp170), coded by the multidrug-resistance gene *MDR1*, transports a range of drugs (eg, glucocorticoids, methotrexate) out of cells.[305] High levels of *MDR1* expression have been found in lymphocytes from patients with Gc-resistant inflammatory bowel disease [343] and rheumatoid arthritis,[344] and polymorphisms of the *MDR1* gene have been examined in children with INS. Jafar *et al.*, found two SNPs of *MDR1* (G2677T/A and C3435T) which increase the risk of developing SRNS,[345] and these findings have been replicated in another study.[346] Data from the Egyptian population of children with INS found a correlation between expression of serum IL-2 expression and P-gp170, with higher expression of both proteins in lymphocytes of children with SRNS.[347] A report from Poland examining children with INS also found higher expression, and pump activity of P-gp170 in lymphocytes of children with SRNS.[348] Interestingly, this higher P-gp170 activity was reduced by calcium channel blockers *in vitro*, suggesting this may be a potential approach to reverse Gc-resistance.

The human cytochrome P450 (CYP) system of enzymes plays a major role in the metabolism of endogenous hormones, xenobiotics and drugs. Chiou *et al.*, analysed the A6986G polymorphism in the *CYP3A5* gene but found no difference in frequency between children with SSNS and SRNS.[349] Additionally, a range of pharmacokinetic

parameters were evaluated in thirteen children treated with prednisolone during an active phase of INS, and no correlation was found between any parameter and response to Gc-therapy.[245] These data suggest that assessment of pharmacokinetics is not able to predict response to Gc-therapy in children with INS.

In summary, glucocorticoids are potent therapy for many clinical conditions, but a major limiting factor in their clinical use is the wide variation observed in responsiveness to therapy. The reasons underpinning this Gc-resistance are currently unclear and are likely to be disease-specific. A number of approaches to enhance Gc-sensitivity are currently being developed including targeting of MIF and P-gp170, as well as the use of selective GR modulators (SGRMs) which would ideally preserve anti-inflammatory activity but lack the side-effect profile of conventional glucocorticoids.[350] Data concerning the utility of such agents in the treatment SRNS is lacking.

1.7 Cell migration

Cell migration is essential for normal development and is an integral part of the responss to tissue damage and infection.[351] Cell migration also occurs in chronic human diseases such as cancer, atherosclerosis, rheumatoid arthritis, and, as described in section 1.3.4, INS. Indeed, agents which specifically reduce cancer cell motility have already been shown to be promising therapeutic agents.[352-355] In the following sections, I will describe the mechanisms regulating cell motility, with a particular focus on the podocyte.

1.7.1 Overview of cell migration

Cell migration is a multi-step, cyclical process, usually initiated in response to extracellular cues, leading to reorganisation of the actin cytoskeleton and cell polarisation. [351] The cell motility cycle may be divided into mechanistically distinct steps:

i) A cell must first interact with its environment and adhere to the ECM. Examples of receptors mediating cell-ECM interaction include integrins, syndecans, and dystroglycan.[356] Integrin-ECM engagement triggers the recruitment of a large number of proteins termed focal adhesion complexes which not only provide physical and regulatory links between the ECM and the cytoskeleton, but also provide influence over other major cellular functions including cell survival and proliferation.[357]

ii) To initiate migration, cells must receive a pro-migratory stimulus, which may be physical (eg, ECM-integrin interaction), or chemical (eg, lysophosphatidic acid or growth factors such as platelet derived growth factor).[358]

iii) Pro-migratory stimuli cause the cell to polarise forming a leading edge and a trailing edge, allowing directional cell movement to occur.[359] In order to migrate, a cell must push its membrane forward at the leading edge and retract it at the trailing edge. Cells extend four different plasma membrane protrusions at the leading edge: lamellipodia, filopodia, blebs and invadopodia.[360]

Lamellipodia are sheet-like protrusions filled with a branched network of actin, while filopodia are ‘finger-like’ structures that are filled with tight

parallel bundles of filamentous (F)-actin.[361] The elongation of these structures pushes the leading edge forward, thus promoting cell migration. Invadopodia are protrusions rich in proteinases such as members of the matrix metalloprotease (MMP) family and the urokinase-type plasminogen activator (uPA) proteolytic system, which allow focal degradation of the ECM to facilitate invasion through tissues.[362] Blebs form when the plasma membrane detaches focally from the underlying actin filament cortex, allowing cytoplasmic flow to push the membrane outwards rapidly due to intracellular hydrostatic pressure, and are thought to be important during development.[360]

iv) The final stage involves the dynamic control of adhesion complex recycling to ensure these complexes do not persist too long (resulting in the ability of a cell to move forward), or for too short a period (which would lead to unstable adhesion to the ECM and limited cell traction). An example of this is how endocytosed integrins are sorted to either the leading or trailing edge of cancer cells based on their activation status: Ras-related protein Rab-25 (Rab25) coordinates cell extension and retraction by regulating recycling of inactive integrin to the cell front, whereas active integrins are recycled to the cell rear where they can promote signals for forward movement.[363, 364]

The Ras superfamily of small guanosine triphosphatases (GTPases) are major regulators of actin dynamics and other processes involved in cell migration and will be discussed below.

1.7.2 Small GTPases

The Ras superfamily of small GTPases (from now on simply referred to as ‘small GTPases’) comprise over 150 human members and are divided into five major branches: Ras, Rho, Rab, Ran and Arf. [365] Small GTPases possess intrinsic phosphatase activity and bind either guanosine triphosphate (GTP) or guanosine diphosphate (GDP). The relative affinity difference of the effector molecules from GTP- versus GDP-loaded states of small GTPases can be as much as 100-fold.[366] Thus, small GTPases function as molecular switches, cycling between inactive (GDP-bound) and active (GTP-bound) states (see **Figure 1.5**).

GDP/GTP cycling is controlled by guanine-nucleotide-exchange factors (GEFs) which promote the formation of the active GTP-bound form,[367] GTPase-activating proteins (GAPs) which accelerate the intrinsic GTPase activity to promote the formation of the inactive GDP-bound form,[368] and GDP disassociation inhibitors (GDIs) which bind GDP-associated GTPases and maintain the small GTPases in an inactive state.[369] Small GTPases within a family branch use both shared and distinct GAPs and GEFs, while small GTPases in different family branches use structurally distinct but mechanistically similar GAPs and GEFs.[365]

1.7.2.1 The Ras family

The Ras sarcoma (Ras) oncoproteins consist of 36 members and interact with multiple downstream effectors regulating gene expression, cell proliferation and cell survival.[365] They have critical roles in human oncogenesis,[370] and in the context of cell migration Rap1 regulates integrin activation,[371] and RaIA promotes the formation of filopodia.[372]

1.7.2.2 The Rho family

The mammalian Ras homologous (Rho) family consist of 20 members, and have well characterised roles in actin cytoskeletal regulation.[373] Several subfamilies exist within the Rho family including Rac (Rac1, Rac2, Rac3 and RhoG), Rho (RhoA, RhoB, RhoC) and Cdc42h (Cdc42, TC10, TCL, Chp).[351] Rho GTPases have been implicated in the regulation of cell polarity, cell movement, cell shape, as well as in the regulation of endocytosis and exocytosis.[374] The members of the Rho family that have received most attention in the context of cell migration (primarily because they were the first to be characterised in the morphological responses of cells to external stimuli in the early 1990s[375]) are RhoA, Cdc42 and Rac1. I will discuss each of these in more detail in later sections, but as a general overview, RhoA activation leads to the assembly of contractile actin-myosin filaments (stress fibres),[358] Rac1 is implicated in the formation of lamellipodia,[376] and Cdc42 has a critical role in the formation of filopodia.[377]

1.7.2.3 The Rab family

Ras-like proteins in the brain (Rab) form the largest branch of the superfamily with 61 members, and regulate intracellular vesicular transport and the trafficking of proteins along endocytic and secretory pathways.[365] Regarding cell migration, Rab proteins

play essential roles in the recycling of adhesion receptors. For example, in cancer cells Rab25 promotes migration by regulating the delivery of integrin receptors to the tip of membrane protrusions at the leading edge.[365]

1.7.2.4 The Ran family

The Ras-like-nuclear (Ran) is the only member of this family but is the most abundant small GTPase in the cell and has well characterised roles in nucleocytoplasmic transport of RNA and proteins.[365] Ran also has role in trafficking intracellular vesicles containing *Legionella pneumophilia* (the causative agent of Legionnaires' disease).[378]

1.7.2.5 The Arf family

Like the Rab proteins, the ADP-ribosylation factor (Arf) proteins regulate intracellular vesicular transport.[365] Arf1 is the best characterised member of this family and controls the formation of vesicle coats in the exocytic and endocytic pathways.[379] Arf6 is involved in integrin recycling during cell migration, remodelling of the actin cytoskeleton and invadopodia formation.[380]

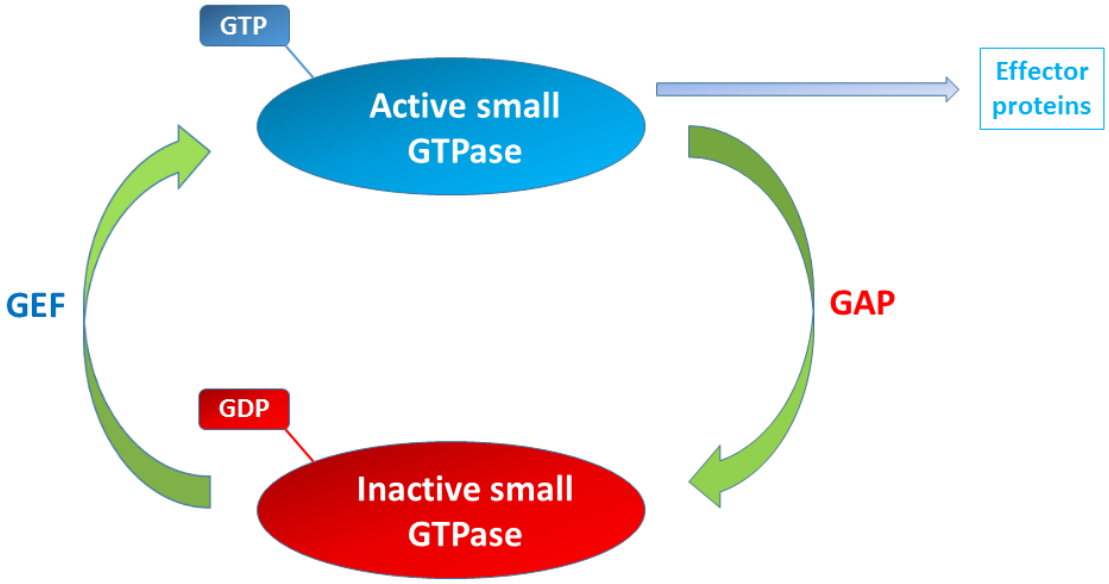

Figure 1.5 The small GTPase cycle
Small GTPases serve as molecular switches, cycling between an active guanosine-triphosphate (GTP)-bound form, and an inactive guanosine diphosphate (GDP)-bound form. Activation of small GTPases is mediated by guanine-nucleotide-exchange factors (GEFs), while GTPase-activating proteins (GAPs) promote the formation of the inactive GDP-bound form.

1.7.3 The Rho sub-family

The three Rho isoforms (RhoA, RhoB, and RhoC) are highly homologous, with the primary protein sequences being approximately 85% identical.[375] Early work on the control of the cytoskeleton was done in fibroblasts, in which actin filaments principally exists in three types of structure: the cortical actin network, actin stress fibres which emanate from adhesion complexes, and membrane protrusions (eg, filopodia).[381] The first data implicating Rho proteins in the control of actin dynamics came from a study in which injection of C3 transferase into cells (which inhibits all three Rho isoforms) causes fibroblasts to lose their actin stress fibres and to round up.[382]

More direct evidence that Rho proteins have effects on the actin cytoskeleton came from microinjection of serum-starved fibroblasts with recombinant RhoA or plasmids overexpressing *rhoA* cDNA, which caused cell contraction and adhesion complex formation.[382] Ridley *et al.*, subsequently demonstrated that serum-starved cells contain few stress fibres, while fibroblasts growing in the presence of serum contain abundant stress fibres, and addition of serum induced rapid cytoskeletal reorganisation.[358] They identified several growth factors including lysophospholipid and platelet derived growth factor responsible for these changes, suggesting these may be critical activators of Rho.

RhoA controls intracellular contractility by regulating both actin severing and actin polymerisation. RhoA activates Rho-associated protein kinases (ROCK1/2), which in turn phosphorylates myosin light chain (MLC) (directly) or MLC phosphatase causing cell contraction and retraction of the cell trailing edge.[383] RhoA also modulates actin depolymerisation by activating ROCK, which in turn activates LIM kinase (LIMK), which phosphorylates the actin severing protein cofilin.[366] Through its severing activity, cofilin increases the number of free barbed ends at the end of filaments, playing a role in the initiation of actin-based cell protrusions in lamellipodia and invadopodia.[384]

Another downstream effector of Rho proteins is the Formin family of proteins. Formins produce straight, unbranched actin fibres involved in the initiation of actin filament assembly.[385] Indeed, active RhoA has been identified at the front of lamellipodia where it may act to stimulate actin polymerisation mediated by the formin mDia1.[386] Thus, RhoA has complex actions on the cytoskeleton with roles in contraction of the trailing edge, as well as being a regulator of membrane protrusions at the leading edge.

The small degree of protein sequence divergence between the three Rho isoforms occurs around the Switch 1 region (which changes conformation between GDP- and GTP-bound forms), suggesting the proteins could have different affinities for regulator or effector proteins.[375] However, few GEFs and GAPs have been compared for their relative activity on RhoA, RhoB, and RhoC, and most have been tested only on RhoA. Of those that have been tested on all three isoforms, very little difference in affinity has been observed.[367]

In terms of effector protein binding, ROCK has higher affinity for RhoC compared to RhoA and RhoB. Moreover, RhoC-mediated ROCK activation is higher than that elicited by RhoA or RhoB.[375] This difference suggests the isoforms may have differing contributions to cellular motility. Differences in cellular localisation have also been observed: RhoA and RhoC localise to the plasma membrane or interact with RhoGDI in the cytoplasm, whereas RhoB localises to the endosomal membranes.[373] The effects of Rho proteins on cell migration also seem to be cell-specific, which probably reflects the basal level of stress fibres and focal adhesions.[351] Vega *et al.*, investigated the role of RhoA and RhoC in invasion and migration using two cancer cells lines: PC3 (prostate cancer cells) and MDA-MB-231 (breast cancer cells).[387] Both RhoA-depleted and RhoC-depleted PC3 cells showed reduced migration speed but through different mechanisms: RhoA-depleted cells extended narrow protrusions simultaneously in two or more opposing directions, resulting in reduced net movement, whereas RhoC-depleted cells were unable to polarise. Additionally, in a 3D invasion assay RhoA-depleted cells showed enhanced invasion compared to control or RhoC-depleted cells, suggesting a link between the protrusive nature of RhoA-depleted cells and an increase in invasive behaviour. In contrast, another study showed that RhoB-depleted PC3 cells showed an *increase* in migration speed (no invasion assay was performed).[388]

In addition to their roles in regulating actin dynamics, Rho proteins have been implicated in the control of endosome trafficking, cell survival and cancer progression. For example, RhoB-null smooth muscle cells have impaired trafficking of the PDGF receptor,[389] RhoC-null mice have reduced number and size of metastatses in a model of lung cancer, with a decreased metastatic cell survival time. [390]

1.7.4 The Rac subfamily

The four members of the Rac subfamily (Rac1, Rac2, Rac3 and RhoG) have different expression patterns. [373] Rac1 is the most studied member of this family and is ubiquitously expressed, whereas Rac2 expression is mostly restricted to cells of haematopoietic origin, and Rac3 is most abundant in the brain.[391, 392] RhoG has the lowest sequence identity to Rac1, is widely expressed, but at varying levels with human tissues: in the human kidney, moderate tubular staining is observed but no glomerular expression.[393] In the following discussion, I will focus on the actions of Rac1.

Rac1 is activated by a variety of stimuli including shear stress,[394] mechanical stretch,[395] reactive oxygen species,[396] inflammatory cytokines (eg, tumour necrosis factor α),[397] growth factors (eg, epidermal growth factor),[398] integrins (eg, β3 integrin),[399, 400] high glucose concentrations,[401] homocysteine,[402] osmotic stress,[403] angiotensin II,[404] and aldosterone.[405, 406] Activation of Rac1 is associated with the regulation of membrane protrusions required for cell migration.[373] This was first shown in a study which showed microinjection of recombinant Rac1 protein into fibroblasts stimulated the formation of lamellipodia.[407] Nobes *et al.*, provided further insight using a wound healing assay.[408] Inhibition of Rac1 had pronounced inhibitory effects on cell movement: in cells injected with dominant negative Rac1 protein, wound size after 5 hours was reduced by 80%, and in cells injected with a dominant negative Rac1 expression plasmid, cell movement was inhibited by 98%. Microinjection of constitutively active Rac1 protein had no effect on cell migration across the wound. The authors concluded that Rac1 is essential for cell movement. Additionally, Rac1-null Schwann cells, endothelial cells and platelets have impaired lamellipodium formation.[409-411] More recent data have revealed that activation of Rac1 alone, using a photoactivatable Rac1, is sufficient to induce lamellipodium extension. [412]

Rac1 regulates actin polymerisation during lamellipodial extension in several ways: i) activation of actin-nucleating proteins [eg, the ARP2/3 complex through WASP-family verprolin-homologous protein (WAVE) proteins] and mDia formins; ii) controlling the availability of free actin barbed ends through cofilin and; iii) increasing the availability of actin monomers via the actions of cofilin.[373, 413]

Additionally, Rac1 has roles in integrin-mediated cell adhesion,[414] reactive oxygen species production,[415] cell cycle progression, phagocytosis, and gene expression (eg, by activation of the MAPK and STAT pathways).[416]

1.7.5 Cdc42

A role for Cdc42 in cytoskeletal regulation was identified in a study in which microinjection of Cdc42 protein in fibroblasts led to the rapid formation of filopodia.[417] Using a wound healing assay, it was subsequently found that Cdc42 inhibition led to a 50% reduction in cell movement, suggesting Cdc42 is required for efficient movement but is not absolutely essential (a 98% reduction in cell movement was found with Rac1 inhibition in the same study).[408] Additionally, other small GTPases can also induce filopodia formation including RhoQ, RhoU, RhoF, and RhoD.[373, 418-420] Another study used a chemotaxis chamber to demonstrate that RhoA and Rac1 are required for cell migration, whereas Cdc42 is required for cells to respond to an attractant chemokine gradient, but is not essential for cell locomotion.[376]

1.7.6 Rho GTPase cross-talk

Many of the early studies examining how Rho GTPases regulate actin dynamics focussed on isolated effects of either RhoA, Rac1 or Cdc42. However, recent data show that these proteins act in complex activation cascades, involving antagonistic regulatory mechanisms.[366] For example, Rac1 and RhoA are mutually inhibitory,[421] and Cdc42 can activate Rac1.[417]

It has also previously been hypothesised that the protrusive phenotype driven primarily by Rac1 must be dominant at the leading edge, and the RhoA-mediated contractile phenotype causing tail retraction must be dominant at the rear of the cell.[366] However, again more recent data indicates that a much finer spatiotemporal control of migratory events occurs in cells. For example, Machacek *et al.*, examined small GTPase coordination in fibroblasts through simultaneous visualisation of GTPase biosensors for RhoA, Rac1, and Cdc42.[422] The group found that all three GTPases (ie, including RhoA), were maximally active proximal to the leading edge. This is not consistent with the hypothesis of dominant Rac1/Cdc42 activity at the leading edge, with dominant RhoA at the trailing edge. Additionally, they found that RhoA was activated at the cell edge synchronous with edge advancement, whereas Rac1 and Cdc42 were activated

2µm behind the edge with a delay of 40 seconds. These data suggest that Rac1 and RhoA operate antagonistically in a precise manner, and that RhoA has a role in the initial protrusion event, whereas Rac1 and Cdc42 activate pathways implicated in reinforcement and stabilisation of the newly expanded protrusion.

1.7.7 Rho GTPases and nephrotic syndrome

Mechanistic links between podocyte motility, proteinuria, and the Rho family of small GTPases were suggested by a study demonstrating suPAR (a serum factor potentially linked to the onset of INS) led to increased podocyte motility *in vitro*, and FP effacement and proteinuria *in vivo* through activation of podocyte β_3-integrin, which in turn promotes Rac1 and Cdc42 activity.[400] These observations were made in the era before the complex spatiotemporal regulatory mechanisms involving the small GTPases (see section 1.7.6) were widely recognised. It was hypothesised that RhoA activation causes a hypomobile podocyte phenotype, stabilising the podocyte FP structure and protecting from effacement and proteinuria, whereas Rac1 and Cdc42 activity promotes podocyte motility and the development of FP effacement and proteinuria (see Figure 1.6).[129, 130] Data supporting this hypothesis includearhg the observation that a mouse line with inducible podocyte-specific constitutively active Rac1 displayed a rapid onset of proteinuria associated with altered FP morphology.[423]

Subsequent *in vivo* work demonstrated that the relationship between small GTPase activity and proteinuria was more complex than initially thought, and both under- and over-activity of small GTPase action in podocytes has a detrimental effect on glomerular barrier function.

Shibata *et al.*, demonstrated that inhibition of ROCK (a downstream effector of RhoA) by fasudil reduced proteinuria in a PAN-nephrosis model in rats, suggesting excessive RhoA activity increases GFB permeability.[424] Podocyte-specific expression of a constitutively active, doxycycline-inducible form of RhoA in mice led to significant proteinuria: weak activation of RhoA led to histological findings consistent with MCD, while stronger activation of RhoA resulted in histological findings similar to FSGS in humans.[425] However, further studies showed podocyte-specific expression of both a constitutively active RhoA construct or a dominant-negative RhoA construct in mice led to proteinuria, FP effacement and disruption of the actin cytoskeleton.[426]

The individual contributions of the Rho GTPases were assessed by Scott *et al.*, who deleted each of these proteins in rodent podocytes. Cdc42 mutant mice displayed proteinuria from birth and died of renal failure within two weeks. In contrast, Rac1 and RhoA mutants did not develop proteinuria by 3 months of age and showed no overt disease phenotype or decline in weight even after 1 year.[427] One confounding issue not tackled in this study is the possibility of molecular redundancy. RhoA shows 84% and 92% amino acid sequence identity with RhoB and RhoC respectively; Rac1, Rac2 and Rac3 all share >90% sequence identity; while Cdc42 shows only 62% and 55% homology with its closest relatives RhoQ and RhoJ.[373] There is a possibility that the lack of an overt phenotype in the RhoA and Rac1 mutants in the study by Scott *et al.*, arises from the ability of related molecules to functionally compensate.

Blattner *et al.*, further studied the role of Cdc42 by demonstrating that although mice with podocyte-specific deletion of Cdc42 appeared normal at birth, they began to experience significant morbidity and proteinuria from approximately 2 weeks of age and the majority of mutants died by the age of 4 weeks.[428] In the same study, podocyte-specific deletion of Rac1 resulted in healthy mice pups experiencing no proteinuria at 6 months of age and displaying no gross renal pathology. However, in an acute protamine sulphate model of podocyte injury, deletion of Rac1 prevented FP effacement, while in a chronic model of glomerular damage (uninephrectomized/ deoxycorticosterone acetate salt-induced hypertension), Rac1 mutants exhibited increased proteinuria compared to control mice. Thus, loss of Rac1 either improves or worsens the effects of agents harmful to the filtration barrier dependent on the context. Yu et al., provided further evidence for a role for Rac1 in the development of proteinuria by generating a podocyte-specific, inducible transgenic mouse line that expressed constitutively-active Rac1.[423] Induction of the transgene resulted in a rapid onset of proteinuria associated with FP effacement.

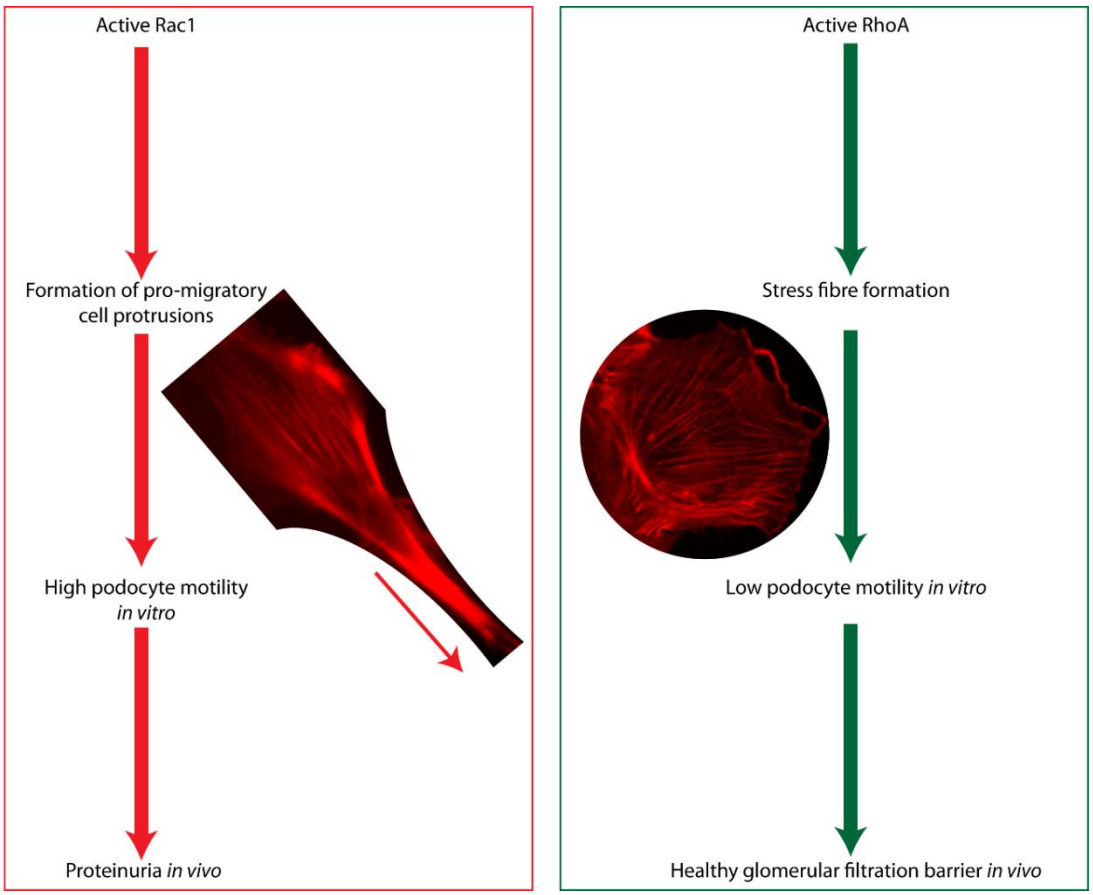

Figure 1.6 Podocyte motility is a determinant of glomerular barrier function

Podocytes are motile cells *in vivo*, and hypermobility is associated with glomerular disease.[132] Key regulators of cellular motility are the small GTPases Ras-related C3 botulinum toxin substrate 1 (Rac1), which stimulates the formation of pro-migratory cell protrusions, [373] and Ras homolog gene family, member A (RhoA), which forms stress fibres when active.[382] Images show human, wild type immortalised podocytes stained with the F-actin fluorescent dye Texas Red®-Y and imaged using a DeltaVision microscope.

1.7.8 Rac1 and chronic kidney disease

Data implicating Rac1 in the development of chronic kidney disease (CKD) comes from a study examining crosstalk between Rac1 and MR. MR and its ligand aldosterone have well-established pathophysiological roles in the progression of kidney disease,[429] and MR antagonists (eg, spironolactone) are used clinically as adjunctive therapy to reduce proteinuria.[430] Shibata *et al.*, transiently transfected constitutively active Rac1 into human embryonic kidney cells (HEK) 293 cells and demonstrated enhanced MR activity, including increased nuclear translocation.[431] Additionally, mice lacking Rho GDI α (*Arhgdia*$^{-/-}$) (GDIs prevent small GTPases from being converted to the active GTP-bound form) developed heavy proteinuria associated with increased Rac1 (but not RhoA) and MR signalling. Treating *Arhgdia*$^{-/-}$ mice with a Rac-inhibitor (NSC23766) reduced MR overactivity and renal damage, and MR-blockade also reduced proteinuria (fasudil, a ROCK inhibitor, was ineffective therapy). This suggests Rac1 enhances the activity of MR in a ligand-independent manner, accelerating kidney damage.[431] The observation that mutations in the *Arhgdia* gene cause SRNS underscores its importance in the pathogenesis of proteinuria.[432]

Further evidence implicating Rac1 in kidney disease comes from a study examining angiotensin-II-induced podocyte injury. This study demonstrated a switch from a stationary to motile phenotype involving Rac1 in cultured mouse podocytes stably expressing the type 1 angiotensin II-receptor.[433] Tian *et al.*, showed, again in a mouse podocyte cell line, that calcium influx via TRPC5 channels activate Rac1 and stimulates podocytes to adopt a motile phenotype, whereas calcium influx via TRPC6 channels activates RhoA and elicits a more stationary podocyte phenotype.[128] Babelova *et al.*, examined a potential role for Rho GTPase inhibition in CKD using the 5/6 nephrectomy model of arterial hypertension and proteinuria in mice, using EHT1846 (Rac1 inhibitor), SAR407899 (ROCK inhibitor) and ramipril (angiotensin converting enzyme inhibitor which is used widely in clinical practice for the treatment of chronic kidney disease).[434] All inhibitors markedly attenuated proteinuria as well as glomerular and tubulointerstitial damage. Additionally, the combination of the ROCK inhibitor and ramipril was more effective in preventing albuminuria than ramipril alone.

Regulators of Rac1 also seem to play a role in the development of kidney disease: when RhoA is activate, a Rac1 GAP, Rho GTPase-activating protein 24, RhoGAP24 (coded

by the *Arhgap24* gene), is phosphorylated by ROCK. This phosphorylation increases the GAP activity of RhoGAP24, resulting in the inactivation of Rac1 and Cdc42.[406, 435] In cultured mouse podocytes, RhoGAP24 knock down results in increased levels of active Rac1 and Cdc42 (but not RhoA), and results in increased motility in a wound healing assay.[436] Furthermore, mutations in *Arhgap24* have been associated with familial FSGS in humans.

1.8 Project aims

Glucocorticoid therapy has been the cornerstone of management of childhood idiopathic nephrotic syndrome for several decades but the clinically-relevant mechanism of action, and the target cell remain poorly understood. An understanding of these unknowns may help to guide the future development of targeted therapeutics with an improved side effect profile.

We hypothesise that glucocorticoids act directly on podocytes to produce potentially clinically useful effects without involvement of the immune system. I will principally use an immortalised human podocyte cell line to:

1. Define the glucocorticoid receptor cistrome in the podocyte to understand the effects glucocorticoids exert on the podocyte.

2. Validate potentially clinically-relevant effects identified in aim (1).

3. Identify any novel mechanistic pathways which may be amenable to therapeutic treatment *in vitro*.

2 General materials and methods

2.1 Materials and reagents

Unless otherwise stated, all cell culture plastic ware were provided by Corning; media and reagents were provided by Sigma-Aldrich. Ultrapure water was obtained using a Milli-Q Synthesis system (Millipore Ltd).

2.2 General buffers

PBS: Dulbecco's phosphate buffered saline (150mM Nacl) without divalent cations.

TBS: Tris buffered saline, 150mM NaCl, 25mM Tris-HCl, pH 7.4

TAE: 50X; 2M Tris-acetate, 50mM EDTA, pH 7.7.

TE: 10mM Tris, 1mM EDTA, pH 8.0.

2.3 SDS-PAGE and western blotting buffers

Laemmli SDS sample loading buffer (5X): 125mM Tris-HCl pH 6.8, 25% (w/v) glycerol, 10% (w/v) sodium dodecyl-sulfate (SDS), 0.001% (w/v) bromophenol blue, 2% (v/v) β-mercaptoethanol.

NuPAGE MES [2-(N-morpholino)ethanesulfonic acid] SDS running buffer (1X): 50mM MES, 50mM Tris base, 0.1% SDS, 1mM EDTA, pH7.3.

Western blotting transfer buffer: 50mM Tris-base, 170mM glycine, 0.1% (w/v) SDS, 20% (v/v) methanol

TBS-Tween: 25mM Tris pH 7.4, 150mM NaCl, 0.1% (w/v) Tween-20.

Blocking buffer(10X): Casein blocking buffer (Sigma-Aldrich, B6429).

2.4 Antibodies

2.4.1 Primary antibodies

See **Table 2.1**.

Table 2.1 Primary antibodies

WB: western blotting; IF:immunofluorescence; IHF: fluorescent immunohistochemistry; CS: chromatin immunoprecipitation sequencing; GR: glucocorticoid receptor; Rac1: Ras-related C3 botulinum toxin substrate 1; RhoA: Ras homolog gene family, member A; MR: mineralocorticoid receptor; GAPDH: Glyceraldehyde 3-phosphate dehydrogenase.

Antibody target	**Species**	**Use and dilution (v/v)**	**Supplier**	**Catalogue number**
Human GR	Rabbit	IF: 1/200 WB: 1/2000 CS: 2µg	Proteintech	24050-1-AP
Human GR	Rabbit	CS: 2µg	Sigma-Aldrich	HPA004248
Mouse GR	Rabbit	IHF: 1/100	Santa-Cruz	M20 : sc-1004
Human phosphorylated-GR (serine 211)	Rabbit	WB:1/1000	Cell Signaling	4161
Rac1	mouse	WB: 1/1000	BD Biosciences	610651
RhoA	mouse	WB: 1/500	Cytoskeleton	ARH03
Mouse nephrin	Guinea pig	IHF: 1/100	Acris	BP5030
Human GAPDH	Mouse	WB: 1/2000	Sigma-Aldrich	G8795
Human MR	Mouse	WB: 1/1000	Life Technologies	MA1-620

2.4.2 Secondary antibodies

See **Table 2.2**.

Table 2.2 Secondary antibodies

WB: western blotting IHF: fluorescent immunohistochemistry; IF: immunofluorescence; Ig: immunoglobulin

Antibody target	**Source Species**	**Fluorescent dye**	**Use and dilution (v/v)**	**Supplier**	**Catalogue number**
Rabbit IgG	Goat	Alexa Fluor 680	WB: 1/5000	Invitrogen	A21109
Mouse IgG	Goat	Alexa Fluor 800	WB: 1/5000	Invitrogen	A11001
Rabbit IgG	Donkey	Alexa Fluor 647	IHF: 1/200	Invitrogen	A31573
Guinea pig IgG	Goat	Alexa Fluor 488	IHF: 1/200	Invitrogen	A11073
Rabbit IgG	Donkey	Cy2	IF:1/200	Jackson immunoresearch laboratories	711225152

2.5 Human cell lines

Human wild type podocytes: a conditionally immortalised human podocyte cell line developed by transfection with the temperature-sensitive SV40-T gene, which proliferate at 33ºC, but at 37ºC enter growth arrest and express markers of differentiated *in vivo* podocytes.[108] Obtained from M. Saleem, University of Bristol, UK.

GEnC: Conditionally immortalised human glomerular endothelial cells.[437] Obtained from S. Satchell, University of Bristol, UK.

A549: Human lung adenocarcinomic alveolar basal epithelial cells.[438] Obtained from T. Poolman, University of Manchester, UK.

HEK 293: Human embryonic kidney cells (Invitrogen).[439]

2.6 Cell Culture

Conditionally immortalised podocytes,[108] were grown in RPMI-1640 medium with L-glutamine and $NaHCO_3$ (R8758) supplemented with 10% (v/v) foetal calf serum (Life Technologies), 1% (v/v) insulin-transferrin-selenium (Life Technologies, 41400045), and 1% penicillin-streptomycin (P0781-stock 10,000 units penicillin and 10mg streptomycin per mL).

Proliferating podocytes were cultured at 33ºC in a 5% (v/v) CO_2 humidified incubator, and passaged when confluent, by detachment with Trypsin-EDTA solution (0.5g porcine trypsin and 0.2g EDTA per litre of Hanks's balanced salt solution with phenol red), and reseeded in fresh tissue culture flasks.

Podocytes underwent 10-14 days differentiation at 37ºC before use. Unless otherwise stated, glucocorticoid (Gc)-treatment refers to 1μM prednisolone dissolved in methanol.; vehicle-treatment refers to administration of an equal, 0.001% (v/v) amount of methanol alone. The Ras-related C3 botulinum toxin substrate 1 (Rac1) inhibitor EHT 1864 (Chapter 5) was used at a dose of 30μM (gift from Dr. Caswell, University of Manchester).

2.7 Protein analysis

2.7.1 Preparation of a total cell lysate

Cells were washed twice with PBS, before harvesting with ice-cold radioimmunoprecipitation assay cell lysis buffer (RIPA) [150mM NaCl, 20mM Tris pH 7.4, 3mM MgCl2, 0.5% (v/v) Triton X-100, supplemented with PhosSTOP protease inhibitor tablets (Roche) and cOmplete protease inhibitor cocktail tablets (Roche)]. Cells were detached by scraping prior to centrifugation at 21,000g for 10 minutes at 4^{o}C.

Supernatant was collected and stored at -80^{o}C prior to analysis by sodium dodecyl sulfate polyacrylamide gel electrophoresis (SDS-PAGE).

2.7.2 Polyacrylamide gel electrophoresis

Protein samples were separated by SDS-PAGE using 4-12% (w/v) NuPAGE Novex Bis-Tris gels (Invitrogen). Precision Plus Protein All Blue standards (Bio-Rad Laboratories) were loaded onto gels as molecular weight markers. Gels were resolved in NuPAGE MES SDS running buffer (Invitrogen) using XCell SureLock mini-cells (Invitrogen) at 150 volts (V) for 50 minutes.

2.7.3 Immunoblotting

2.7.3.1 Electrophoretic transfer

Proteins resolved by SDS-PAGE were transferred onto Protran nitrocellulose blotting membrane (Whatman International Ltd.) using XCell II blot modules (Invitrogen) according to the manufacturer's instructions. Proteins were transferred in transfer buffer at 30V for 90 minutes.

2.7.3.2 Membrane blocking, antibody probing and detection

Nitrocellulose membranes were blocked with blocking buffer diluted in ultrapure water (Millipore Ltd) for 45 minutes at room temperature. Membranes were probed with primary antibodies (see Table 2.1) resuspended to the appropriate concentration in blocking buffer diluted in TBS-Tween and incubated overnight at 4^{o}C. Membranes were washed five times with TBS-Tween and incubated with the appropriate fluorescent dye-conjugated secondary antibody (see Table 2.2) diluted in TBS-Tween for 45 minutes at room temperature, protected from sources of light. Membranes were washed

five times with TBS-Tween and visualised using the Odyssey IR imaging system (700nm and 800nm channels, 169µm resolution, without focus offset).

2.8 Immunofluorescence staining

Cells on coverslips were fixed in 4& (w/v) paraformaldehyde for 10minutes at room temperature. Following two washed with PBS, cells were permeabilised with 0.5% (v/v) Triton X-100 in PBS for 10 minutes at room temperature, before blocking with 1% (w/v) bovine serum albumin (BSA) diluted in PBS for 10 minutes at room temperature. Coverslpis were incubated with primary antibodies diluted in 1% BSA for 1 hour at room temperature. Coverslips were then washed three times with PBS before incubation with an appropriate secondary antibody (Table 2.2) diluted in 1% BSA for 1 hour at room temperature. After a further 3 washes with PBS, nuceli were stained with 4',6-diamidino-2-phenylindole (DAPI) before mounting onto glass slides using Polyvinyl alcohol mounting medium with DABCO® antifading reagent. Coverslips were imaged on a Delta Vision fluorescence microscope.

2.9 Widefield fluorescence microscopy

Fluorescent images were acquired on a Delta Vision [RT] (Applied Precision) restoration microscope using a 40x/ numerical aperture 0.85 Uplan Apo objective and the Sedat filter set (86000v2). The images were collected using a Coolsnap HQ (Photometrics) camera with a Z optical spacing of 0.2µm. All images were taken with constant exposure time between all the conditions of the same staining. Images were processed using ImageJ 1.49c.

2.10 Electric Cell Substrate Impedance Sensing

Time course analysis and resistance measurement was performed using an automated cell monitoring system, Electrical Cell-Substrate Impedance Sensing (ECIS 1600R, Applied Biophysics), as used in previous studies of podocyte function.[440] Differentiated podocytes were seeded at a density 25,000 cells per well onto 8W10E+ arrays (Applied Biophysics) coated with 10mM cysteine and 10µg/mL fibronectin. Each experiment measured the resistance in two 8W10E+ arrays, each 8W10E+ array contained five wells. The electrical resistance in each well was measured using ten electrodes. The resistance was measured at regular time intervals of 30 seconds.

3 Human podocytes respond directly to glucocorticoid exposure *in vitro*

3.1 Overview

Although glucocorticoid (Gc) therapy has been used for several decades to treat children with NS, the target cell and mechanism of action have never been clearly identified. The well-characterised immunosuppressive effects of glucocorticoids have previously been taken as indirect evidence that the therapeutically-relevant mechanism of action on the kidney involves an indirect effect via immune cells. More recently, data have emerged to demonstrate that glucocorticoids act directly on podocytes. For example, a murine podocyte cell line expresses key components of the GR complex, and GR-mediated signalling is intact following exposure to dexamethasone.[105] Additionally, human podocytes express GR *in vivo*,[104] and treating cultured murine podocytes with dexamethasone protects them from actin filament disruption.[109]

In this chapter, I demonstrate that the GR-signalling mechanism is intact in a human podocyte cell line following exposure to prednisolone (the GR-ligand used in clinical practice for the treatment of NS). Specifically, I show that: i) podocytes express GR and exposure to ligand reduces GR levels; ii) GR is phosphorylated at serine 211 following prednisolone exposure; iii) GR translocates to the nucleus following ligand activation and; iv) podocyte messenger RNA (mRNA) levels for a known Gc-regulated gene increase following prednisolone exposure. I also show that prednisolone has a direct protective effect on human podocytes, without immune cell involvement, by using electrical resistance across a monolayer of podocytes as a functional marker of barrier integrity.

3.2 Chapter-specific methods

3.2.1 Quantitative real-time polymerase chain reaction

Fully differentiated human, wild-type podocytes were treated with either prednisolone (1nM, 3nM, 10 nM, 30 nM, 100nM, or 1000nM) or vehicle (standard culture medium supplemented with 0.001% v/v methanol) for 6 hours. Total RNA was prepared using the RNeasy mini kit with on-column DNase I digestion (Qiagen). The concentration of the RNA was quantified using a Nanodrop ND1000 ultra low volume spectrophotometer (Lab Tech) and 1µg RNA per sample was used to prepare complementary DNA (cDNA) using a High Capacity RNA to cDNA kit, and was analysed using the Power SRBR Green PCR Master Mix (Applied Biosystems) on a StepOnePlus Real-Time PCR system (Life Technologies). Primers used for Glyceraldehyde 3-phosphate dehydrogenase (*GAPDH*) and Glucocorticoid-induced leucine zipper (*GILZ*), were obtained from the 10x QuantiTect Primer Assay (Qiagen). Relative expression levels were calculated using the ΔΔCT method, normalizing to GAPDH control.

3.3 Results

3.3.1 The podocyte GR-signalling pathway is functionally active *in vitro*

I first confirmed that human immortalised wild type podocytes express GR using western blotting (Figure 3.1). Exposure to the GR ligand prednisolone resulted in reduced GR expression by the 2 hour time point, a nadir of GR expression at 12 hours, followed by a gradual recovery in expression levels over the remaining 2 days of the experiment. Phosphorylation of GR at serine residue 211 peaked at the 2 hour time point following prednisolone exposure, and subsequently decreased until reaching a steady level at the 24 hour time point.

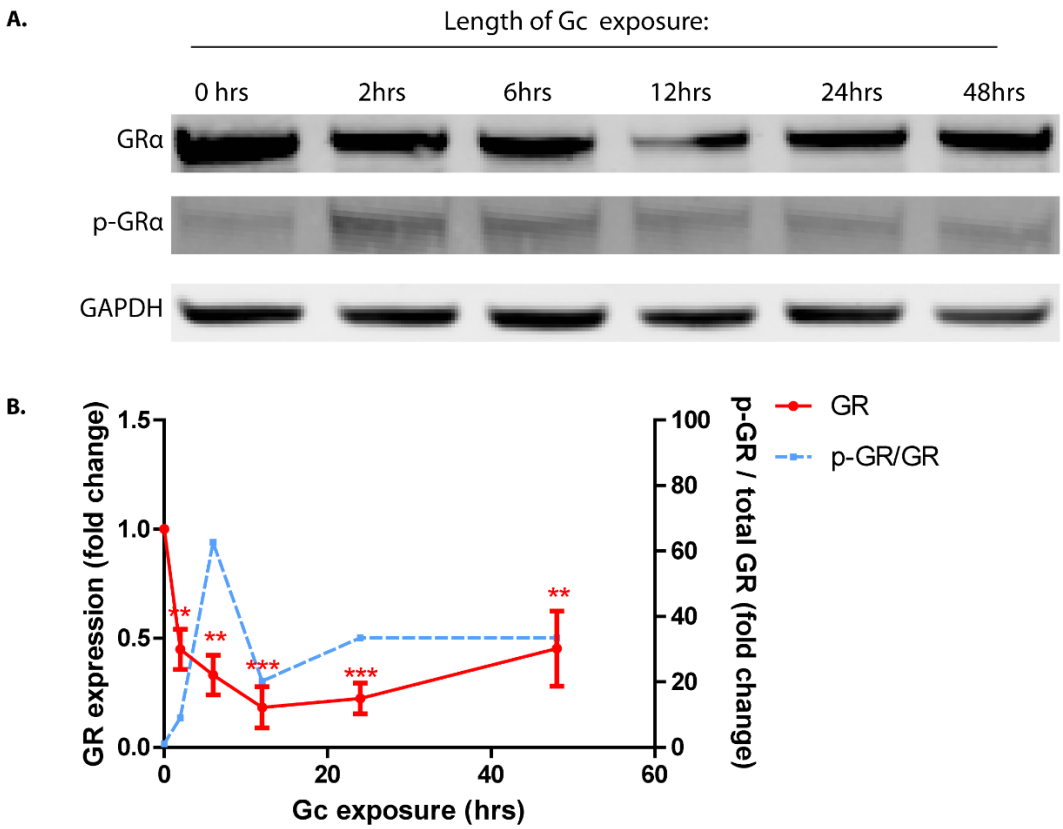

Figure 3.1 Podocyte GR expression and response to Gc exposure.

(A) Wild type podocytes express GRα as demonstrated by western blotting. Exposure to the GR-ligand prednisolone results in decreased GR expression. **(B)** Quantification of western blotting results. GR expression is reduced as early as 2 hours following prednisolone exposure. The solid red line represents the mean GR expression and error bars represent the standard error of the mean (SEM). Results were analysed by one-way ANOVA followed by Dunnett's multiple comparisons test. ** = adjusted p value <0.05 ; *** = adjusted p value <0.005. Blue line represents the mean GR phosphorylated at serine residue 211 divided by total GR. No significant difference in phospho-GR levels were found. The experiment was repeated 3 times (n=3).

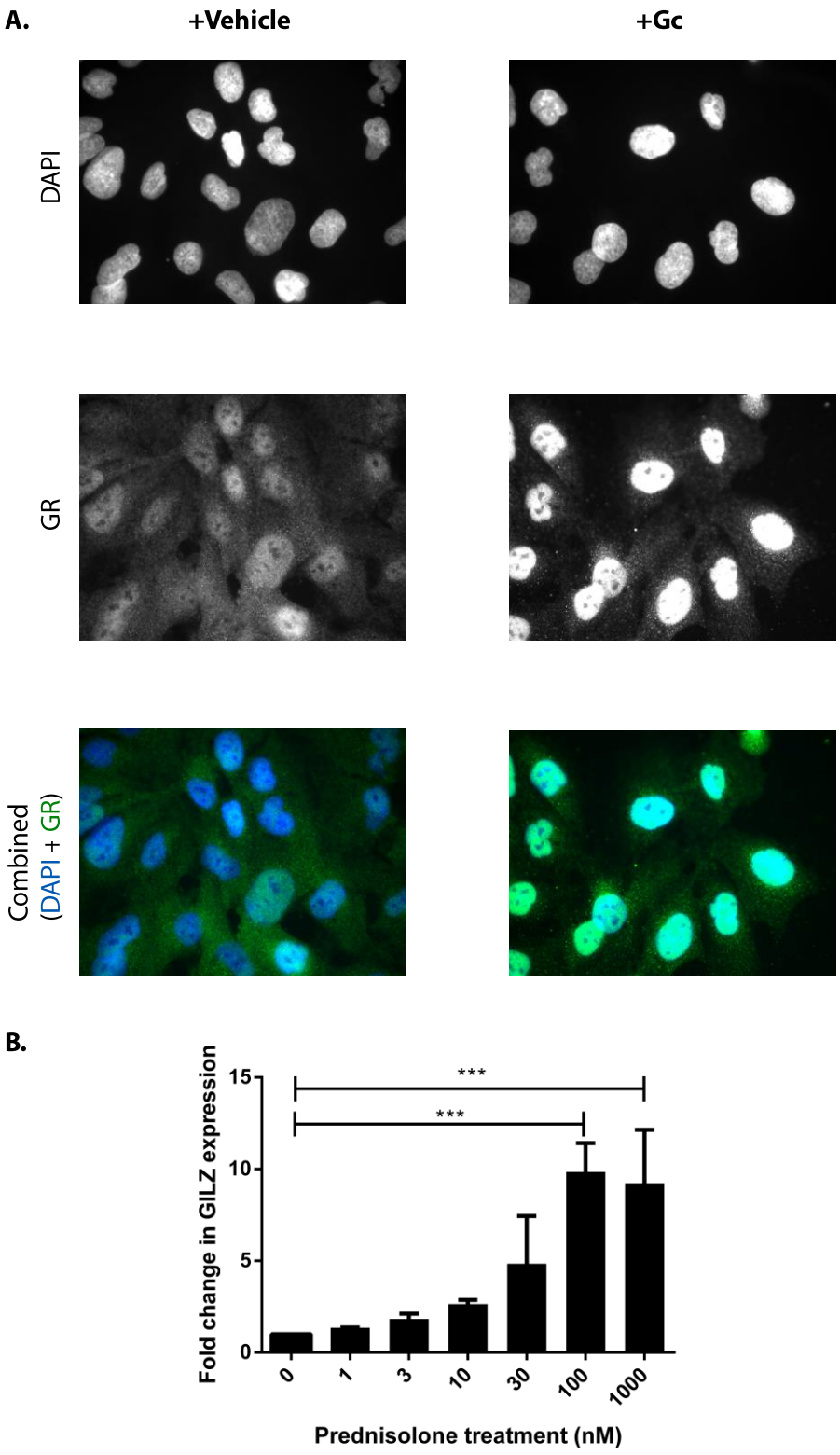

Figure 3.2 Ligand-dependent nuclear translocation of GR and transcriptional response.

(A) Immunofluorescence data demonstrating GR nuclear translocation following 3 hours of prednisolone exposure. **(B)** Graph showing fold change in messenger RNA (mRNA) levels for a known Gc-regulated gene, glucocorticoid-induced leucine zipper (*GILZ*), following exposure to different concentrations of prednisolone for 6 hours. mRNA levels were quantified using real-time polymerase chain reaction (qPCR). The experiment was performed three times. Results were analysed using one way ANOVA followed by Dunnet's multiple comparisons test.*** = adjusted p value <0.005. n=3.

Ligand-dependent translocation of GR into the nucleus was observed (**Figure 3.2**), as was a dose-dependent increase in levels of mRNA for a known Gc-regulated gene, glucocorticoid-induced leucine zipper (*GILZ*). In summary, these results demonstrate that the basic GR-signalling mechanism is intact in the human podocyte *in vitro*, and functionally active as shown by the transcriptional output elicited by prednisolone exposure.

3.3.2 Podocyte-specific GR isoform expression and MR levels

Next, I further characterised the human wild type podocyte cell line (AB) by examining the GR-isoform expression pattern in relation to three other cell lines: human glomerular endothelial cells (GEnC), human embryonic kidney 293 (HEK 293) cells, and adenocarcinomic human alveolar basal epithelial (A549) cells. Thus, wild type podocytes were compared with two other kidney cell lines, and another non-kidney cell line. **Figure 3.3-A** shows that total GR antibody identified three dominant GR isoforms in podocytes following western blotting of total cell lysate. The molecular weights corresponded to known GR isoforms, specifically: GRα (94kDa), GR-P (74 kDa), and GR-A (65 kDa).[441] AB podocytes were found to have higher GRα expression than GEnC cells (**Figure 3.3-B**), no statistically significant difference in GR-P expression levels were found between the four cell lines (**Figure 3.3-C**), and podocytes had higher GR-A expression levels than HEK 293 and A549 cells (**Figure 3.3-D**).

Many Gc ligands also have high affinity for MR. However, unlike GR, MR has a very tissue-specific distribution (see Section 1.6.1.3). Therefore, to investigate the possibility that some cellular effects of Gc-ligands may be mediated via MR in the podocyte, MR expression patterns were compared across the four cell lines (**Figure 3.3-E**). Only a very faint band was observed in podocytes, with HEK 293 cells showing 6 fold higher expression levels (**Figure 3.3–G**). It is therefore unlikely that Gc effects are mediated via MR in the wild type podocytes *in vitro*.

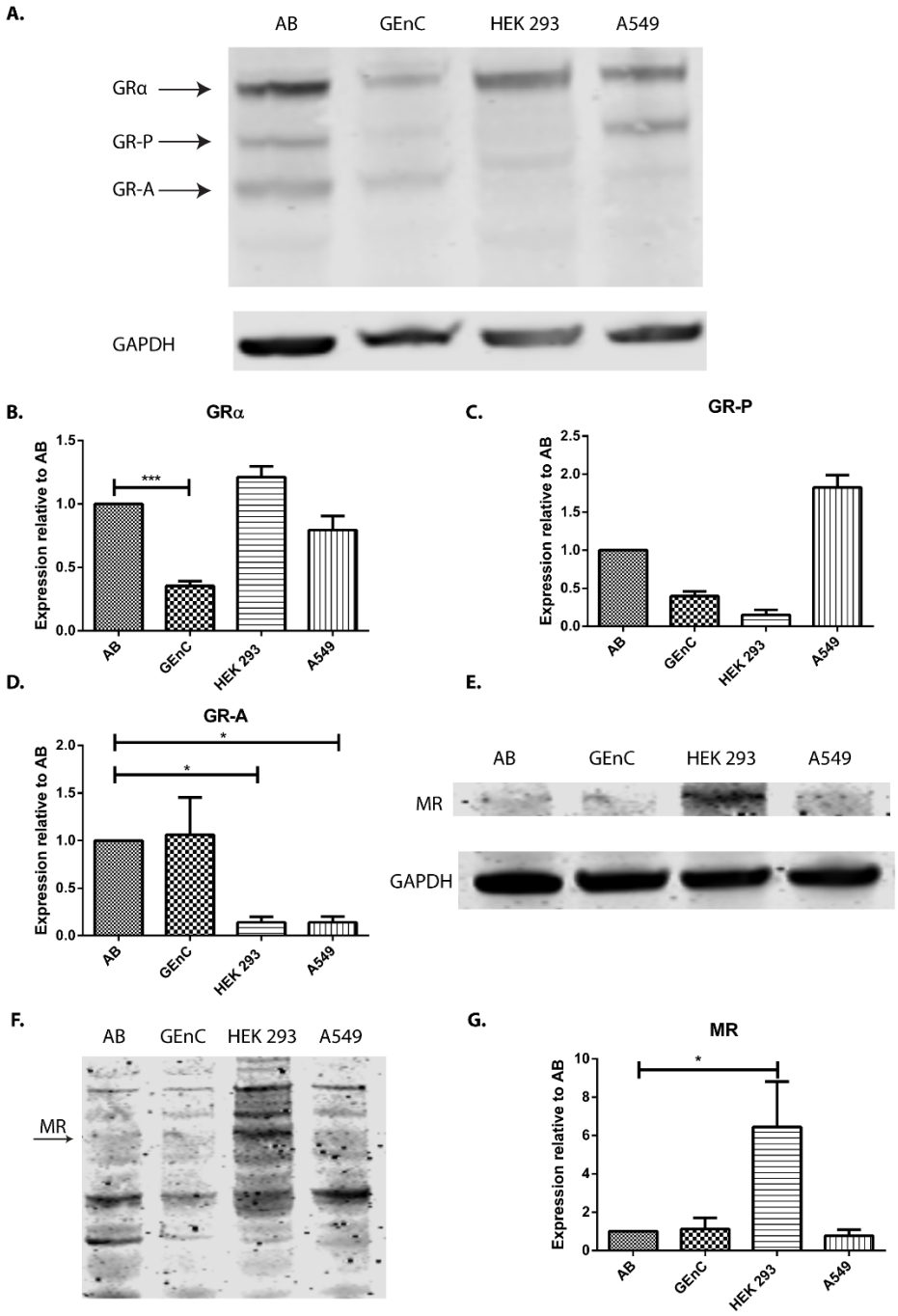

Figure 3.3 GR isoform and MR expression pattern in podocytes.
(A) Western blot demonstrating three dominant GR isoforms expressed by wild type podocytes (AB) in comparison to GEnC, HEK 293 and A549 cells. Quantification of GRα **(B)**, GR-P **(C)** and GR-A **(D)** expression patterns between the cell lines. Expression **(E)/(F)** and quantification **(G)** of mineralocorticoid receptor (MR) expression between the cell lines. Results analysed using one way ANOVA followed by Dunnett's multiple comparisons test. *=adjusted p value<0.05, ***=adjusted p value <0.005. For western blotting, all wells were loaded with 40µg of total cell lysate. n=3.

3.3.3 Prednisolone exerts a direct protective effect on human podocytes

After demonstrating that GR-signalling was intact in the podocyte cell line, I investigated the possibility that prednisolone has direct, protective effects against a damaging insult on podocytes, without the involvement of immune cells *in vitro*. In order to do this, I used an assay called Electric Cell-Substrate Impedance Sensing (ECIS). The assay consists of a series of wells with an electrode at the bottom of each well. When cells are added to the ECIS arrays and attached to the electrodes, they form a monolayer and act as insulators, increasing the electrical resistance. The data generated are resistance versus time. In the assay, electrical resistance is taken as a surrogate marker for monolayer or barrier integrity, with higher resistance corresponding to higher barrier integrity. In support of this approach, electrical charge across the glomerular filtration barrier (GFB) has been shown to be an integral component of a functioning renal filtration system (see Section 1.2.2.3).

I chose to use the well-characterised puromycin aminonucleoside (PAN)-model of podocyte damage for use in the ECIS assay. This model is used both *in vitro* and *in vivo*. Following PAN administration to rats, podocyte injury is manifest by podocyte effacement, reduction of charge across the GFB and proteinuria.[442] I first confirmed that the *in vitro* dose of PAN frequently described in the literature (5.0 μg/mL) did produce disruption of the podcyte actin cytoskeleton.[109] **Figure 3.4** shows that the well-defined actin fibres apparent in the vehicle-treated podocytes are lost in podocytes treated with PAN for 24 hours, confirming the efficacy of this dose of PAN.

Following plating of podocytes into the wells of the ECIS array, the resistance across the cell monolayer markedly increased (**Figure 3.5-B**). Cells were subsequently treated with culture medium containing either vehicle alone, prednisolone alone, PAN alone, or PAN and prednisolone together. The subsequent changes in resistance reflect changes in cell morphology and the nature of the cell-electrode attachments. As expected, the resistance across cells treated with PAN alone markedly decreased, signifying podocyte damage. Cells treated with prednisolone alone showed higher resistance than vehicle-treated cells. Interestingly, Gc exposure seemed to provide some protective effect against PAN-damage, as demonstrated by the higher resistance recorded for PAN/Gc cells compared to cells treated with PAN alone (**Figure 3.5-A**).

3.4 Discussion

The target cell of action of Gc therapy in NS unclear. In this project, I propose that podocytes are the target of Gc action. In this chapter, I investigated whether human podocytes *in vitro* can respond directly to Gc exposure, and whether this exerts a functionally protective effect in a PAN-model of podocyte damage. Prior to this investigation, it had already been established that podocytes express GR in homogenates of isolated normal human glomeruli.[104] Key components of the GR signalling pathway were shown to be expressed in a murine podocyte cell line, and it was demonstrated that the GR signalling pathway can be activated by the GR-ligand dexamethasone.[105] It was also known that wild type human podocytes express GR.[102]

In this chapter I demonstrated that the GR signalling pathway is intact in human podocytes following exposure to the GR-ligand prednisolone. I also demonstrated homologous regulation of GR expression levels by prednisolone (**Figure 3.1-A**), with GR levels reduced by 55% compared to baseline after only 2 hours of Gc exposure, and maximal downregulation occurring at 12 hours of exposure. Several studies investigating the impact of Gc-ligand on GR expression have been performed but most have focussed on GR messenger RNA (mRNA) levels rather than protein levels. The vast majority of reports suggest Gc-ligand downregulates GR expression. In a study by Rosewicz *et al.* from 1988, dexamethasone maximally decreased GR mRNA levels to 43% of control after 6 hours of incubation with dexamethasone in human IM-9 lymphocytes, whereas in AR42J rat pancreatic cells mRNA levels were maximally decreased to 50% of control after 12 hours.[443] Incubation with dexamethasone for up to 72 hours caused no further down-regulation. In another study using mouse AtT-20 pituitary tumour cells treated with the GR-ligand triamcinolone acetonide, GR mRNA levels decreased to approximately 60% of control levels at 4 hours of treatment, 48% of control levels at 48 hours of treatment, and then increased slightly to 67% at 72 hours.[444] Interestingly, the authors also performed a series of *in vitro* studies demonstrating that GR is degraded in an ATP-dependent manner, suggesting a role for the ubiquitin proteolytic pathway. One study found that homologous regulation of GR may be cell type specific: dexamethasone caused an upregulation of GR mRNA in

human CEM-C7 T-lymphoblast cells, but a downregulation of GR mRNA in IM-9 lymphocytes.[445]

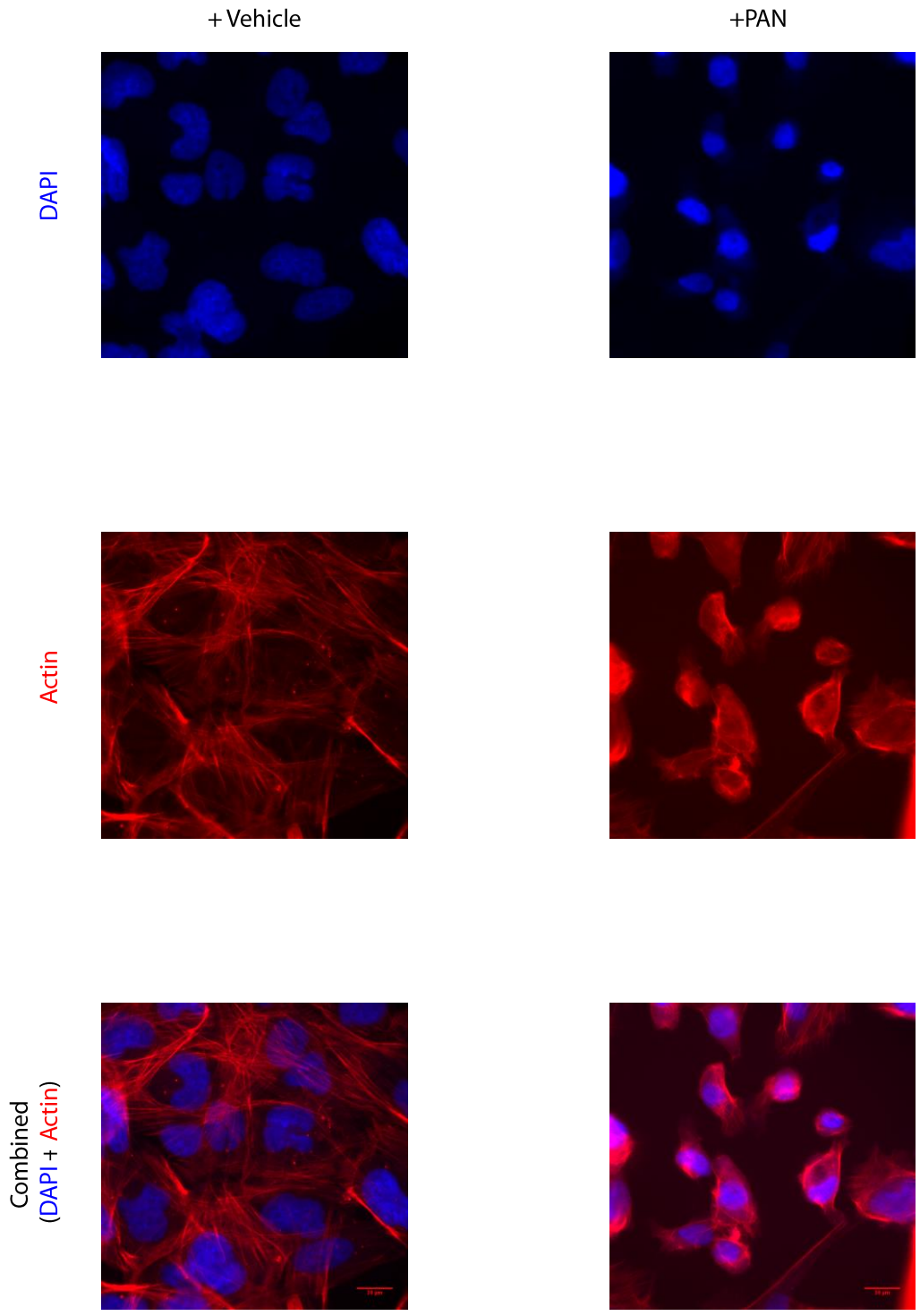

Figure 3.4 The effect of puromycin aminonucleoside (PAN) treatment on podocytes

Human podocytes were cultured in growth medium containing either vehicle or 5.0µg/mL of PAN. Immunofluorescence staining was performed using 4',6-diamidino-2-phenylindole (DAPI) for nuclear staining, and Texas Red-X phalloidin F-actin dye. Scale bars are included on the bottom right of the combined images.

Figure 3.5 Direct Gc effect on podocyte barrier integrity

Direct effects of prednisolone on a monolayer of podocytes were investigated using Electric Cell-Substrate Impedance Sensing (ECIS) which measures resistance across a monolayer of podocytes over time. Higher resistance is a surrogate marker for higher barrier integrity. **(A)** shows combined data from 3 separate experiments, normalised to the vehicle control. Data was analysed using one way ANOVA followed by Tukey's multiple comparison test. ***= adjusted p value <0.0001. The grey dotted line surrounding each continuous coloured line denotes the standard error of the mean (SEM). **(B)** shows a single, representative experiment with the time of cell plating and cell treatment labelled.

Later studies looked directly at GR protein levels. Sathiyaa *et al.*, exposed primary cultures of trout hepatocytes to cortisol and found a significantly decreased GR protein content at 24 hours of treatment (no earlier time points were examined).[446] In a murine podocyte cell line, the effect of dexamethasone on GR protein expression was examined at the 2 hour and 24 hour time point. Although no statistically significant difference in GR protein expression was observed at 2 hours, levels were significantly lower at 24 hours.[105] This decrease in GR protein level occurred without a change in GR mRNA level, suggesting post-transcriptional processes are responsible for autologous GR degradation. Xing *et al.*, presented data using the human podocyte cell line used in the current study.[102] The group examined a single time point at an extended 14 days of culture in dexamethasone-containing medium and surprisingly found an upregulation of GR expression levels. The discrepancy with the data presented here may be due to the different length of the time course examined (48 hours compared to 2 weeks).

Further work examining the mechanism of the ligand-dependent reduction in GR levels has been performed in COS-1 (African Green monkey kidney) cells, which showed that GR protein levels fall to 42% of control levels after 12 hours of treatment with dexamethasone (no earlier time point was examined), and this downregulation was blocked by a proteasome inhibitor.[301] This implicates the ubiquitin-proteasome mediated degradation pathway as an important system in controlling GR expression levels. Interestingly, phosphorylation of GR may be a key-step in initiating this process as mutation of all phosphorylation sites in GR increased receptor half-life and abolished ligand-dependent downregulation.[230]

Figure 3.1 shows a peak of GR phosphorylation at serine residue 211 at 2 hours following exposure to prednisolone. As described in Section 1.6.4, phosphorylation of human GR at serine 211 is induced by ligand binding, and is also associated with increased transcriptional activity of GR, and translocation to the nucleus.[230] Results from the present study are consistent with data from the murine podocyte cell line, which showed at peak in phosphorylation at serine 220 at the 2 hour time point following dexamethasone exposure.[105] Further data presented here suggesting the GR-signalling pathway is intact in human podocytes includes the demonstration of GR

translocation from the cytoplasm to the nucleus, and activation of transcriptional output of a known Gc-responsive gene following exposure to GR-ligand (**Figure 3.2**).

The vast majority of *in vitro* studies have used dexamethasone as the GR-ligand. I was unable to identify any *in vitro* studies involving podocytes where prednisolone was used. Key studies investigating the effects of dexamethasone on cells *in vitro* have used a wide range of concentrations from 0.01μM [109] to 100 μM.[105] However, the most commonly used concentration is 100nM (0.1μM).[447-450] A pharmokinetic study found the mean peak plasma concentration of prednisolone in children with NS following an oral dose of the pro-drug prednisone was 0.1μM.[245] However, in another study involving 11 children with relapsed steroid-sensitive NS, the mean peak serum concentrations of prednisolone following an intravenous (prednisolone) bolus was approximately 3μM.[451] *In vivo*, it is unclear how the plasma concentration of prednisolone relates to the Gc concentration of the ultrafiltrate surrounding the podocyte, and how the 11 beta-hydroxysteroid dehydrogenase system affects this (see Section 1.6.1.2). As the most common *in vitro* dose of dexamethasone used in the literature is 0.1μM, and dexamethasone has been shown to be a ten-fold more potent GR-agonist than prednisolone in luciferase transactivation assays (see Section 1.6.1.3),[263] a dose of 1μM prednisolone was used in the current study, unless otherwise stated.

In this chapter, I characterised the GR isoform expression profile of human wild type podocytes for the first time (**Figure 3.3**). It is already known that one single human GR gene produces several GR isoforms through a combination of alternative splicing and alternative translation initiation. Although GRα is the dominant, ubiquitously expressed isoform, the other variants have differing tissue distribution patterns and transcriptional regulatory patterns, and this may play a role in the cell-specific response to glucocorticoids.[268, 452] By performing western blotting on total cell lysate from human podocytes, I identify bands corresponding to GR-P (74 kDa) and GR-A (65 kDa) in addition to GRα. GR-A and GR-P both have low transactivation activities and the manner in which these may interact with GRα to control podocyte-specific responses to Gc exposure is incompletely understood at present.[441] GR-P has been identified in normal lymphocytes as well as several haematological tumour cells.[453] There is controversy regarding its role in Gc-sensitivity, with some studies suggesting that it may contribute to a Gc-resistant phenotype,[454] and others providing evidence that GR-P

can enhance the activity of GRα.[455] One study examining GR-A in human myeloma cells suggested high expression levels may be associated with Gc-resistance.[453]

GR-ligands typically also have high affinity for MR. However, unlike GR, MR has a tissue-restricted expression pattern (section 1.6.1.3). For example, within the kidney, MR expression is found at high levels in the distal nephron, but several studies have demonstrated that MR is not present in the human,[255, 261] and rabbit glomerulus.[261] **Figure 3.3** confirms the finding that podocytes express only low levels of MR. These data suggest MR has a limited role in mediating the effects of Gc-ligand within the glomerulus. However, definitive data to support this would require the use of a MR-antagonist.

Although direct protective effects of Gc exposure on the murine podocyte actin cytoskeleton *in vitro* have been demonstrated previously,[109] here I use the ECIS assay to demonstrate that prednisolone exposure protects human podocytes from PAN-induced damage, by using electrical resistance across a cell monolayer as a surrogate marker of barrier integrity. This approach is strengthened by the recent insights suggesting charge across the GFB *in vivo* contributes to normal functioning of the renal filtration system (see Section 1.2.2.3). **Figure 3.5** shows that Gc exposure increases resistance across the podocyte cell layer compared to vehicle-treated cells in the unchallenged state, and also provides protection against PAN-induce damage. This demonstrates that, *in vitro*, Gc exposure can protect podocytes directly against a damaging insult causing proteinuria *in vivo*, without involvement of immune cell mediators. In the following chapters, I will provide data suggesting mechanisms underpinning this podocyte-protective effect.

4 Glucocorticoid-regulated changes in podocyte transcriptional output

4.1 Overview

The mechanism(s) whereby Gc-exposure results in beneficial clinical effects and altered podocyte function remain poorly understood. GR is a transcription factor which is activated by Gc-ligand binding, and this is the dominant signalling pathway whereby glucocorticoids exert biologically-relevant actions.[456] In order to provide mechanistic insight to understand Gc-effects on podocytes *in vitro*, I used microarray expression analysis to identify Gc-regulated genes. Target genes subsequently underwent gene ontology analysis to reveal key biological functions regulated by Gc-exposure. From the biological functions identified by this analysis, I aimed to gain insight into mechanisms underpinning the protective effect observed in podocytes following Gc-exposure.

Analysis of the microarray data highlighted some already well-characterised effects of Gc exposure such as regulating apoptosis,[457] providing confidence the dataset was robust. However, the anlaysis also revealed that Gc treatment exerted prominent effects on genes regulating cellular motility. As described in Section 1.3.4, podocyte hypermotility is associated with glomerular barrier dysfunction, and the microarray results suggest that reversing the hypermotility phenotype may be a novel mechanism whereby Gc-exposure exerts podocyte-protective effects.

4.2 Chapter-specific methods

4.2.1 Microarrays

Fully differentiated human wild type podocytes cultured in RPMI 1640 medium (see Section 0) were treated with 1µM prednisolone or an equal volume (0.001%,v/v) of methanol as a vehicle control for 5 hours at 37ºC. Total cellular RNA was isolated using the RNeasy mini kit with on-column DNase I digestion (Qiagen). RNA integrity was assessed by a Nanodrop ND100 ultralow volume-spectrophotometer (Lab Tech) followed by a 2100 Bioanalyser (Agilent). Only samples with an absorbance 260nm/280nm ratio 1.9-2.1 were processed further. Sample processing was performed by Michal Smiga of the Genomic Technologies Core research facility (University of Manchester). Total RNA from each sample was used to prepare biotinylated fragmented complementary RNA according to the GeneChip® Expression Analysis Protocol (Affymetrix). GeneChip® Human Genome U133A Plus 2.0 Array were hybridised and scanned using the GeneArray® 2500, according to the GeneChip® Expression Analysis Protocol (Affymetrix). Treatments were done in triplicates and the same batch of microarrays was used for all treatments.

4.2.2 Data Analysis

Technical quality control and outlier analysis was performed with dChip (V2005) (www.dchip.org)[458], using the default settings. Background correction, quantile normalization, and gene expression analysis were performed using RMA in Bioconductor.[459] To establish relationships and compare variability between patients, principal components analysis (PCA) was used since this method is able to reduce the effective dimensionality of complex gene-expression space without significant loss of information.[460] PCA was performed with Partek Genomics Solution (version 6.5, Copyright 2010, Partek Inc.) Differential expression analysis was performed using Limma using the functions lmFit and eBayes.[461] Gene lists of differentially expressed genes were controlled for false discovery rate (fdr) errors using the method of q value.[462] Probsets were selected for further analysis if the fold-change was >1.5 and q value <0.05. Gene ontology anlaysis was performed using Ingenuity® Pathway Analysis software.

4.3 Results

4.3.1 Initial processing of microarray data

In order to understand Gc-effects on the podocyte *in vitro*, the transcriptional output of fully differentiated wild-type human podocytes following a 5 hour treatment with either prednisolone or vehicle was performed using whole-genome Affymetrix U133 Plus 2.0 Arrays. The 5 hour time point was chosen to ensure primary-response genes were analysed.[107] Triplicate samples for each condition were analysed. Probe intensity levels were similar between all arrays as shown by the box-plot in in **Figure 4.1-A** and the close overlap between arrays in the histogram in **Figure 4.1–B**. These results suggest none of the arrays contained a spacial artifact or abnormally high background interference. Principal component analysis revealed a clear separation between prednisolone- and vehicle-treated samples (**Figure 4.1-C**). These results indicated good technical quality of the data, and therefore indicated that further analysis was warranted.

In order to derive a list of Gc-regulated genes, transcripts showing a fold change of >1.5 fold (either up or down) and a q-value of <0.05 were considered to be significantly altered between vehicle and Gc conditions, in line with other Gc-microarray studies.[107, 463] The volcano plot in **Figure 4.2-A** shows the distribution of Gc-regulated transcripts in relation to the total transcript population detected. This cut-off resulted in 606 significantly altered transcripts/probe set identifiers (ids) corresponding to 397 unique genes [full details in Compact Disc 1 (back cover insert)]. The difference between 606 and 397 is due to probe-set redundancy, as shown in **Figure 4.2**. 267/397 genes were upregulated, while 130/397 showed reduced expression following treatment with Gc (**Figure 4.2-C**).

The list of 397 Gc-regulated genes was analysed using Ingenuity Pathway Analysis® (IPA®) software. IPA software is underpinned by the Ingenuity® Knowledge Base, which is a highly curated repository of biological interactions, allowing modelling of relationships between observed, experimental transcriptional changes and how these may impact biological functions *in vivo* and *in vitro*.

IPA® also can also independently identify upstream regulators and predict whether they are activated or inhibited, given the observed gene expression changes in the experimental dataset. The expected causal effects are derived from the literature compiled in the Ingenuity® Knowledge Base. The analysis examines the known targets

of each upstream regulator (UR) in the data submitted by the user, and compares the targets' actual direction of change to the predicted direction of change derived from the literature, then issues a prediction for each upstream regulator. An 'upstream regulator' in this context covers the range of molecules found in the literature, including transcription factors, cytokines, microRNAs, kinases chemicals and drugs. For each potential UR two statistical measures, an overlap p-value and activation z-score are computed. The overlap p-value identifies likely upstream regulators based on significant (p value <0.01) overlap between dataset genes and the genes that are regulated by a regulatory molecule. The activation z-score is used to infer the activation states of predicted upstream regulators (ie, whether the observed transcriptional dataset is best explained by activation or inhibition of a particular regulator). When the list of Gc-regulated genes from the current study were analysed in IPA®, activated GR was clearly identified as the UR which best explained the gene changes observed in the dataset, with a p-value of overlap of $3x10^{-12}$ and an z-activation score of 4.1 (**Table 4.1**). This provided further confidence that the dataset was suitable for further analysis, and reflected changes caused by GR activation. The top 10 most upregulated and downregulated genes are listed in **Table 4.2**.

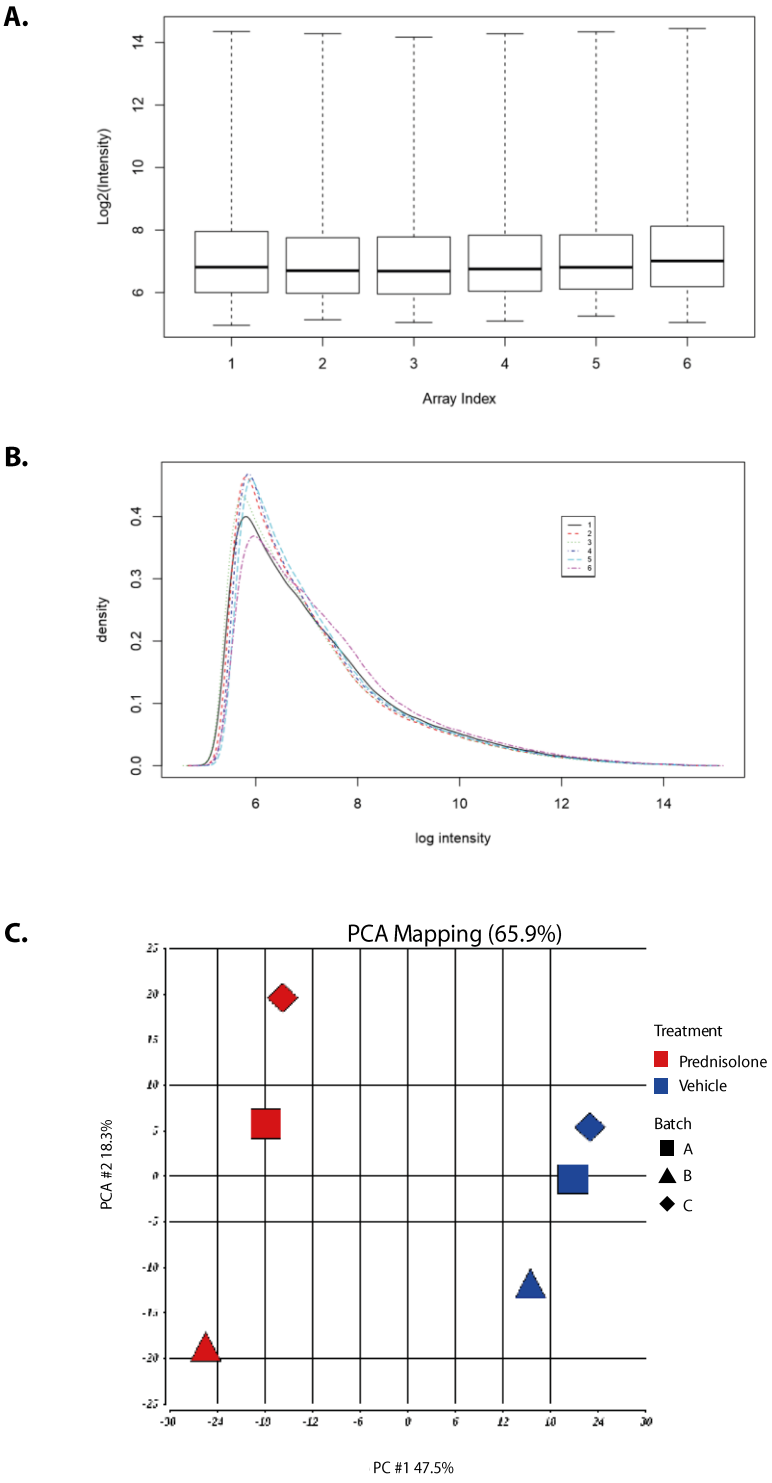

Figure 4.1 Quality control of microarray data
Microarray analysis using biotin-labelled complementary RNA derived from human podocytes following 5 hour treatment with either vehicle (arrays 1,3,5) or prednisolone (arrays 2,4,6) was performed using Affymetrix U133 Plus 2.0 arrays. **(A)** boxplot comparing probe intensity levels between arrays of the dataset. Either end of the box represents the upper and lower quartile. The line in the middle of the box represents the median. Horizontal lines connected to the box by 'whiskers' indicate the largest and smallest values not considered outliers. **(B)** histogram of probe density compared to probe intensity. **(C)** Principal component analysis (PCA) of array data.

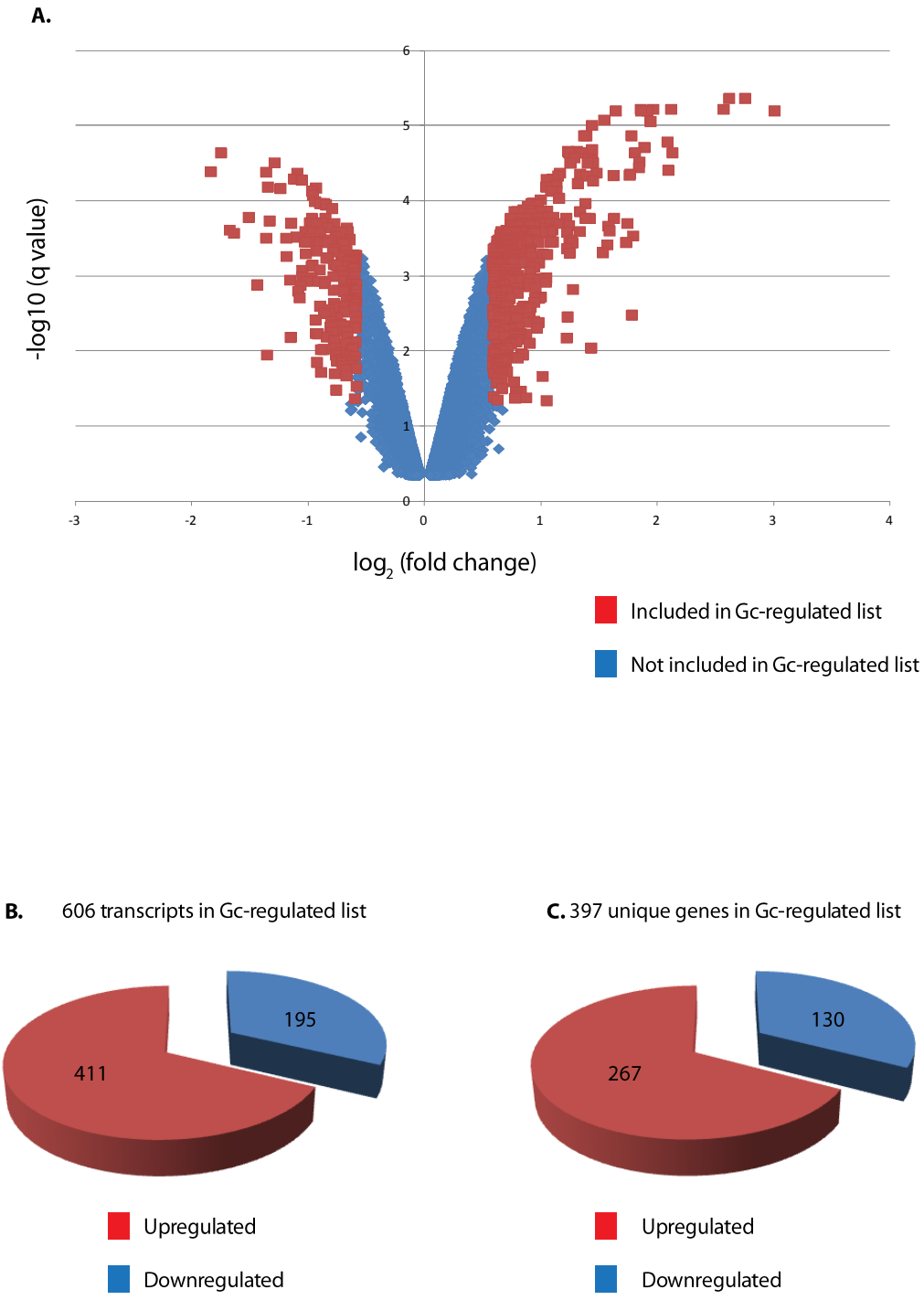

Figure 4.2 Identification of Gc-regulated genes

A fold-change in transcript expression of ±1.5 and a q-value of <0.05 between vehicle- and prednisolone-treated samples was considered significant, and this defined the list of Gc-regulated genes. **(A)** is a volcano plot showing the distribution of Gc-regulated transcripts. **(B)** and **(C)** are pie-charts showing the number of Gc-regulated transcripts and unique genes, respectively.

Table 4.1 Upstream regulator analysis using IPA® software

A list of 397 genes identified as being 'Gc-regulated' following microarray analysis from samples obtained from wild type podocytes underwent analysis using IPA® to independently identify likely upstream regulators. Overlap p-values are used to quantify the significance of overlap between dataset genes and genes known to be regulated by different upstream regulators. Activation z-scores infer the likely activation state of regulators. This analysis was performed to understand which regulators would be most likely to cause the transcriptional changes observed in the dataset, using data from existing literature. GR was the regulator most likely to cause the observed changes, suggesting that the dataset is a valid list of Gc-regulated genes, and warranted further analysis. NP=not predicted (insufficient/conflicting data).

Upstream Regulator	**Molecule Type**	**Predicted Activation State**	**Activation z-score**	**p-value of overlap**
NR3C1 (Glucocorticoid receptor)	Ligand-dependent nuclear receptor	Activated	4.149	3.00E-12
NFKBIA (Nuclear factor of kappa light polypeptide gene enhancer In B-cells inhibitor, alpha)	Transcription regulator	NP	0.064	4.00E-09
STAT3 (Signal transducer and activator of transcription 3)	Transcription regulator	NP	0.104	5.31E-09
NR3C2 (Mineralocorticoid receptor)	Ligand-dependent nuclear receptor	NP	1.213	6.48E-09
PGR (Progesterone receptor)	Ligand-dependent nuclear receptor	Activated	2.338	1.06E-08
CTNNB1 [Catenin (Cadherin-Associated Protein), Beta 1]	Transcription regulator	NP	0.942	1.38E-08
EZH2 (Enhancer Of Zeste 2 Polycomb Repressive Complex 2 Subunit)	Transcription regulator	NP	-0.756	3.18E-08
FOXL2 (Forkhead Box L2)	Transcription regulator	NP	-0.451	2.12E-07
JUN (Jun proto-oncogene)	Transcription regulator	Np	-1.347	5.64E-07
NFKB1 (Nuclear Factor Of Kappa Light Polypeptide Gene Enhancer In B-Cells 1)	Transcription regulator	NP	0.095	6.38E-07

Table 4.2 Genes showing largest changes in transcription following Gc exposure

Microarray analysis was performed on human podocytes following 5 hour exposure to either vehicle prednisolone. **(A)** shows genes that were mostly highly upregulated ; **(B)** shows genes that were most strongly downregulated.

A.

Gene Symbol	Gene Name	Fold change
AREG	Amphiregulin	↑ 8.028
PDK4	Pyruvate Dehydrogenase Kinase, Isozyme 4	↑ 6.738
KIAA1211L	Uncharacterized Protein KIAA1211-Like	↑ 6.126
CCL20	Chemokine (C-C Motif) Ligand 20	↑ 4.375
GILZ	Glucocorticoid-Induced Leucine Zipper Protein	↑ 4.339
NPR3	Natriuretic Peptide Receptor 3	↑ 4.265
FKBP5	FK506 Binding Protein 5	↑ 4.248
SLC46A3	Solute Carrier Family 46, Member 3	↑ 3.899
IRS2	Insulin Receptor Substrate 2	↑ 3.762
HPGD	Hydroxyprostaglandin Dehydrogenase 15-(NAD)	↑ 3.696

B.

Gene Symbol	Gene Name	Fold Change
IL11	Interleukin 11	↓ 3.365
KRTAP1-1	Keratin Associated Protein 1-1	↓ 3.192
TRPC4	Transient Receptor Potential Cation Channel, Subfamily C, Member 4	↓ 3.115
KMO	Kynurenine 3-Monooxygenase (Kynurenine 3-Hydroxylase)	↓ 2.852
MAB21L3	Protein Mab-21-Like 3	↓ 2.710
IL1A	Interleukin 1, Alpha	↓ 2.570
KCTD4	Potassium Channel Tetramerization Domain Containing 4	↓ 2.519
TNFRSF11B	Tumor Necrosis Factor Receptor Superfamily, Member 11b	↓ 2.361
CYP1B1	Cytochrome P450, Family 1, Subfamily B, Polypeptide 1	↓ 2.280
C4orf26	Chromosome 4 Open Reading Frame 26	↓ 2.276

4.3.2 Genes involved with tissue damage

The list of 397 Gc-regulated genes underwent toxicology analysis using IPA® software to identify those genes involved in organ-specific tissue damage (in either a protective or deleterious manner). The IPA® Knowledge Base contains a database of molecules known to be involved with particular types of organ toxicity. Understanding which Gc-regulated genes identified in my dataset have known roles in preventing (or causing) kidney damage may help to develop an understanding of mechanism underpinning the Gc-mediated protective effects on the kidney.

A key aspect of IPA® is its ability to predict the direction of change in a given biological function elicited by changes in expression of particular genes using the curated IPA® Knowledge Base, which is quantified by the z-score. In this context, if an activating molecule of a particular biological process had increased gene expression, that biological process would be expected to be enhanced (positive z-score). Conversely, if an inhibitory molecule of particular biological process had increased gene expression, that biological process would be expected to be reduced (negative z score). IPA® only makes predictions concerning the direction of change in biological processes with activation scores either ≤ 2 or ≥ 2.

Genes from the Gc-regulated list identified by IPA® as having roles in kidney-specific damage are shown in **Table 4.3**. **Figure 4.3** represents the tissue-type and disease processes with which genes from the dataset involved with tissue damage are involved. The top-ranking kidney-specific terms are 'glomerular injury,' 'kidney failure' and 'renal fibrosis.' In order to ascertain whether effects on the kidney were predicted to be beneficial or damaging, pathway analysis was performed (**Figure 4.4**). This analysis links changes in experimentally-observed gene expression to predictions in changes of biological function. IPA predicted the changes in expression levels observed in the microarray dataset would have effects on six kidney-related terms (ie, z-activation score ≤ 2 or ≥ 2): all six kidney toxicology terms were predicted to be inhibited (exact activation z-scores are provided in **Table 4.3**). These data further underscore the protective effects of Gc-exposure on the kidney.

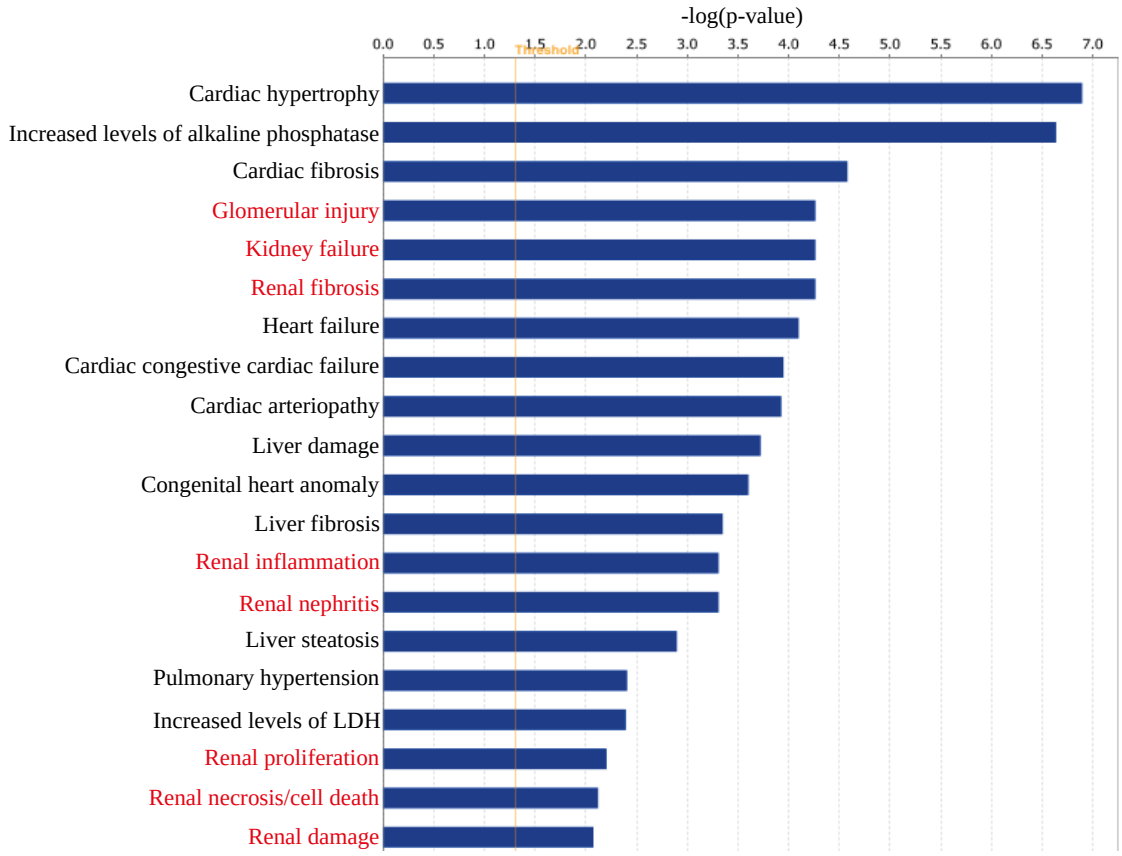

Figure 4.3 Predicted effects of microarray-determined transcriptional changes on organ toxicity

Gc-regulated genes were identified by microarray analysis on human wild type podocytes. The IPA® Knowledge Base contains a dataset of genes known to be involved with various types of organ-damage (toxicology lists). To understand if the genes identified in the microarray had known roles in specifically reducing *kidney* damage, the dataset was analysed to produce a list of organ-specific toxicology terms known to be affected by the genes in the dataset. The bar chart displays these terms in order of statistical significance. Terms in red denote kidney-related terms. The orange line denotes a threshold significance value corresponding to a p-value of 0.05.

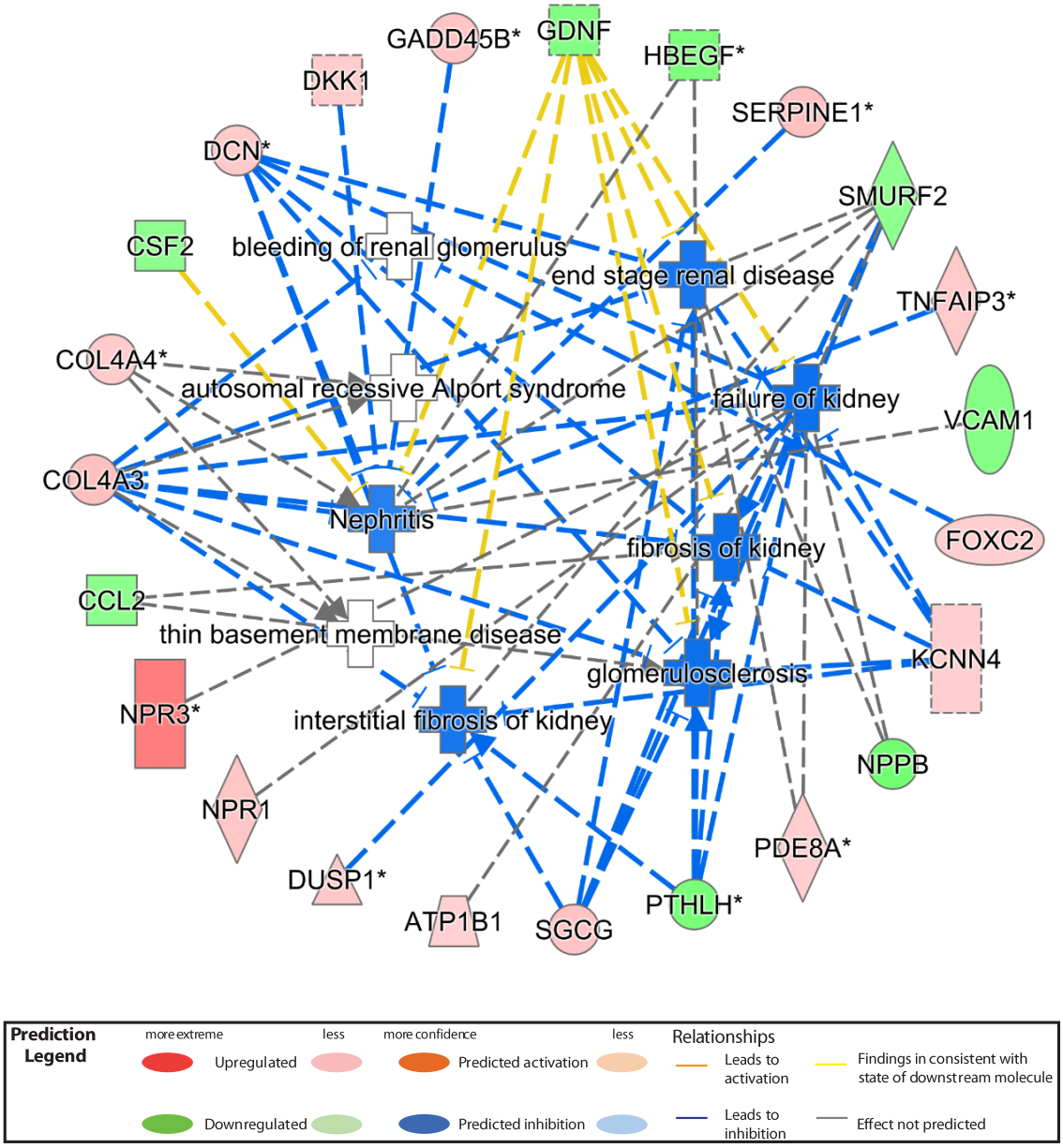

Figure 4.4 Pathway analysis for kidney-specific toxicology terms

IPA® software was used to predict whether the transcriptional changes observed in the microarray dataset would have beneficial or deleterious effects on kidney function. Gc-regulated genes from the dataset, identified using IPA® Knowledge Base as having a role in kidney damage, are displayed around the outside circle. Toxicology-terms are displayed in the central circle. Out of the nine toxicology terms identified, changes observed in the microarray dataset were predicted to have a beneficial effects on six of them (coloured blue) ; IPA did not make a prediction about the change in direction of the remaining two terms (coloured white).

Table 4.3 Gc-regulated genes involved with kidney damage

Gc-regulated genes from the microarray dataset underwent analysis using the toxicology component of IPA® software. This table lists specific Gc-regulated genes involved with each kidney-specific term, the level of significance, and the activation z-score which provides an *in silico* prediction of whether the gene expression changes observed experimentally would be damaging (positive activation z-score) or beneficial/protective (negative activation z-score). N.P.=Not predicted/insufficient data.

Categories	**Diseases or Functions Annotation**	**p-Value**	**Activation z-score**	**Molecules**
Glomerular Injury, Kidney Failure, Renal Fibrosis	interstitial fibrosis of kidney	5.43E-05	-1.698	COL4A3,DCN,GDNF,KCNN4,PTHLH,SGCG, SMURF2
Glomerular Injury, Renal Fibrosis	fibrosis of kidney	2.26E-04	-1.969	CCL2,COL4A3,DCN,GDNF,KCNN4,PTHLH, SGCG,SMURF2
Renal Inflammation, Renal Nephritis	autosomal recessive Alport syndrome	4.89E-04	N.P.	COL4A3,COL4A4
Renal Inflammation, Renal Nephritis	thin basement membrane disease	4.89E-04	N.P.	COL4A3,COL4A4
Kidney Failure	end stage renal disease	7.57E-04	-1.698	COL4A3,DCN,GDNF,KCNN4,NPPB,PDE8A, PTHLH,SGCG,SMURF2
Kidney Failure	failure of kidney	1.45E-03	-1.941	ATP1B1,COL4A3,DCN,DUSP1,GDNF,KCNN4, NPPB,NPR1,NPR3,PDE8A,PTHLH,SGCG,SMURF2

Glomerular Injury	glomerulosclerosis	1.77E-03	-1.968	CCL2,COL4A3,DCN,GDNF,HBEGF,KCNN4, PTHLH,SGCG,SMURF2
Glomerular Injury	bleeding of renal glomerulus	2.85E-03	N.P.	COL4A3,FOXC2
Renal Inflammation, Renal Nephritis	Nephritis	4.99E-03	-1.429	COL4A3,COL4A4,CSF2,DCN,DKK1,GADD45B, GDNF,HBEGF,SERPINE1,SMURF2,TNFAIP3, VCAM1
Renal Proliferation	proliferation of glomerular cells	6.23E-03	-1.98	DCN,DUSP1,IL1B,PLAU,PTHLH
Renal Proliferation	proliferation of kidney cells	6.33E-03	-1.446	DCN,DUSP1,GDNF,IL1B,PLAU,PTHLH
Renal Inflammation, Renal Nephritis	tubular nephritis	6.92E-03	N.P.	COL4A3,DCN
Renal Necrosis/Cell Death	cell death of kidney cells	7.56E-03	-0.345	AREG,BCL2A1,BIRC3,CFLAR,CRYAB,DCN, DUSP1,EMP1,HIPK2,IL1B,PTHLH,RASSF4, SLC47A1,TCF4,TNFRSF19,TNFSF10,UNC5A
Renal Damage	damage of kidney	8.41E-03	0	DKK1,DUSP1,HBEGF,IL1R1,ITGB6,POU2F2, RGCC,SERPINE1
Glomerular Injury	formation of glomerular crescent	9.29E-03	N.P.	COL4A3,PLAU,SERPINE1

4.3.3 Predicted Gc-effects on biological function

In order to understand the biological processes regulated by Gc exposure in the podocyte, the Gc-regulated list of genes derived from the microarray study underwent gene ontology analysis using IPA®. Individual genes in the Gc-regulated gene list will have one or more known biological functions identified using the IPA® Knowledge Base. If enough genes with the same biological function are found in the gene list, that biological function was considered to be enriched. Understanding the key biological functions that Gc regulates in the podocyte may help to identify mechanisms responsible for the protective effect exerted by Gc during periods of glomerular filtration barrier dysfunction.

Figure 4.5 displays the biological functions linked to the gene expression changes ranked in order of statistical significance (using the search term 'molecular and cellular functions'). As expected, these data show that glucocorticoids regulate a wide variety of functions within the cell including growth, apoptosis and metabolism. However, unexpectedly, 'cellular movement' was a highly ranked term (third overall). As it is already known that a hypermotile podocyte phenotype is associated with proteinuria *in vivo* (see Section 1.3.4), this *in silico* prediction of an effect of Gc exposure on podocyte motility was intriguing, and I decided to pursue this further.

Gene ontology analysis in IPA® can also be used to understand which diseases and general physiological functions are altered by the changes observed in the dataset. **Figure 4.6** displays the results of expanding the gene ontology analysis to include all three gene ontology terms available on IPA®, viz., 'disease and disorders,' 'molecular and cellular functions' and 'physiological system development and function' with an example of a pathway analysis relevant to each displayed significant term. This highlights the wide range of effects that glucocorticoids exert on tissues, including roles in cancer and apoptosis. These findings are consistent with the clinical use of Gc-therapy as the cornerstone of lymphoid cancer treatment.[457]

Gc-regulated genes involved with cellular movement identified by IPA® are displayed in **Figure 4.7** and **Supplementary Table 10.1**. As described in Section 1.3.4, gene effects on motility are highly cell-specific. As the IPA® Knowledge Base is based on the general scientific published literature (ie, not podocyte-specific), predictions regarding the direction of change in cellular movement (ie, increasing or decreasing) are difficult to interpret. As shown in **Figure 4.7**, **Table 4.4** and **Supplementary Table 10.1**, many

of the individual Gc-regulated genes have predicted antagonistic effects on cellular movement, and the net effect cannot be accurately predicted from this *in silico* analysis. These data can alternatively be visualised with a gene ontology heat map as shown in **Figure 4.8**. The parent gene ontology term 'cellular movement' is sub-divided into smaller boxes each corresponding to a lower-order gene ontology term (eg, migration of smooth muscle cells). Each of these smaller boxes is coloured according to activation z-score, providing an *in silico* prediction of whether the transcriptional changes observed in the microarray dataset would be expected to increase or decrease cellular motility relating to the corresponding lower order term. Out of the 46 lower-order cellular motility terms recognized by IPA as being significantly enriched in the current dataset, 29/46 were predicted to be inhibited by the changes observed in the microarray (ie, reducing cellular movement), 10/46 were predicted to be enhanced by the observed changes, and IPA did not make a prediction for 7/46 terms. Although this provides a very weak prediction that the observed transcriptional changes in the microarray dataset would overall act to reduce cellular motility, it needs to be emphasised again that this *in silico* prediction relied on existing published general literature and is not podocyte-specific.

IPA® software also helps to generate hypotheses for how a phenotype is altered by experimentally-observed transcriptional changes, using an algorithm based on pre-established connections known from the published literature. In order to understand how the Gc-responsive regulators of cellular motility may be exerting phenotypic change, I performed IPA® downstream analysis. This provided a visual representation of known links between genes in my dataset on effects on cellular motility in a range of cell types. These data ares shown in **Figure 4.9**.

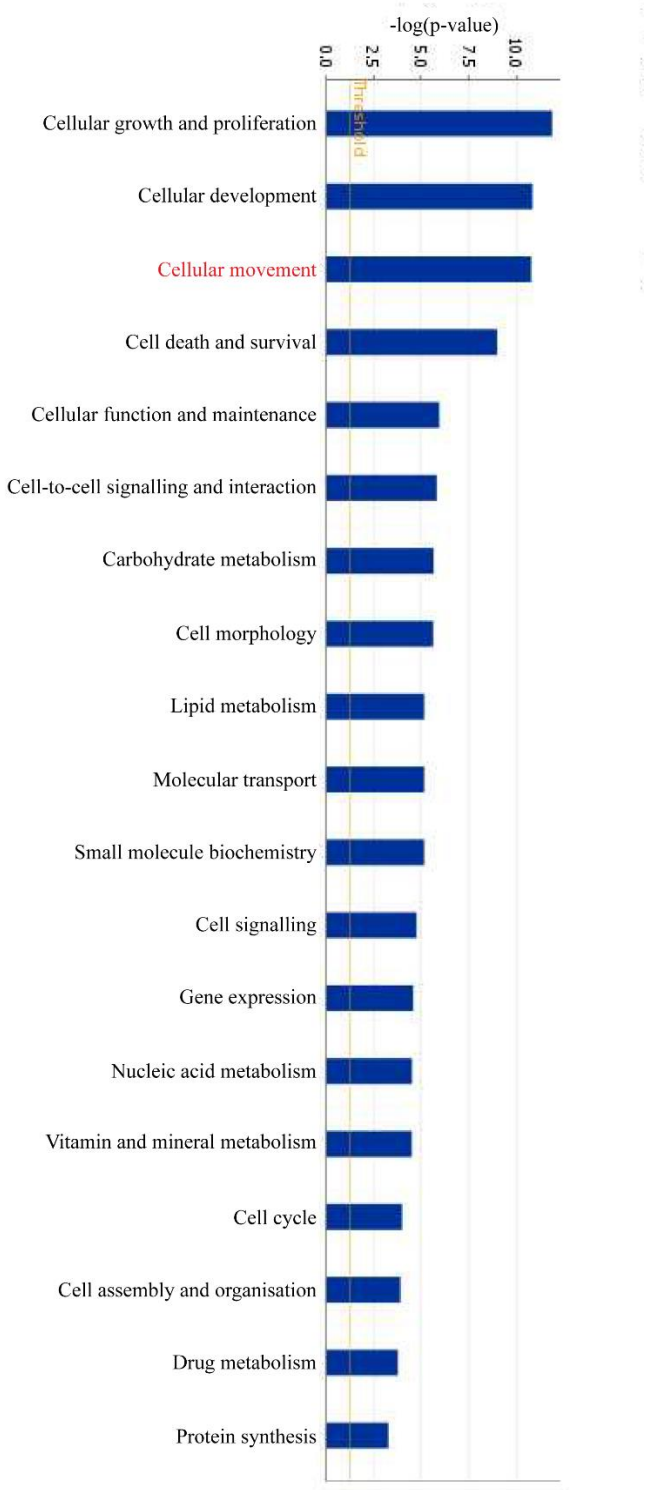

Figure 4.5 Bar chart illustrating Gc-effects on podocyte cellular functions

Podocyte Gc-regulated genes identified by microarray analysis underwent gene ontology analysis with IPA® software using the term 'molecular and cellular functions.' Enriched terms are listed in order of significance. The orange line denotes a threshold level of significance corresponding to a p-value of 0.05. 'Cellular movement' was a term selected for further analysis and is highlighted in red.

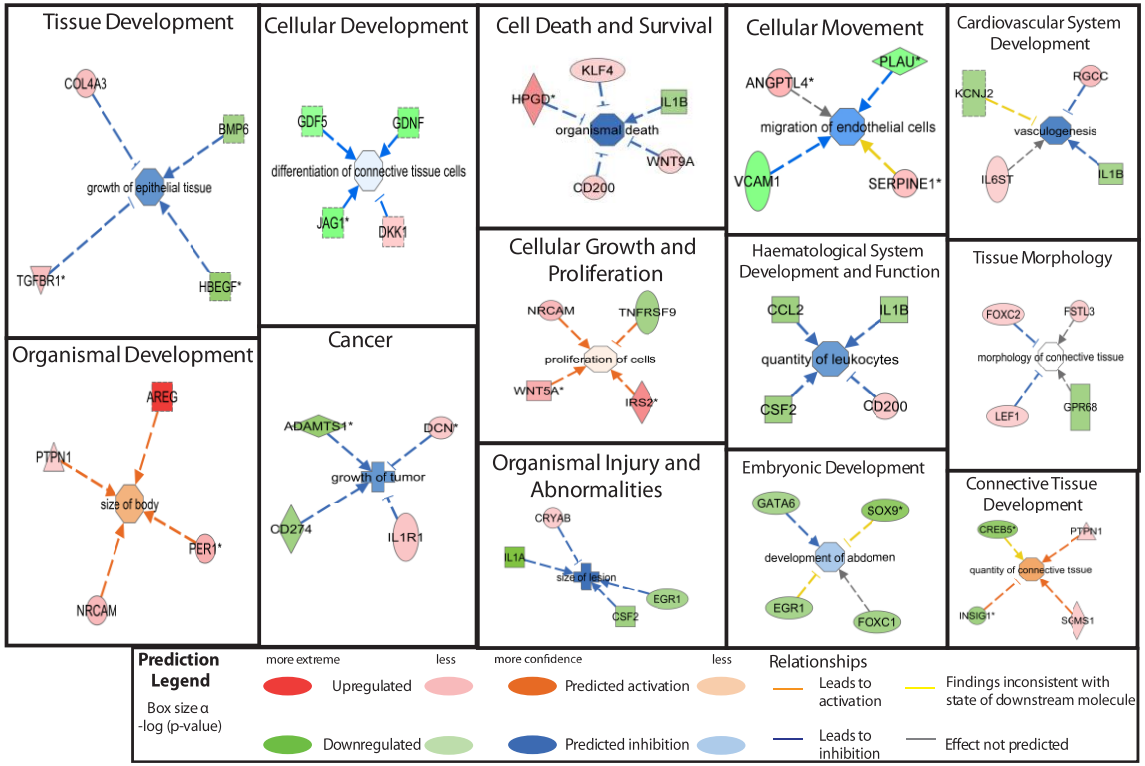

Figure 4.6 Expanded gene ontology anlalysis of microarray results.

Legend on next page.

Gc-regulated genes were identified by comparing the transcriptional output of vehicle- and prednisolone- treated human podocytes using microarray technology. This list of genes underwent gene ontology analysis using the following terms: ‘disease and disorders,’ ‘molecular and cellular functions’ and ‘physiological system development and function’ to understand the range of processes regulated by Gc. Significantly enriched terms are displayed, with the size of each box being inversely proportional to the p-value. Each displayed term has a pathway analysis example contained within the box, illustrating the relationship between transcriptional changes and effects on lower-order gene ontology terms.

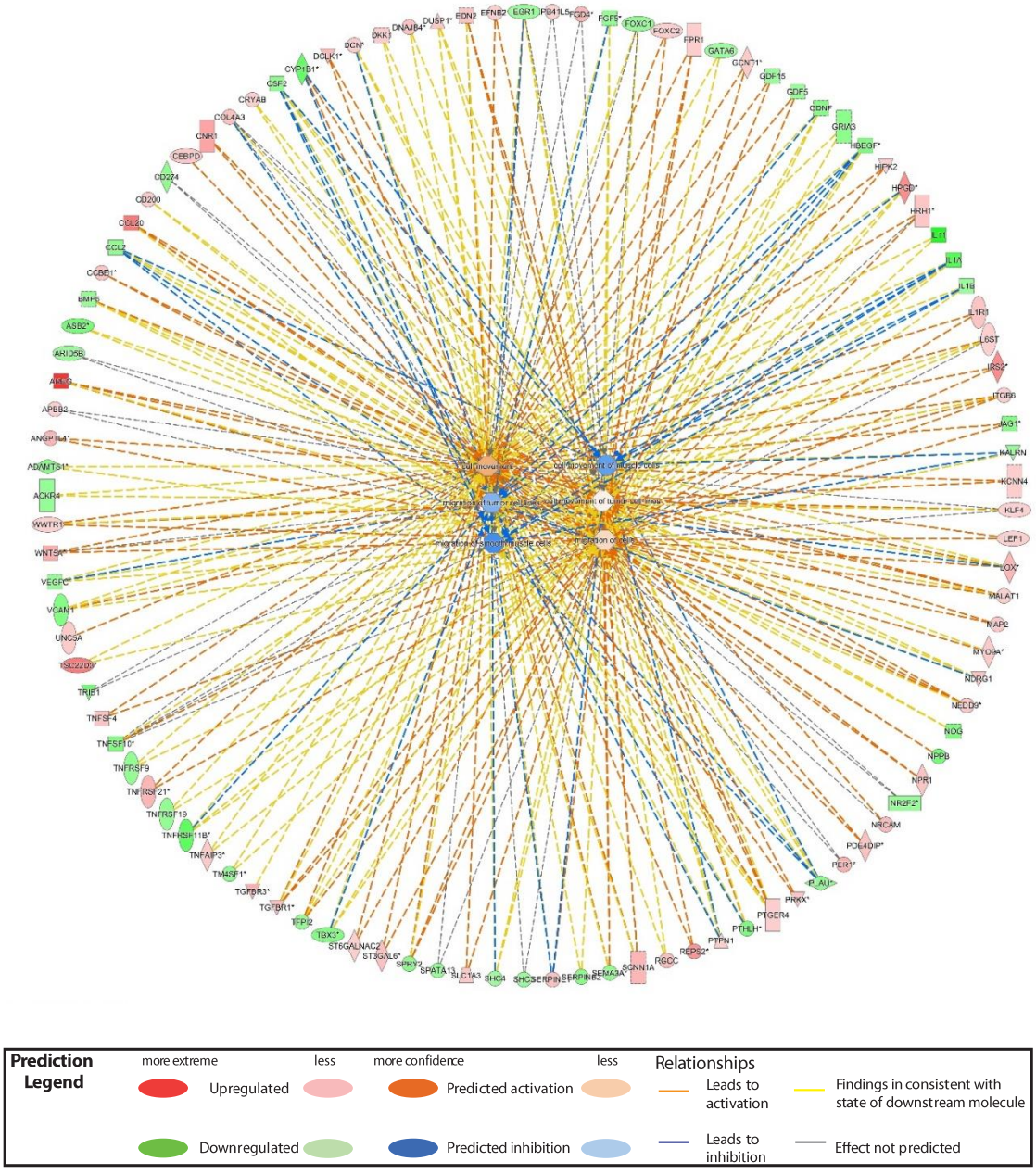

Figure 4.7 Gc-regulated genes with known connection to cellular movement

Chart displaying Gc-regulated genes from the microarray analysis identified by IPA® as having a role in cellular movement, as established by existing scientific literature. Chart also shows direction in change of expression for each gene observed in the microarray dataset, and provides an *in silico* prediction of how this observed change in gene expression will affect cellular movement.

Table 4.4 Activation z-scores of cellular movement gene ontology terms

Figure 4.7 illustrates genes from the microarray dataset involved with cellular motility. This table provides activation z-scores quantifying *in silico* predictions generated by IPA® software of whether Gc-effect on the podocyte are pro-migratory (positive activation z-scores) or anti-migratory (negative activation z-scores).

Categories	Functions annotation	p-value	Activation z-score
Cellular Movement	cell movement	1.72E-11	0.728
Cellular Movement	invasion of cells	1.86E-10	-1.395
Cellular Movement	migration of cells	3.92E-09	0.302
Cellular Movement	invasion of tumor cell lines	1.37E-08	-1.187
Cellular Movement	cell movement of tumor cell lines	2.64E-08	0.1
Cellular Movement	migration of tumour cell lines	2.23E-06	-0.674

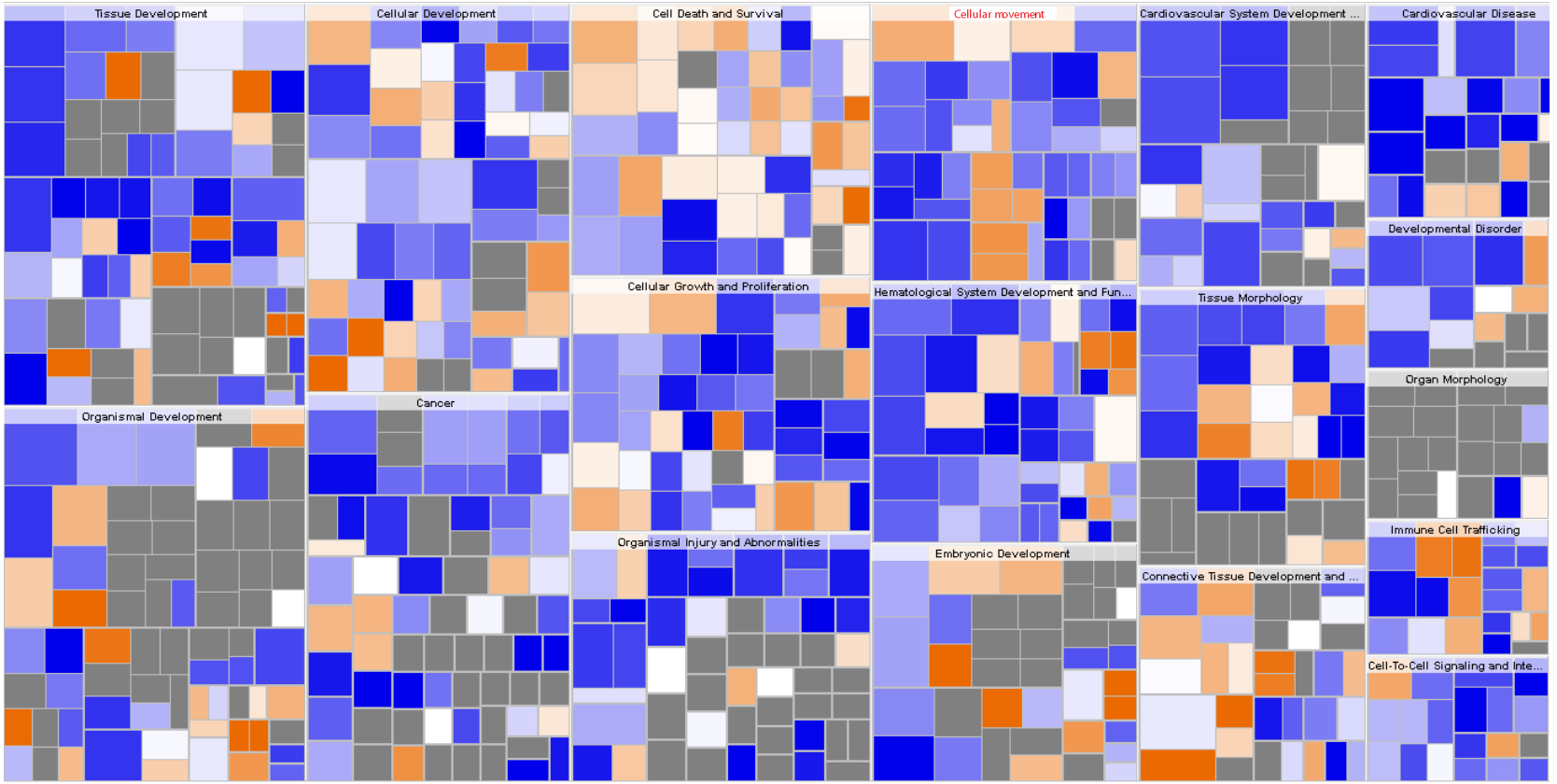

Figure 4.8 Gene ontology heatmap

Legend on next page.

Gc-regulated genes identified by microarray experiments underwent gene ontology (GO) analysis using the following GO terms: ‘disease and disorders,’ ‘molecular and cellular functions’ and ‘physiological system development and function.’ The size of the box is inversely proportional to the level of significance; significantly enriched parent GO terms form the large boxes. Each large parent GO term box is subdivided in smaller boxes representing lower-order terms, relating to the parent term. Each of these smaller boxes is coloured according to the activation z-score (ie, an *in silico* prediction of the change in direction for that GO term elicited by the expression changes from the microarray datset). Gene ontology heat maps represent not only which GO terms are enriched, but also whether each GO term is predicted to be up- or –downregulated following Gc-exposure.

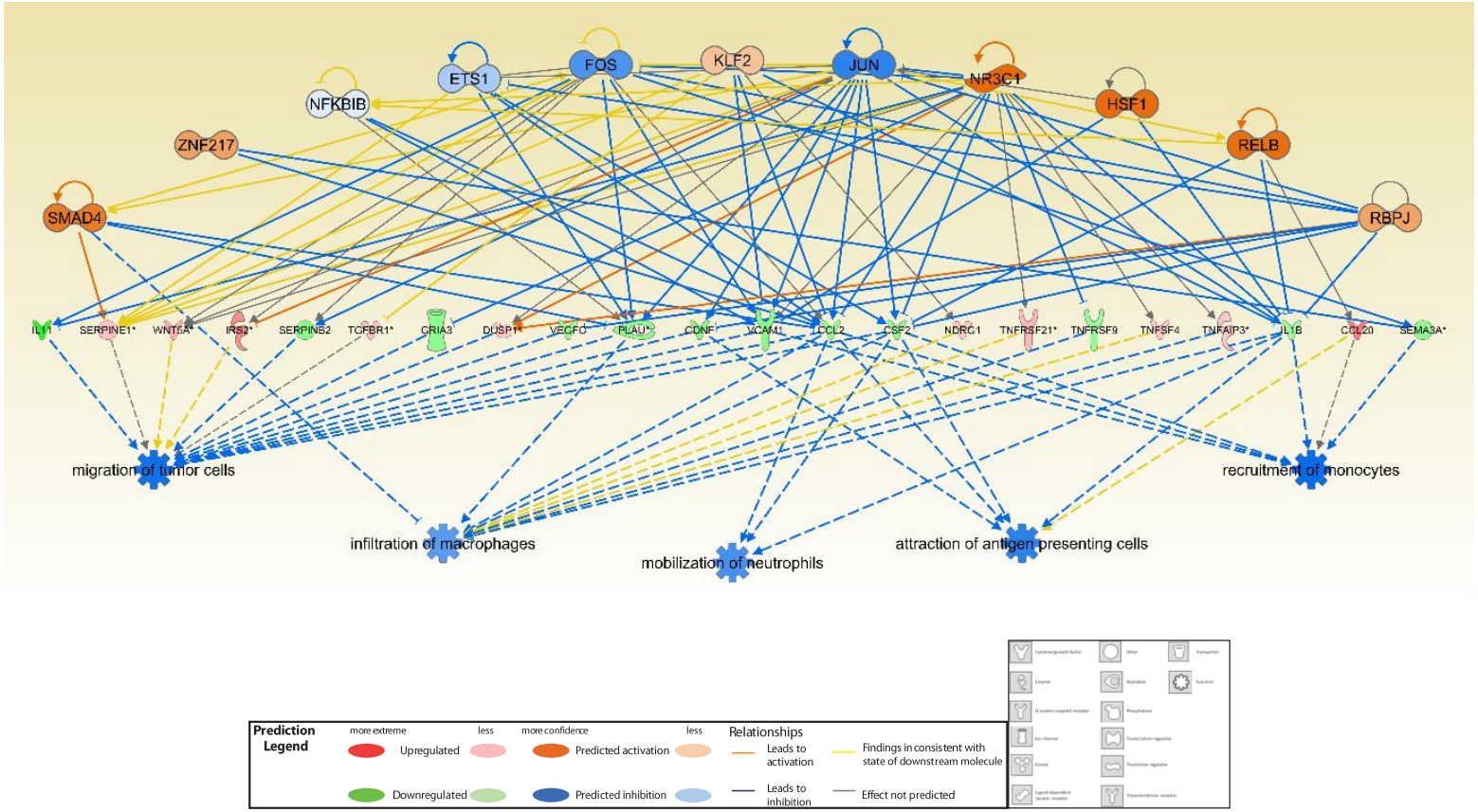

Figure 4.9 Example of how observed microarray changes may relate to changes in cellular motility
IPA® software connects upstream regulators, experimentally observed changes in gene expression following Gc-exposure to provide *in silico* predictions of how these may affect cell phenotype. This diagram represents an example of how Gc-regulated genes observed in my dataset may alter cellular motility.

4.4 Discussion

The mechanism(s) underlying the ability of glucocorticoids to protect podocytes from damage is poorly understood. In order to provide insight into potential mechanisms underlying these direct protective effects, I identified Gc-regulated genes using microarray analysis following a 5 hour exposure of human, wild type AB podocytes to either vehicle or prednisolone. This revealed a list 397 genes whose expression changed significantly following Gc treatment. Initial analysis involved identification of Gc-regulated genes involved with aspects of kidney tissue damage. *In silico* predictions using IPA software® suggest Gc-exposure would have direct protective effects on the kidney. This supports existing literature, as well as data provided in Chapter 3 of the current study.[109, 110]

Subsequent gene ontology categorisation of the microarray dataset illustrated Gc-regulated gene involvement in a diverse range of cellular functions (**Figure 4.5**), and suggested a prominent role for effects on cellular motility, which was the third most significantly enriched gene ontology term. Recent data have highlighted that podocyte hypermotility is a feature of a dysfunctional renal filtration barrier disease (see Section 1.3.4); it is thus possible that glucocorticoids may exert a protective effect on podocytes by reversing this hypermotility phenotype.

In the present study, I identified direct Gc-gene targets using a short exposure (5 hours) of the GR-agonist prednisolone to fully differentiated (differentiation time of 14 days) human podocytes. Cheng *et al.*, have previously used a microarray approach to investigate the effect Gc-treatment has on podocyte differentiation. The group identified direct and indirect Gc-targets using a prolonged 3 day exposure of the GR-agonist dexamethasone to minimally differentiated (differentiation time 2 days) AB podocytes.[107] In a similar fashion to the current study, "negative regulation of smooth muscle cell migration" was identified as an enriched gene ontology term following treatment with Gc.

Table 4.5 details examples of other studies examining whole-genome changes in gene expression following treatment with a variety of GR-agonists, in various cell lines, for variable lengths of treatment. 'Cellular motility' has been identified as an enriched gene-ontology term in Gc-regulated genes in human primary monocytes and an

endometrial cancer cell line, but not in an A549 lung cancer cell line or in lens epithelial cells.

Although analysis of the microarray data strongly suggests prednisolone exposure affects podocyte motility *in vitro*, whether this would be a pro-migratory or anti-migratory effect is difficult to determine from this analysis alone. The cell type-specific nature of motility regulation combined with the antagonistic effects resulting from the *in silico* predictions suggest experimental, podocyte-specific, validation of Gc-effects on motility are warranted. This validation is the subject of the following chapter.

Table 4.5 Examples of published studies identifying Gc-regulated genes

In the current study, genes whose expression significantly changed following a 5 hour treatment with the GR-agonist prednisolone using the human podocyte cell line. Here, I provide examples of other studies examining genome-wide changes in gene expression in a variety of cell types, using different GR-ligands and for variable lengths of treatment.

Cell-type	**GR-agonist**	**Length of treatment with GR-agonist**	**Number of Gc-regulated genes identified**	**Cell motility identified as enriched gene ontology term**	**Reference**
Human AB podoctyte cell line (Differentiating)	Dexamethasone	3 days	517	✓	[107]
Human primary peripheral monocytes	Fluticasone	16 hours	133	✓	[464]
Human uterine endometrial cancer cell line (ECC1 cells)	Dexamethasone	6 hours	1802	✓	[465]
Human primary lens epithelial cells	Dexamethasone	4 and 16 hours	4 hour treatment- 136 genes ; 16 hours- 86 genes	×	[466]
Human adenocarcinomic alveolar basal epithelial cell line (A549 cells)	Dexamethasone	1 hour	234	×	[449]

5 Glucocorticoid effects on podocyte motility

5.1 Overview

In the previous chapter, gene ontology analysis of glucocorticoid (Gc)-regulated genes suggested that Gc exposure may be exerting effects on podocyte motility. In this chapter, I present data examining Gc effects on podocyte motility using complementary *in vitro* assays. Live-cell imaging of podocytes coupled with tracking analysis using MTrackJ/ImageJ software confirmed that Gc-exposure does indeed reduce the speed of podocytes and also causes podocytes to adopt more directionally persistent movement.

To gain insight into how Gc-exposure may be causing a change in podocyte motility, I focussed on two small GTPases, Rac1 and RhoA, which exert mutually antagonistic effects on cell movement (see Section 1.7.6). These small GTPases cycle between an inactive, guanosine diphosphate (GDP)-bound form, and an active, guanine triphosphate (GTP)-bound form. Active Rac1 stimulates the formation of pro-migratory lamellipodial cell protrusions,[407] while active RhoA stimulates stress-fibre formation.[382] Data presented here suggest that Gc exposure reduces Rac1 activity in a time-dependent manner.

As podocyte hypermotility has been associated with the development of proteinuria,[132] and Rac1 overactivity has been implicated in the development of chronic kidney disease,[406] the observation that Gc exposure reduced podocyte motility and Rac1 activity suggested some of the protective effects of Gc on podocytes may be through reducing Rac1 activity. I subsequently showed that damaging podocytes by exposure to puromycin aminonucleoside (PAN) increases Rac1 activity, before investigating whether inhibiting Rac1 activity has any direct, protective effect on podocytes against PAN-damage. Using the electric cell substrate impedance sensing (ECIS) assay (see Section 2.10), which uses electrical resistance across a monolayer of podocytes as a surrogate marker for barrier integrity, I demonstrated that Rac1 inhibition using the small molecule EHT 1864 does indeed increase electrical resistance compared to cells treated with PAN alone, and interestingly Rac1 inhibition and Gc in combination seem to exert a cumulatively protective effect. This suggests that Rac1 inhibitors and downstream effectors of the Rac1 pathway may be useful starting points for future *in vitro* and animal studies investigating novel anti-proteinuric therapeutic strategies.

5.2 Chapter-specific methods

5.2.1 Live cell imaging

Differentiated wild type podocytes were seeded at a density of 5,000 cell/mL per well in a 24 well cell culture cluster plate (Costar). Two wells were used for each treatment condition. Cells were then filmed using an AS MDW live cell imaging system (Leica) with a 5x/NA 0.15 HC Plan Fluotar air objective (magnification 1.5x). Point visiting was used to allow multiple positions to be imaged within the same time course, and cells were maintained at 37^{o}C and 5% (vol/vol) CO_2. Images were collected using a Coolsnap HQ camera, and six movies (3 movies per well) were generated for each condition. To assess cell migration, the speed and directionality of 120 cells per condition (20 cells per movie) was measured using the MTrackJ plug-in of ImageJ. Cell tracking was performed over a 24-hour period.

5.2.2 Rac1 activity assay

Active Rac1 was affinity purified from lysates using an effector pull-down approach with GST-PAK beads. Cells were serum starved for 24 hours before treatment. At the relevant time, cells were lysed in ice-cold lysis buffer [20mM Hepes pH 7.5, 140mM NaCl, 1% (v/v) Igepal, 4mM EDTA, 4mM EGTA, 0.5% (wt/vol) sodium deoxycholate, 10% (vol/vol) glycerol] supplemented with EDTA-free protease inhibitor tablets (Roche). Lysates were clarified by centrifugation at 12,000 g, 4^{o}C for 5 minutes prior to snap-freezing in liquid nitrogen to preserve GTPase-activity while other batched samples were processed.

Thawed lysates were then incubated with 20µg GST-PAK beads (Cytoskeleton) for 1 hour at 4^{o}C. Beads were washed three times with ice-cold lysis buffer, and active Rac1 was eluted off beads by addition of Laemmli reducing sample buffer. For each condition, equal volumes of GTP-Rac1 eluted from the GST-PAK beads, and equal volume of 'total' extract obtained prior to snap-freezing were resolved by SDS-PAGE and analysed by Western blotting. The ratio between GTP-Rac1 and total Rac1 was quantified to determine the Rac1 activation state.

5.2.3 RhoA activity assay

Active RhoA was affinity purified from lysates using an effector pull-down approach with Rhotekin RBD beads. Cells were serum starved for 24 hours before treatment. At the relevant time, cells were lysed in ice-cold lysis buffer[50mM Tris pH 7.5, 10mM

$MgCl_2$, 0.5M NaCl, and 2% (vol/vol) Igepal] supplemented with protease inhibitor cocktail (Cytoskeleton). Lysates were clarified by centrifugation at 10,000g, 4^{o}C for 1 minute prior to snap-freezing in liquid nitrogen to preserve GTPase-activity while other batched samples were processed.

Thawed lysates were then incubated with 50µg Rhotekin RBD beads (Cytoskeleton) for 1 hour at 4^{o}C. Beads were washed once with ice-cold wash buffer (25mM Tris pH 7.5, 30mM $MgCl_2$, 40 mM NaCl), and active RhoA was eluted off beads by addition of Laemmli reducing sample buffer. For each condition, equal volumes of GTP-RhoA eluted from the Rhotekin-RBD beads, and equal volume of 'total' extract obtained prior to snap-freezing were resolved by SDS-PAGE and analysed by Western blotting. The ratio between GTP-RhoA and total RhoA was quantified to determine the RhoA activation state.

5.3 Results

5.3.1 Gc effects on podocyte motility

To validate the findings of the microarray and subsequent gene ontology analysis suggesting Gc exposure affects podocyte motility, live-cell imaging of podocytes over a 24 hour period was performed. Representative movies are provided in Compact Disc 1 (back cover insert). The imaging commenced 24 hours after treatment with Gc. Podocytes in these movies were manually tracked using the MTrackJ plugin on ImageJ software to generate quantifiable data for analysis.

As shown in **Figure 5.1-A**, Gc-exposure reduced the mean speed of podocytes over the 24 hour period by approximately 36%, from 0.0053 μm/sec (vehicle-treated) to 0.0034 μm/sec (Gc-treated). Confidence in the assay was enhanced by the observation that damaging podocytes with PAN caused a statistically significant increase in podocyte motility from 0.0053 μm/sec (vehicle-treated) to 0.0063 μm/sec (PAN-treated). Interestingly, the hypermobile PAN-treated podocytes also responded to Gc-treatment by reducing speed from 0.0063 m/sec (PAN-treated) to 0.0035 μm/sec (PAN+Gc-treated).

To determine if Gc-treatment also affected the directional persistence of podocyte movement, the ratio of the Euclidean distance travelled by each podocyte (ie, distance between the starting and final point of each track) compared to the total distance travelled was calculated. A cell persistence ratio of 1 corresponds to a cell that travels in a perfectly straight line during the whole period of imaging, while a ratio tending towards 0 would imply a cell constantly changing direction. **Figure 5.1-B** shows a very modest, but statistically significant increase in podocyte persistent movement from 0.50 (vehicle-treated) to 0.57 (Gc-treated). In order to visualise movement patterns of podocytes in the different treatment conditions, rose plots were constructed which displayed movement of individual cells over the imaging period using the x,y coordinates generated by the tracking software (**Figure 5.1C-F**). **Figure 5.1–G** plots the movement of PAN-treated cells and PAN+Gc treated cells on the same axes to demonstrate the shorter distance travelled by PAN+Gc-treated podocytes during the same time interval.

To ascertain Gc-effects on cell motility in the context of another podocyte-damaging agent, the live cell imaging was repeated using lipopolysaccharide (LPS) instead of

PAN, with the remainder of the experimental design remaining the same. The results are shown in **Figure 5.2**. The manual cell tracking in this experiment was performed by a different individual to reduce the risk of observer-bias.

Figure 5.2-A again shows a reduction in podocyte motility following Gc-treatment. Here, a 51% decrease in podocyte speed was observed: from 0.021 µm/sec (vehicle-treated) to 0.010 µm/sec (Gc-treated). LPS-exposure also increased podocyte motility from 0.021 µm/sec (vehicle-treated) to 0.031 µm/sec (LPS-treated). The hypermobile LPS-treated podocytes displayed reduced motility when LPS was co-administered with Gc (0.014 µm/sec). Also, Gc-treated podocytes (cell persistence ratio 0.58) showed a small increase in persistence compared to vehicle-treated podocytes (0.51), and LPS-treated podocytes displayed reduced directional movement (0.43).

To determine the time taken for Gc to have an effect on podocyte motility, another set of live-cell imaging experiments was performed comparing vehicle- and Gc-treated podocytes during the first 24 hours following treatment. **Figure 5.3-B** shows the instantaneous speed of podocytes at each time point. The first statistically-significant difference in the mean speed of the vehicle- and Gc-treated podocyte populations occurred 120 minutes following treatment (p-value 0.013). The statistical significance of this difference had increased at the 180 minute time-point (p value 0.0004) and again at the 220 minute time-point (p value <0.0001).

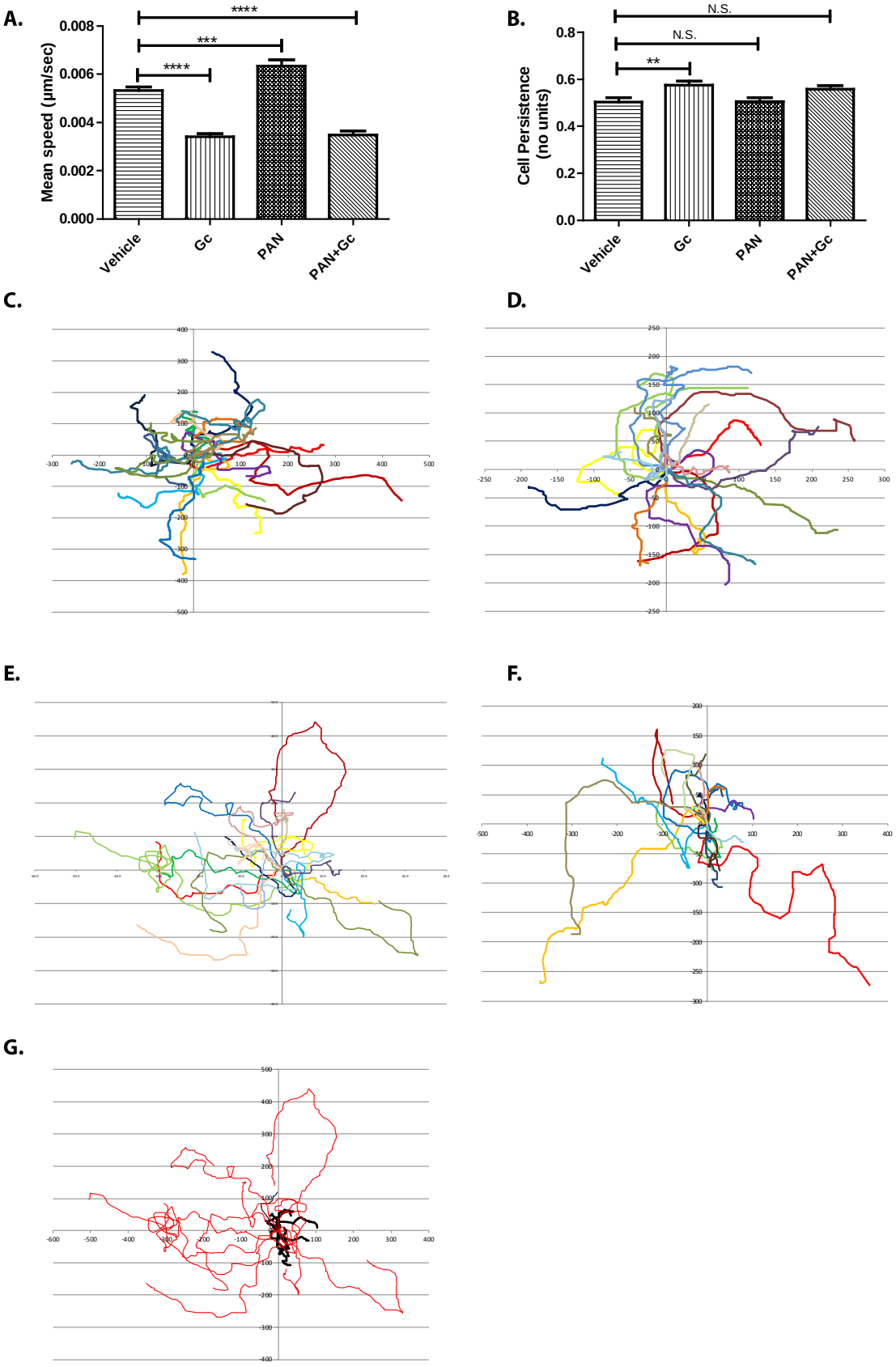

Figure 5.1 Effects of Gc and puromycin aminonucleoside exposure on podocyte motility

Legend on next page

Microarray analysis of Gc-regulated genes from wild-type podocytes suggested Gc exposure affected podocyte motility. In order to test this, live cell imaging of podocytes was performed for a 24 hour period, beginning 24 hours following treatment. Subsequently, manual cell tracking was performed using the MTrackJ plugin on ImageJ software to allow analysis of podocyte speed and cell directional persistence. Each experiment consisted of tracking 120 cells per condition. The experiment was performed 3 times. **(A)** quantifies mean podocyte speed over the 24 hour period. **(B)** quantifies podocyte directional persistence. Rose plots were created for each condition to visualize the path travelled for 20 cells (the path of each cell is marked with a different colour). The x- and y-axis refer to x,y coordinates of each cell over time generated by the cell tracking software: **(C)** vehicle-treated; **(D)** Gc-treated; **(E)** PAN-treated; **(F)** PAN+Gc-treated. **(G)** is a rose plot comparing the movement of 10 PAN-treated podocytes (red) compared with 10 podocytes treated with PAN+Gc (black) over the 24 hour period. Results were analysed by one-way ANOVA followed by Dunnett's multiple comparisons test. **= adjusted p value 0.091; ***= adjusted p value 0.0003; ****= adjusted p value <0.0001. N.S.= not significant. Error bars represent standard error of the mean.

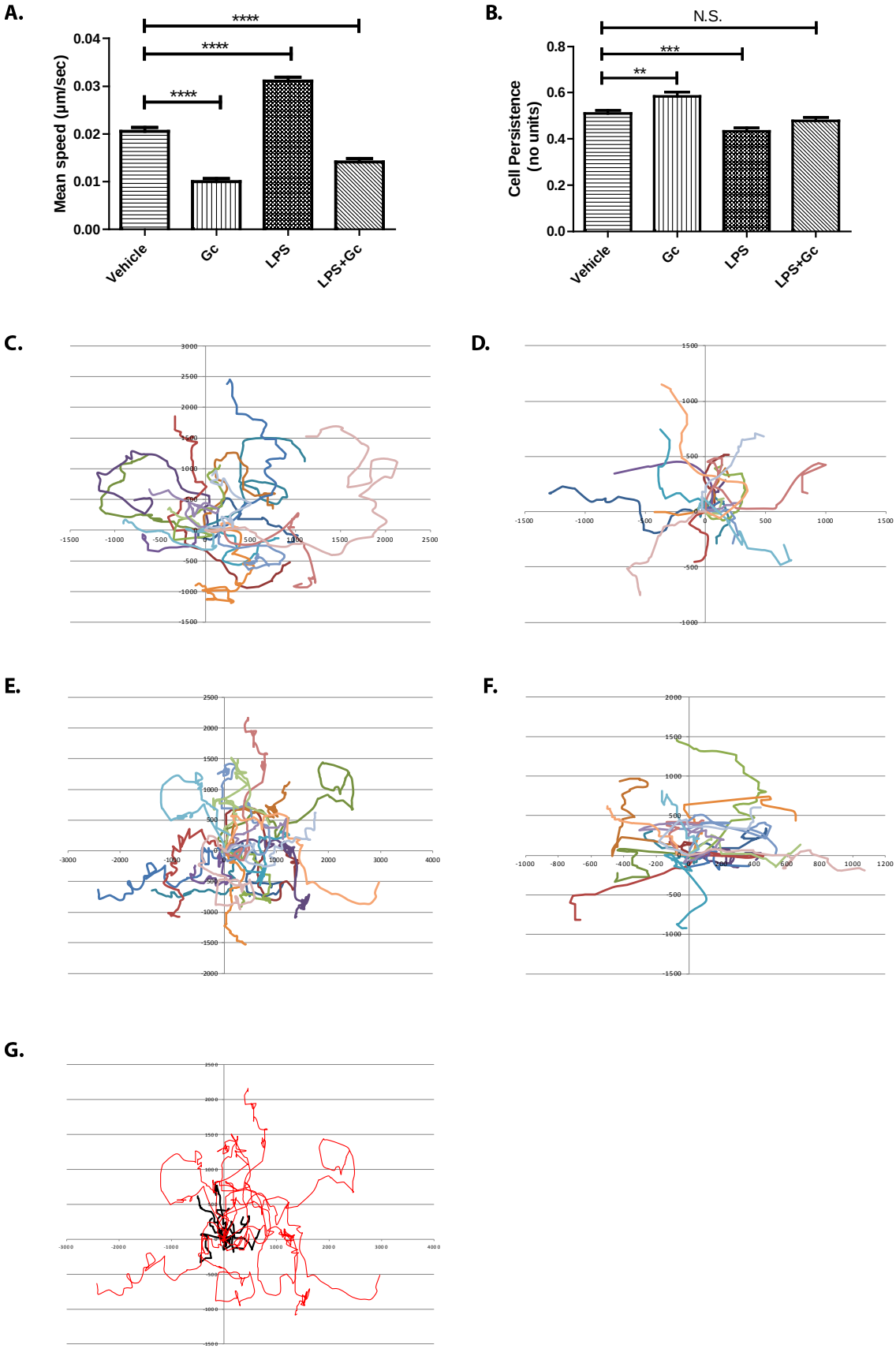

Figure 5.2 Effects of Gc and lipopolysaccharide exposure on podocyte motility.

Legend on next page.

Figure 5.1 shows analysis of effects of Gc and the podocyte-damaging agent puromycin aminonucleoside (PAN) on podocyte motility. This figure shows analysis of the effects on podocyte motility of Gc and another podocyte-damaging agent, lipopolysaccharide (LPS). Again, live cell imaging was performed on wild type podocytes for a 24 hour period, beginning 24 hours after treatment. Each experiment consisted of tracking 120 cells per condition. The experiment was performed three times. Manual tracking using ImageJ software was performed by a different individual for the PAN- and LPS- experiments to reduce the risk of observer bias. **(A)** quantifies mean podocyte speed over the 24 hour period. **(B)** quantifies podocyte directional persistence. Rose plots were created for each condition to visualize the path travelled for 20 cells (the path of each cell is marked with a different colour). The x- and y-axis refer to x,y coordinates of each cell over time generated by the cell tracking software: **(C)** vehicle-treated; **(D)** Gc-treated; **(E)** LPS-treated; **(F)** LPS+Gc-treated. **(G)** is a rose plot comparing the movement of 10 LPS-treated podocytes (red) compared with 10 podocytes treated with LPS+Gc (black) over the 24 hour period. Results were analysed by one-way ANOVA followed by Dunnett's multiple comparisons test. ****=adjusted p value <0.0001; ***= adjusted p value 0.0009; **=adjusted p value 0.0027. N.S.= not significant. Error bars represent standard error of the mean. I (JM) prepared the cells or the experiment, performed the video imaging and data anlaysis. Ms. Cressida Moxey (University of Manchester Medical School) performed the manual cell tracking.

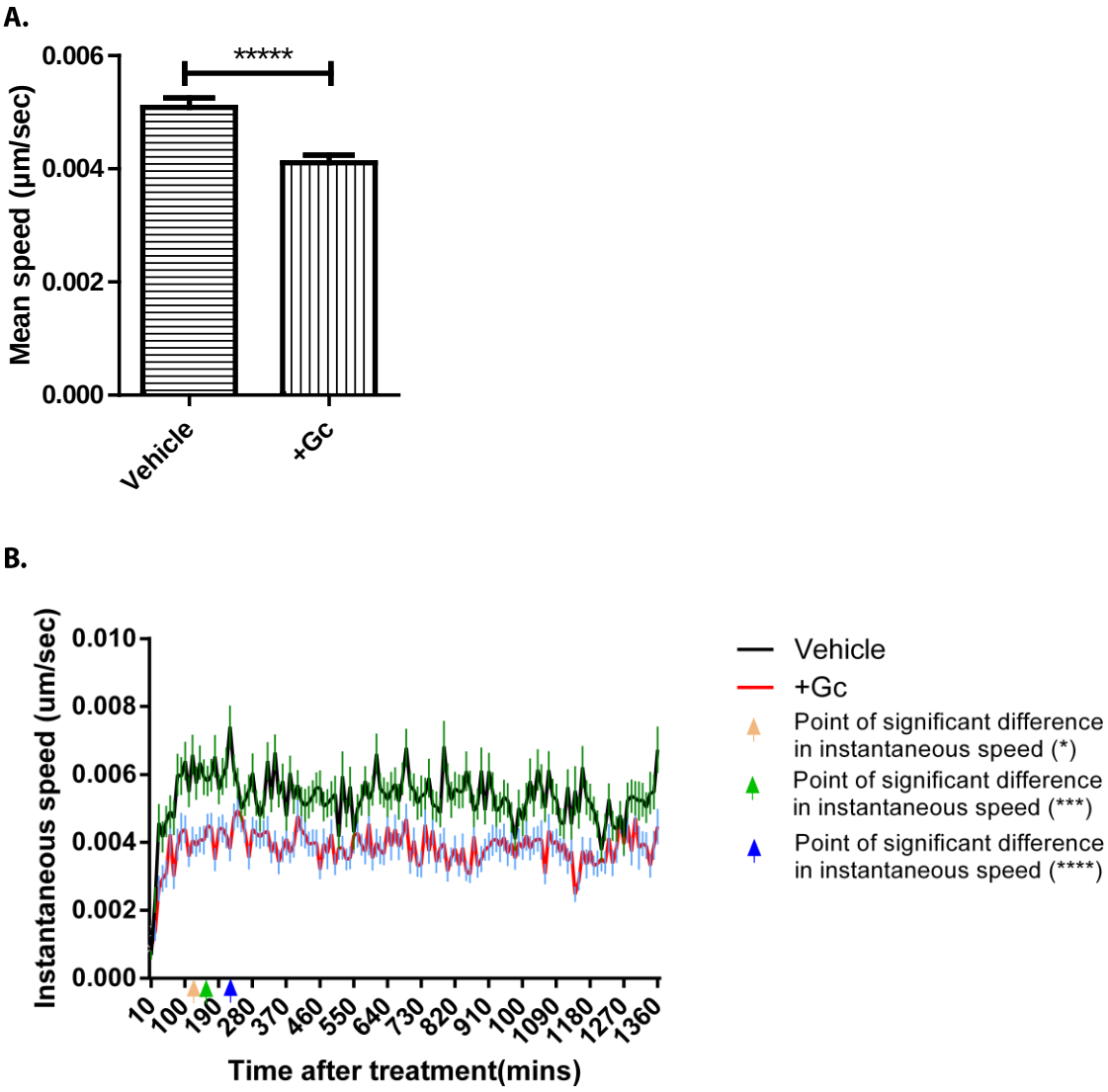

Figure 5.3 Early effects of Gc on podocyte motility.

To analyse the length of time taken for Gc to affect podocyte speed, live cell imaging of WT podocytes was performed in the 24 hour period following treatment. Each experiment consisted of manually tracking 120 cells per condition using ImageJ software. The experiment was performed twice. **(A)** shows the mean cell speed during the whole period of imaging. (B) shows the instantaneous speed for the podocytes during the 24 hour period. Coloured arrows on the X-axis refer to the level of significance of the difference between the means of cell speed between vehicle- and Gc-treated cells. The first time of significant difference is shown by the arrow at 120 minutes. Results were analysed by two-way repeated measures ANOVA followed by Šídák's multiple comparisons test. *=adjusted p value 0.0134; ***=adjusted p value 0.0004; ****=adjusted p value <0.0001. Error bars represent standard error of the mean.

5.3.2 Gc effects on Rac1 and RhoA

The small GTPases Rac1 and RhoA are important regulators of cell motility and are mutually inhibitory.[421] To understand if Gc action affected the activity of either of these proteins, pull-down assays using beads specific for the active, GTP-bound protein were performed, and the active protein component was normalised to the total (inactive plus active) protein content. Data were obtained at the 3 hour time point as this corresponded to the approximate time at which differences in cellular motility following Gc-exposure were first observed in the live-cell imaging experiment (**Figure 5.3**), and also at the 24 hour time point.

Figure 5.4-A shows that Gc reduced Rac1 activity at both the 3 hour time point and 24 hour time point compared to vehicle-treated cells harvested at the same time point. Although RhoA showed a trend towards increased activity following Gc exposure, this was not statistically significant (p value 0.9 at both 3 hour time point and 24 hour time point). Gc exposure did not significantly affect total Rac1 or RhoA protein expression (**Figure 5.4 C-F**).

As Gc-exposure reduced Rac1 activity, I investigated whether the converse was true by performing pull-down assays for active Rac1 following 24 hours of PAN-exposure. Indeed, PAN-damaged podocytes did show an increase in Rac1 activity following treatment (**Figure 5.5**).

The association between a hypermobile podocyte phenotype and proteinuria has already been established.[132] As Gc exposure resulted in reduced podocyte speed (**Figure 5.1**) and reduced activity of the pro-migratory regulator Rac1 (**Figure 5.4**), I investigated whether inhibiting Rac1 with the small molecule EHT 1864 may have any protective function on podocytes against PAN-induced damage. To do this, I returned to the electric cell substrate impedance sensing assay (ECIS) used in Chapter 3, which measures electrical resistance across a monolayer of podocytes. Electrical resistance is used as a surrogate marker for barrier integrity, with higher electrical resistance implying higher barrier function. In accordance with other studies, a dose of 30μM EHT 1864 was used.[467] **Figure 5.6** demonstrates that podocytes simultaneously treated with PAN and EHT 1864 had higher trans-barrier electrical resistance compared to podocytes treated with PAN alone (p value <0.0001). Also, the electrical resistance across a podocyte cell layer exposed to PAN was higher when EHT 1864 and Gc were

co-administered, compared to when either Gc or EHT 1864 were used as single treatments (p value <0.0001).

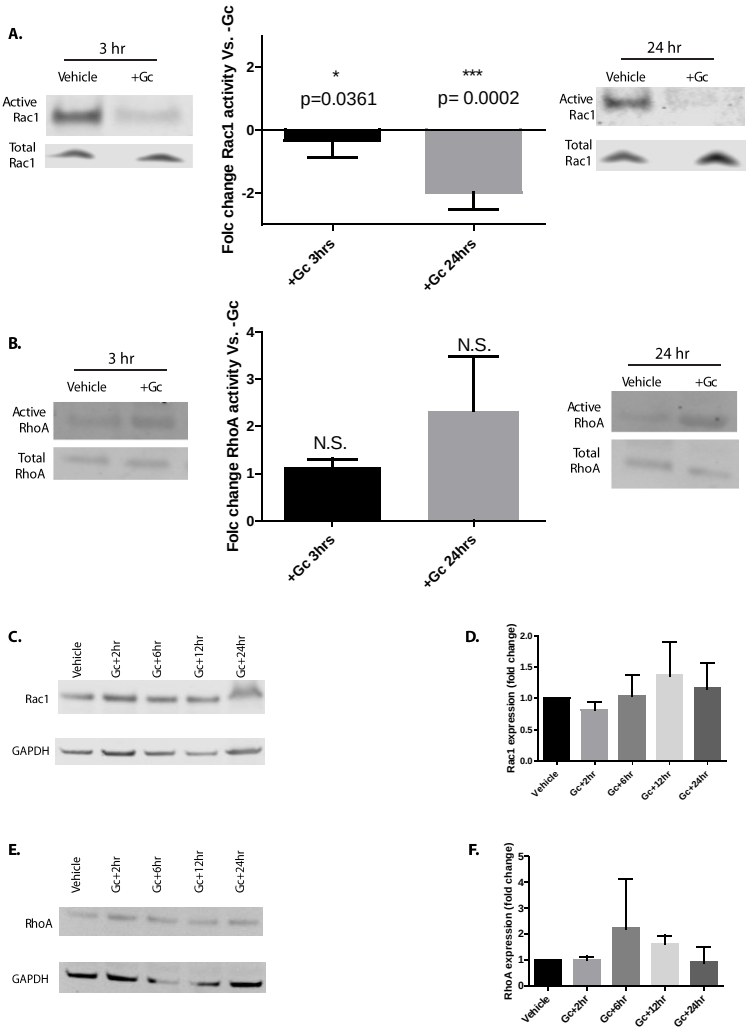

Figure 5.4 Gc effects on Rac1 and RhoA activity and expression.

To understand effects of Gc exposure on the activity of two key regulators of cell motility, Rac1 and RhoA, pull-down assays using beads specific for the active form of these proteins was performed. This allowed quantification of the active protein : total protein. **(A)** demonstrates Rac1 activity at 3 hours and 24 hours following Gc exposure. **(B)** demonstrates RhoA activity at 3 hours and 24 hours following Gc exposure. Results were analysed using the nonparametric Mann-Whitney U test: vehicle-control treated cells were compared with Gc-treated cells at the 3 hour time point, and separate vehicle-control treated cells were compared with Gc-treated cells at the 24 hour time point for each experiment. The experiment was performed at least six times. N.S.= not significant. Western blot **(C)** and quantification **(D)** of total Rac1 expression following Gc exposure (n=3), and western blot **(E**) and quantification **(F)** of RhoA expression (n=2), showed no significant change in expression following analysis using one way ANOVA and Dunnett's multiple comparisons test for any time point measured. Error bars represent standard error of the mean.

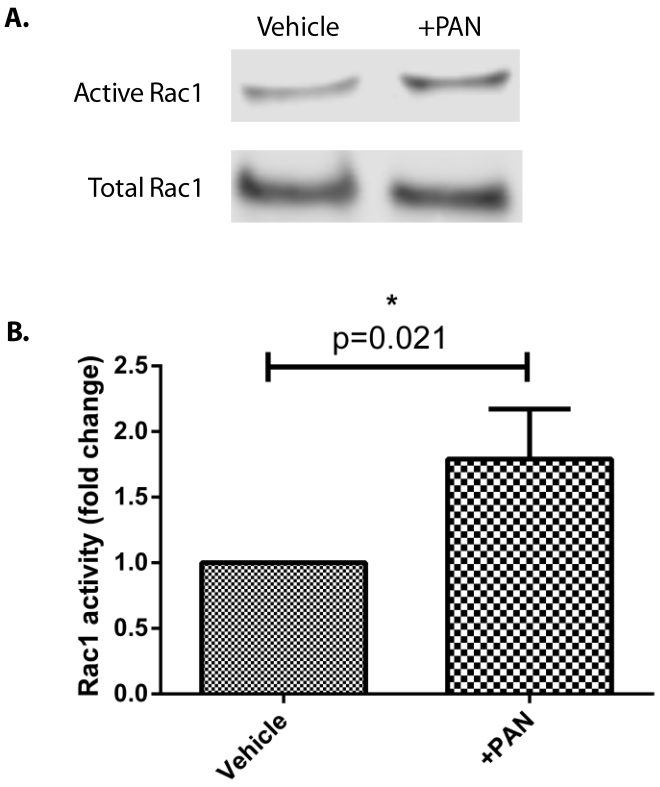

Figure 5.5 Rac1 activity following exposure to puromycin aminonucleoside (PAN).

To understand if injuring podocytes with PAN affected Rac1-activity, pull-down assays using beads specific for active Rac1were performed following 24 hours of PAN exposure. This allowed quantification of the ratio of active Rac1 : total Rac1. **(A)** shows a representative western blot; **(B)** shows quantification. Results were analysed using the nonparametric Mann-Whitney U test. The experiment was performed four times. Error bars represent standard error of the mean.

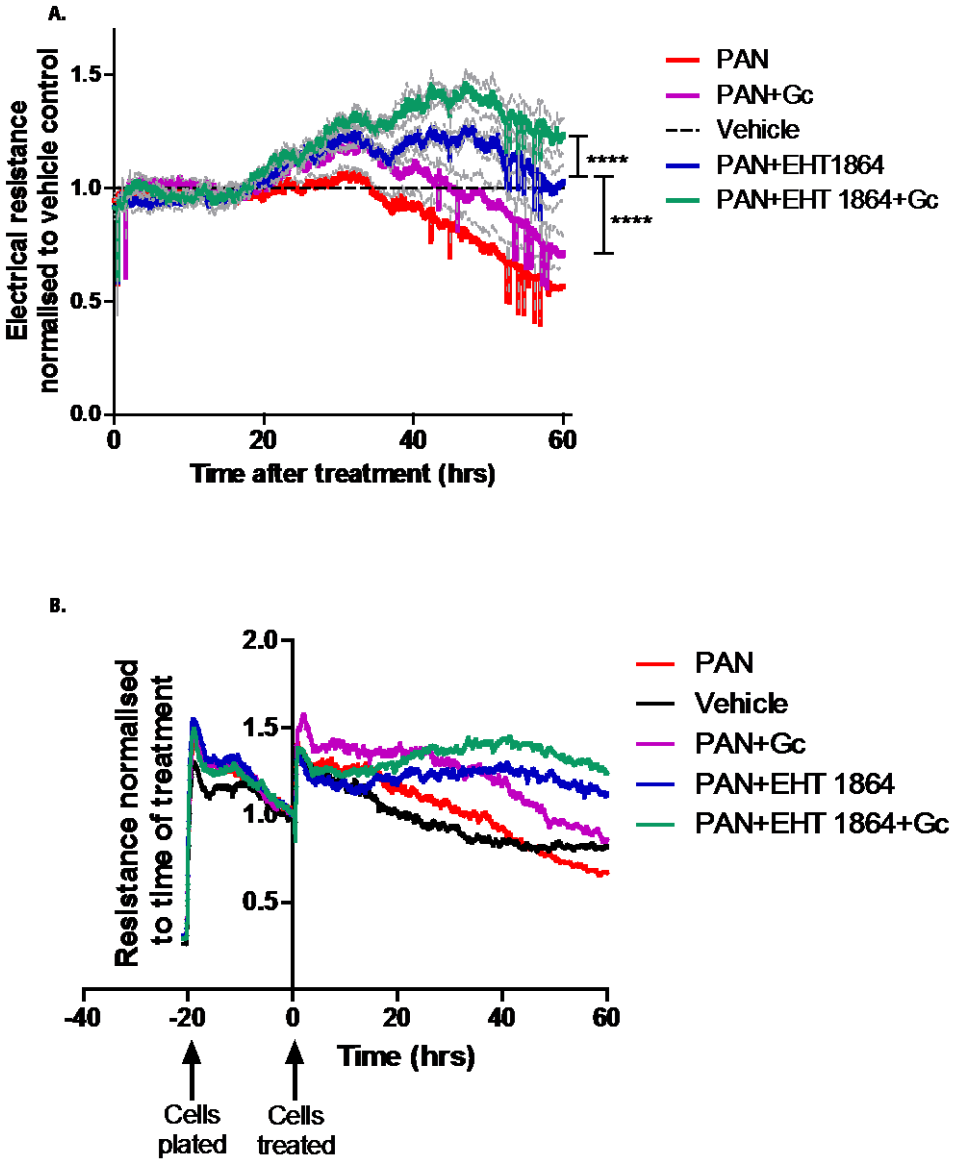

Figure 5.6 Effect of Rac1 inhibition on podocyte barrier function.

The effects of Rac1 inhibition with the small molecule EHT 1864 on electrical resistance across a monolayer of podocytes was examined using electrical cell-substrate impedance sensing (ECIS). Here, electrical resistance is used as a surrogate marker for cell barrier integrity, with higher electrical resistance implying higher barrier integrity. **(A)** shows the combined results of three experiments normalised to the vehicle control. Each experiment consisted of 3 plated wells of cells per condition, with each experiment lasting for 60 hours following treatment. The experiment was performed three times. Measured electrical resistances during the final 30 minutes of the experiment for each condition were used for final statistical analysis. Statistical analysis was performed using one-way ANOVA followed by Tukey's multiple comparisons test. ****= p value <0.0001. The thin grey lines represent standard error of the mean. **(B)** shows an example of a single experiment, with the resistance on the y-axis normalised to measured resistance at the time of treatment for each condition.

5.4 Discussion

Cell motility is essential during embryogenesis, development and immune responses, and is known to play a prominent role in pathological conditions such as cancer metastasis, atherosclerosis, wound healing and arthritis.[359] The majority of studies examining the role of cell migration in disease processes to date have focussed on understanding the pathways governing tumour invasiveness [degradation of the extracellular matrix (ECM)], and tumour motility (actual movement of the cancerous cell). In order for a cell to move, it must adhere to the ECM, polarise to form a leading edge and trailing edge, push the leading edge forward and retract the trailing edge, and re-internalise cell-environment interactors (eg, integrins) to repeat the cycle (see Section 1.7.1). These processes are highly complex, tightly regulated, and carefully coordinated.[468] The concept that tumour progression is a disease of dysregulated cell motility has recently gained recognition,[469] and accumulating evidence suggests therapies targeting motility would be effective at treating metastasis.[468]

In a similar manner, the concept of podocyte motility as a determinant of glomerular filtration barrier (GFB) function is an emerging theme in renal biology.[129, 130] This idea originated from the *in vitro* observation that exposing podocytes to proteinuric stimuli such as PAN caused cells to adopt a hypermobile phenotype. Recent advances with *in vivo* imaging have confirmed that podocytes are motile along the GFB, and migrate at a higher rate during periods of proteinuric renal disease.[132]

In the current Chapter, I build on microarray data from Chapter 4 suggesting Gc therapy may be exerting prominent effects on podocyte motility. I demonstrate using *in vitro* live-cell imaging that podocytes show reduced motility (as quantified by cell speed) following exposure to Gc, and Gc reduces the motility of podocytes exposed to two proteinuria-inducing agents: PAN (**Figure 5.1**) and LPS (**Figure 5.2**). In combination, these observations raise the possibility that some of the beneficial effects of Gc during periods of proteinuria may be through directly preventing the increased podocyte motility associated with renal disease.

Numerous regulators of cell motility have been identified. These include the Rho family of small GTPases which, when bound to GTP, recruit a range of proteins which regulate the cytoskeleton.[470] Active Rac1 promotes the formation of large membrane protrusions called lamellipodia that drive the motility of many cell types,[407] while

active RhoA can recruit the Rho kinase (ROCK) family of kinases that phosphorylate a range of cytoskeletal proteins, promoting the formation of actin stress fibres and the generation of contractile force.[471] It has also been shown that active Rac1 inhibits RhoA and *vice versa*.[421] Additionally, mutations in genes associated with Rac1 regulation have been shown to cause INS. For example, mutations in the Rho guanosine nucleoside dissociation inhibitor α gene *Arhgdia*, which normally functions to prevent inactive Rac1 from being converted to active Rac1, cause SRNS,[432] and mutations in *Arhgap24* (RhoGAP24), which inactivates Rac1in the non-mutated form, has been associated with familial FSGS.[436] Podocyte-specific under- and over-activity of these small GTPases in animal models have also been shown to cause proteinuria.[426, 428] I therefore proceeded to investigate Gc effects on the activity of Rac1 and RhoA to gain a small degree of mechanistic insight.

These small GTPase activity assays revealed that Gc exposure reduced (pro-migratory) Rac1 activity, and showed a (non-statistically significantly) trend to increase the activity of RhoA. Previously, Ransom *et al.*, performed a similar experiment using cultured murine podocytes. In this paper, cells were treated with dexamethasone for 30 minutes, cultured in fresh medium for a further 3 days, before cells were harvested for analysis.[109] The group found a statistically significant increase in RhoA activity in Gc-treated cells, but no difference in Rac1 activity. Discrepancies between these data and mine may be due to the GR ligand investigated (dexamethasone compared to prednisolone), the podocyte cell line used (murine compared to human) or length of time of Gc exposure. As my data suggested a prominent Gc-effect on reducing Rac1 activity consistent with the anti-migratory effect of Gc I had observed in the live-cell imaging experiments, I confirmed that damaging podocytes with PAN-exposure increased Rac1 activity (**Figure 5.5**).

As well as quantifying podocyte speed, I also investigated Gc effects on the pattern of podocyte migration. Data illustrated in **Figure 5.1-B** and **Figure 5.2-B** demonstrates that I found a small increase in directionally persistent cell movement in podocytes treated with Gc (ie, podocytes exposed to Gc displayed less frequent changes in direction of movement). Weiger *et al.*, demonstrated that the directionality of 2 dimensional cell motion clearly distinguishes benign and tumorigenic cell lines, with tumorigenic cell lines harbouring less directed, more random motion.[472] In data presented here, Gc promotes persistent cell movement, and LPS (but not PAN) causes

more random motion, similar to the dysregulated motility pattern observed in tumorigenic cells.

Directional migration is regulated by multiple mechanisms including microtubules,[473] Cdc42,[417] integrins,[474] and chemotactic stimuli.[475] Duning et al., reported that the protein KIBRA (for kidney and brain) bound to synaptopodin, an important regulator of the podocyte cytoskeleton, and that stable knockdown of KIBRA in immortalised podocytes impaired directional cell migration.[476] It has been shown that chemotaxis imposes more persistent migration in cells via activation of phosphatidylinositol 3'-kinase (PI3K).[477, 478] However, many migratory processes occur with no evidence of extrinsic chemotactic signalling, and use intrinsic cell migration properties. Pankov *et al.*, investigated mechanisms underpinning intrinsic control of directionally persistent cell migration, and identified Rac1 as a molecular switch responsible for determining whether cells move in a random or directionally persistent manner.[479] Using cultured human fibroblast cells, the group identified that high Rac1 activity resulted in increased random migration (low cell persistence), increased cell speed and increased lamellae formation. Conversely, low Rac1 activity switched cells to a directionally persistent, low-speed phenotype with fewer lamellae cell protrusions. The data presented in **Figure 5.2** of LPS treated podocytes displaying increased motility and lower directional persistence, which was reversed following Gc exposure to a more directionally persistent, lower-speed phenotype gave me confidence that Gc was reducing Rac1 activity.

In the context of cancer, the Rac1-specific inhibitor NSC23766 has been shown to reduce the motility of non-small-cell lung cancer cells *in vitro*, and reduce tumour size in mice *in viv*o (no robust systemic toxicology analysis was performed, but the authors reported that the treated animals did not experience severe side effects or a loss in body weight compared to control mice).[480] Regarding kidney disease, the Rac1 inhibitor EHT 1864 has been shown to markedly attenuate proteinuria as well as glomerular and tubulointerstitial damage in the 5/6 nephrectomy chronic model of arterial hypertension and proteinuria in mice.[434] EHT 1864 also attenuated renal injury and fibrosis with the chronic angiotensin II-salt-induced kidney injury model of double transgenic Tsukuba hypertensive mice.[481] I therefore returned to the ECIS assay to investigate whether Rac1 inhibition with EHT 1864 had any direct protective effect on podocytes undergoing acute damage with PAN *in vitro*.

ECIS provides a reading of the electrical resistance across a monolayer of cells plated into wells of the assay. As *in vivo* studies have revealed that a potential difference exists across the GFB, and loss of this potential difference is associated with proteinuria, ECIS provides a good *in vitro* functional measurement of podocyte barrier function.[54] ECIS experiments demonstrated that EHT 1864 did indeed increase the electrical resistance across the PAN-treated podocyte cell layer compared to podocytes treated with PAN alone. Also interestingly, PAN-treated podocytes co-administered with Gc and EHT 1864 had a higher electrical resistance compared to podocytes treated with either agent in isolation (**Figure 5.6**). Whether this observation is due to the two agents in combination reducing Rac1 activity levels below those reached with either agent alone, or whether Gc and EHT 1864 work via multiple, distinct mechanisms is unclear from the current data.

Direct, podocyte-specific, effects of medication frequently used in current clinical practice for the treatment of INS have already been established. Until relatively recently, the potent immunosuppressive effect of ciclosporin A was assumed to underlie its therapeutic efficacy. However, Faul *et al.*, demonstrated the key anti-proteinuric mechanism of ciclosporin A was through direct stabilization of the podocyte actin cytoskeleton.[103] In a similar manner, it is possible that Gc efficacy in INS results from direct effects on the podocyte, and does not rely on the potent immunosuppressive action of Gc. Specifically, promotion of a hypomobile podocyte phenotype and effects on the Rac1 pathway may be important.

As described in Section 1.7.4, Rac1 has a wide range of effects in addition to regulating cell motility, including roles in cell cycle progression and phagocytosis. Additionally, it has already been demonstrated that either podocyte-specific over- or under-activity of small GTPases *in vivo* can result in proteinuria,[426] and it has been proposed that a low, basal-level of podocyte motility is necessary to ensure the GFB remains clear of filtered plasma proteins.[123] As physiological podocyte motility may have a role in the normal functioning of the GFB, and Rac1 has roles in a range of biological processes, drugs affecting cell motility must be subtly targeted. Any future *in vitro* or animal studies examining the potential therapeutic benefits of Rac1 inhibition in reducing the acute-onset proteinuria observed in INS must be careful to ensure robust toxicology screening is performed, although the possibility of anti-proteinuria medication targeted at reducing disease-associated podocyte hypermotility is an intriguing possibility.

6 The podocyte GR cistrome

6.1 Overview

GR translates the glucocorticoid (Gc) signal into genomic outputs. In the absence of Gc, GR resides primarily in the cytoplasm of the cell, but Gc-GR interaction results in the translocation of GR into the nucleus where it binds DNA to regulate gene expression.[237] Both GR-binding patterns and Gc-regulated transcriptional output are highly cell specific.[285] To date, a comprehensive map of GR binding sites (GBS) in podocytes has not been produced. Tackling this issue is key to understand how GR produces transcriptional change.

In this chapter, I identify GBS on a genome-wide scale in human podocytes scale using a combination of chromatin immunoprecipitation coupled with high throughput DNA sequencing (ChIP-Seq). I then proceed to characterise GBS in relation to important functional genetic units, before overlying the microarray analysis from Chapter 4, to identify links between GR-binding and Gc-regulated genes. A striking observation, in agreement with data from other cell types, is that a large proportion of GR-binding occurs at significant linear distances away from Gc-regulated genes, suggesting GR causes changes in gene expression by long-range looping interactions, and, as yet, other unidentified mechanisms.

6.2 Chapter-specific methods

6.2.1 Cell treatment and harvest

Twenty 15cm-diameter culture dishes of confluent wild-type human podocytes, approximating to $6x10^7$ cells, were used for each treatment condition. Twenty four hours prior to harvest, cell culture medium containing standard 10% fetal bovine serum (FBS) was exchanged with cell culture medium containing 10% charcoal-stripped FBS (CSFBS) (Gibco™) to prevent endogenous Gc activating GR. One hour prior to harvesting, cells in culture medium containing CSFBS were treated with either 1µM prednisolone dissolved in methanol or an equal volume (0.001% v/v) of methanol alone as a vehicle control.

Following treatment, cells were cross-linked in 0.1% (v/v) 11% formaldehyde solution for 10 minutes at room temperature, followed by quenching of the cross-linking reaction using 0.05% (v/v) 2.5 M glycine. Each plate was then washed twice with 1 x phosphate-buffered saline (PBS), before cells were harvested using a cell scraper. Cells were pooled into a 50mL conical tube (separate tubes for Gc-treated and vehicle-treated samples) and centrifuged at 700x*g* for 5 minutes at 4ºC. The supernatant was discarded and the cell pellet was resuspended in 10mL PBS. Tubes were centrifuged at 700x*g* for 5 minutes at 4ºC and the supernatant was discarded. Samples were flash-frozen in liquid nitrogen and stored at -80ºC.

6.2.2 Chromatin immunoprecipitation

Samples were processed using reagents from the ChIP-IT® High Sensitivity kit (Active Motif). Cell pellets from -80ºC were resuspended in 5mL Chromatin Prep Buffer supplemented with 5µL of protease inhibitor cocktail (PIC) and 5µL 100nM phenylmethylsulfonyl fluoride (PMSF) at room temperature. Samples were homogenized using a Qiagen TissueRuptor® (power setting '4' for 45 seconds), before a 5 minute incubation on ice. Samples then underwent 90 stokes with a chilled Dounce homogeniser, before transfer to a 15 mL tube, which was centrifuged at 1250g for 3 minutes at 4ºC. The supernatant was discarded and the pellet was resuspended in 500µL ChIP Buffer supplemented with 5µL PIC and 5µL 100nM PMSF. Following a 10 minute incubation on ice, samples were sonicated using an Active Motif EpiShear® probe sonicator in combination with an EpiShear cooled sonication platform (35% power; 45 cycles- each cycle consisted of 30 seconds of sonication followed by 30 seconds of inactivity).

Samples were then centrifuged at 4ºC at maximum speed for 2 minutes to pellet the cellular debris. 100µL from the vehicle treated sample (for 'input' DNA) and 100µL from the +Gc sample were removed at this point to confirm that sonication produced appropriately sized DNA fragments. The remaining samples were stored in aliquots at -80ºC.

100µL Tris-EDTA (TE) buffer, pH 8.0 and 2µL RNAase A (10ug/µL) were added to the 100µL chromatin samples before a 1 hour incubation at 37ºC. 5µL proteinase K (10µg/µL) was then added before a 3 hour incubation at 37ºC. The samples then underwent a 16 hour incubation at 65ºC with 10µL 5M NaCl.

DNA from the 100µL samples was purified using the Macherey-Nagel Nucleospin® kit. 1mL NTB was added to the sheared chromatin, and samples were spun through purification columns for 30 seconds at 11,000g, and the flow-through was discarded. 700µL NT3 was then added to the columns before centrifugation for 30 seconds at 11,000 g, and the flow-through was discarded. The step involving NT3 was performed twice, before the column was dried by 11,000g spin for 1 minute. The column was then inserted into a new holding 1.5mL tube and 20µL NE buffer was added before a 1 minute incubation at room temperature. The column was centrifuged at 11,000g for 1 minute. 18µL of the sample was placed into a PCR tube with 2µL 5M NaCl before a 20 minute incubation at 100ºC, and the sonication efficiency was checked by running the sample on a 1.5% agarose gel (100 volts, 60 minutes).

The chromatin aliquots stored at -80ºC were thawed on ice, and spun at maximum speed at 4ºC for 2 minutes. Overnight incubation at 4ºC on an end to end rotator was performed with the following components: 205µL chromatin, 5µL blocker, 2µg Proteintech™ anti-human GR antibody (24050-1-AP) with 2µg of Sigma® anti- human GR antibody (HPA004248), and 5µL PIC (total volume 240µL).

30µL protein G agarose beads per reaction were washed twice in 30µL TE buffer. The chromatin/antibody mixture was centrifuged at 1250g for 1 minute and 30µL protein G agarose beads were added for a 3 hour period at 4ºC on an end to end rotator. ChIP reactions were centrifuged at 1250g for 1 minute before 600µL ChIP buffer was added, and the mixture was transferred to a ChIP filtration column. The column was washed five times with 900µL AM1 wash buffer. The column was transferred to a 1.5mL tube before centrifugation for 3 minutes at 1250g. Following transfer to a new 1.5mL tube,

warm AM4 elution buffer was added to the column before centrifugation at 1250g for 3 minutes. 2µL of proteinase K (10µg/µL) was added to the 100µL solution before a 30 minute incubation at 55^{o}C. The cross-links were then reversed with a 2 hour incubation at 80^{o}C. 500µL DNA purification binding buffer was added and the pH was adjusted to ensure pH<7.5 using 5µL aliquots of 3M sodium acetate. The sample was then added to the DNA purification column before centrifugation at 14,000 rpm for 1 minute, and the flow through was discarded. 750µL DNA purification wash buffer was added prior to another 14,000 rpm centrifugation for 1 minute. The column was dried with a 2 minute 14,000 centrifugation before transfer to a new 1.5mL tube. Warm purification elution buffer was added to the column before a 1 minute incubation at room temperature, followed by collection of purified ChIP DNA by centrifugation at 14,000rpm for 1 minute.

Prior to sample sequencing, real-time polymerase chain reaction (qPCR) was performed to ensure enrichment of the +Gc samples over vehicle-treated samples for a known GR-binding site (GBS) (**Figure 6.3**). Quantification of the concentration of DNA was performed using the Qubit™ fluorometer.

6.2.3 ChIP-Seq

Following Chromatin-immunoprecipitation (ChIP), DNA libraries were constructed according to the TruSeq® ChIP Sample Preparation Guide (Illumina). Briefly, sample DNA (5–10 ng) was blunt-ended and phosphorylated, and a single 'A' nucleotide added to the 3' ends of the fragments in preparation for ligation to an adapter with a single-base 'T' overhang. The ligation products were then purified and PCR-amplified to enrich for fragments with adapters on both ends. The final purified product was then quantitated prior to cluster generation on a cBot instrument and the loaded flow-cell then paired-end sequenced on an Illumina HiSeq2500 instrument.

Data from the finished sequencing run was transferred to the Bioinformatics Core Facility (University of Manchester), on dedicated off-instrument storage space and converted to .fastq formatted reads using the software CASAVA. Quality control was performed using FastQC v0.11.2. Read pairs (R1 and R2) were filtered using Trimmomatic v0.32 using paired-end mode, to remove adapters, and truncate reads (3') with a base sequence quality of <Q20, taken as an average of a 4bp moving window. Filtered reads <50b were removed. Default settings were applied.

Filtered paired reads were mapped to human reference sequence (HG19/GRCh37; minus haplotypes) using Bowtie2 v2.2.3 with default parameters. Mapped paired-reads were filtered with 'samtools view' v0.1.19, to remove reads with mapping quality <Q30 and discordant pairs (i.e. incorrect orientation and/or >500bp apart). Only paired reads belonging to chromosomes 1-22, X and Y were used in downstream analyses (reads mapping to unassembled contigs and particularly the mitochondrial genome adversely affect the statistics generated by the peak caller).

Regions of the genome significantly enriched with GR read-pairs, considered as fragments of DNA, compared to a background model using the input DNA fragments, were identified using model-based analysis for ChIP-Seq (MACS) 2 v2.1.0.20140616. Paired-end mapped reads enabled MACS2 to take the observed mean of DNA fragments, as opposed to approximating by cross-correlation when single-end reads are used. Binding regions were reported with a minimum q-value of 0.05, and fold enrichment was set at a cut-off of 5 over background.

The University of California, Santa Cruz (UCSC) human canonical genes for HG19 were associated with the summit regions (200bp centred on binding region summits) using RnaChipIntegrator (unpublished, by the BCF core facility). The two closest genes, by closest edges, up to 1 million bases away. Promoter region was designated as -2000b to 100b of transcriptional start site (TSS).

Motif analysis was performed using the Pscan-ChIP.[482]

6.3 Results

6.3.1 Development of methods

ChIP-Seq is a powerful method for identifying genome-wide binding sites for DNA-associated proteins such as transcription factors. An overview of ChIP-Seq is provided in **Figure 6.1**. Two key steps in ChIP-Seq are ensuring adequate sonication of DNA samples and optimising the immunoprecipitation conditions. When performing ChIP-seq for low-abundance transcription factors such as GR (in comparison to ChIP-Seq involving histone modifications), ensuring a sufficient mass of purified DNA is obtained after immunoprecipitation for sequencing is also challenging.

6.3.1.1 Sonication

Sonication is a highly variable step and will vary greatly dependent on the cell type, cell culture conditions, quantity of cells, degree of crosslinking and specifics of the sonicator being used.[483] Undersonication results in a loss of resolution of binding events. Smaller DNA fragments allow for more precise localisation of GR-binding events, as a smaller region of DNA will be pulled down in the immunoprecipitation. The Illumina protocol for pre-sequencing sample preparation involves a size selection step which selects for libraries that are 250-300 base pairs (bp) long. Prior to this, 60 bp adapters have been ligated onto DNA fragments to be sequenced (adding 120 bp to the DNA fragment size). Therefore, 100-200 bp DNA fragments are required prior to immunoprecipitation.

To optimise sonication conditions, I performed a time course experiment, removing aliquots of DNA isolated from human wild type podocytes at discrete points throughout an extended sonication run using a Diagenode® waterbath bioruptor. Each cycle lasted 1 minute and consisted of 30 seconds of sonication and 30 seconds of inactivity (periods of inactivity are introduced to preventing samples overheating). Following crosslink reversal and purification, the DNA samples were run on a 2% agarose gel to estimate the degree of sonication. **Figure 6.2-A** displays results from a published protocol[483] using a Misonix® 3000 sonicator, where each cycle lasted 90 seconds and consisted of 30 seconds of sonication followed by 90 seconds of rest, for comparison. This group suggested 12 cycles of sonication (**Figure 6.2-A**) provided a good degree of sonication. My results in **Figure 6.2-B** similarly show decreased fragment size with longer periods of sonication, and I achieved similar results with 20-25 sonication cycles.

However, in both **Figure 6.2–A** and **–B**, a significant proportion of the total DNA exceeds the 200 bp size-selection cut-off, and would not be sequenced. I therefore attempted to improve the sonication step by using an Active Motif EpiShear® probe sonicator in combination with an EpiShear cooled sonication platform. Each cycle lasted for 1 minute and consisted of 30 seconds of sonication followed by 30 seconds of inactivity. In comparison to the waterbath sonicator, a much higher proportion of the total DNA was found at levels compatible with downstream sequencing. 45 cycles produced shorter DNA fragments lower than those resulting from 30 cycles (**Figure 6.2-C**), and an increase to 60 cycles did not produce additional benefit (**Figure 6.2-D**). As 60 cycles would expose the DNA to unnecessary mechanical shearing and heat, I concluded that 45 cycles of sonication was optimal.

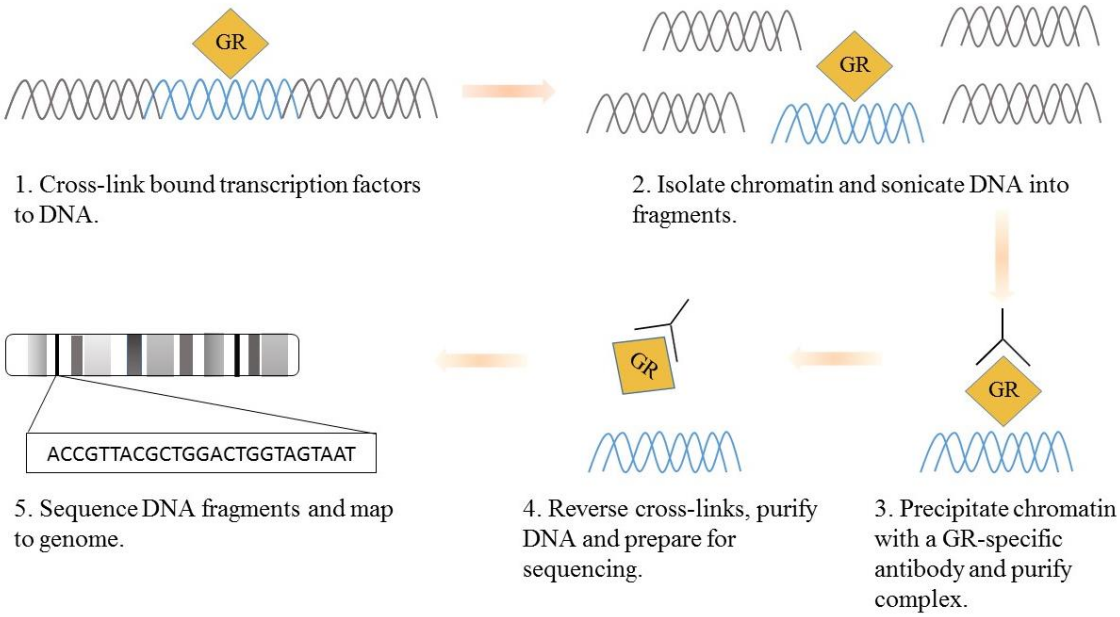

Figure 6.1 Chromatin immunoprecipitation coupled with high throughput DNA sequencing (ChIP-Seq) methodology.

To perform ChIP-Seq, DNA:protein interactions are first stabilised using a cross-linker (eg, formaldehyde). Chromatin is then isolated from cells and fragmented. An antibody against the protein of interest [eg, the glucocorticoid receptor (GR)] is used to enrich for specific chromatin fragments. DNA bound with the protein of interest undergoes cross-link reversal, and the DNA is then sequenced. Aligning these specific DNA fragments with a reference genome allows specific protein-binding loci to be determined.

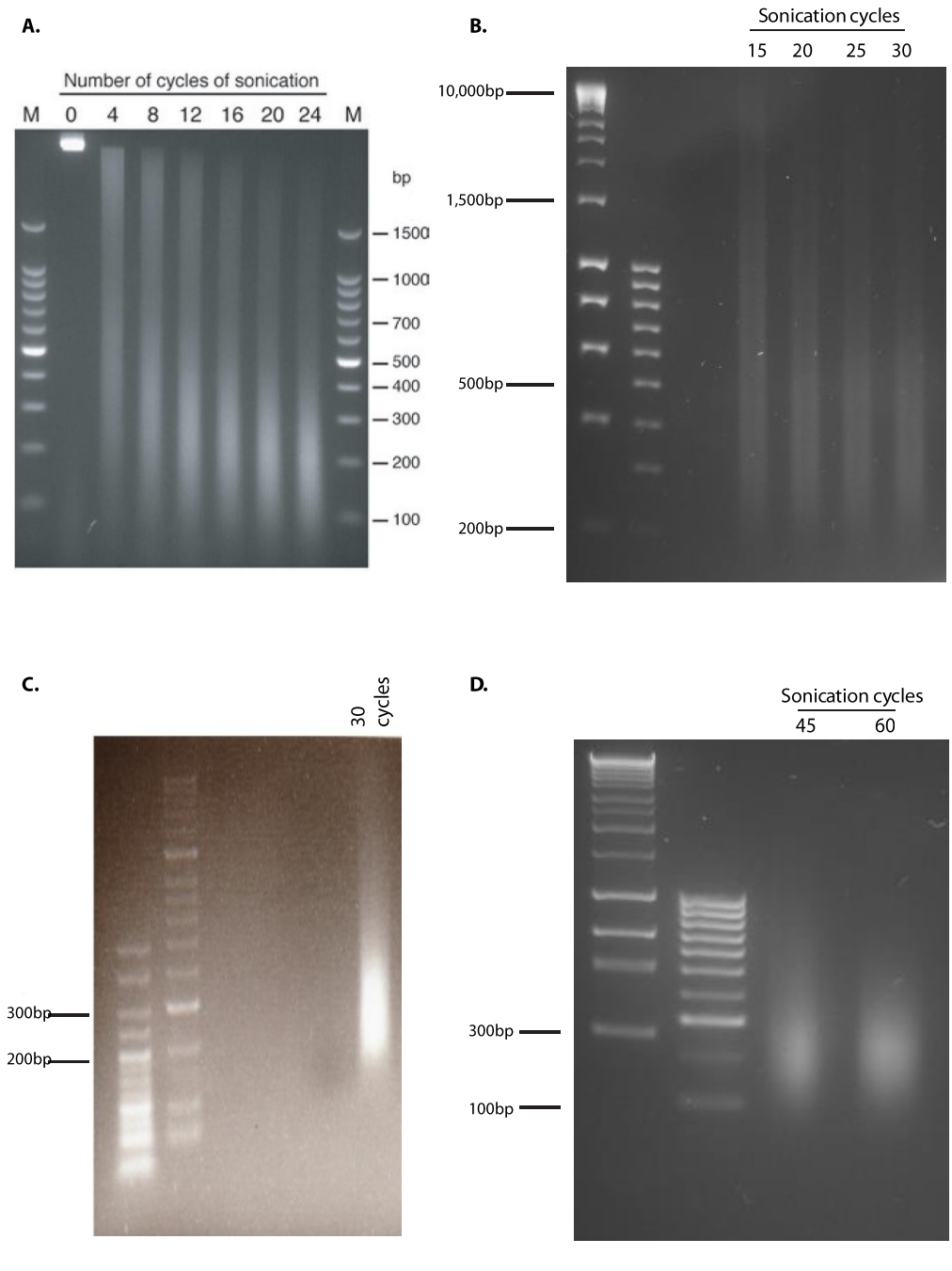

..

Figure 6.2 Sonication Optimisation

Sonication is an important step in preparing samples for ChIP-Seq. Small DNA fragments are required to allow precise localisation of GR-binding sites. 100-200 base pair (bp) DNA fragments are optimal for the current protocol. **(A)** shows a published example of $2x10^8$ crosslinked human Jurkat cells sonicated using a Misonix 3000 sonicator with microtip (power setting 7) with aliquots after a discrete number of cycles (each cycle consisted of 30 seconds of sonication, followed by 90 seconds rest) and run on a 2% agarose gel following DNA purification and cross-link reversal.[483] (**B**) Samples from $6x10^7$ wild type human podocytes sonicated using a Diagenode® waterbath bioruptor (each cycle consists of 30 seconds sonication, followed by 30 seconds of inactivity). (**C**) and (**D**) podocyte samples were sonicated using an Active Motif EpiShear® probe sonicator.

6.3.1.2 Antibody choice

Some published GR ChIP-Seq studies have used a 'cocktail' of several GR antibodies to perform ChIP-Seq.[285, 484] At the time of performing the experiment, the majority of GR ChIP-Seq studies had been performed using murine cell lines, and data regarding successful human GR ChIP-Seq experiments was scarce. In previous small-scale ChIP-Seq optimisation experiments using human A549 cells performed by Dr. Toryn Poolman at the University of Manchester, the Proteintech™ anti-human GR antibody 24050-1-AP had performed well, providing significant enrichment above background (personal communication). I therefore decided to compare the performance of 24050-1-AP in isolation, and in combination with the Sigma® anti- human GR HPA004248 antibody, which had performed well when used by members of Dr. Lennon's laboratory for immunostaining of human kidney specimens.

Following preparation of two ChIP-Seq optimisation samples (one vehicle-treated, one Gc-treated) (see Section 6.2), I performed immunoprecipitations for each sample under the following two conditions (four immunoprecipitations in total; total volume for each immunoprecipitation was 155µL): i) 4µg of 24050-1-AP; and ii) 2µg of 24050-1-AP with 2µg of HPA004248.

To test the efficiency of the two antibody conditions in pulling down GR/DNA cross-linked complexes, I planned to use real-time polymerase chain reaction (qPCR) to identify known GR binding sites in the various samples. However, no GR ChIP-Seq had previously been performed in podocytes (murine or human), and it was already known that GR-occupancy of genetic loci is highly cell-selective. For example, only 11.4% of GBS are shared between murine pituitary and mammary cells.[285]

I therefore had to first identify a human podocyte GBS. To do this, I prepared another set of ChIP-Seq optimisation samples. As I had previously demonstrated that the *GILZ* gene was Gc-responsive (see Chapter 3), I first used qPCR primers for the *GILZ* proximal promoter region, but this only showed a 2.53 fold enrichment (using the $2^{-\Delta\Delta Ct}$ method)[485] over background, which is insufficient for downstream ChIP-Seq analysis. A possible reason for this became clear following the publication of a human GR ChIP-Seq dataset in A549 cells, which did not identify a GBS in the *GILZ* proximal promoter.[449] The minimal *GILZ* enrichment observed in my sample was therefore probably due to GR/DNA complexes with long DNA strands (DNA fragment size selection had not yet occurred).

However, a human GBS dataset did identify a binding region 86 kilobases (kb) upstream of the *FKBP5* gene (FKBP+86) which had been shown to be Gc-responsive in my podocyte microarray dataset (see Chapter 4), and also provided primer sequences for a region 97 kb upstream of *FKBP5* (FKBP+97) with no GBS, to act as a control.[486] After performing qPCR on my samples previously analysed for *GILZ* proximal promoter enrichment, I found a fold-enrichment of 15.8 for the FKBP+86 site, and a fold enrichment of 1.25 for the FKBP+97 site, suggesting primers for the *FKBP*+86 site were suitable to use to test the efficiency of my GR immunoprecipitation. The results for the samples submitted for sequencing are shown in **Figure 6.3**.

Using the *FKBP*+86 primers, I found a 56-fold enrichment for the Gc-treated sample over the vehicle-treated sample when using the 24050-1-AP antibody and HPA004248 antibody together, but DNA purified from the immunoprecipitations involving the 24050-1-AP antibody alone did not record a signal. Ideally, I would have wished to perform another optimisation experiment investigating the HPA004248 alone. However, as it took approximately 6 weeks just to culture sufficient numbers of cells for optimisation experiments, I decided to proceed using the 24050-1-AP antibody and HPA004248 antibody combination.

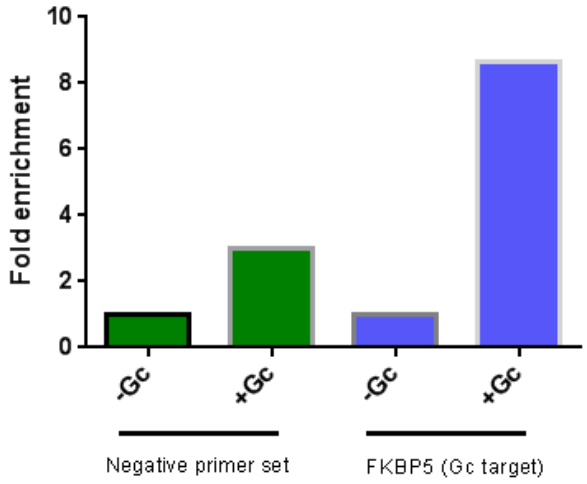

Figure 6.3 Sample enrichment prior to ChIP-Seq

Prior to the sequencing step of ChIP-Seq, it is common practice to ensure samples are suitable by performing real time polymerase chain reaction (qPCR) to ensure a known GR-binding site (GBS) is enriched. Results above demonstrate an 8.6 fold enrichment of vehicle (-Gc) over prednisolone (+Gc) treated samples. Fold enrichment was calculated using the $2^{-\Delta\Delta Ct}$ method.[485] Primers used for the qPCR reaction were for a known GBS near to the *FKBP5* gene,[486] and for a 59 bp fragment from a gene desert on human chromosome 4 as a negative control (Active Motif®).

6.3.2 GR-binding characteristics

I used ChIP-Seq to identify the genomic locations bound by GR in human wild type podocytes following one hour treatment with the GR-ligand prednisolone. Since GR binding to DNA precedes effects on gene expression (as analysed in Chapter 4), one hour was chosen as the length of Gc exposure, consistent with other GR ChIP-Seq studies.[107, 285] ChIP DNA was sequenced with an Illumina 2500 system and mapped to a human reference sequence using the Bowtie programme. The model-based analysis of ChIP-Seq (MACS) algorithm was then used to identify enriched genomic regions in Gc-treated samples compared to DNA input ('background'). To ensure the specificity of the GR antibody, a vehicle-treated control was prepared (without GR-ligand, little GR-DNA interaction should occur). As expected, an insufficient mass of DNA for sequencing was obtained after immunoprecipitation in the vehicle-treated sample (using the high-sensitivity setting on the Qubit® fluorometer, the DNA concentration following immunoprecipitation in the Gc-treated samples was 0.23 ng/µL,

whereas the concentration in vehicle-treated sample was too low for quantification). A fold-enrichment of 5 over background levels was used to identify 1,130 genomic positions occupied by GR following Gc-exposure. This fold-enrichment over background is at least as conservative as published studies: some groups have used fold-enrichments of 3[487, 488] and 4.[489] RnaChipIntegrator was used to assign the two closest human genes based to each GR-binding site (GBS). The 50 GR-binding sites (GBS) showing the highest fold-enrichment over background are shown in **Supplementary Table 10.2**. Details of the full list of 1,130 GBS are provided in Compact Disc 1 (back cover insert).

Visualisation of GBS/human gene alignment was performed using the University of California, Santa Cruz (UCSC) genome browser. Two examples are shown in **Figure 6.4**. GBS peak 1 in the *TTI1* gene locus and GBS peak 1 in the *Per1* gene locus have previously been identified as GR-binding regions in A549 lung adenocarcinoma cells as part of the ENCODE project (https://genome.ucsc.edu/ENCODE/).

The *Cis*-regulatory element annotation system (CEAS) was used to characterise GBS in terms of alignment with functionally important genomic regions such as gene promoters or exons. **Figure 6.5** shows the distribution of GBS over chromosomes. In general, GBS were distributed evenly throughout the genome. The only statistically significant differences when comparing the percentage of GBS on each chromosome to the percentage of total mappable regions of the genome occupied by each chromosome occurred for chromosomes 19 and 20 (more GBS than would be expected) and the X chromosome (fewer GBS than would be expected).

Figure 6.6-A shows how GBS are distributed over important genomic features. Consistent with data from previous studies (see 'Discussion'), the majority of GBS were located outside the intragenic and immediate proximal promoter region of genes. 56.6% of the GBS observed in my dataset were located >2.5 kilobases (kb) away from the nearest transcriptional start site, with 41.2% of GBS located intragenically. An alternative way to visualise this is shown in **Figure 6.6-B**, which illustrates the average binding GBS profile for a hypothetical 3,000 bp gene. The two genomic regions with the highest frequency of GBS are distal to the proximal-promoter, and intragenic.

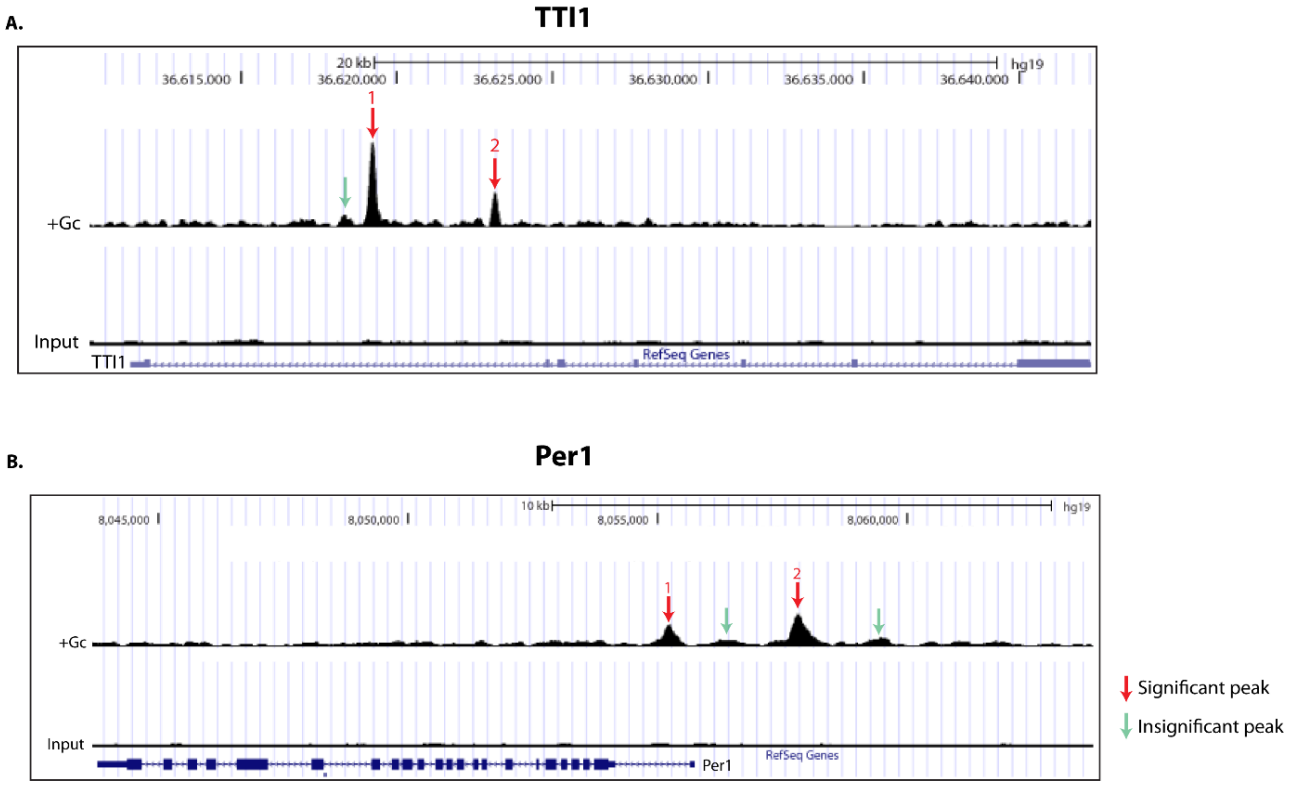

Figure 6.4 GR binding sites in relation to a reference human genome.

GR binding sites (GBS) in human wild type podocytes were identified using ChIP-Seq. Significant GBS were defined as those showing ≥5 fold-enrichment in Gc-treated podocytes compared to DNA input. Results were visualised using the University of California, Santa Cruz (UCSC) genome browser. Two significant intragenic GBS for the *TTI1* gene **(A)**, and a significant peak approximately 400bp downstream of the transcriptional start site (peak 1) and in the promoter region (peak 2) of the *Per1* gene **(B)** are displayed.

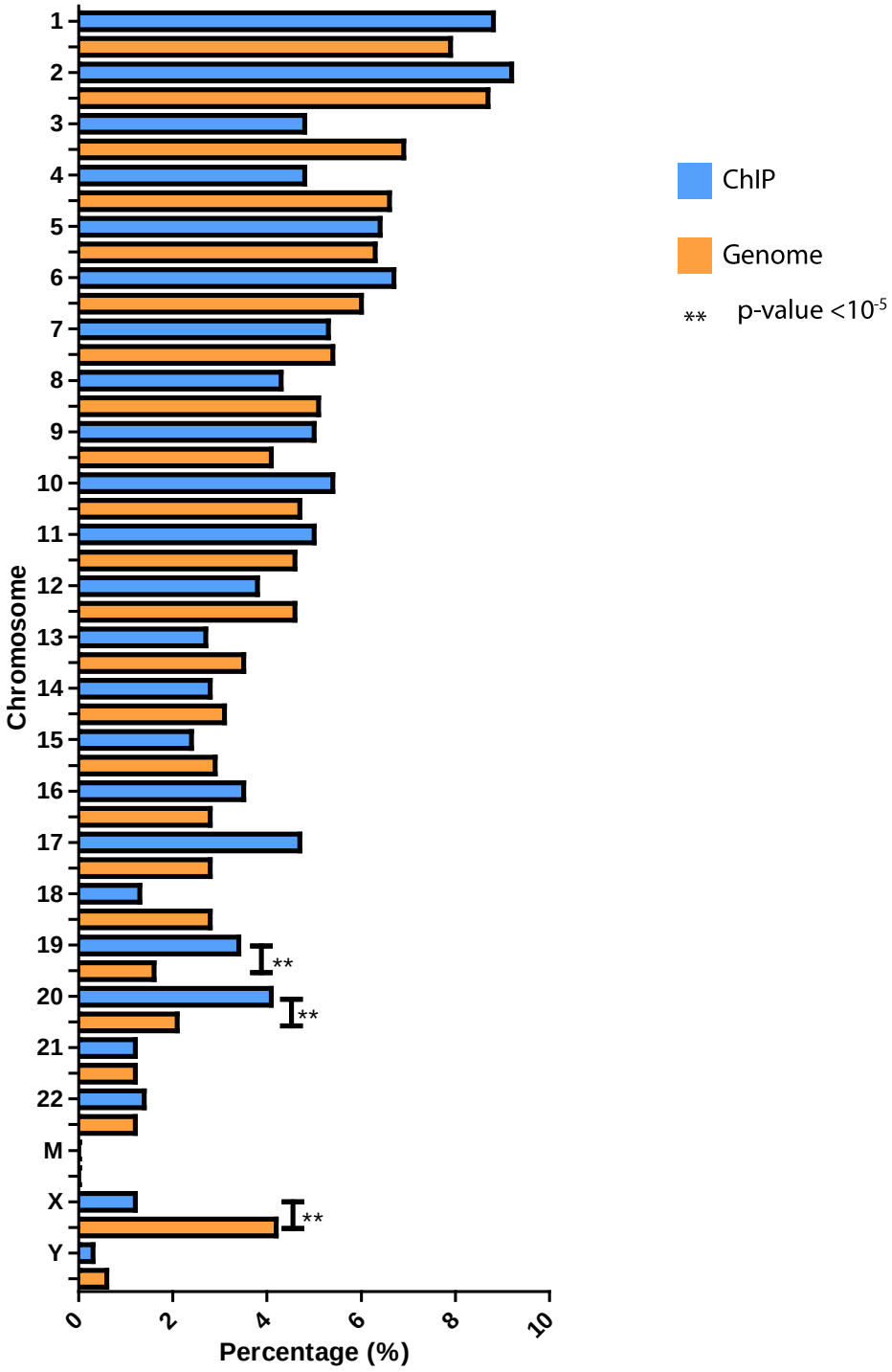

Figure 6.5 Chromosomal distribution of GR-binding sites.

The distribution of 1,130 significant GR-binding sites (GBS) identified by ChIP-Seq over chromosomes was analysed using the *cis*-regulatory element annotation system (CEAS). The orange bars represent the percentage of total mappable regions in the chromosome (genome background) and the blue bars the percentage of total GBS found in that chromosome. For example, 4.1% of GBS reside in chromosome 20, whereas 2.1% of total mappable regions occupy chromosome 20.

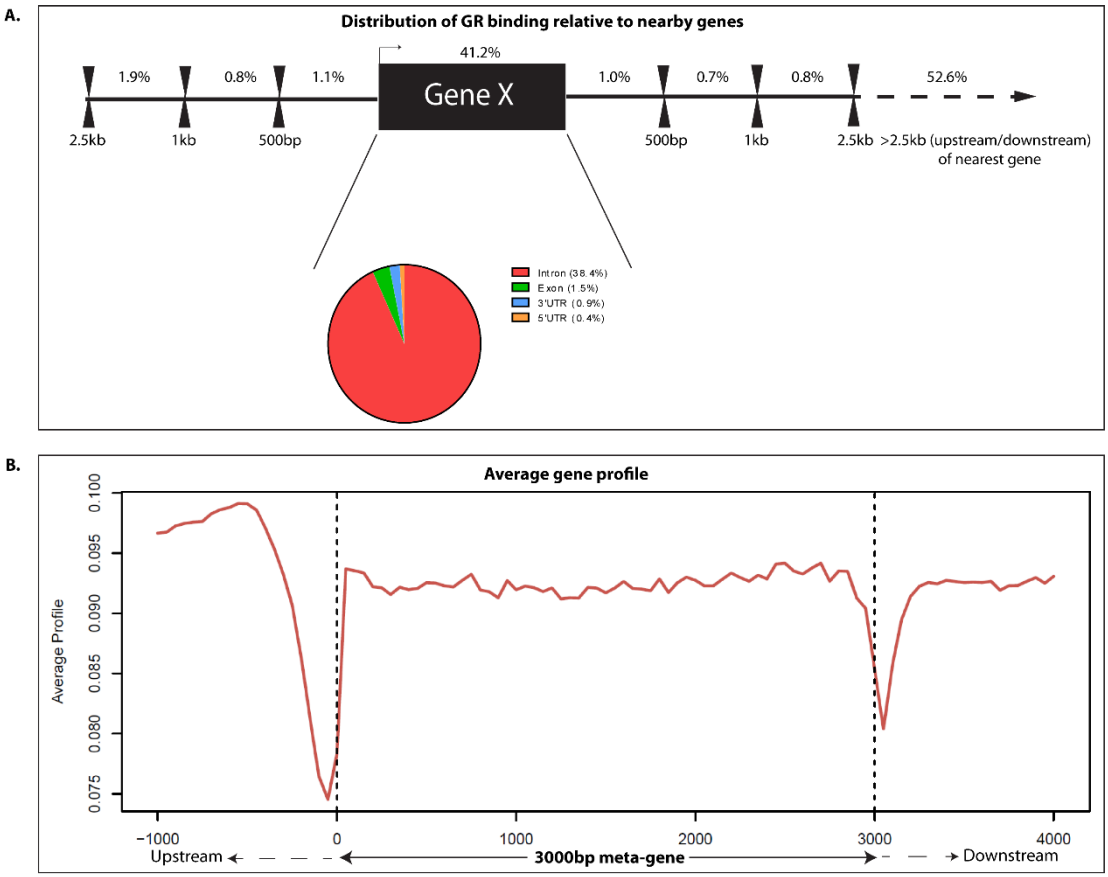

Figure 6.6 Genomic distribution of GR binding sites.

GR-binding sites (GBS) in human wild type podocytes identified by ChIP-Seq were analysed using the *cis*-regulatory element annotation system (CEAS). **(A)** illustrates the percentage of GBS located in different functional genomic units. **(B)** represents the average GBS binding profile on a hypothetical 3kb meta-gene, which shows that GBS are enriched in upstream distal and intragenic regions.

6.3.3 Association between GR-binding and Gc-responsiveness of genes

I then investigated the relationship between the location of GBS and the Gc-responsive genes identified in the microarray dataset from Chapter 4. Frequently, genes have been operationally defined as the coding sequence plus a fixed physical distance in each direction.[490] Lengths of the extensions have been from 0 to 500 kb,[491, 492] but most often of 20kb[493-495] or 50kb.[496-500] For analysis, I separated GBS into 3 categories: i) GBS located ≥50kb away from the coding sequence of any gene; ii) GBS located ≤50kb away from a Gc-regulated gene (as defined by my microarray dataset); and iii) GBS located ≤50kb away from a Gc-unresponsive gene (as defined by my microarray dataset).

Figure 6.7 shows that 32.4% of GBS are located ≥50kb from the nearest gene. I then performed separate CEAS analysis on GBS within 50kb of a Gc-regulated gene and compared this to CEAS analysis on GBS within 50kb of a Gc-unresponsive gene to gain insight into whether the site of GR-binding impacts gene Gc-responsiveness. This revealed that when a GBS is located within 50kb of a Gc-responsive gene it has a higher likelihood of binding in the immediate 2.5kb upstream promoter region. The bar chart in **Figure 6.7** shows greater enrichment of GBS in the 2.5kb upstream promoter region for Gc-responsive genes compared to Gc-unresponsive genes.

I then focussed my analysis on the Gc-regulated genes from my microarray dataset in Chapter 4. Although when GBS do occur within 50kb of a Gc-responsive gene, binding within the 2.5kb upstream region is enhanced, GBS are found within 50kb of a Gc-responsive gene only in a minority of cases. **Figure 6.8** shows that only 83/397 (20.9%) of Gc-regulated genes are located within 50kb of a GBS. 81/83 of these Gc-regulated genes were upregulated following treatment with Gc, with only *DYRK2* and *SOX9* displaying reduced expression. Seven genes were found to have a GR binding site in the 2.5kb upstream promoter region including the classically Gc-regulated genes *Per1* and *DUSP1*.[284] Twenty Gc-regulated genes were located within 50kb of more than one GBS and are listed in **Table 6.3**.

I next went onto investigate the likelihood of GR binding in a particular genetic functional module being associated with transcriptional change of that gene. Focussing on the 764 GBS located within 50kb of any gene, I quantified the number of times a GBS is found within a particular genetic unit (2.5kb upstream promoter, gene body, or GBS within 50kb of gene but outside gene body and immediate upstream promoter) and

expressed the probability of GR-residency in that locus being associated without transcriptional change of that gene as a percentage. **Figure 6.9** shows that GR-residency in any of these genetic loci does not predict Gc-responsiveness, eg, if GR is located in the 2.5kb upstream regulatory region, there is only a 11.8% chance of that gene undergoing a change in transcriptional output.

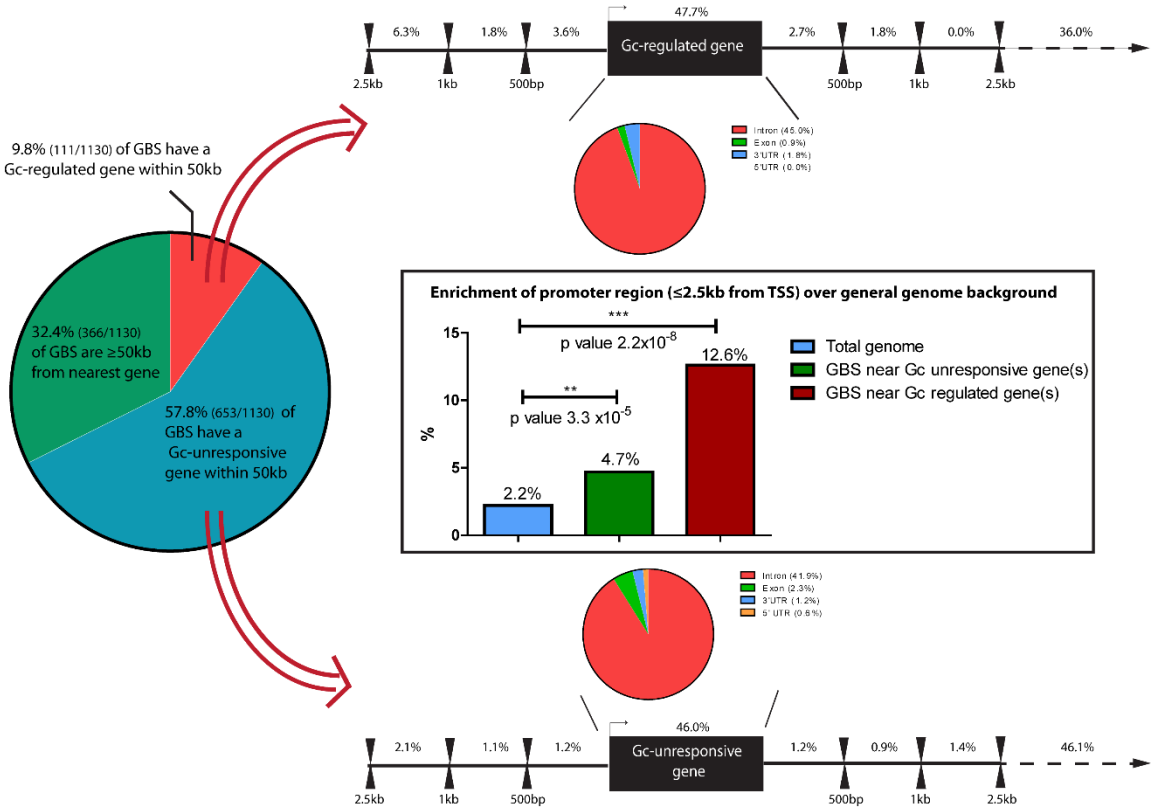

Figure 6.7 Combining the podocyte microarray and ChIP-Seq dataset.

The relation between the GR binding sites (GBS) in wild type podocytes identified by ChIP-Seq and the transcriptional output elicited by Gc-exposure, as identified by microarray, was compared. The large pie chart shows division of GBS according to distance from Gc-regulated genes. Linked diagrams shows the percentage of GBS sites found in areas surrounding Gc –responsive and –unresponsive genes. Bar chart shows GBS enrichment in 2.5 kb promoter region over general genome background for Gc –responsive and –unresponsive genes.

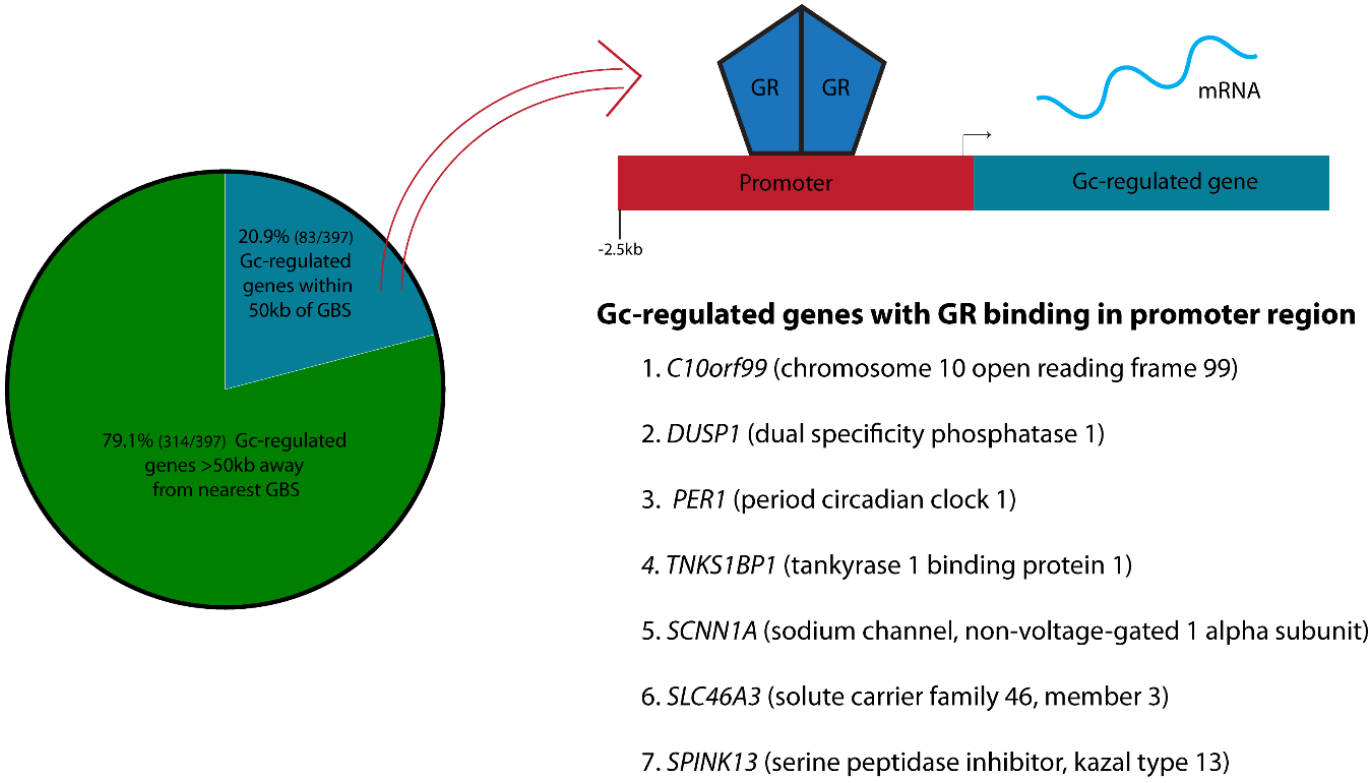

Figure 6.8 Relation between Gc-regulated genes and GR-binding sites

Gc-regulated genes in wild-type human podocytes were identified using microarray analysis and GR-binding sites (GBS) identified using ChIP-Seq. Pie-chart shows proportion of Gc-regulated genes found within 50 kb of a GBS. Seven Gc-regulated genes had a GBS within their 2.5kb upstream promoter.

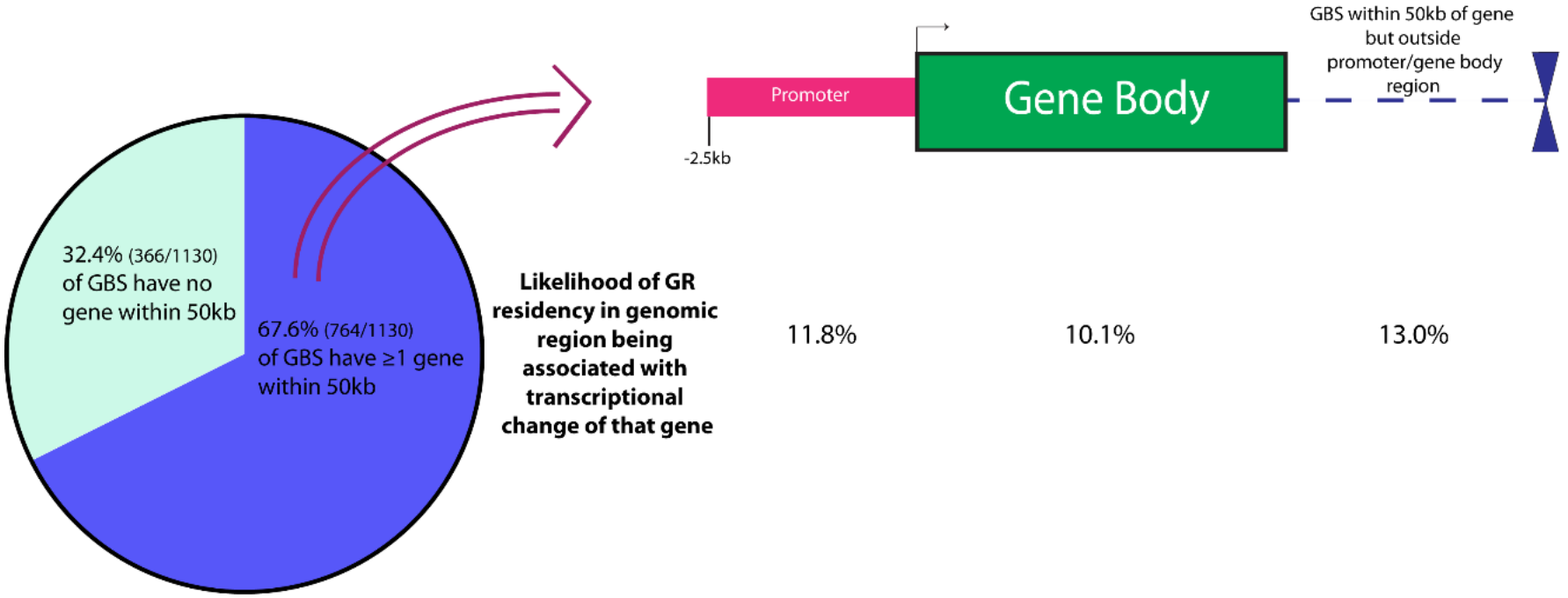

Figure 6.9 Transcriptional output and site of GR-binding

Pie chart shows proportion of GR-binding sites (GBS) in wild type podocytes with a gene within 50kb. Chart shows likelihood of GR residency in particular genomic locations being associated with a change in gene expression following Gc-exposure.

6.3.4 Motif analysis

To gain insight into the nucleotide sequences where GR preferentially bound, I used the Pscan-ChIP programme,[482] which searches the JASPAR database (http://jaspar.binf.ku.dk/) for known binding nucleotide motifs of transcription factors. Pscan-ChIP identified nucleotide sequences in the 1,130 GBS which were found more frequently than would be expected if GR was binding randomly, before linking these enriched nucleotide sequences with known binding motifs of transcription factors. **Figure 6.10-A** shows the most enriched binding motif was a 15bp known glucocorticoid responsive element (GRE). **Figure 6.10-B** shows that, as expected, the location of this binding motif is located in the central region of GBS (typical GREs are 15bp in length, but DNA sonication step in the ChIP-Seq protocol produces DNA strands 100-200 bp in length).

Table 6.1 shows the most enriched binding motifs identified, and the transcription factor associated with that motif. To understand more about potential co-regulators of GR, I performed a 'motif-centred' analysis. For regions in my dataset containing a known GRE, PScanChIP processed the 150bp region around the oligonucleotide to identify known binding sites for other transcription factors. The results are shown in **Table 6.2** and include the Jun and Fos monomeric subunits of activator protein 1 (AP1), which is known to be critical for GR-regulated transcription, partly through maintaining baseline chromatin accessibility.[501] I then investigated whether any differences in binding motif patterns existed between those GBS located within 50kb of a Gc-responsive gene and GBS located within 50kb of a Gc-unresponsive gene. As shown in **Figure 6.11**, no differences of obvious functional importance were observed.

A summary overview of the data is provided in **Figure 6.12**.

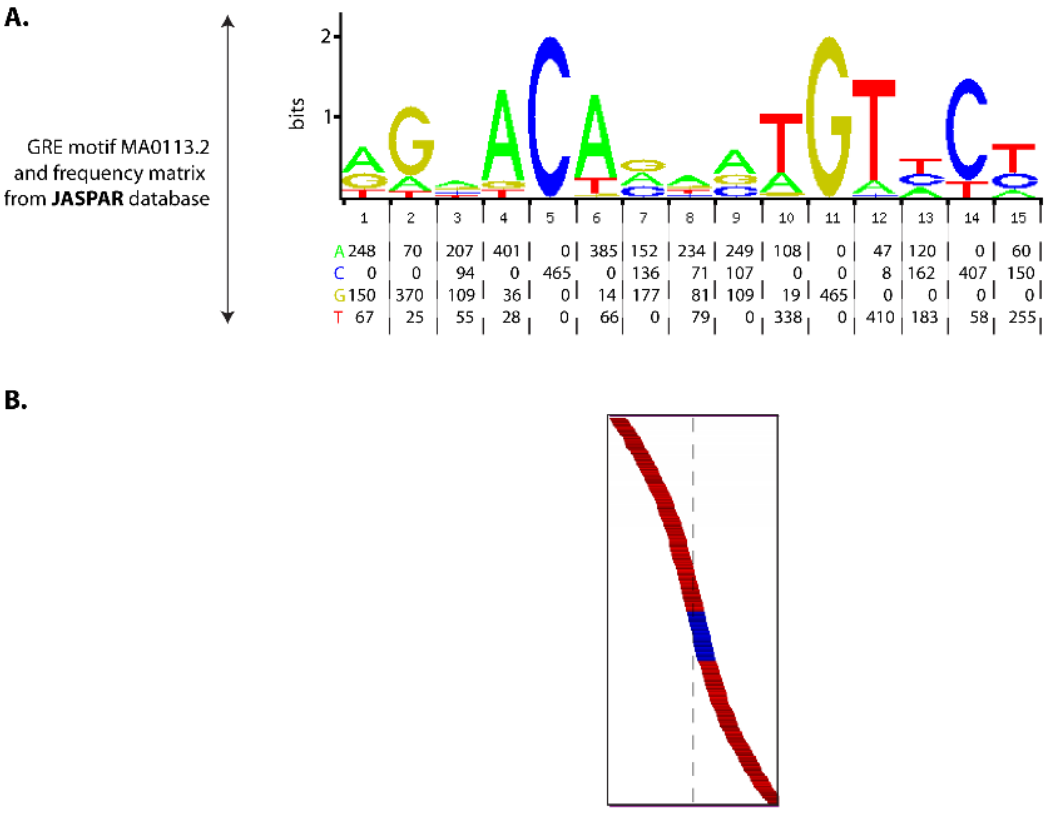

Figure 6.10 Motif analysis

Nucleotide sequence motifs where GR was preferentially binding were identified using Pscan-ChIP.[482] **(A)** shows the sequence motif which was most enriched; a known GR-binding motif. The size of the letter for each nucleotide position relates to how dominant the base is for that position, and the matrix below quantifies this. For example, at base 4, adenine was found most commonly, but guanine and thymine are sometimes located in this position. **(B)** shows an average representation of where the best matching oligonucleotides in the binding region (blue) were found in relation to total DNA fragment (red). A= adenine, C=cytosine, T=thymine, U=uracil.

Table 6.1 Enriched transcription factor binding motifs

1,130 GR-binding sites (GBS) in human wild type podocytes were identified using ChIP-Seq. These nucleotide sequences were analysed by Pscan-ChIP,[482] and the most enriched transcription-factor specific binding motifs are listed below. GR= glucocorticoid receptor, AR=androgen receptor, ESR= oestrogen receptor, RXRA=retinoid receptor alpha, VDR= vitamin D receptor, HSF1= heat shock transcription factor 1, TBP= TATA-binding protein, SOX10=sex determining region Y-box 10, PAX5=paired box 5.

Transcription factor with enriched binding motif	**JASPAR ID**	**Local enrichment p-value**	**Motif over-(↑) or under-(↓) represented**
GR	MA0113.2	1.4×10^{-137}	↑
AR	MA0007.2	2.6×10^{-136}	↑
Ar	MA0007.1	2.6×10^{-129}	↑
GR	MA0113.1	2.4×10^{-58}	↑
ESR2	MA0258.1	1.3×10^{-32}	↑
ESR1	MA0112.2	6.2×10^{-11}	↑
ESR2	MA0258.2	7.3×10^{-8}	↑
RXRA::VDR	MA0074.1	5.4×10^{-7}	↑
HSF1	MA0486.1	1.0×10^{-6}	↑
TBP	MA0108.2	4.2×10^{-5}	↓
SOX10	MA0442.1	4.7×10^{-5}	↑
PAX5	MA0014.2	5.1×10^{-5}	↑
TBP	MA0108.1	5.3×10^{-5}	↓

Table 6.2 GR coregulators

1,130 GR-binding sites in human wild-type podocytes identified by ChIP-Seq underwent 'motif centred' analysis using Pscan-ChIP.[482] Regions in the dataset containing a known GR binding motif were extended 150bp in both directions to identify other known transcription factor binding motifs which may be acting as co-regulators with GR. GR= glucocorticoid receptor, AR=androgen receptor, ESR= oestrogen receptor, RXRA=retinoid receptor alpha, Fos= cellular oncogene c-fos, HSF1= heat shock transcription factor 1, JUND= Jun D proto-oncogene, ARID3A= AT rich interactive domain 3A, PAX5= paired box 5, CDX2= caudal type homeobox 2.

Transcription factor with enriched binding motif	**JASPAR ID**	**Local enrichment p-value**	**Motif over-(↑) or under-(↓)represented**
GR	MA0113.2	2.3×10^{-262}	↑
AR	MA0007.2	9.7×10^{-226}	↑
Ar	MA0007.1	1.9×10^{-213}	↑
GR	MA0113.1	8.4×10^{-101}	↑
ESR2	MA0258.1	2.2×10^{-33}	↑
RXRA::VDR	MA0074.1	4.0×10^{-13}	↑
ESR1	MA0112.2	7.2×10^{-11}	↑
ESR2	MA0258.2	1.8×10^{-9}	↑
FOS	MA0476.1	2.1×10^{-8}	↑
HSF1	MA0486.1	9.7×10^{-7}	↑
JUND	MA0491.1	1.5×10^{-6}	↑
ARID3A	MA0151.1	4.5×10^{-6}	↓
PAX5	MA0014.2	8.1×10^{-6}	↑
CDX2	MA0465.1	9.1×10^{-6}	↓
SOX10	MA0442.1	4.1×10^{-5}	↑
FOSL1	MA0477.1	5.2×10^{-5}	↑

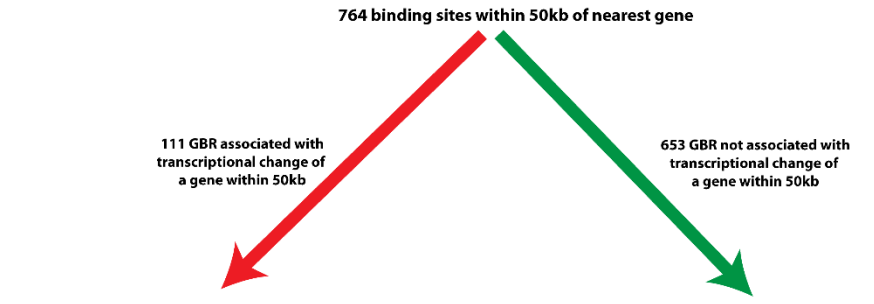

Transcription factor with enriched binding motif	JASPAR ID	Local enrichment p-value	Motif over-(↑) or under-(↓) represented
GR	MA0113.2	9.9×10^{-37}	↑
AR	MA0007.2	1.6×10^{-35}	↑
Ar	MA0007.1	6.3×10^{-32}	↑
GR	MA0113.1	6.5×10^{-16}	↑

Transcription factor with enriched binding motif	JASPAR ID	Local enrichment p-value	Motif over-(↑) or under-(↓) represented
GR	MA0113.2	2.1×10^{-72}	↑
AR	MA0007.2	5.4×10^{-68}	↑
Ar	MA0007.1	2.8×10^{-67}	↑
GR	MA0113.1	5.4×10^{-26}	↑
ESR2	MA0258.1	3.5×10^{-19}	↑
ESR1	MA0122.2	2.2×10^{-7}	↑
ESR2	MA0258.2	7.6×10^{-6}	↑

Figure 6.11 GR co-regulators in Gc-sensitive and –insensitive sites

ChIP-Seq identified GR-binding sites in wild type podocytes and microarray analysis revealed Gc-regulated genes. Pscan-ChIP was used to perform a 'motif-centred' analysis to identify potential transcriptional co-regulators in Gc-responsive and –unresponsive genes. GR= glucocorticoid receptor, AR=androgen receptor, ESR= oestrogen receptor.

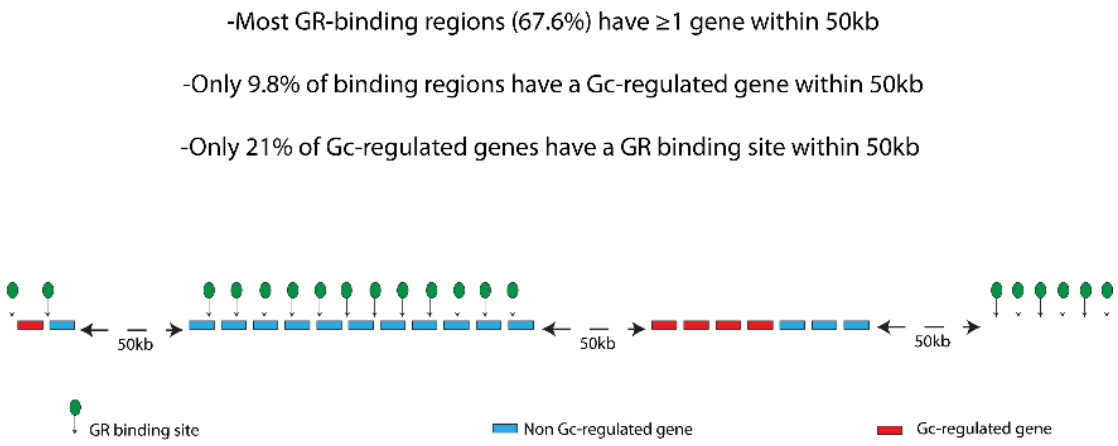

Figure 6.12 Summary of GR binding pattern in human podocytes

ChIP-Seq identified 1,130 GR binding sites in human wild-type podocytes, and their location in relation to Gc-regulated genes was investigated. The diagram above shows a cartoon summary of the GR binding pattern observed.

6.4 Discussion

In this chapter I analysed the GR-binding pattern in human wild type podocytes, and how this relates to the transcriptional changes observed in the microarray study from Chapter 4. GR ChP-Seq has previously been performed in other cell lines, and a striking feature of these datasets is the large proportion of GR binding events occurring significant distances away from the gene coding region. A comparison summary of locations of GBS identified in my data with other studies is shown in **Figure 6.13**.

John *et al.*, performed GR ChIP-Seq in 3134 murine mammary adenocarcinoma cells and found 93% of GBS were located >2.5kb away from the nearest gene (in comparison to 52.6% of GBS in my dataset).[285] In a similar manner, the group were unable to identify any clear relationship between GR-occupancy patterns and transcriptional activation of nearby genes. Yu *et al.*, found that 54% of Gc-regulated genes in murine adipocytes had a GBS within 100kb,[502] and Reddy et al., found that 30% of Gc-responsive genes had a GBS within 10kb,[449] whereas my analysis revealed 20.9% of Gc-regulated genes had a GBS within 50kb. These data raise the possibility that GR acts through long-range mechanisms, or that many binding events are opportunistic and do not necessarily affect transcriptional output. Indeed, long-range looping interactions between regulatory sequences and their target genes have been analysed using chromosome conformation-capture (3C)-based techniques, and identified chromatin interactions that span a linear genomic distance from several hundred base pairs to over 1 million base pairs.[503] Wilms' tumour 1 (*WT1*) is a transcription factor with a key role in kidney development, and *WT1* mutations lead to a range of renal manifestations including Denys-Drash syndrome, the Frasier syndrome, and steroid-resistant NS. Several WT1 ChIP-Seq experiments have been performed in podocytes, and these show around 45% of WT1 genomic binding sites are located more than 50kb away from transcription start sites.[33-35] This suggests WT1 regulates gene expression via both proximal and distal regulatory elements in a similar manner to GR.

Another prominent observation from my data was that of the 83 Gc-regulated genes located within 50kb of a GBS, only 2 genes (*DYRK2* and *SOX9*) showed transcriptional downregulation. This raises the possibility that linear genomic distance between the GR-binding site and gene may be a factor in determining the directionality of transcriptional change. A similar observation was made in lung adenocarcinoma A549 cells by Reddy *et al.*, who found genes activated by Gc have GR bound within a median

distance of 11kb, whereas the GR binding site for genes repressed by Gc were a median of 146kb from the gene.[449]

Motif analysis (**Figure 6.11**) revealed little difference between GBS close to Gc-responsive genes and Gc-unresponsive genes. Additionally, Uhlenhaut *et al.*, found that identical nucleotide motifs directed positive and negative transcriptional regulation in macrophages.[284] Overall, my data are consistent with existing studies and suggests long-range interaction of GR with target genes is important, but a full understanding of the mechanism whereby GR exerts transcriptional change is a major future challenge.

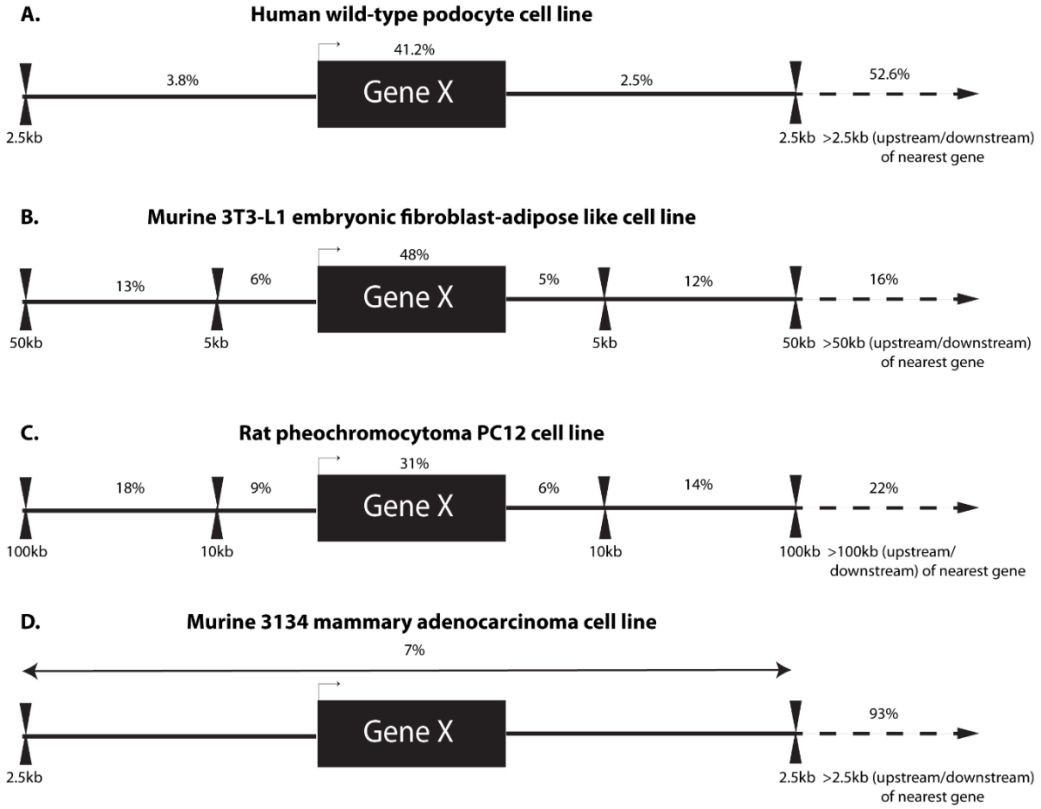

Figure 6.13 Comparison of human podocyte ChIP-Seq dataset to other cell lines

In the current study, GR binding sites (GBS) were identified in human wild type podocytes using ChIP-Seq. The percentage of GBS found in particular genomic locations is shown in **(A)**. For comparison, the location of GBS found in murine adipocytes **(B)**,[502] rat pheochromocytoma **(C)**,[448] and murine mammary adenocarcinoma cells **(D),**[285] from published studies are shown.

Table 6.3 Genes near multiple GR-binding sites

GR-binding sites (GBS) in human wild type podocytes were identified using ChIP-Seq, and Gc-regulated genes were identified using microarray analysis. 1,130 GBS were found in total, and the twenty Gc-regulated genes located with 50 kb of more than one GBS are listed below.

Gene Symbol	Gene name	#GR binding sites within 50kb
SERPINE1	Serpin peptidase inhibitor, clade E (nexin, plasminogen activator inhibitor type 1),	5
FKBP5	FK506 binding protein 5	4
CRISPLD2	Cysteine-rich secretory protein LCCL domain containing 2	3
PRKAG2	protein kinase, AMP-activated, gamma 2 non-catalytic subunit	3
ST6GALNAC2	ST6 (alpha-N-acetyl-neuraminyl-2,3-beta-galactosyl-1,3)-N-acetylgalactosaminide	3
TSC22D3	Glucocorticoid-induced leucine zipper	
ACPL2	acid phosphatase-like 2	2
CFLAR	CASP8 and FADD-like apoptosis regulator	2
DUSP1	Dual Specificity Phosphatase 1	2
FAM134B	Family With Sequence Similarity 134, Member B	2
JPH2	Junctophilin 2	2
KLF6	Krippel-Like Factor 6	2
LEF1	Lymphoid enhancer-binding factor 1	2
MT1M	Metallothionein 1M	2
NPAS2	Neuronal PAS domain protein 2	2
PER1	Period circadian clock 1	2
RASSF4	Ras association (RalGDS/AF-6) domain family member 4	2
RERE	Arginine-glutamic acid dipeptide repeats	2
TFCP2L1	Transcription factor CP2-like 1	2
VSTM2L	V-Set And Transmembrane Domain Containing 2 Like	2

7 Proteomic analysis of human wild type podocytes

7.1 Overview

Characterisation of the podocyte proteome is an important step in understanding the role this cell plays in maintaining normal glomerular function. In this chapter, I use recent developments in label-free mass spectrometry (MS) to identify the protein constituents of human wild type podocytes, and to identify proteins whose abundance significantly alters following Gc exposure. These analyses reveal that the podocyte is rich in actin cytoskeletal regulators, consistent with observations that the podocyte is a motile and contractile cell (see Section 1.3.4). Gene ontology (GO) analysis of proteins whose expression alters following Gc exposure validates the analysis performed on the Gc-regulated transcriptomic data (Chapter 4), with seven of the top ten most significantly enriched GO terms being common to both datasets. In particular, 'cellular movement' is an enriched term in both datasets, suggesting Gc exerts prominent effects on podocyte motility.

7.2 Chapter specific methods

7.2.1 Sample preparation

One confluent 10cm-diamater cell culture dish of fully differentiated wild type human podocytes was used for each replicate. Twenty four hours prior to treatment cells were placed into serum-free medium. Cells in culture medium then underwent 24 hours of treatment with either 1μM prednisolone dissolved in methanol or an equal volume (0.001% v/v of media) of methanol alone as a vehicle control. Cells were lysed using radioimmunoprecipitation (RIPA) buffer [150mM NaCl, 20mM Tris pH 7.4, 2mM $MgCl_2$, 0.5% Triton X-100 supplemented with cOmplete protease inhibitor cocktail tablets (Roche) and PhosSTOP protease inhibitor cocktail tablets (Roche)] to produce whole cell extracts.

7.2.2 Digestion

Protein samples were separated by SDS-PAGE and allowed to migrate 10mm into a 4-12% polyacrylamide gel. Following staining with InstantBlue (Expedeon), bands of interest were excised from the gel and dehydrated using acetonitrile followed by vacuum centrifugation. Dried gel pieces were reduced with 10 mM dithiothreitol and alkylated with 55 mM iodoacetamide. Gel pieces were then washed alternately with 25 mM ammonium bicarbonate followed by acetonitrile. This was repeated, and the gel pieces dried by vacuum centrifugation. Samples were digested with trypsin overnight at 37^{o}C.

7.2.3 Mass spectrometry

Digested samples were analysed by Liquid chromatography-tandem mass spectrometry(LC-MS/MS) using an UltiMate® 3000 Rapid Separation LC (RSLC, Dionex Corporation) coupled to an Orbitrap Elite (Thermo Fisher Scientific) mass spectrometer.

Peptide mixtures were separated using a gradient from 92% A (0.1% FA in water) and 8% B (0.1% FA in acetonitrile) to 33% B, in 44 min at 300 nL min^{-1}, using a 250 mm x 75 μm i.d. 1.7 μM BEH C18, analytical column (Waters). Peptides were selected for fragmentation automatically by data dependant analysis.

7.2.4 Progenesis data analysis

Profile .raw files were imported into Progenesis LC-MS (Nonlinear Dynamics) version 4.1. Alignment of chromatograms was carried out using the automatic alignment algorithm. Progenesis created the peak list file that was exported to an in-house Mascot server (Matrix Science).[504] Carbamidomethylation of cysteine was set as a fixed modification and oxidation of methionine was allowed as a variable modification. Only tryptic peptides were considered, with up to one missed cleavage permitted. Monoisotopic precursor mass values were used and only doubly and triply charged precursor ions were considered. Mass tolerances for precursor and fragment ions were 5 parts per million (ppm) and 0.5 Daltons (Da) respectively.

Data were re-imported in Progenesis to assign peptide identification to features. Peptide and protein data were then exported from Progenesis as .csv files to be analysed in Excel 2007 (Microsoft®).

7.2.5 Functional analysis of data

Proteins were only considered for further analysis if they were identified using ≥2 unique peptides.[505] Gc-regulated proteins were identified by a fold-change of >2 and a false discovery rate adjusted p value (q value) of <0.05. Global proteomic data were analysed using output from DAVID (Gene Ontology) version 6.7,[506, 507] coupled to the Enrichment map plug-in on Cytoscape version 2.8.3 (p value 0.001, q value 0.05, similarity cut-off 1.0).[508] Gene ontology (GO) analysis using the term ‘molecular and cellular functions’ was performed using IPA® software (Ingenuity). Enriched lower-order GO terms were ranked according to significance with a minimum threshold p value of 0.05.

7.3 Results

7.3.1 Optimisation of experimental conditions

Gc-mediated effects on translational output typically occur on the scale of hours, but are variable between specific Gc-regulated proteins.[509] In order to choose a suitable time point for analysis of Gc-mediated effects on translational change in human podocytes, I first performed an optimisation experiment comparing the protein content of total cell lysate preparations obtained from podocytes following treatment with vehicle, 12 hours of Gc, and 24 hours of Gc (biological duplicates prepared for each condition).

Samples were analysed using a Thermo Scientific Orbitrap Elite mass spectrometry system with a 1 hour run-time per sample. Data processing with Progenesis QI software (Nonlinear Dynamics) in conjunction with Mascot (Matrix science) to identify peptides, revealed a raw protein identification count of 1,921. Principal component analysis (PCA) showed vehicle-treated samples clustered together, as did samples treated for 24 hours with Gc (**Figure 7.1**). Samples treated with Gc for 12 hours were widely separated, suggesting an intermediate phenotype between vehicle- and 24 hour Gc-treated samples. Therefore, I proceeded to prepare triplicate samples to compare the protein differences between vehicle-treated podocytes and podocytes treated with Gc for 24 hours. Additionally, MS run-times were extended to 2 hours per sample to further improve the number of proteins identified.

7.3.2 Protein composition of human wild type podocytes

Total cell lysates from wild-type human podocytes treated with vehicle or Gc for 24 hours were prepared. Prior to MS analysis, sample quality was checked to ensure Gc-exposure had resulted in translational change for a known Gc-regulated protein, and to ensure minimal sample degradation had occurred during processing. As I had already demonstrated that Gc-exposure resulted in reduced expression of GR (Chapter 3), I performed western blotting using a GR primary antibody on sample aliquots. Western blotting demonstrated downregulation of GR in the samples following Gc-exposure, and I therefore proceeded with MS analysis (**Figure 7.2-A**).

Samples were run on a Thermo Scientific Orbitrap Elite mass spectrometer with 2 hour run times per sample to improve the number of peptides detected and therefore proteins identified. Data were analysed using Progenesis QI software. Progenesis produces an ion intensity map, which is representative of the sample's MS signal by mass/charge

and retention time. The software automatically selects the most appropriate sample to act as a 'reference' with which other samples are aligned. Aligning ion intensity peaks from different samples is key to quantifying differences in protein abundance. Alignment scores >50% are generally considered acceptable, and 68.8%-90.8% were recorded for my samples (**Figure 7.2-B**). PCA showed a clear separation of samples according to treatment group (**Figure 7.3**).

A raw protein identification count of 3,866 was found on the 2 hour runs, in contrast to the 1,921 proteins identified on the optimisation 1 hour sample run times. To ensure protein identification was robust, proteins identified by less than 2 unique peptides were discarded (**Figure 7.2-C**).[505] The 2,062 proteins remaining represented the measurable protein content of podocytes. MS analysis of total cell lysates will not produce an exhaustive list of all proteins contained in a cell, as low-abundance proteins are likely to remain undetected. However, processing of the data observed may still be informative. Proteins detected by MS of known importance to podocyte function[510] included: CD2-associated protein, α-actinin 4, zonula occludens protein 1, utrophin, erzin, integrin β1, integrin αV, and integrin β5. Important podocyte proteins that were not detected included: nephrin, podocin, synaptopodin and podocalyxin.

In order to understand the cellular compartments from which these 2,062 proteins originated, gene ontology analysis was performed using a combination of DAVID,[506, 507] and the Enrichment map software plug-in for Cytoscape.[508] Results are shown in **Figure 7.4** and show that proteins were sampled from a wide range of cellular compartments including the cytosol, nucleus, mitochondria, and cell membrane. I proceeded to investigate the function of the proteins identified, and one of the biological processes enriched was cytoskeletal regulation (**Figure 7.5**).

Next I focussed on proteins whose expression changed significantly following 24 hours of treatment with Gc. Proteins which showed a 2-fold change (either up or down) and a false discovery rate adjusted p value (q value) of <0.05 were considered to be Gc-regulated (**Figure 7.2-C**). 53 proteins were identified and are listed in **Supplementary Table 10.3**. Gene ontology analysis was performed using Ingenuity software for the term 'molecular and cellular functions' and 'cell movement' was a highly enriched term (**Figure 7.6**). 'Cell death and survival' was the most significant term, in keeping with previous links to Gc and apoptosis.[110, 511]

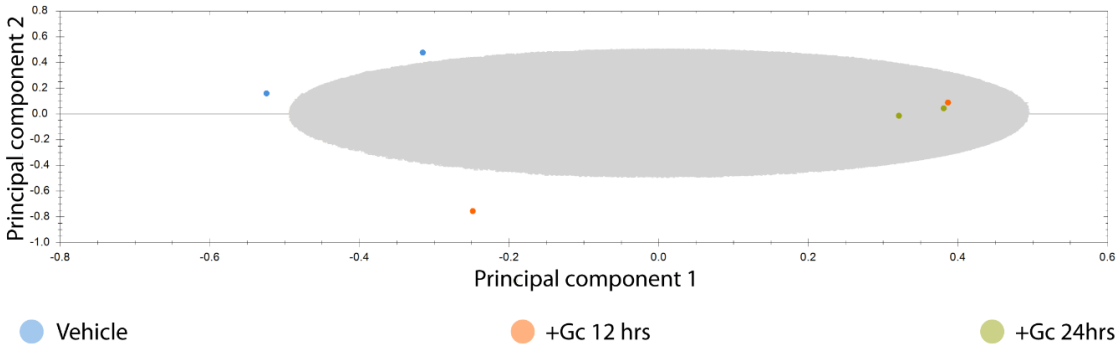

Figure 7.1 Principal component analysis of optimisation samples

To decide whether 12 hours or 24 hours of treatment with Gc was a more appropriate time to assess the global translational change exerted by Gc on wild-type podocytes, total cell lysates were prepared and compared with samples from vehicle-treated podocytes using mass spectrometry. Principal component analysis of identified peptides revealed a clustering of 24 hour treated samples, while samples treated for 12 hours were more widely dispersed.

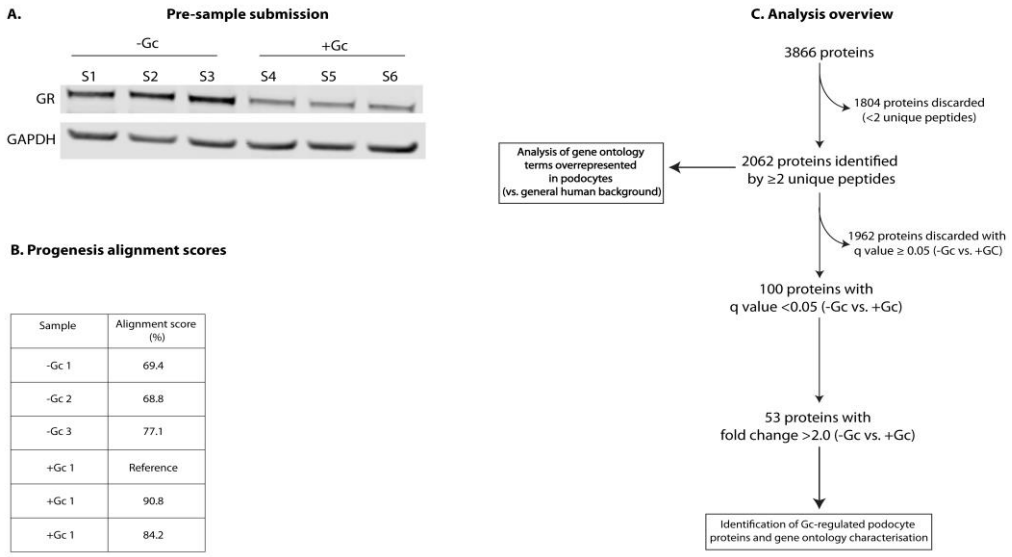

Figure 7.2 MS samples

Total cell lysates were prepared from wild type podocytes treated with vehicle (-Gc) or Gc (+Gc) for 24 hours. Samples were analysed by mass spectrometry (MS) to define the podocyte proteome and understand global proteomic changes exerted by Gc exposure. **(A)** shows western blot of vehicle-treated samples (S1-S3) and Gc-treated samples (S4-S6) using a human GR antibody. Reduced expression of GR is demonstrated, suggesting Gc treatment had been effective and samples were suitable for MS analysis. **(B)** Data were processed using Progenesis QI software which aligns ion intensity peaks generated by MS to allow protein quantification. The software automatically selects a reference sample to which all others are aligned. Alignment scores for the samples are shown; scores >50% are considered acceptable. **(C)** For analysis of the global podocyte proteome, only proteins identified by 2 or more unique peptides were used, and Gc-regulated proteins were considered to be those showing a fold change of > 2.0 and a false discovery rate adjusted p value (q value) of <0.05.

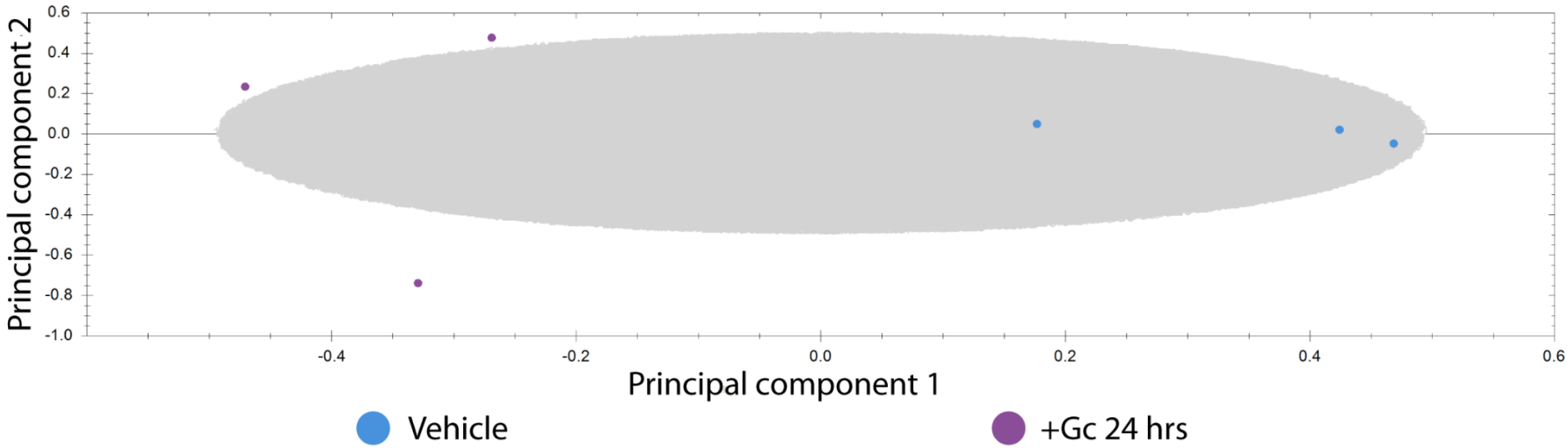

Figure 7.3 Principal component analysis of peptide ions detected by mass spectrometry

Mass spectrometry (MS) analysis was performed on samples from human wild type podocytes treated for 24 hours with either vehicle or Gc. Principal component analysis of MS data was performed using Progenesis QI software, and revealed a clear separation of samples according to group, suggesting further data analysis was warranted.

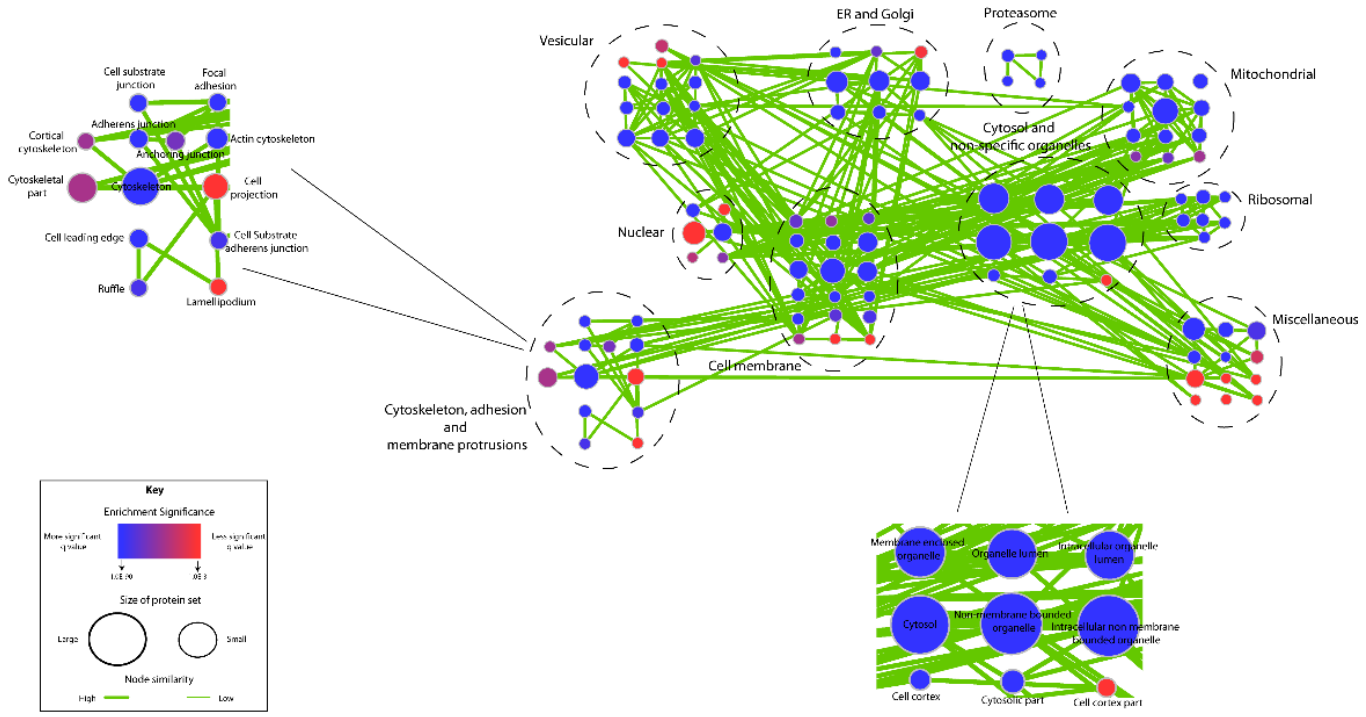

Figure 7.4 Sub-cellular origin of podocyte proteins identified by mass spectrometry

Mass spectrometry (MS) analysis was performed on total cell lysates from wild type human podocytes treated with vehicle or Gc for 24 hours. 2,062 proteins were identified in total. The sub-cellular localisation of these proteins was identified using a combination of the DAVID web-based analysis tool (https://david.ncifcrf.gov/) (Gene ontology_BP) and the Enrichment map plug-in on Cytoscape.[508] Settings used in Cytoscape were as follows: p-value 0.001, q-value 0.05, similarity cut-off (ranging from 0.5-1.0, with 0.5 being least conservative) 1.0.

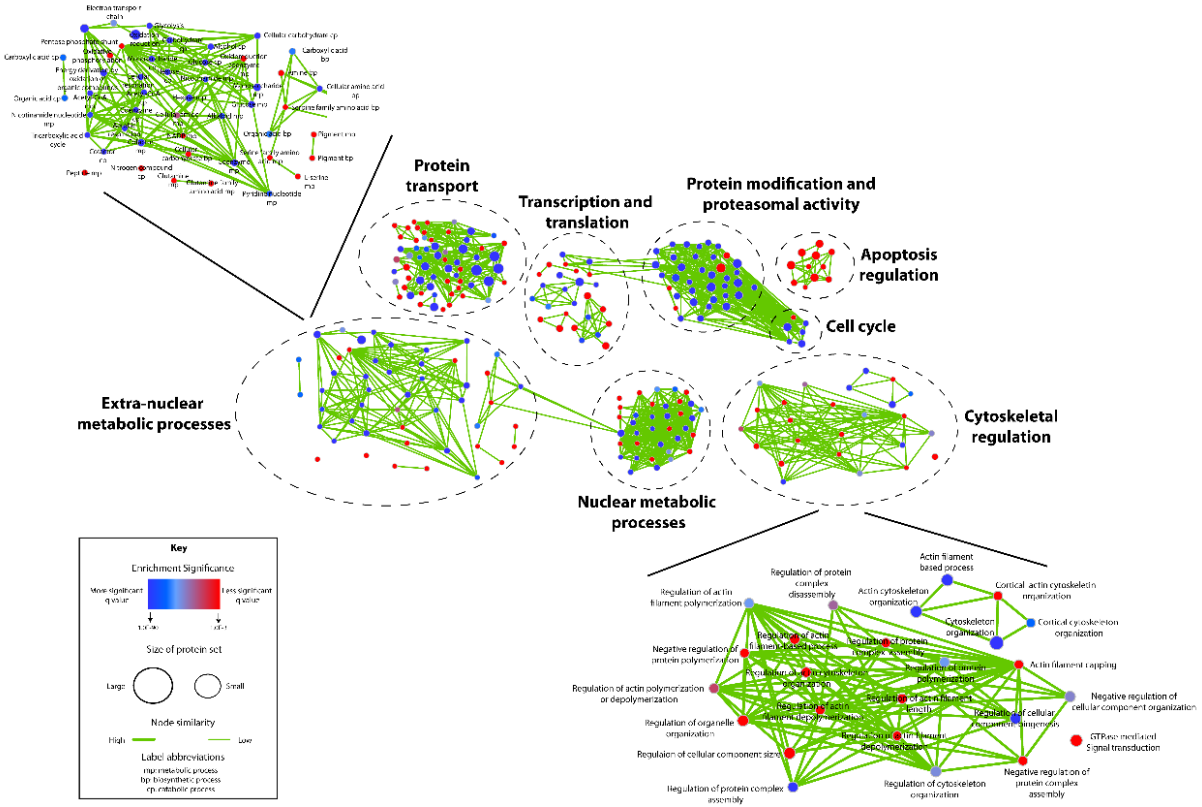

Figure 7.5 Biological functions of proteins identifed by global mass spectrometry anlaysis

Total cell lysates from human wild type podocytes underwent mass spectrometry (MS) analysis to define the podocyte proteome. The 2,062 proteins identified were analysed using DAVID online software (Gene ontology_BP) coupled with the Enrichment map plug-in on Cytoscape to understand the biological processes with which these proteins were involved. Settings used in Cytoscape were as follows: p-value 0.001, q-value 0.05, similarity cut-off (ranged from 0.5-1.0, with 0.5 being least conservative) 1.0.

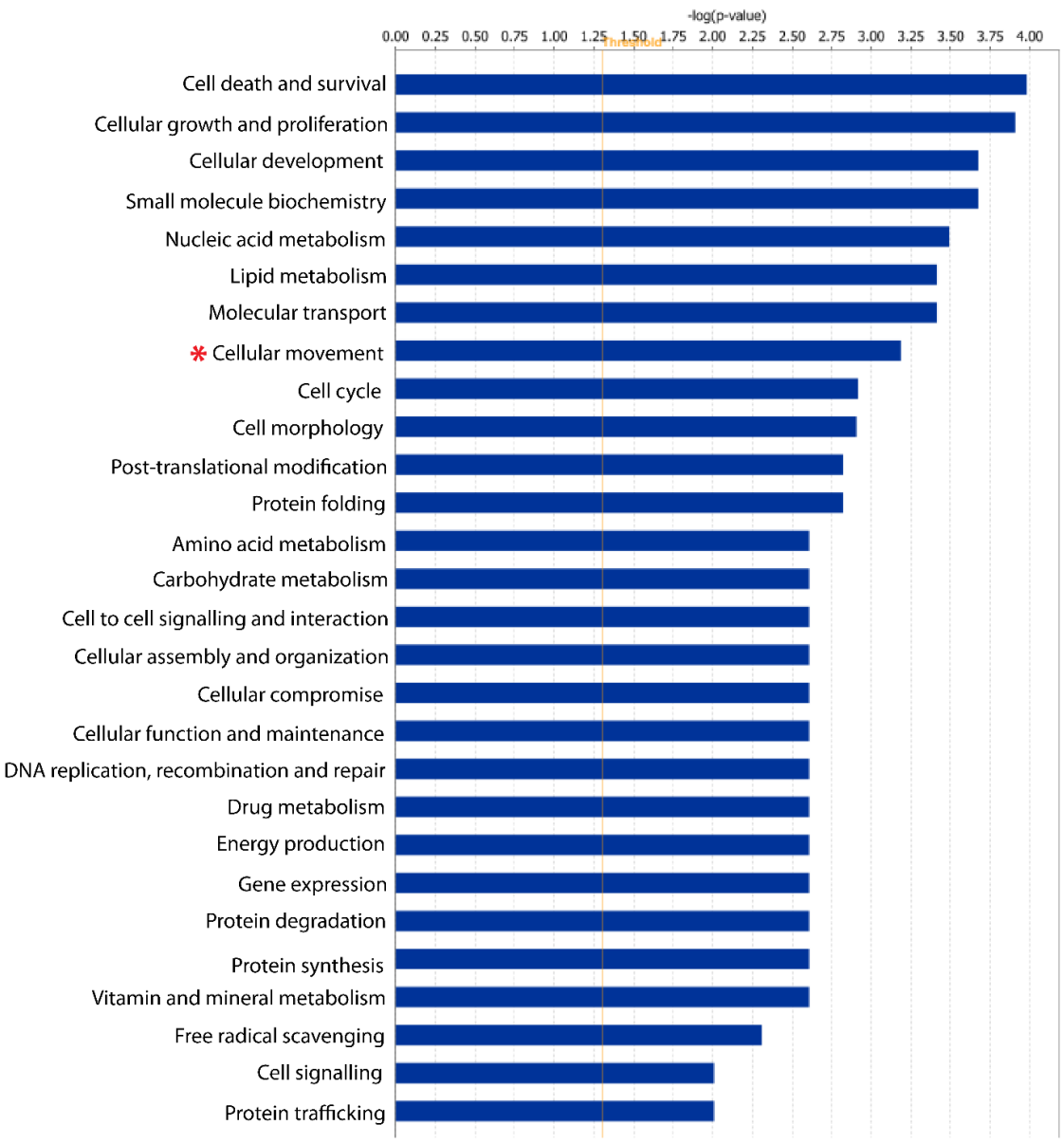

Figure 7.6 Gene ontology anlaysis of Gc-regulated proteins

Mass spectrometry analysis of wild type human podocytes treated for 24 hours with either vehicle or Gc revealed 53 proteins which changed significantly following Gc exposure. Gene ontology analysis (using the term 'molecular and cellular functions') using IPA (Ingenuity) software revealed important functions with which the GC-regulated proteins were involved. Terms are listed in order of significance of enrichment. Only terms with –log (p value) > 2 are displayed.

7.4 Discussion

MS is frequently used to study the differential protein expression in complex biological samples.[512] The classical method for quantitative analysis of protein mixtures involved protein separation and comparison by two-dimensional polyacrylamide gel electrophoresis (2D-PAGE), followed by MS.[513] However, spots on a 2D gel often contain more than one protein, making quantification ambiguous. The development of 'shotgun' label-free quantitative proteomics marked a significant advance in our ability to study complex biological samples.[512]

In this chapter, I used label-free high resolution MS quantification coupled with Progenesis software to characterise the proteome of human wild type podocytes, and understand the translational changes stimulated by Gc exposure. I identified 2,062 proteins obtained from podocyte total cell lysates, and demonstrated that the extraction method isolated proteins from a range of sub-cellular localisations including the nucleus, cell membrane and cytosol (**Figure 7.4**). Characterisation of the biological functions of these podocyte constituent proteins revealed a prominent role for regulators of the cytoskeleton (**Figure 7.5**).

A 2005 study from Ransom *et al.*, analysed the proteome of a murine podocyte cell line using 2D-PAGE to separate proteins before identification by matrix-assisted laser desorption time-of-flight (MALDI-TOF) MS and peptide fingerprinting.[106] 88 proteins were identified in total. The group reported that the largest class of proteins found in this group was cytoskeletal proteins, consistent with the view of the podocyte as a contractile, motile cell (see Section 1.3.4). Podocyte proteins were also extracted 3 days after a 30-minute treatment with either dexamethasone or vehicle, although the rationale for this time point is not clear in this study. Overall, the study identified 6 proteins, which altered following Gc treatment and none of these were found in my Gc-regulated protein dataset. This may be due to a variety of factors including: the different cell line used; the different GR-ligand and length of treatment; or the different MS method.

Following developments in MS technology, a 2013 study from Boerries *et al.*, used a linear trap quadrupole (LTQ) Orbitrap mass spectrometer to characterise the proteome of freshly isolated murine podocytes, and identified 1,280 proteins. In agreement with my data, cytoskeletal and plasma membrane proteins were prominent constituents of the podocyte proteome.

In order to understand the function of the proteins whose levels altered significantly following Gc treatment in my dataset, I performed gene ontology analysis. There was a high correlation between the enriched gene ontology terms found in the Gc-regulated proteomic dataset and the Gc-regulated transcriptomic dataset (see Chapter 4). Seven gene ontology terms were common to the top ten most enriched terms in both datasets: cellular growth and proliferation, cellular development, cellular movement, cell death and survival, cell morphology, lipid metabolism and molecular transport. The finding that cellular movement is an enriched gene ontology term following Gc treatment at both transcriptomic and proteomic level further emphasises the prominent effects that Gc exposure has on altering the motility of podocytes.

8 Podocyte-specific GR deletion *in vivo*

8.1 Overview

Although Gc treatment has been used for many decades to treat nephrotic syndrome (NS), the target cell of action has not been defined. Data presented in this thesis and elsewhere,[102, 109, 110, 119] suggests that Gc has direct effects on the podocyte, and I hypothesise that the podocyte is the target cell of Gc action in NS. To evaluate this, I generated a mouse line with a podocyte-specific deletion of GR using the Cre-LoxP site-specific system.[514]

The *Cre* (cyclisation recombination) gene encodes a 38 kilo Dalton (kDa) site-specific DNA recombinase, called Cre, which recognises 34 base-pair (bp), LoxP (locus of X-over of P1) sites and catalyses recombination between two LoxP sites, excising all DNA sequences located between. When Cre expression is placed under the control of a tissue-specific gene promoter, tissue-specific excision of selected genes can occur.[515]

By breeding mice expressing Cre under the control of the podocyte-specific podocin (*Nphs2*) promoter, with mice harbouring two LoxP sites in the GR gene ('GR floxed' mice), mice with specific deletion of GR in the podocyte were generated. In this chapter, I show that these mice show no overt baseline phenotype. This work is a prelude to proposed experiments in which these mice will receive a proteinuria-inducing challenge [eg, an intraperitoneal lipopolysaccharide injection (LPS)] before treating with Gc and observing for differences in response between mice with podocyte GR deletion and control mice.

8.2 Chapter-specific methods

8.2.1 Transgenic mouse lines and genotyping

Podocyte-specific GR-knockout mice (Cre+ $GR^{fl/fl}$) were generated by breeding $GR^{fl/fl}$ mice,[516] with *Nphs2-Cre* mice (Jackson Labs 008205). Both lines were on a C57BL/6 background. Expression of Cre was assessed by reverse transcriptase polymerase chain reaction (PCR) performed on a DNA template extracted from ear punches (see **Table 8.1** for primers). DNA was isolated using the QIAamp DNA Min Kit (Qiagen) and PCR performed using the Go Taq Polymerase Kit (Promega) according to the supplier instructions. Samples were separated by electrophoresis using 1.5% (w/v) agarose gels prepared in 1 X Tris-acetate-EDTA (TAE) buffer (see Section 2.2) supplemented by 1:10,000 (vol/vol) SYBR Safe DNA stain (Life Technologies). Gels were run at 60 volts for 90 minutes, and the size of the DNA fragments was determined by comparison with hyperladder IV (Bioline). The size of the DNA bands are as follows: GR flox allele 275 bp; GR wild-type allele 225 bp; and Cre 600 bp.

Table 8.1 Primers used for mouse genotyping

Primer	**Sequence (5' -3')**
Cre forward	GGATCATCAGCTACACCAGAGACG
Cre reverse	CGCAGAACCTGAAGATGTTCGCGA
GR flox forward	GGCATGCACATTACTGGCCTTCT
GR reverse -4	GTGTAGCAGCCAGCTTACAGGA
GR reverse -8	CCTTCTCATTCCATGTCAGCATGT

8.2.2 Isolation of primary murine podocytes using a differential sieving technique

Mice were culled using neck dislocation, in accordance with 'The Humane Killing of Animals under Schedule 1 to the Animals (Scientific Procedures) Act 1986.' Kidneys were immediately extracted and washed in 1 X phosphate buffered saline (PBS). Kidneys were decapsulated and the medulla was removed. After cutting the kidney cortex into small pieces, the tissue was pressed through a 100 µm cell strainer (Becton Dickinson) and washed with PBS. This crude isolate was then passed through a 70 µM cell strainer (Becton Dickinson), which trapped glomeruli. Glomeruli were washed with

PBS and seeded onto 10-cm diameter culture dishes. Following 10 days of incubation at 37ºC with 5% CO_2 to allow podocyte outgrowth from glomeruli, cells underwent immunofluorescence staining (see Section 2.8).

8.2.3 Phenotyping mice

Cre+ $GR^{fl/fl}$ were compared to age- and sex- matched Cre- $GR^{fl/fl}$ controls. 22 mice were analysed in total (11 per group); the age range was 3 months – 13 months old; further details are provided in **Supplementary Table 10.4**. Prior to cull, mice were weighed and urine obtained (stored at 4ºC). 10µL urine sample aliquots were incubated at 95ºC for 5 minutes with an equal volume of sodium dodecyl sulfate (SDS) loading buffer before electrophoresis on a 4-12% polyacrylamide gel, and staining with InstantBlue (Expedeon). This allowed visualisation of the degree of albuminuria.

Immediately following culling of the mice, blood samples were obtained. Blood samples underwent centrifugation at 1,800g at 4ºC for 15 minutes to obtain serum. Both serum creatinine and the urinary protein:creatinine ratio was quantified using an ILAB 600 clinical chemistry analyser (Instrumentation Laboratory).

Kidneys were extracted from the mice. One kidney per animal was prepared for cryosectioning; one half-kidney per animal was fixed for electron microscopy (EM); the remaining half-kidney per animal was fixed in 4% paraformaldehyde (PFA) prior to fixation in paraffin for Hematoxylin and eosin (H&E) staining.

8.2.3.1 Cryosections

Kidneys for cryosectioning were placed in OCT CryoCompond (Klinipath) before a 30 minute incubation on dry ice, and subsequent transfer to -80ºC storage. 30µm cryosections were obtained using a CM3050 (Leica) cryostat. Immunofluorescence staining on cryosections involved blocking with 1.5% bovine serum albumin (BSA) in donkey serum for 30 minutes at room temperature before overnight incubation at 4ºC with anti-mouse GR antibody [M20; Santa Cruz; rabbit immunoglobulin G (IgG)] and anti-nephrin antibody [BP5030; Acris; guinea pig IgG], both using 1:100 dilution. Five washes with PBS was followed by a 1 hour incubation at room temperature with 1:200 dilution of Alexa Fluor 647 (rabbit) and Alexa Fluor 488 (guinea pig) (Life Technologies). Five further PBS washes preceeded 10 minute room temperature incubation with 4',6-diamidino-2-phenylindole (DAPI) nuclear stain (1µg/mL) (Cell

Signalling). Slides were washed once with PBS, and twice with Milli Q water (Millipore) before mounting with ProLong Gold antifade reagent (Molecular Probes).

8.2.3.2 Electron microscopy

Hemi-kidneys were placed immediately into 4% PFA/2.5% glutaraldehyde in 0.1 M 4-(2-hydroxyethyl)-1-piperazineethanesulfonic acid (HEPES) buffer for 30 minutes at room temperature. The renal pelvis and medulla was then removed, before specimens were cut into 2-4 mm^2 pieces. These were then re-placed into 4% PFA/2.5% glutaraldehyde in 0.1 M HEPES for 2 hours at 4^{o}C, before 2 washes with 0.1M HEPES.

Samples were incubated with reduced osmium (OsO4 1% + K4Fe(CN)6 1.5%) for 1 hour, followed by 1% tannic acid in 0.1 M cacodylate buffer for 1 hour and finally with 1% uranyl acetate in water overnight. The next day, samples were dehydrated in a series of alcohols, and permeated with TAAB LV resin. Ultrathin 70 nm sections were cut with Leica Ultracut S ultramicrotome and put on formvar/carbon-coated slot grids. The grids were visualised using a Tecnai 12 Biotwin transmission electron microscope at 80 kV.

8.2.3.3 Hematoxylin and eosin staining

Kidney samples were fixed in 4% PFA prior to processing with a Shandon Citadel 2000 automated tissue processor (Thermo Scientific). Specimens were then embedded in wax using a ThermoShandon Histocentre2. 5µm sections were prepared using a RM 2155 microtome (Leica).

For H&E staining, sections were deparaffinized and hydrated by incubation of the slides in xylene, followed by decreasing ethanol series (100%, 95%, 85%, 70%), and finally washed with PBS. Slides were stained with filtered hematoxylin for 5 seconds, rinsed with water, dipped five times in acidic solution 1% hydrogen chloride, again rinsed with water, dipped five times in sodium bicarbonate solution and again rinsed in water. The slides were transferred to eosin solution for 30 seconds and dehydrated by increasing percentage of Ethanol (80%, 90%, 100%, 100%) until the slides were incubated in xylene. Samples were mounted using Roti Histokitt (Roth) mounting medium and imaged using a 3D Histech Pannoramic 250 Flash II slide scanner.

8.3 Results

In order to investigate the role of podocyte GR in mediating the therapeutic effects of systemic Gc treatment in nephrotic syndrome, a podocyte-specific GR knock-out mouse line was generated using the Cre-LoxP site-specific recombination system (**Figure 8.1-A**).[515] The knockout mouse was generated by crossing mice harbouring LoxP sites in the GR gene with mice expressing Cre under the control of the gene promoter for the podcoyte-specific marker podocin (*Nphs2*).

To verify the genotype of mice, PCR analysis on DNA isolated from ear punches was performed using primers for the floxed GR gene and the podocin-Cre gene. Back-crossing of heterozygous floxed mice generated offspring which were either heterozygous floxed ($GR^{fl/-}$) or homozygous floxed ($GR^{fl/fl}$). Cre+ $GR^{fl/fl}$ mice were expected to have undergone podocyte-specific GR-excision, while Cre- $GR^{fl/fl}$ mice served as experimental controls (**Figure 8.1-B**).

To ensure GR-excision had been successful, fluorescent immunohistochemistry was performed. This showed that GR had successfully been knocked out in Cre+ $GR^{fl/fl}$ mice, but not in Cre- $GR^{fl/fl}$ mice (**Figure 8.1-C**). To validate this finding, primary podocytes were isolated from mice using a differential sieving technique and immunofluorescence staining was undertaken. This demonstrated the presence of GR in primary podocytes derived from Cre- $GR^{fl/fl}$ mice, and in non-podocyte glomerular cells from Cre+ $GR^{fl/fl}$ mice, but not in primary podocytes from Cre+ $GR^{fl/fl}$ mice (**Figure 8.2**).

These mice were generated with the intention of experimentally inducing proteinuria (eg, using an LPS intraperitoneal injection),[517] to be followed by systemic Gc administration and characterisation of the response of Cre+ $GR^{fl/fl}$ and Cre- $GR^{fl/fl}$ mice. Here, I present data examining the phenotype of the mice without induced kidney damage. Twenty-two mice (11 Cre+ $GR^{fl/fl}$ mice and 11 Cre- $GR^{fl/fl}$ age- and sex-matched controls; see **Supplementary Table 10.4**) were investigated using a variety of methods (**Figure 8.3**). No difference in kidney size, total body weight, degree of proteinuria, serum creatinine (a biomarker for kidney function) or kidney structure at light microscopy or ultrastructural level was detected **(Figure 8.4**).

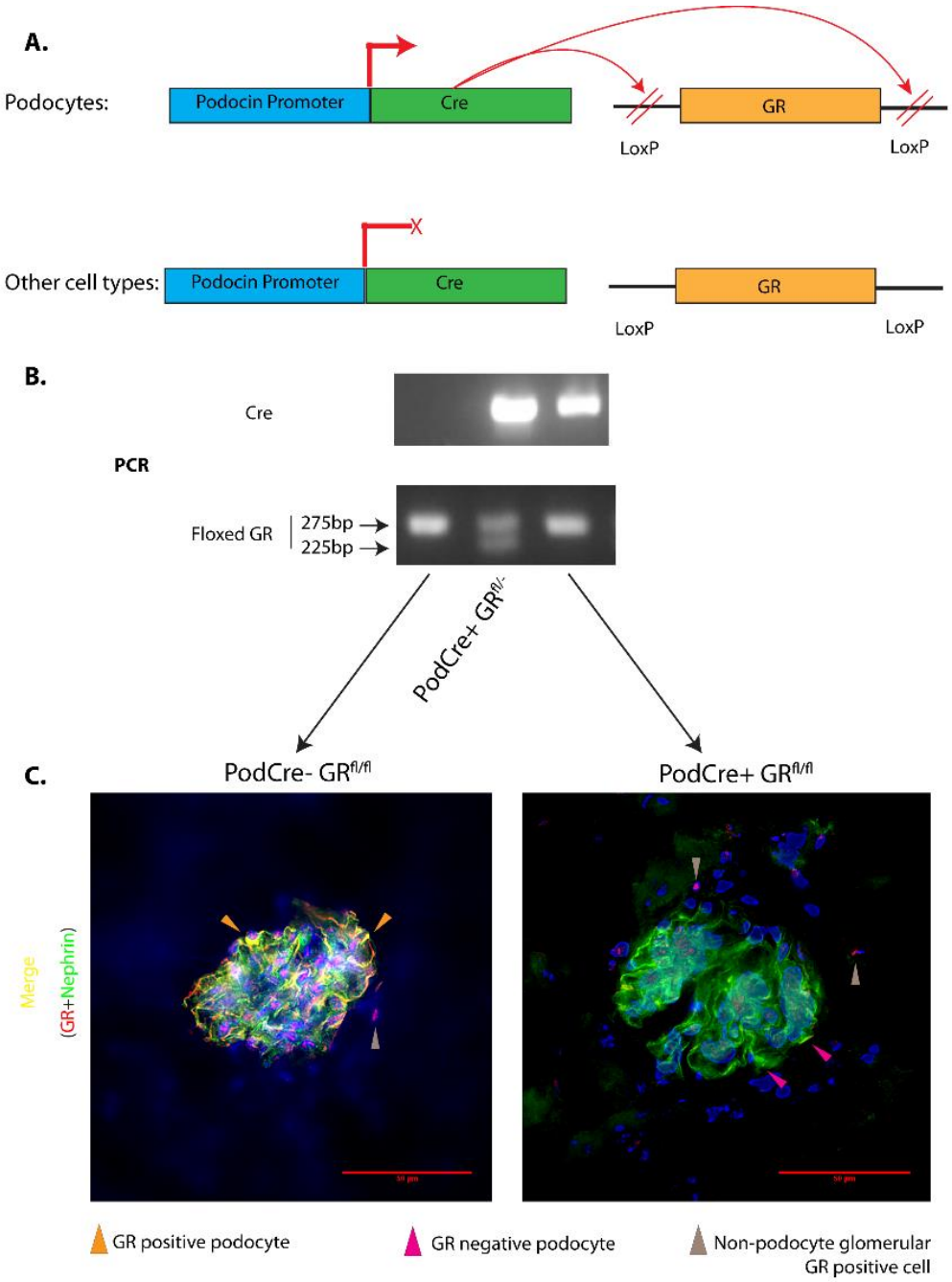

Figure 8.1 Generation of Cre+ GR $^{fl/fl}$ mice

In order to achieve a podocyte-specific knock-out of GR, mice harbouring Cre recombinase whose expression was driven by the podocyte-specific promoter of the *NPHS2* (podocin) gene were crossed with mice containing LoxP sites in the GR gene. Only podocytes expressed Cre, and therefore experienced cell-specific GR knock-out **(A)**. DNA from mice extracted from ear punches was genotyped using polymerase chain reaction (PCR). Third generation mice contained either one GR LoxP allele (GR $^{fl/-}$) or two (GR$^{fl/fl}$). Cre- GR $^{fl/fl}$ mice acted as controls, while Cre+ GR$^{fl/fl}$ mice underwent podocyte-specific GR excision The GR flox allele was identified as a 275 base pair (bp) band, and the wild type allele as a 225bp band following gel electrophoresis **(B)**. To ensure GR had been excised from podocytes in Cre+ GR$^{fl/fl}$ mice, fluorescence immunohistochemistry was performed on murine kidney cryosections using antibodies for mouse GR, the podocyte-specific marker nephrin, as well as 4',6-diamidino-2-phenylindole (DAPI) nuclear stain. Podocyte-specific GR deletion was demonstrated in Cre+ GR$^{fl/fl}$ mice **(C)**.

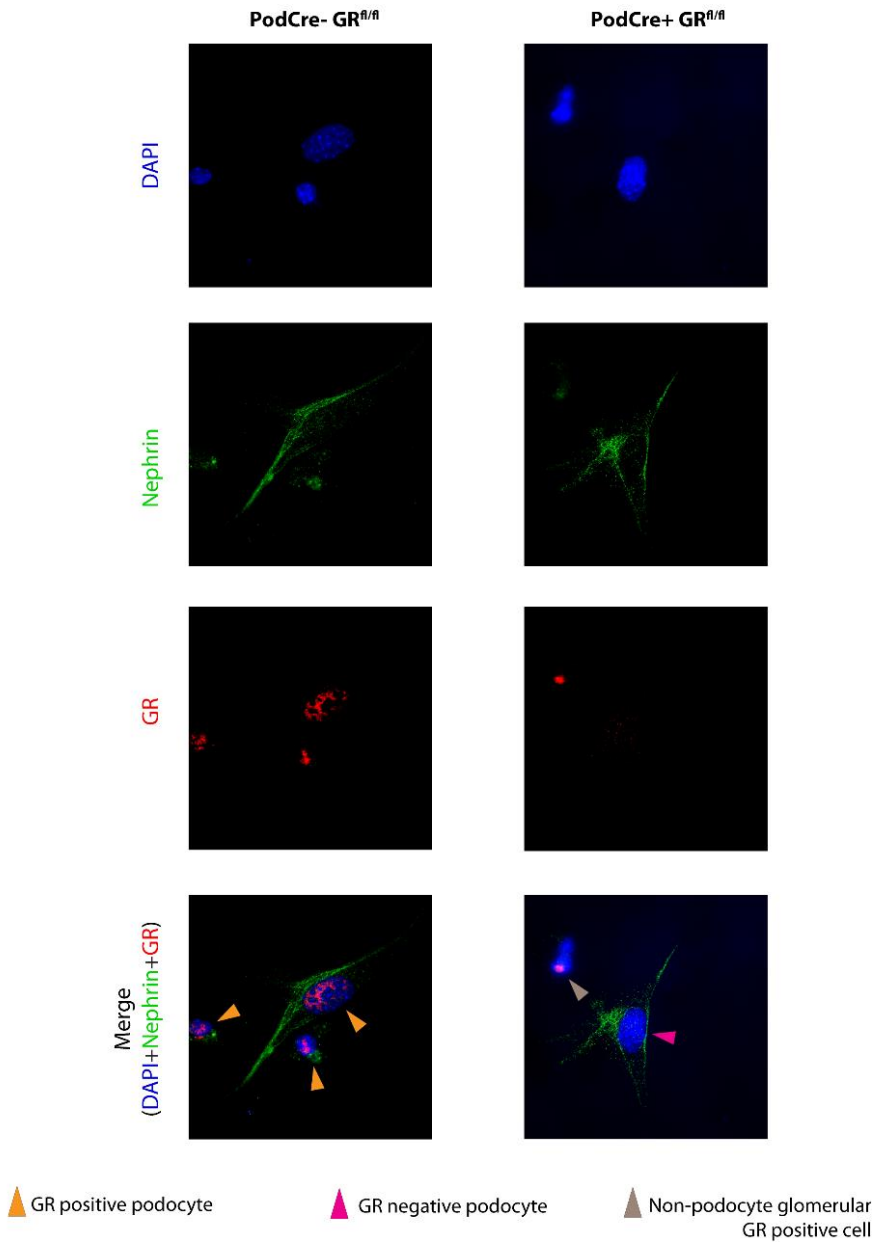

Figure 8.2 Immunofluorescence images of murine primary podocytes in culture

To verify that podocyte-specific deletion of GR had been achieved in Cre+ $GR^{fl/fl}$ mice but not in control Cre- $GR^{fl/fl}$ mice, primary podocytes were isolated from murine kidney samples using a differential sieving technique. Primary podocytes subsequently underwent immunofluorescence using 4',6-diamidino-2-phenylindole (DAPI) nuclear stain, and antibodies for mouse GR, and the podocyte-specific marker nephrin. Cre- $GR^{fl/fl}$ mice showed GR staining in podocytes, while Cre+ $GR^{fl/fl}$ mice showed staining in non-podocyte cells of glomerular origin, but not in podocytes, verifying the knock-out had been successful. Podocytes used for staining in this figure were obtained from 10 month old male mice. Immunofluorescence images were visualised on a Delta Vision (Applied Precision) restoration microscope using a 40x/ 0.85 objective and collected using a Coolsnap HQ (Photometrics) camera.

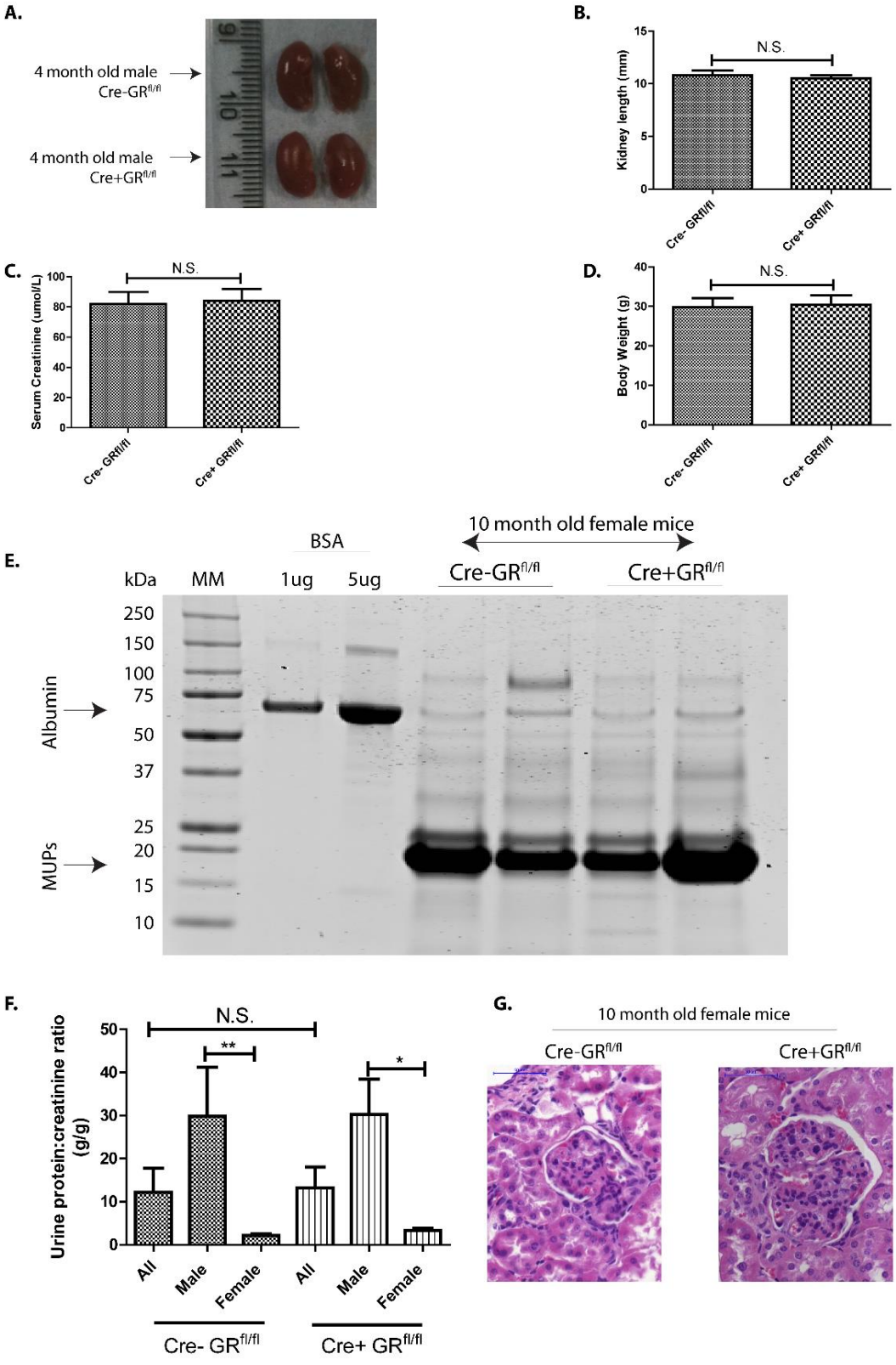

Figure 8.3 Phenotype of Cre+ GR$^{fl/fl}$ mice.

Legend on next page.

To understand if the loss of GR in the podocyte causes a disturbance of glomerular function without inducing kidney damage, mice with podocyte specific deletion of GR (Cre+ $GR^{fl/fl}$) were generated and compared to age- and sex-matched controls (Cre- $GR^{fl/fl}$). Twenty-two mice were examined in total (eleven in each group). The mice varied in age from 3 months-13 months old. No difference in kidney size **(A)** and **(B)**; serum creatinine **(C)**; or body weight **(D)** was observed between groups. **(E)** shows a 4-12% polyacrylamide gel stained with InstantBlue after 10µL mouse urine was loaded into each lane. Bovine serum albumin (BSA) was loaded as a control to non-quantitatively demonstrate the degree of albuminuria, which is a marker of glomerular filtration. Total urinary protein excretion normalised to urinary to creatinine (to correct for urinary flow rates) is shown in **(F)**. The observation that males have a higher level of proteinuria at baseline than females is well-known, and reproducing this finding here provides confidence the assay is functioning adequately.[518] No gross structural glomerular defects are observed following hematoxylin and eosin staining of mice kidney specimens. Groups in (F) were compared using the nonparametric Mann-Whitney U test. **=p value 0.0061, *=p value 0.0106, N.S= not significant. MM=molecular marker, kDa= kilo Daltons; MUPs=major urinary proteins.[519]

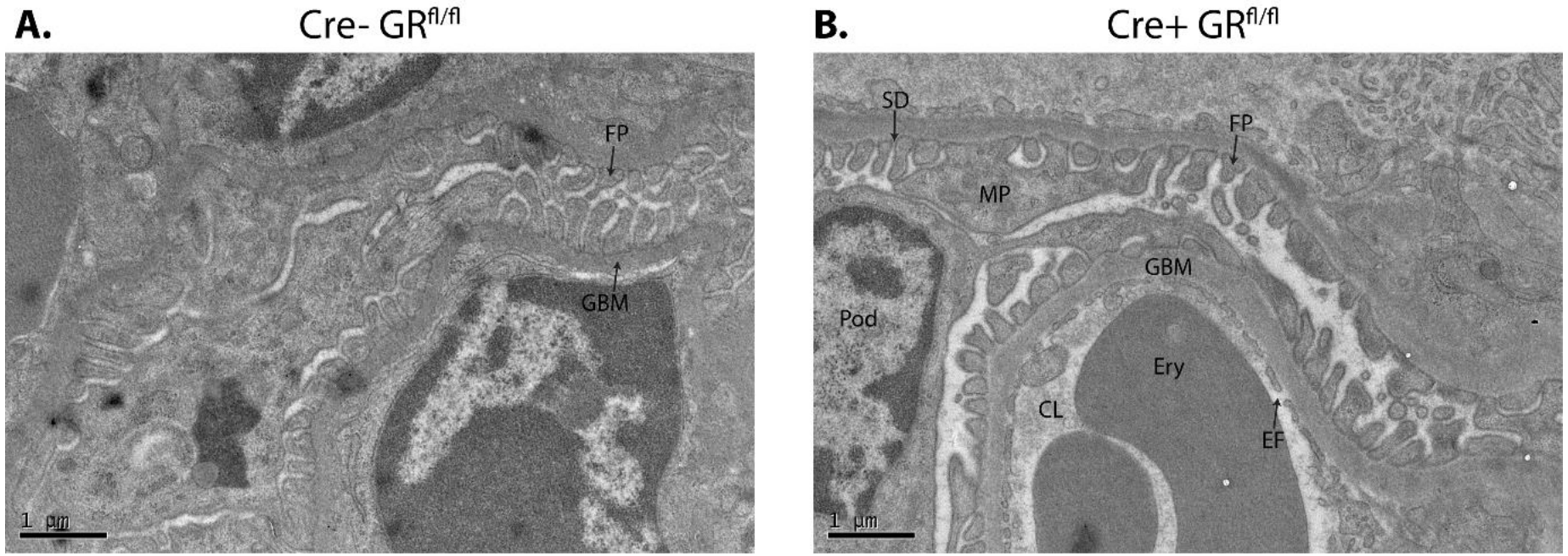

Figure 8.4 Glomerular ultrastructure of Cre+ GR$^{fl/fl}$ mice

Electron microscopy was performed on kidney specimens obtained from control mice (Cre- GR$^{fl/fl}$) **(A)** and mice with a podocyte specific deletion of GR (Cre+ GR$^{fl/fl}$) **(B).** Glomerular ultrastructure of Cre+ GR$^{fl/fl}$ mice appeared normal. Images shown are from two female 11-month old mice born in the same litter. GBM=glomerular basement membrane; FP=foot process; SD=slit diaphragm; Pod=podocyte cell body; CL=capillary lumen, Ery=erythrocyte, EF=endothelial fenestra; MP=major process.

8.4 Discussion

Targeted GR deletion has been performed in several tissues using the Cre-LoxP system. These have included GR excision from neuronal cells, which led to impairment in regulation of the hypothalamus-pituitary-adrenal (HPA)-axis (and the development of a Cushingoid-like phenotype),[516, 520] and the demonstration that monocyte-specific loss of GR confers resistance to Gc-treatment in LPS-induced acute lung injury.[521]

With regards to the kidney, Goodwin *et al.*, investigated the mechanism of Gc-induced hypertension, which had traditionally been attributed to promiscuous activation of the mineralocorticoid receptor (MR) by Gc. However, global MR-knockout mice still experience a Gc-induced increase in systemic blood pressure,[522] and RU28362, a pure GR-agonist devoid of MR-activity induces mineralocorticoid-like effects in cultured collecting duct cells, which is blocked by Gc-, but nor MR-, antagonists.[523] These data suggest Gc-induced hypertension is independent of MR. The group generated mice with a GR knockout in the distal nephron, and found these mice had a mild elevation of baseline blood pressure, but a similar hypertensive response to Gc compared to control mice, suggesting GR in the distal nephron is not necessary for Gc-induced hypertension.[524]

Here, I generated a mouse line with a specific GR deletion in the podocyte. These mice do not appear to have an overt phenotype at baseline. To understand the role podocyte GR has in mediating the therapeutically beneficial effects of systemic Gc therapy in NS, Dr. Lennon's group will experimentally induce proteinuria in these mice, before treating with Gc and observing if any difference in response between Cre+ $GR^{fl/fl}$ mice and Cre- $GR^{fl/fl}$ mice is observed. A diminished response to Gc in Cre+ $GR^{fl/fl}$ mice would be strong evidence that the podocyte is the key cell mediating therapeutically beneficial effects in NS and would help to inform future discovery of novel drug targets.

9 General discussion and perspectives

Work presented in this thesis has demonstrated that podocytes *in vitro* are directly responsive to Gc exposure and produce effects which may be clinically relevant (Chapter 3). Analysis of the Gc-regulated transcriptome (Chapter 4) suggested that effects on podocyte motility may be responsible for this protective effect. Interrogation of the mechanisms underpinning the Gc-induced hypomobile cell phenotype highlighted a potential role for Rac1, and demonstrated that Rac1 inhibition may have a functionally protective effect against puromycin aminonucleoside (PAN) or lipopolysaccharide (LPS), which are both proteinuria-inducing agents (Chapter 5). The development of a mouse line with a podocyte-specific deletion of GR (Chapter 6) may provide data in the future addressing the importance of the podocyte in mediating therapeutically useful anti-proteinuric effects *in vivo*, and contribute to an understanding of the target of novel tissue-specific drug therapies.

Currently, the clinical response to treatment with Gc separates children with nephrotic syndrome (NS) into two groups: a Gc-resistant group (SRNS) in which patients have a high chance of developing chronic kidney disease (CKD), and a Gc-sensitive group (SSNS) who typically experience a favourable long-term outcome, but risk short-term morbidity from disease relapses and Gc-exposure.[525] Although the pathogenesis of the disease in the two groups, and between individuals within the same group, is known to be different in many cases,[179] the drug-therapies employed for SSNS and SRNS are very similar.

NS has traditionally been viewed as a disease of immune system dysfunction, and following the discovery of Gc-efficacy in the treatment of proteinuria, strategies to identify new drug therapies have focussed on alternative immunosuppressive agents.[525] Although the majority of agents known to be effective in NS have immunosuppressive properties, direct podocyte-specific effects have been identified as the key mechanism for some drugs including ciclosporin and the anti-CD20 antibody rituximab.[103, 526] These observations have built on extensive evidence demonstrating that the podocyte is the key target-site of injury in NS,[36, 527] and stimulated the search for podocyte-specific therapies, which may yield more efficacious drugs with an improved side-effect profile.

For example, Clement *et al.*, noted increased podocyte expression of a hyposialylated version of the glycoprotein angiopoietin-like-4 (Angptl4) in human minimal change disease (see Section 1.5.1.1). The group also developed a transgenic rat model, the *NPHS2-Angpltl4* rat, and found that these rats developed classical features of NS including proteinuria, foot process effacement and loss of glomerular basement membrane charge. Furthermore, conversion of this hyposialylated Angptl4 to sialylated Angptl4 in rodents using oral administration of the sialic acid precursor acetyl-D-mannosamine (ManNAc) reduced proteinuria.[199] Sialylation-based therapies hold promise for the treatment of NS in the future.[528]

Some evidence has implicated the p38 mitogen-activated protein kinase (p38 MAPK) pathway in the development of NS, including the observation of increased p38 MAPK activation in podocytes in biopsy samples from adults with NS. Additionally, treatment with an inhibitor of the p38 MAPK pathway led to reduced proteinuria in puromycin aminonucleoside (PAN)- and adriamycin –induced nephropathy.[529] p38 MAPK is downstream of protein kinase C α (PKCα), and both kinases are activated by transforming growth factor β (TGF-β).[530] It has been shown that loss of PKCα had podocyte-protective effects in mice following streptozotocin-induced diabetic nephropathy.[531] Therefore, inhibition of p38 MAPK and PKC α represent a potential strategy to treat patients with NS.[525]

Stress-induced disturbance of protein-folding in the endoplasmic reticulum, called the unfolded protein response (UPR), may have a role in some genetic forms of NS, caused by mutations in nephrin, podocin and α–actinin-4.[532, 533] Potential future therapeutic approaches to stabilise protein folding homeostasis in podocytes may involve increasing the expression of relevant protein chaperones or increasing proteasome system activity.[525] NS in some patients is caused by mutations in the *TRPC6* gene (transient receptor potential cation channel, subfamily C, member 6). The observation that ciclosporin can downregulate *TRPC6* mRNA, suggests this may be an effective approach in patients with mutations resulting in elevated TRPC6 activity.[534] Podocyte replacement therapy using stem cells for genetic aetiologies of NS may be possible in the future, but this approach is in its infancy.[535]

It is not yet known whether other therapies currently used to treat NS also have effects on Rac1, or whether this is a Gc-specific effect. An approach which may prove useful to identify alternative medication for NS would be to investigate whether drugs currently

used for other indications could be ‘re-purposed ‘as anti-proteinuric agents. For example, the thiazolidinediones are ligands of the nuclear hormone receptor peroxisome proliferator-activated receptor γ (PPARγ), which are used for the treatment of type 2 diabetes.[525] The thiazolinedione pioglitazone has been shown to protect against the progression of PAN-induced glomerulosclerosis *in vivo*,[536] and to protect cultured podocytes against PAN-induced cytoskeletal disruption, to increase GR phosphorylation and enhance the transcriptional activity of GR *in vitro*.[537] This suggests the thiazolidinediones may have potential clinical utility as either primary or adjunctive therapy in NS.

The transcriptomic analysis presented in Chapter 4 may act as a resource for hypothesis-generation for other studies aiming to understand how Gc exerts an anti-migratory effect on podocytes. Gene ontology analysis suggested Gc has prominent effects on podocyte motility, but it is currently unclear whether this occurs through a single, key mechanism or via multiple, contributory pathways. It is also unclear at which stage of the cell motility cycle (cell-extracellular matrix interaction; signalling instigated by a pro-migratory stimulus; cell polarisation; or recycling of cellular motility machinery) (see Section 1.7.1) Gc acts. The family of small GTPases regulate many aspects of the cell motility cycle, eg, Rac1 has roles in regulating the turnover of cell-extracellular matrix adhesions as well as in the formation of lamellipodia.[373]

One striking feature of the transcriptomic data was the lack of guanine nucleotide exchange factors (GEFs), GTPase-activating proteins (GAPs), and guanine nucleotide-dissociation inhibitors (GDIs), which constitute the immediate regulators of the small GTPases. This suggests that Gc-effects are mediated further upstream. Indeed, many of the Gc-regulated genes identified by IPA® as having roles in cell motility would be predicted to be regulating the interaction of the podocyte with external stimuli (**Supplementary Table 10.1**). Examples of this include transforming growth factor receptor β (TGF-β) 1 and 3, responsible for signal transduction of proteinuria-inducing agents such as tumour necrosis factor α and TGF-β [538] and urokinase plasminogen activator, which acts as a ligand at the urokinase-type plasminogen activator receptor (see Section 1.5.1.1), which may affect podocyte motility via β3 integrin.[202]

In this thesis, I presented *in vitro* evidence suggesting Rac1 inhibition may warrant further study as a potential novel anti-proteinuric therapy. Previous data supporting the use of drugs affecting podocyte motility in reducing proteinuria include the use of

inhibitors of ROCK (a downstream effector of RhoA) in acute PAN-nephrosis in rats,[424] as well as ROCK and Rac1 inhibition in a murine 5/6th nephrectomy model of chronic kidney damage.[434] Furthermore, in mice with mutations in the *Arhgdia* gene, which is known to cause NS in humans,[432] Rac1 inhibition has been shown to be effective at reducing proteinuria. Whether Rac1 inhibition is effective in non-genetic forms of NS (and genetic forms other than those arising from *Arhgdia* mutations) has not been evaluated. Robust data concerning the systemic side-effect profile of Rac1 inhibition in animal models is currently lacking.

Podocyte hypermotility is a prominent feature of proteinuric kidney disease,[132] and data in this thesis has demonstrated that Gc, which represent the first-line therapy for NS in children, reduces podocyte motility. Although future studies targeting pathways involving the small GTPases may uncover new and efficacious anti-proteinuric therapies, another potential strategy which is currently unexplored may be to block pro-migratory signals (or provide anti-migratory signals), rather than directly target the cellular motility machinery.[539] Additionally, the potential role of selective GR agonists (SEGRAs) in clinical practice, which preferentially induce the transrepression and the not the transactivation function of GR, is still unclear.[540] The next step in understanding whether Rac1 inhibition may play a role in the treatment of NS will be to investigate whether these agents are effective in rodent models of acute proteinuria. More broadly, a deeper understanding of the various aetiologies underpinning NS in discrete patient groups, may one day yield not only podocyte-specific, but also patient-specific, therapies.

10 Supplementary Tables

Supplementary Table 10.1 Genes involved with cell movement

Genes from the microarray dataset identified using IPA software as having roles in cellular motility.

Genes in dataset	**Predicted effect on cellular movement (based on expression direction)**	**Fold Change in gene expression following Gc-treatment**
AREG	Increased	8.028
CCL20	Increased	4.375
TSC22D3	Decreased	4.339
IRS2	Increased	3.762
HPGD	Decreased	3.696
REPS2	Increased	3.498
CNR1	Increased	2.964
WNT5A	Increased	2.637
TGFBR3	Decreased	2.618
PER1	Affected	2.618
ANGPTL4	Increased	2.439
SCNN1A	Increased	2.37
LOX	Increased	2.363
TNFRSF21	Increased	2.363
FGD4	Affected	2.323
DCLK1	Increased	2.226
NRCAM	Affected	2.225

RGCC	Decreased	2.132
TGFBR1	Increased	2.069
COL4A3	Affected	2.063
ST3GAL6	Increased	2.036
SERPINE1	Increased	2.017
TNFSF4	Increased	1.975
DNAJB4	Decreased	1.967
PDE4DIP	Increased	1.95
EDN2	Increased	1.932
CCBE1	Increased	1.905
NDRG1	Decreased	1.891
NPR1	Increased	1.881
PRKX	Increased	1.869
IL1R1	Increased	1.85
HRH1	Increased	1.826
DUSP1	Decreased	1.794
NEDD9	Increased	1.789
MAP2	Increased	1.773
CEBPD	Increased	1.77
SLC1A3	Increased	1.751
TNFAIP3	Decreased	1.741
MYO9A	Decreased	1.73

DCN	Decreased	1.725
UNC5A	Increased	1.7
CD200	Decreased	1.688
GCNT1	Increased	1.684
DKK1	Decreased	1.621
EFNB2	Increased	1.616
ITGB6	Increased	1.608
CRYAB	Decreased	1.588
MALAT1	Increased	1.583
PTPN1	Decreased	1.581
APBB2	Affected	1.578
FOXC2	Increased	1.574
FPR1	Increased	1.57
PTGER4	Increased	1.568
KCNN4	Increased	1.559
LEF1	Increased	1.543
HIPK2	Increased	1.532
ST6GALNAC2	Increased	1.52
WWTR1	Increased	1.518
KLF4	Decreased	1.517
IL6ST	Increased	1.516
EPB41L5	Affected	1.503

GATA6	Decreased	-1.504
SHC4	Decreased	-1.523
EGR1	Decreased	-1.526
IL1B	Decreased	-1.535
SHC3	Affected	-1.544
GDF15	Increased	-1.546
KALRN	Decreased	-1.559
ACKR4	Decreased	-1.56
GDF5	Increased	-1.576
NR2F2	Affected	-1.579
ARID5B	Affected	-1.59
VEGFC	Decreased	-1.593
TNFRSF9	Decreased	-1.593
SPATA13	Affected	-1.595
TNFRSF19	Decreased	-1.596
FOXC1	Decreased	-1.601
BMP6	Decreased	-1.61
TFPI2	Increased	-1.629
CD274	Decreased	-1.67
FGF5	Decreased	-1.676
SEMA3A	Increased	-1.693
CSF2	Decreased	-1.702

CCL2	Decreased	-1.707
TM4SF1	Decreased	-1.711
GRIA3	Decreased	-1.712
PLAU	Decreased	-1.749
SERPINB2	Decreased	-1.774
SPRY2	Increased	-1.8
VCAM1	Decreased	-1.827
GDNF	Decreased	-1.859
JAG1	Increased	-1.866
TBX3	Decreased	-1.902
ADAMTS1	Decreased	-1.905
TNFSF10	Affected	-1.945
HBEGF	Decreased	-1.949
NOG	Decreased	-1.958
PTHLH	Decreased	-2.015
ASB2	Decreased	-2.076
NPPB	Increased	-2.104
TRIB1	Affected	-2.176
CYP1B1	Affected	-2.28
TNFRSF11B	Decreased	-2.361
IL1A	Decreased	-2.57
IL11	Decreased	-3.365

Supplementary Table 10.2 Fifty most enriched GR-binding sites

GR binding sites (GBS) were found in human wild type podocytes using ChIP-Seq. Significant peaks were considered to be those enriched ≥5 fold over background. 1,130 significant peaks were identified, and the fifty most enriched GBS are listed here.

Region	Chr	Start	End	Fold Enrichment	Nearest gene (bp)	Gene Symbol	Gene description
1	chr2	223317027	223317545	29.1	27936	SGPP2	Sphingosine-1-phosphate phosphatase 2
2	chr7	50569772	50571094	26.5	29192	LOC100129427	LOC100129427
3	chr1	214366320	214367099	26.4	87655	SMYD2	SET and MYND domain containing 2
4	chr6	35569364	35570046	26.2	28417	FKBP5	FK506 binding protein 5
5	chr20	36618962	36619683	24.1	3240	AK123872	AK123872
6	chr5	172295520	172296569	24.0	2723	BX648961	BX648961
7	chr11	114033325	114035178	23.9	87600	ZBTB16	Zinc finger and BTB domain containing 16
8	chr6	12354677	12355272	23.4	57398	EDN1	Endothelin 1

9	chr5	150159635	150160516	22.2	2359	C5orf62	Small integral membrane protein 3
10	chr6	11621331	11621909	22.1	37613	TMEM170B	Transmembrane protein 170B
11	chr3	183088238	183089228	21.8	56992	MCF2L2	MCF.2 cell line derived transforming sequence-like 2
12	chr4	154925049	154926354	21.4	215773	SFRP2	Secreted frizzled-related protein 2
13	chr10	30235653	30236933	20.3	65672	KIAA1462	KIAA1462
14	chr6	35699388	35700360	20.3	4962	ARMC12	Armadillo repeat containing 12
15	chr3	193586491	193587594	19.5	24912	AK091265	AK091265
16	chrY	58838291	58838985	19.2	261714	SPRY3	Sprouty homolog 3
17	chr3	138316178	138316661	19.0	3209	CEP70	Centrosomal protein 70kDa

18	chr10	45459545	45460255	18.7	4441	RASSF4	Ras association (RalGDS/AF-6) domain family member 4
19	chr14	61932752	61933343	18.6	84580	PRKCH	Protein kinase C, eta
20	chr6	11364641	11365641	18.6	52111	BC030116	BC030116
21	chr5	148345006	148346551	18.5	15509	SH3TC2	SH3 domain and tetratricopeptide repeats 2
22	chr2	20638385	20638921	18.4	8163	RHOB	Ras homolog family member B
23	chr15	31657936	31658300	18.2	11871	KLF13	Kruppel-like factor 13
24	chr2	201988454	201989492	18.2	7892	CFLAR	CASP8 And FADD-like apoptosis regulator
25	chr12	15341067	15341529	18.0	33058	RERG	RAS-like, estrogen-regulated, growth inhibitor
26	chr5	148514863	148515393	17.8	5807	ABLIM3	Actin binding LIM protein family, member 3

27	chr3	156533918	156535227	17.7	93	LOC730091	LOC730091
28	chr20	45945734	45946666	17.6	968	LOC100131496	LOC100131496
29	chr11	18287113	18287811	17.5	118	SAA1	Serum amyloid A1
30	chr11	117685197	117685812	17.4	5109	FXYD6-FXYD2	FXYD6-FXYD2 readthrough
31	chr20	39876961	39877667	17.3	51181	ZHX3	Zinc fingers and homeoboxes 3
32	chr14	95065420	95065978	17.2	6111	SERPINA5	Serpin peptidase inhibitor, clade A (alpha-1 antiproteinase, antitrypsin), Member 5
33	chr3	137906808	137907408	17.1	827	ARMC8	Armadillo repeat containing 8
34	chrX	3615747	3616222	16.7	15597	PRKX	Protein kinase, X-linked
35	chrX	53100807	53101239	16.7	8712	GPR173	G protein-coupled receptor 173
36	chr2	28021744	28022146	16.5	17604	RBKS	Ribokinase

37	chr19	3336548	3337745	16.5	29562	NFIC	Nuclear factor I/C (CCAAT-binding transcription factor)
38	chr17	8057351	8058251	16.3	1956	PER1	Period circadian clock 1
39	chr2	95981725	95983724	16.0	18763	KCNIP3	Kv channel interacting protein 3, calsenilin
40	chrX	106920267	106920942	15.9	26068	PRPS1	Phosphoribosyl pyrophosphate synthetase 1
41	chr9	118412097	118412738	15.8	84114	U2	U2 (snRNA)
42	chr7	40261462	40261820	15.7	86968	C7orf10	Succinate-hydroxymethylglutarate CoA-transferase
43	chr3	187938677	187939318	15.7	8164	LPP	LIM domain containing preferred translocation partner in lipoma
44	chr7	100743474	100744126	15.7	9649	TRIM56	Tripartite motif containing 56

45	chr1	206921884	206922428	15.5	14510	MAPKAPK2	Mitogen-activated protein kinase-activated protein kinase 2
46	chr5	133801837	133802405	15.4	33547	U6	U6 (snRNA)
47	chr10	123880372	123880897	15.4	131925	TACC2	Transforming, acidic coiled-coil containing protein 2
48	chr15	85874112	85875071	15.3	49131	AKAP13	A kinase (PRKA) anchor protein 13
49	chr17	46560857	46561607	15.3	45310	HOXB1	Homeobox B1
50	chr2	28884400	28885163	15.0	17851	PLB1	Phospholipase B1

Supplementary Table 10.3 Gc-regulated proteins

Human wild type podocytes were treated with Gc or vehicle for 24 hours, and proteins significantly changing following Gc exposure were identified by mass spectrometry. In total 2,062 proteins were identified and the 53 proteins whose expression level significantly altered following Gc treatment are listed below.

Gene Symbol	**Protein**	**Fold Change (+Gc/-Gc)**
OLA1	Obg-like ATPase 1	25.2
PPP6R3	Isoform 5 of Serine/threonine-protein phosphatase 6 regulatory subunit 3	22.2
RTN4	Reticulon	12.0
GSR	Glutathione reductase, mitochondrial	7.8
FDFT1	Squalene synthase	6.5
SAA1	Serum amyloid A-1 protein	6.5
4 SV	Uncharacterized protein	6.0
SMARCC2	SWI/SNF complex subunit SMARCC2	5.9
ADK	Adenosine kinase	5.9
CAPNS1	Calpain small subunit 1	5.1
CDC42	Cdc42 effector protein 1	4.8
HSP90AB3P	Putative heat shock protein HSP 90-beta-3	4.8
AFG3L2	AFG3-like protein 2	4.6
HAUS6	HAUS augmin-like complex subunit 6	4.3
PSME2	Proteasome activator complex subunit 2	4.1
NAGA	Alpha-N-acetylgalactosaminidase	3.9
RAB34	Ras-related protein Rab-34, isoform NARR	3.7

CTSD	Cathepsin D	3.3
NUP93	Nuclear pore complex protein Nup93	3.2
PSMB2	Proteasome subunit beta type-2	3.1
SERPINB8	Serpin B8	3.1
LGALS1	Galectin-1	3.0
NAP1L4	Nucleosome assembly protein 1-like 4	2.8
DOK1	Docking protein 1	2.6
CCT6A	T-complex protein 1 subunit zeta	2.6
GOLT1B	Vesicle transport protein GOT1B	2.4
ATL3	Atlastin-3	2.4
LYPLA1	Acyl-protein thioesterase 1	2.3
NIT1	Nitrilase homolog 1	2.2
PDXK	Pyridoxal kinase	2.2
AKR1A1	Alcohol dehydrogenase [NADP(+)]	2.2
NUBP2	Cytosolic Fe-S cluster assembly factor NUBP2	2.2
ERP44	Endoplasmic reticulum resident protein 44	2.1
PHB	Prohibitin	2.1
CDC2	Cell division cycle 2, G1 to S and G2 to M, isoform CRA_a	2.0
HSPD1	60 kDa heat shock protein, mitochondrial	2.0
SPTLC2	Serine palmitoyltransferase 2	0.49
TRIM25	E3 ubiquitin/ISG15 ligase TRIM25	0.49
HSPBP1	Hsp70-binding protein 1	0.47
ADH5	Alcohol dehydrogenase class-3	0.43
ABR	Active breakpoint cluster region-related protein	0.42

PFAS	Phosphoribosylformylglycinamidine synthase	0.42
RRM2	Isoform 2 of Ribonucleoside-diphosphate reductase subunit M2	0.40
TUBA1C	Tubulin alpha-1C chain	0.37
SPNS1	Isoform 5 of Protein spinster homolog 1	0.34
DDOST	Dolichyl-diphosphooligosaccharide--protein glycosyltransferase 48 kDa subunit	0.34
MRPL19	39S ribosomal protein L19, mitochondrial	0.27
KRT8	Keratin, type II cytoskeletal 8	0.22
METAP2	Methionine aminopeptidase 2	0.14
GPX8	Glutathione peroxidase	0.14
CES2	Carboxylesterase 2 (Intestine, liver), isoform CRA_b	0.12
TSN	Translin-associated protein X	0.057

Supplementary Table 10.4 Details of mice

Mice with a podocyte-specific deletion of GR (Cre+ $GR^{fl/fl}$) underwent a variety of analyses with control mice (Cre- $GR^{fl/fl}$) to understand if GR has a role in maintaining baseline glomerular function. No overt phenotype was detected. Details of the mice are provided here.

	Sex	Age at Cull (months)	Body weight (g)	Kidney length (mm)	Urine protein:Cr ratio	Serum Creatinine (umol/L)		Sex	Age at Cull (months)	Body weight (g)	Kidney length (mm)	Urine protein:Cr ratio	Serum Creatinine (umol/L)
Cre - $GR^{fl/fl}$	M	13	45.6	13	13.11	79	Cre + $GR^{fl/fl}$	M	13	45.38	9	6.12	67
	F	10	36.7	10	3.45	n/a		F	10	28.1	10	4.44	n/a
	F	10	30.2	11	3.01	84		F	10	36.4	11	2.58	50
	F	10	28.9	10	2.02	58		F	10	28.5	10	4.44	62
	M	9	30.3	13	7.61	n/a		M	9	32.9	12	37.55	n/a
	F	6	34.5	10	0.94	57		F	6	34.3	10	2.89	71
	F	4	22.9	11	2.7	77		F	4	24.5	11	4.85	91
	M	4	32.3	11	45.13	113		M	4	36.2	12	39.06	108
	M	4	27.1	12	53.32	71		M	4	30.1	11	38.51	115
	F	3	20.1	9	2.03	130		F	3	19.9	10	1.08	78
	F	3	19.2	9	0.73	67		F	3	18.4	10	3.13	113

11 Formal acknowledgements

I thank Leo Zeef (Bioinformatics Chapter 4), Ian Donalson (Bioinformatics Chapter 6) and Andy Hayes of the Bioinformatics and Genomic Technologies Core Facilities at the University of Manchester for providing support with regard to microarrays and ChIP-Seq.

The Bioimaging Facility microscopes used in this study were purchased with grants from BBSRC, Wellcome and the University of Manchester Strategic Fund. Special thanks goes to Peter March, Roger Meadows, and Steve Mardsen for their help with the microscopy.

Thanks to David Knight, Ronan O'Cualain, and Julian Selley of the Mass Spectrometry Core Facility who helped with experimental planning and the use of Progenesis® software. Also to thanks to Emma Keevill who prepared the mass spectrometry samples analysed in Chapter 7.

I am grateful to Aleksandr Mironov from the Electron Microscopy Core Facility for the prepraration and imaging of samples, and to Peter Walker of the Histology Core Facility for training and use of the immunohistology equipment. Thanks to all the staff at the BSF animal facility, and Graham Morrissey in particular for use of his transgenic mouse breeding licence. Also thanks to Cressida Moxey of Manchester Medical School, who performed the manual cell tracking for the LPS-experiments in Chapter 5. Thanks to Mike Randles for culturing HEK 293 and GEnC cells, and for Toryn Poolma for culturing A549 cells, used in Chapter 3. Franziska Lausecker performed the extraction of primary murine podocytes in Chapter 8.

Finally, thanks to my funders, without whom this PhD would not have been possible. I was awarded an MRC Clinical Training Fellowship, supported by the North West England Medical Research Council Fellowship Scheme in Clinical Pharmacology and Therapeutics, which is funded by the Medical Research Council (grant number G1000417/94909), ICON, GlaxoSmithKline, AstraZeneca and the Medical Evaluation Unit.

12 References

1. Arneil, G.C. and C.N. Lam, *Long-term assessment of steroid therapy in childhood nephrosis.* Lancet, 1966. **2**(7468): p. 819-21.
2. *Minimal change nephrotic syndrome in children: deaths during the first 5 to 15 years' observation. Report of the International Study of Kidney Disease in Children.* Pediatrics, 1984. **73**(4): p. 497-501.
3. Chang, R.L., et al., *Permselectivity of the glomerular capillary wall: III. Restricted transport of polyanions.* Kidney Int, 1975. **8**(4): p. 212-8.
4. Hogg, R.J., et al., *Evaluation and management of proteinuria and nephrotic syndrome in children: Recommendations from a pediatric nephrology panel established at the National Kidney Foundation Conference on Proteinuria, Albuminuria, Risk, Assessment, Detection, and Elimination (PARADE).* Pediatrics, 2000. **105**(6): p. 1242-1249.
5. Eddy, A.A. and J.M. Symons, *Nephrotic syndrome in childhood.* Lancet, 2003. **362**(9384): p. 629-39.
6. *Chapter 3: Steroid-sensitive nephrotic syndrome in children.* Kidney Int Suppl (2011), 2012. **2**(2): p. 163-171.
7. Keller, G., et al., *Nephron number in patients with primary hypertension.* The New England journal of medicine, 2003. **348**: p. 101-8.
8. Orth, S.R. and E. Ritz, *The nephrotic syndrome.* N Engl J Med, 1998. **338**(17): p. 1202-11.
9. Farquhar, M.G., *The glomerular basement membrane: not gone, just forgotten.* The Journal of clinical investigation, 2006. **116**: p. 2090-3.
10. Salmon, A.H., C.R. Neal, and S.J. Harper, *New aspects of glomerular filtration barrier structure and function: five layers (at least) not three.* Curr Opin Nephrol Hypertens, 2009. **18**(3): p. 197-205.
11. Sorensson, J., et al., *Synthesis of sulfated proteoglycans by bovine glomerular endothelial cells in culture.* Am J Physiol Renal Physiol, 2003. **284**(2): p. F373-80.
12. Adamson, R.H. and G. Clough, *Plasma proteins modify the endothelial cell glycocalyx of frog mesenteric microvessels.* J Physiol, 1992. **445**: p. 473-86.
13. Osterloh, K., U. Ewert, and A.R. Pries, *Interaction of albumin with the endothelial cell surface.* Am J Physiol Heart Circ Physiol, 2002. **283**(1): p. H398-405.
14. Kanwar, Y.S. and M.G. Farquhar, *Isolation of glycosaminoglycans (heparan sulfate) from glomerular basement membranes.* Proc Natl Acad Sci U S A, 1979. **76**(9): p. 4493-7.
15. Singh, A., et al., *Glomerular endothelial glycocalyx constitutes a barrier to protein permeability.* J Am Soc Nephrol, 2007. **18**(11): p. 2885-93.
16. Jeansson, M. and B. Haraldsson, *Glomerular size and charge selectivity in the mouse after exposure to glucosaminoglycan-degrading enzymes.* J Am Soc Nephrol, 2003. **14**(7): p. 1756-65.
17. Bulger, R.E., et al., *Endothelial characteristics of glomerular capillaries in normal, mercuric chloride-induced, and gentamicin-induced acute renal failure in the rat.* J Clin Invest, 1983. **72**(1): p. 128-41.
18. Haraldsson, B., J. Nystrom, and W.M. Deen, *Properties of the glomerular barrier and mechanisms of proteinuria.* Physiol Rev, 2008. **88**(2): p. 451-87.
19. Sugio, S., et al., *Crystal structure of human serum albumin at 2.5 A resolution.* Protein Eng, 1999. **12**(6): p. 439-46.

20. Stan, R.V., M. Kubitza, and G.E. Palade, *PV-1 is a component of the fenestral and stomatal diaphragms in fenestrated endothelia.* Proc Natl Acad Sci U S A, 1999. **96**(23): p. 13203-7.
21. Lennon, R., M.J. Randles, and M.J. Humphries, *The importance of podocyte adhesion for a healthy glomerulus.* Front Endocrinol (Lausanne), 2014. **5**: p. 160.
22. Abrahamson, D.R., et al., *Cellular origins of type IV collagen networks in developing glomeruli.* J Am Soc Nephrol, 2009. **20**(7): p. 1471-9.
23. Hironaka, K., et al., *Pores in the glomerular basement membrane revealed by ultrahigh-resolution scanning electron microscopy.* Nephron, 1993. **64**(4): p. 647-9.
24. Miner, J.H., et al., *Compositional and structural requirements for laminin and basement membranes during mouse embryo implantation and gastrulation.* Development, 2004. **131**(10): p. 2247-56.
25. Hudson, B.G., et al., *Alport's syndrome, Goodpasture's syndrome, and type IV collagen.* N Engl J Med, 2003. **348**(25): p. 2543-56.
26. Lennon, R., et al., *Global analysis reveals the complexity of the human glomerular extracellular matrix.* J Am Soc Nephrol, 2014. **25**(5): p. 939-51.
27. Neal, C.R., et al., *Three-dimensional reconstruction of glomeruli by electron microscopy reveals a distinct restrictive urinary subpodocyte space.* J Am Soc Nephrol, 2005. **16**(5): p. 1223-35.
28. Sterk, L.M., et al., *Glomerular extracellular matrix components and integrins.* Cell Adhes Commun, 1998. **5**(3): p. 177-92.
29. Has, C., et al., *Integrin alpha3 mutations with kidney, lung, and skin disease.* N Engl J Med, 2012. **366**(16): p. 1508-14.
30. Wartiovaara, J., et al., *Nephrin strands contribute to a porous slit diaphragm scaffold as revealed by electron tomography.* J Clin Invest, 2004. **114**(10): p. 1475-83.
31. Rodewald, R. and M.J. Karnovsky, *Porous substructure of the glomerular slit diaphragm in the rat and mouse.* J Cell Biol, 1974. **60**(2): p. 423-33.
32. Gagliardini, E., et al., *Imaging of the porous ultrastructure of the glomerular epithelial filtration slit.* J Am Soc Nephrol, 2010. **21**(12): p. 2081-9.
33. Kann, M., et al., *Genome-Wide Analysis of Wilms' Tumor 1-Controlled Gene Expression in Podocytes Reveals Key Regulatory Mechanisms.* J Am Soc Nephrol, 2015. **26**(9): p. 2097-104.
34. Dong, L., S. Pietsch, and C. Englert, *Towards an understanding of kidney diseases associated with WT1 mutations.* Kidney Int, 2015.
35. Dong, L., et al., *Integration of Cistromic and Transcriptomic Analyses Identifies Nphs2, Mafb, and Magi2 as Wilms' Tumor 1 Target Genes in Podocyte Differentiation and Maintenance.* J Am Soc Nephrol, 2015. **26**(9): p. 2118-28.
36. Hinkes, B.G., et al., *Nephrotic syndrome in the first year of life: two thirds of cases are caused by mutations in 4 genes (NPHS1, NPHS2, WT1, and LAMB2).* Pediatrics, 2007. **119**: p. e907-19.
37. Salmon, A.H., et al., *Evidence for restriction of fluid and solute movement across the glomerular capillary wall by the subpodocyte space.* Am J Physiol Renal Physiol, 2007. **293**(6): p. F1777-86.
38. Neal, C.R., et al., *Glomerular filtration into the subpodocyte space is highly restricted under physiological perfusion conditions.* Am J Physiol Renal Physiol, 2007. **293**(6): p. F1787-98.
39. Tojo, A. and H. Endou, *Intrarenal handling of proteins in rats using fractional micropuncture technique.* Am J Physiol, 1992. **263**(4 Pt 2): p. F601-6.

40. Norden, A.G., et al., *Glomerular protein sieving and implications for renal failure in Fanconi syndrome.* Kidney Int, 2001. **60**(5): p. 1885-92.
41. Weyer, K., et al., *Mouse model of proximal tubule endocytic dysfunction.* Nephrol Dial Transplant, 2011. **26**(11): p. 3446-51.
42. Russo, L.M., et al., *The normal kidney filters nephrotic levels of albumin retrieved by proximal tubule cells: retrieval is disrupted in nephrotic states.* Kidney Int, 2007. **71**(6): p. 504-13.
43. Moeller, M.J. and V. Tenten, *Renal albumin filtration: alternative models to the standard physical barriers.* Nat Rev Nephrol, 2013. **9**(5): p. 266-77.
44. Lazzara, M.J. and W.M. Deen, *Model of albumin reabsorption in the proximal tubule.* Am J Physiol Renal Physiol, 2007. **292**(1): p. F430-9.
45. Comper, W.D., B. Haraldsson, and W.M. Deen, *Resolved: normal glomeruli filter nephrotic levels of albumin.* J Am Soc Nephrol, 2008. **19**(3): p. 427-32.
46. Tanner, G.A., *Glomerular sieving coefficient of serum albumin in the rat: a two-photon microscopy study.* Am J Physiol Renal Physiol, 2009. **296**(6): p. F1258-65.
47. Peti-Peterdi, J., *Independent two-photon measurements of albumin GSC give low values.* Am J Physiol Renal Physiol, 2009. **296**(6): p. F1255-7.
48. Peti-Peterdi, J. and A. Sipos, *A high-powered view of the filtration barrier.* Journal of the American Society of Nephrology : JASN, 2010. **21**: p. 1835-41.
49. Birn, H. and E.I. Christensen, *Renal albumin absorption in physiology and pathology.* Kidney Int, 2006. **69**(3): p. 440-9.
50. Farquhar, M.G., *Editorial: The primary glomerular filtration barrier--basement membrane or epithelial slits?* Kidney Int, 1975. **8**(4): p. 197-211.
51. Ryan, G.B. and M.J. Karnovsky, *Distribution of endogenous albumin in the rat glomerulus: role of hemodynamic factors in glomerular barrier function.* Kidney Int, 1976. **9**(1): p. 36-45.
52. Moeller, M.J. and C. Kuppe, *Point: Proposing the electrokinetic model.* Perit Dial Int, 2015. **35**(1): p. 5-8.
53. Hausmann, R., et al., *The glomerular filtration barrier function: new concepts.* Curr Opin Nephrol Hypertens, 2012. **21**(4): p. 441-9.
54. Hausmann, R., et al., *Electrical forces determine glomerular permeability.* Journal of the American Society of Nephrology : JASN, 2010. **21**: p. 2053-8.
55. Moeller, M.J. and G.A. Tanner, *Reply: podocytes are key-although albumin never reaches the slit diaphragm.* Nat Rev Nephrol, 2014. **10**(3): p. 180.
56. Fujigaki, Y., et al., *Intra-GBM site of the functional filtration barrier for endogenous proteins in rats.* Kidney Int, 1993. **43**(3): p. 567-74.
57. Pavenstadt, H., W. Kriz, and M. Kretzler, *Cell biology of the glomerular podocyte.* Physiol Rev, 2003. **83**(1): p. 253-307.
58. Scott, R.P. and S.E. Quaggin, *The cell biology of renal filtration.* J Cell Biol, 2015. **209**(2): p. 199-210.
59. Faul, C., et al., *Actin up: regulation of podocyte structure and function by components of the actin cytoskeleton.* Trends in cell biology, 2007. **17**: p. 428-37.
60. Reiser, J., et al., *The glomerular slit diaphragm is a modified adherens junction.* J Am Soc Nephrol, 2000. **11**(1): p. 1-8.
61. Kestilä, M., et al., *Positionally cloned gene for a novel glomerular protein--nephrin--is mutated in congenital nephrotic syndrome.* Molecular cell, 1998. **1**: p. 575-82.
62. Khoshnoodi, J., et al., *Nephrin promotes cell-cell adhesion through homophilic interactions.* Am J Pathol, 2003. **163**(6): p. 2337-46.

63. Schwarz, K., et al., *Podocin, a raft-associated component of the glomerular slit diaphragm, interacts with CD2AP and nephrin.* J Clin Invest, 2001. **108**(11): p. 1621-9.
64. Shih, N.Y., et al., *CD2AP localizes to the slit diaphragm and binds to nephrin via a novel C-terminal domain.* Am J Pathol, 2001. **159**(6): p. 2303-8.
65. Lehtonen, S., F. Zhao, and E. Lehtonen, *CD2-associated protein directly interacts with the actin cytoskeleton.* Am J Physiol Renal Physiol, 2002. **283**(4): p. F734-43.
66. Hutchings, N.J., et al., *Linking the T cell surface protein CD2 to the actin-capping protein CAPZ via CMS and CIN85.* J Biol Chem, 2003. **278**(25): p. 22396-403.
67. Lynch, D.K., et al., *A Cortactin-CD2-associated protein (CD2AP) complex provides a novel link between epidermal growth factor receptor endocytosis and the actin cytoskeleton.* J Biol Chem, 2003. **278**(24): p. 21805-13.
68. Asanuma, K., et al., *Synaptopodin regulates the actin-bundling activity of alpha-actinin in an isoform-specific manner.* The Journal of clinical investigation, 2005. **115**: p. 1188-98.
69. Hartleben, B., et al., *Neph-Nephrin proteins bind the Par3-Par6-atypical protein kinase C (aPKC) complex to regulate podocyte cell polarity.* J Biol Chem, 2008. **283**(34): p. 23033-8.
70. Fukasawa, H., et al., *Slit diaphragms contain tight junction proteins.* J Am Soc Nephrol, 2009. **20**(7): p. 1491-503.
71. Shih, N.Y., et al., *Congenital nephrotic syndrome in mice lacking CD2-associated protein.* Science, 1999. **286**(5438): p. 312-5.
72. Pierchala, B.A., M.R. Munoz, and C.C. Tsui, *Proteomic analysis of the slit diaphragm complex: CLIC5 is a protein critical for podocyte morphology and function.* Kidney Int, 2010. **78**(9): p. 868-82.
73. Yaoita, E., et al., *Up-regulation of connexin43 in glomerular podocytes in response to injury.* Am J Pathol, 2002. **161**(5): p. 1597-606.
74. Patrakka, J., et al., *Expression and subcellular distribution of novel glomerulus-associated proteins dendrin, ehd3, sh2d4a, plekhh2, and 2310066E14Rik.* J Am Soc Nephrol, 2007. **18**(3): p. 689-97.
75. Hashimoto, T., et al., *Ephrin-B1 localizes at the slit diaphragm of the glomerular podocyte.* Kidney Int, 2007. **72**(8): p. 954-64.
76. Inoue, T., et al., *FAT is a component of glomerular slit diaphragms.* Kidney Int, 2001. **59**(3): p. 1003-12.
77. Shimizu, M., et al., *Expression of galectin-1, a new component of slit diaphragm, is altered in minimal change nephrotic syndrome.* Lab Invest, 2009. **89**(2): p. 178-95.
78. Hirabayashi, S., et al., *MAGI-1 is a component of the glomerular slit diaphragm that is tightly associated with nephrin.* Lab Invest, 2005. **85**(12): p. 1528-43.
79. Lehtonen, S., et al., *Cell junction-associated proteins IQGAP1, MAGI-2, CASK, spectrins, and alpha-actinin are components of the nephrin multiprotein complex.* Proc Natl Acad Sci U S A, 2005. **102**(28): p. 9814-9.
80. Donoviel, D.B., et al., *Proteinuria and perinatal lethality in mice lacking NEPH1, a novel protein with homology to NEPHRIN.* Mol Cell Biol, 2001. **21**(14): p. 4829-36.
81. Gerke, P., et al., *NEPH2 is located at the glomerular slit diaphragm, interacts with nephrin and is cleaved from podocytes by metalloproteinases.* J Am Soc Nephrol, 2005. **16**(6): p. 1693-702.
82. Ruotsalainen, V., et al., *Nephrin is specifically located at the slit diaphragm of glomerular podocytes.* Proc Natl Acad Sci U S A, 1999. **96**(14): p. 7962-7.

83. Holthofer, H., et al., *Nephrin localizes at the podocyte filtration slit area and is characteristically spliced in the human kidney.* Am J Pathol, 1999. **155**(5): p. 1681-7.
84. Roselli, S., et al., *Podocin localizes in the kidney to the slit diaphragm area.* Am J Pathol, 2002. **160**(1): p. 131-9.
85. Schnabel, E., J.M. Anderson, and M.G. Farquhar, *The tight junction protein ZO-1 is concentrated along slit diaphragms of the glomerular epithelium.* J Cell Biol, 1990. **111**(3): p. 1255-63.
86. Kurihara, H., et al., *The altered glomerular filtration slits seen in puromycin aminonucleoside nephrosis and protamine sulfate-treated rats contain the tight junction protein ZO-1.* Am J Pathol, 1992. **141**(4): p. 805-16.
87. Grahammer, F., C. Schell, and T.B. Huber, *The podocyte slit diaphragm--from a thin grey line to a complex signalling hub.* Nat Rev Nephrol, 2013. **9**(10): p. 587-98.
88. Verma, R., et al., *Fyn binds to and phosphorylates the kidney slit diaphragm component Nephrin.* The Journal of biological chemistry, 2003. **278**: p. 20716-23.
89. Jones, N., et al., *Nck adaptor proteins link nephrin to the actin cytoskeleton of kidney podocytes.* Nature, 2006. **440**: p. 818-23.
90. George, B., et al., *Crk1/2-dependent signaling is necessary for podocyte foot process spreading in mouse models of glomerular disease.* J Clin Invest, 2012. **122**(2): p. 674-92.
91. George, B., et al., *Crk1/2 and CrkL form a hetero-oligomer and functionally complement each other during podocyte morphogenesis.* Kidney Int, 2014. **85**(6): p. 1382-94.
92. Bisson, N., et al., *The adaptor protein Grb2 is not essential for the establishment of the glomerular filtration barrier.* PLoS One, 2012. **7**(11): p. e50996.
93. Huber, T.B., et al., *Nephrin and CD2AP associate with phosphoinositide 3-OH kinase and stimulate AKT-dependent signaling.* Mol Cell Biol, 2003. **23**(14): p. 4917-28.
94. Zhu, J., et al., *Nephrin mediates actin reorganization via phosphoinositide 3-kinase in podocytes.* Kidney Int, 2008. **73**(5): p. 556-66.
95. Garg, P., et al., *Neph1 cooperates with nephrin to transduce a signal that induces actin polymerization.* Mol Cell Biol, 2007. **27**(24): p. 8698-712.
96. Schell, C., et al., *N-wasp is required for stabilization of podocyte foot processes.* J Am Soc Nephrol, 2013. **24**(5): p. 713-21.
97. Fan, X., et al., *Inhibitory effects of Robo2 on nephrin: a crosstalk between positive and negative signals regulating podocyte structure.* Cell Rep, 2012. **2**(1): p. 52-61.
98. Robson, A.M., et al., *Normal glomerular permeability and its modification by minimal change nephrotic syndrmone.* J Clin Invest, 1974. **54**(5): p. 1190-9.
99. Boute, N., et al., *NPHS2, encoding the glomerular protein podocin, is mutated in autosomal recessive steroid-resistant nephrotic syndrome.* Nat Genet, 2000. **24**(4): p. 349-54.
100. Ciani, L., et al., *Mice lacking the giant protocadherin mFAT1 exhibit renal slit junction abnormalities and a partially penetrant cyclopia and anophthalmia phenotype.* Mol Cell Biol, 2003. **23**(10): p. 3575-82.
101. Winn, M.P., et al., *A mutation in the TRPC6 cation channel causes familial focal segmental glomerulosclerosis.* Science, 2005. **308**(5729): p. 1801-4.
102. Xing, C.-Y., et al., *Direct effects of dexamethasone on human podocytes.* Kidney international, 2006. **70**: p. 1038-45.

103. Faul, C., et al., *The actin cytoskeleton of kidney podocytes is a direct target of the antiproteinuric effect of cyclosporine A.* Nature medicine, 2008. **14**: p. 931-8.
104. Yan, K., et al., *Subcellular localization of glucocorticoid receptor protein in the human kidney glomerulus.* Kidney Int, 1999. **56**(1): p. 65-73.
105. Guess, A., et al., *Dose- and time-dependent glucocorticoid receptor signaling in podocytes.* Am J Physiol Renal Physiol, 2010. **299**(4): p. F845-53.
106. Ransom, R.F., et al., *Differential proteomic analysis of proteins induced by glucocorticoids in cultured murine podocytes.* Kidney international, 2005. **67**: p. 1275-85.
107. Cheng, X., et al., *Microarray analyses of glucocorticoid and vitamin D3 target genes in differentiating cultured human podocytes.* PLoS One, 2013. **8**(4): p. e60213.
108. Saleem, M.a., et al., *A conditionally immortalized human podocyte cell line demonstrating nephrin and podocin expression.* Journal of the American Society of Nephrology : JASN, 2002. **13**: p. 630-8.
109. Ransom, R.F., et al., *Glucocorticoids protect and enhance recovery of cultured murine podocytes via actin filament stabilization.* Kidney international, 2005. **68**: p. 2473-83.
110. Wada, T., et al., *Dexamethasone prevents podocyte apoptosis induced by puromycin aminonucleoside: role of p53 and Bcl-2-related family proteins.* Journal of the American Society of Nephrology : JASN, 2005. **16**: p. 2615-25.
111. Tufro, A. and D. Veron, *VEGF and podocytes in diabetic nephropathy.* Semin Nephrol, 2012. **32**(4): p. 385-93.
112. Veron, D., et al., *Overexpression of VEGF-A in podocytes of adult mice causes glomerular disease.* Kidney Int, 2010. **77**(11): p. 989-99.
113. Schonenberger, E., et al., *The podocyte as a direct target of immunosuppressive agents.* Nephrol Dial Transplant, 2011. **26**(1): p. 18-24.
114. Simon, M., et al., *Expression of vascular endothelial growth factor and its receptors in human renal ontogenesis and in adult kidney.* Am J Physiol, 1995. **268**(2 Pt 2): p. F240-50.
115. Bailey, E., et al., *Vascular endothelial growth factor mRNA expression in minimal change, membranous, and diabetic nephropathy demonstrated by non-isotopic in situ hybridisation.* Journal of clinical pathology, 1999. **52**: p. 735-8.
116. Huber, T.B., et al., *Expression of functional CCR and CXCR chemokine receptors in podocytes.* J Immunol, 2002. **168**(12): p. 6244-52.
117. Fujii, Y., et al., *The effect of dexamethasone on defective nephrin transport caused by ER stress: a potential mechanism for the therapeutic action of glucocorticoids in the acquired glomerular diseases.* Kidney international, 2006. **69**: p. 1350-9.
118. Uchida, K., et al., *Decreased tyrosine phosphorylation of nephrin in rat and human nephrosis.* Kidney Int, 2008. **73**(8): p. 926-32.
119. Ohashi, T., et al., *Dexamethasone increases the phosphorylation of nephrin in cultured podocytes.* Clinical and experimental nephrology, 2011. **15**: p. 688-93.
120. Xing, Y., et al., *Diversities of podocyte molecular changes induced by different antiproteinuria drugs.* Exp Biol Med (Maywood), 2006. **231**(5): p. 585-93.
121. Wu, J., et al., *Downregulation of microRNA-30 facilitates podocyte injury and is prevented by glucocorticoids.* J Am Soc Nephrol, 2014. **25**(1): p. 92-104.
122. Endlich, N. and K. Endlich, *Stretch, tension and adhesion - adaptive mechanisms of the actin cytoskeleton in podocytes.* Eur J Cell Biol, 2006. **85**(3-4): p. 229-34.

123. Welsh, G.I. and M.A. Saleem, *The podocyte cytoskeleton--key to a functioning glomerulus in health and disease.* Nat Rev Nephrol, 2012. **8**(1): p. 14-21.
124. Saleem, M.A., et al., *The molecular and functional phenotype of glomerular podocytes reveals key features of contractile smooth muscle cells.* Am J Physiol Renal Physiol, 2008. **295**(4): p. F959-70.
125. Coward, R.J., et al., *The human glomerular podocyte is a novel target for insulin action.* Diabetes, 2005. **54**(11): p. 3095-102.
126. Friedrich, C., et al., *Podocytes are sensitive to fluid shear stress in vitro.* Am J Physiol Renal Physiol, 2006. **291**(4): p. F856-65.
127. Morton, M.J., et al., *Human podocytes possess a stretch-sensitive, Ca2+-activated K+ channel: potential implications for the control of glomerular filtration.* J Am Soc Nephrol, 2004. **15**(12): p. 2981-7.
128. Tian, D., et al., *Antagonistic regulation of actin dynamics and cell motility by TRPC5 and TRPC6 channels.* Sci Signal, 2010. **3**(145): p. ra77.
129. Mundel, P. and J. Reiser, *Proteinuria: an enzymatic disease of the podocyte?* Kidney international, 2010. **77**: p. 571-80.
130. Kistler, A.D., M.M. Altintas, and J. Reiser, *Podocyte GTPases regulate kidney filter dynamics.* Kidney international, 2012. **81**: p. 1053-5.
131. Reiser, J., et al., *Podocyte migration during nephrotic syndrome requires a coordinated interplay between cathepsin L and alpha3 integrin.* The Journal of biological chemistry, 2004. **279**: p. 34827-32.
132. Hackl, M.J., et al., *Tracking the fate of glomerular epithelial cells in vivo using serial multiphoton imaging in new mouse models with fluorescent lineage tags.* Nature medicine, 2013. **19**: p. 1661-6.
133. Ma, H., et al., *Inhibition of podocyte FAK protects against proteinuria and foot process effacement.* J Am Soc Nephrol, 2010. **21**(7): p. 1145-56.
134. Harris, J.J., et al., *Active proteases in nephrotic plasma lead to a podocin-dependent phosphorylation of VASP in podocytes via protease activated receptor-1.* J Pathol, 2013. **229**(5): p. 660-71.
135. Park, S.J. and J.I. Shin, *Complications of nephrotic syndrome.* Korean J Pediatr, 2011. **54**(8): p. 322-8.
136. Iversen, P. and C. Brun, *Aspiration biopsy of the kidney.* The American journal of medicine, 1951. **11**: p. 324-30.
137. Churg, J., R. Habib, and R.H. White, *Pathology of the nephrotic syndrome in children: a report for the International Study of Kidney Disease in Children.* Lancet, 1970. **760**: p. 1299-302.
138. Waldman, M., et al., *Adult minimal-change disease: clinical characteristics, treatment, and outcomes.* Clin J Am Soc Nephrol, 2007. **2**(3): p. 445-53.
139. *The primary nephrotic syndrome in children. Identification of patients with minimal change nephrotic syndrome from initial response to prednisone. A report of the International Study of Kidney Disease in Children.* J Pediatr, 1981. **98**(4): p. 561-4.
140. Ferrario, F. and M.P. Rastaldi, *Histopathological atlas of renal diseases: Minimal Change disease and focal glomerulosclerosis.* Journal of nephrology. **18**: p. 1-4.
141. Gipson, D.S., et al., *Differential risk of remission and ESRD in childhood FSGS.* Pediatric nephrology (Berlin, Germany), 2006. **21**: p. 344-9.
142. Bonilla-Felix, M., et al., *Changing patterns in the histopathology of idiopathic nephrotic syndrome in children.* Kidney international, 1999. **55**: p. 1885-90.
143. Hoyer, J.R., et al., *Recurrence of idiopathic nephrotic syndrome after renal transplantation.* Lancet, 1972. **2**: p. 343-8.

144. Cho, M.H., et al., *Pathophysiology of minimal change nephrotic syndrome and focal segmental glomerulosclerosis.* Nephrology (Carlton, Vic.), 2007. **12 Suppl 3**: p. S11-4.
145. McKinney, P.A., et al., *Time trends and ethnic patterns of childhood nephrotic syndrome in Yorkshire, UK.* Pediatr Nephrol, 2001. **16**(12): p. 1040-4.
146. Sharples, P.M., J. Poulton, and R.H. White, *Steroid responsive nephrotic syndrome is more common in Asians.* Arch Dis Child, 1985. **60**(11): p. 1014-7.
147. Jalanko, H., *Congenital nephrotic syndrome.* Pediatr Nephrol, 2009. **24**(11): p. 2121-8.
148. Ruf, R.G., et al., *Patients with mutations in NPHS2 (podocin) do not respond to standard steroid treatment of nephrotic syndrome.* J Am Soc Nephrol, 2004. **15**(3): p. 722-32.
149. Arneil, G.C., *Treatment of nephrosis with prednisolone.* Lancet, 1956. **270**: p. 409-11.
150. *Short versus standard prednisone therapy for initial treatment of idiopathic nephrotic syndrome in children. Arbeitsgemeinschaft fur Padiatrische Nephrologie.* Lancet, 1988. **1**(8582): p. 380-3.
151. Ehrich, J.H. and J. Brodehl, *Long versus standard prednisone therapy for initial treatment of idiopathic nephrotic syndrome in children. Arbeitsgemeinschaft fur Padiatrische Nephrologie.* Eur J Pediatr, 1993. **152**(4): p. 357-61.
152. Gipson, D.S., et al., *Management of childhood onset nephrotic syndrome.* Pediatrics, 2009. **124**(2): p. 747-57.
153. Tarshish, P., et al., *Prognostic significance of the early course of minimal change nephrotic syndrome: report of the International Study of Kidney Disease in Children.* J Am Soc Nephrol, 1997. **8**(5): p. 769-76.
154. McIntyre, P. and J.C. Craig, *Prevention of serious bacterial infection in children with nephrotic syndrome.* J Paediatr Child Health, 1998. **34**(4): p. 314-7.
155. Patiroglu, T., A. Melikoglu, and R. Dusunsel, *Serum levels of C3 and factors I and B in minimal change disease.* Acta Paediatr Jpn, 1998. **40**(4): p. 333-6.
156. Trompeter, R.S., et al., *Long-term outcome for children with minimal-change nephrotic syndrome.* Lancet, 1985. **1**(8425): p. 368-70.
157. Lewis, M.A., et al., *Nephrotic syndrome: from toddlers to twenties.* Lancet, 1989. **1**(8632): p. 255-9.
158. Ruth, E.M., et al., *Children with steroid-sensitive nephrotic syndrome come of age: long-term outcome.* J Pediatr, 2005. **147**(2): p. 202-7.
159. Fakhouri, F., et al., *Steroid-sensitive nephrotic syndrome: from childhood to adulthood.* Am J Kidney Dis, 2003. **41**(3): p. 550-7.
160. Niaudet, P., *Long-term outcome of children with steroid-sensitive idiopathic nephrotic syndrome.* Clin J Am Soc Nephrol, 2009. **4**(10): p. 1547-8.
161. Hayasaka, Y., S. Hayasaka, and H. Matsukura, *Ocular findings in Japanese children with nephrotic syndrome receiving prolonged corticosteroid therapy.* Ophthalmologica. Journal international d'ophtalmologie. International journal of ophthalmology. Zeitschrift für Augenheilkunde, 2006. **220**: p. 181-5.
162. Abeyagunawardena, A.S., P. Hindmarsh, and R.S. Trompeter, *Adrenocortical suppression increases the risk of relapse in nephrotic syndrome.* Arch Dis Child, 2007. **92**(7): p. 585-8.
163. Sumboonnanonda, A., et al., *Adrenal function after prednisolone treatment in childhood nephrotic syndrome.* J Med Assoc Thai, 1994. **77**(3): p. 126-9.
164. Barragry, J.M., et al., *Vitamin-D metabolism in nephrotic syndrome.* Lancet, 1977. **2**(8039): p. 629-32.
165. Gulati, S., et al., *Are children with idiopathic nephrotic syndrome at risk for metabolic bone disease?* Am J Kidney Dis, 2003. **41**(6): p. 1163-9.

166. *Recommendations for the prevention and treatment of glucocorticoid-induced osteoporosis. American College of Rheumatology Task Force on Osteoporosis Guidelines.* Arthritis Rheum, 1996. **39**(11): p. 1791-801.
167. Chesney, R.W., et al., *Effect of prednisone on growth and bone mineral content in childhood glomerular disease.* American journal of diseases of children (1960), 1978. **132**: p. 768-72.
168. Elzouki, A.Y. and O.P. Jaiswal, *Long-term, small dose prednisone therapy in frequently relapsing nephrotic syndrome of childhood. Effect on remission, statural growth, obesity, and infection rate.* Clin Pediatr (Phila), 1988. **27**(8): p. 387-92.
169. Leonard, M.B., et al., *Long-term, high-dose glucocorticoids and bone mineral content in childhood glucocorticoid-sensitive nephrotic syndrome.* N Engl J Med, 2004. **351**(9): p. 868-75.
170. Cecka, J.M., D.W. Gjertson, and P.I. Terasaki, *Pediatric renal transplantation: a review of the UNOS data. United Network for Organ Sharing.* Pediatric transplantation, 1997. **1**: p. 55-64.
171. De Geest, S. and E. Sabaté, *Adherence to long-term therapies: evidence for action.* European journal of cardiovascular nursing : journal of the Working Group on Cardiovascular Nursing of the European Society of Cardiology, 2003. **2**: p. 323.
172. Mekahli, D., et al., *Long-term outcome of idiopathic steroid-resistant nephrotic syndrome: a multicenter study.* Pediatr Nephrol, 2009. **24**(8): p. 1525-32.
173. Trautmann, A., et al., *Spectrum of steroid-resistant and congenital nephrotic syndrome in children: the PodoNet registry cohort.* Clin J Am Soc Nephrol, 2015. **10**(4): p. 592-600.
174. White, R.H., E.F. Glasgow, and R.J. Mills, *Clinicopathological study of nephrotic syndrome in childhood.* Lancet, 1970. **1**: p. 1353-9.
175. Webb, N.J., et al., *Childhood steroid-sensitive nephrotic syndrome: does the histology matter?* Am J Kidney Dis, 1996. **27**(4): p. 484-8.
176. Vivarelli, M., et al., *Time for initial response to steroids is a major prognostic factor in idiopathic nephrotic syndrome.* J Pediatr, 2010. **156**(6): p. 965-71.
177. Saleem, M.A., *New developments in steroid-resistant nephrotic syndrome.* Pediatr Nephrol, 2013. **28**(5): p. 699-709.
178. Heeringa, S.F., et al., *COQ6 mutations in human patients produce nephrotic syndrome with sensorineural deafness.* J Clin Invest, 2011. **121**(5): p. 2013-24.
179. Machuca, E., G. Benoit, and C. Antignac, *Genetics of nephrotic syndrome: connecting molecular genetics to podocyte physiology.* Human molecular genetics, 2009. **18**: p. R185-94.
180. Mahan, J.D., et al., *Congenital nephrotic syndrome: evolution of medical management and results of renal transplantation.* J Pediatr, 1984. **105**(4): p. 549-57.
181. Norio, R., *Heredity in the congenital nephrotic syndrome. A genetic study of 57 finnish FAMILIES WITH A REVIEW OF REPORTED CASES.* Ann Paediatr Fenn, 1966. **12**: p. Suppl 27:1-94.
182. Niaudet, P., *Genetic forms of nephrotic syndrome.* Pediatr Nephrol, 2004. **19**(12): p. 1313-8.
183. Schultheiss, M., et al., *No evidence for genotype/phenotype correlation in NPHS1 and NPHS2 mutations.* Pediatr Nephrol, 2004. **19**(12): p. 1340-8.
184. Koziell, A., et al., *Genotype/phenotype correlations of NPHS1 and NPHS2 mutations in nephrotic syndrome advocate a functional inter-relationship in glomerular filtration.* Hum Mol Genet, 2002. **11**(4): p. 379-88.

185. Landau, D., et al., *Familial steroid-sensitive nephrotic syndrome in Southern Israel: clinical and genetic observations.* Pediatr Nephrol, 2007. **22**(5): p. 661-9.
186. Fuchshuber, A., et al., *Clinical and genetic evaluation of familial steroid-responsive nephrotic syndrome in childhood.* J Am Soc Nephrol, 2001. **12**(2): p. 374-8.
187. Ruf, R.G., et al., *Identification of the first gene locus (SSNS1) for steroid-sensitive nephrotic syndrome on chromosome 2p.* J Am Soc Nephrol, 2003. **14**(7): p. 1897-900.
188. Weber, S., et al., *NPHS2 mutation analysis shows genetic heterogeneity of steroid-resistant nephrotic syndrome and low post-transplant recurrence.* Kidney Int, 2004. **66**(2): p. 571-9.
189. Buscher, A.K., et al., *Immunosuppression and renal outcome in congenital and pediatric steroid-resistant nephrotic syndrome.* Clin J Am Soc Nephrol, 2010. **5**(11): p. 2075-84.
190. Hinkes, B., et al., *Positional cloning uncovers mutations in PLCE1 responsible for a nephrotic syndrome variant that may be reversible.* Nature genetics, 2006. **38**: p. 1397-405.
191. Montini, G., C. Malaventura, and L. Salviati, *Early coenzyme Q10 supplementation in primary coenzyme Q10 deficiency.* N Engl J Med, 2008. **358**(26): p. 2849-50.
192. Cochat, P., et al., *Disease recurrence in paediatric renal transplantation.* Pediatr Nephrol, 2009. **24**(11): p. 2097-108.
193. Ding, W.Y., et al., *Initial steroid sensitivity in children with steroid-resistant nephrotic syndrome predicts post-transplant recurrence.* J Am Soc Nephrol, 2014. **25**(6): p. 1342-8.
194. Ali, A.A., et al., *Minimal-change glomerular nephritis. Normal kidneys in an abnormal environment?* Transplantation, 1994. **58**: p. 849-52.
195. Artero, M.L., et al., *Plasmapheresis reduces proteinuria and serum capacity to injure glomeruli in patients with recurrent focal glomerulosclerosis.* American journal of kidney diseases : the official journal of the National Kidney Foundation, 1994. **23**: p. 574-81.
196. Lagrue, G., et al., *[Transmission of nephrotic syndrome to two neonates. Spontaneous regression]*. Presse médicale (Paris, France : 1983), 1991. **20**: p. 255-7.
197. Zimmerman, S.W., *Increased urinary protein excretion in the rat produced by serum from a patient with recurrent focal glomerular sclerosis after renal transplantation.* Clinical nephrology, 1984. **22**: p. 32-8.
198. Savin, V.J., et al., *Circulating factor associated with increased glomerular permeability to albumin in recurrent focal segmental glomerulosclerosis.* The New England journal of medicine, 1996. **334**: p. 878-83.
199. Clement, L.C., et al., *Podocyte-secreted angiopoietin-like-4 mediates proteinuria in glucocorticoid-sensitive nephrotic syndrome.* Nat Med, 2011. **17**(1): p. 117-22.
200. Bakker, W.W., et al., *Altered activity of plasma hemopexin in patients with minimal change disease in relapse.* Pediatric nephrology (Berlin, Germany), 2005. **20**: p. 1410-5.
201. Lennon, R., et al., *Hemopexin induces nephrin-dependent reorganization of the actin cytoskeleton in podocytes.* Journal of the American Society of Nephrology : JASN, 2008. **19**: p. 2140-9.
202. Wei, C., et al., *Circulating urokinase receptor as a cause of focal segmental glomerulosclerosis.* Nature medicine, 2011. **17**: p. 952-60.

203. Cobos, E., C. Jumper, and C. Lox, *Pretreatment determination of the serum urokinase plasminogen activator and its soluble receptor in advanced small-cell lung cancer or non-small-cell lung cancer.* Clin Appl Thromb Hemost, 2003. **9**(3): p. 241-6.
204. Giamarellos-Bourboulis, E.J., et al., *Risk assessment in sepsis: a new prognostication rule by APACHE II score and serum soluble urokinase plasminogen activator receptor.* Crit Care, 2012. **16**(4): p. R149.
205. Toldi, G., et al., *Plasma soluble urokinase plasminogen activator receptor (suPAR) levels in systemic lupus erythematosus.* Biomarkers, 2012. **17**(8): p. 758-63.
206. Maas, R.J., J.K. Deegens, and J.F. Wetzels, *Serum suPAR in patients with FSGS: trash or treasure?* Pediatr Nephrol, 2013. **28**(7): p. 1041-8.
207. Meijers, B., et al., *The soluble urokinase receptor is not a clinical marker for focal segmental glomerulosclerosis.* Kidney Int, 2014. **85**(3): p. 636-40.
208. Wada, T., et al., *A multicenter cross-sectional study of circulating soluble urokinase receptor in Japanese patients with glomerular disease.* Kidney Int, 2014. **85**(3): p. 641-8.
209. Sinha, A., et al., *Serum-soluble urokinase receptor levels do not distinguish focal segmental glomerulosclerosis from other causes of nephrotic syndrome in children.* Kidney Int, 2014. **85**(3): p. 649-58.
210. Schlondorff, D., *Are serum suPAR determinations by current ELISA methodology reliable diagnostic biomarkers for FSGS?* Kidney Int, 2014. **85**(3): p. 499-501.
211. Shalhoub, R.J., *Pathogenesis of lipoid nephrosis: a disorder of T-cell function.* Lancet, 1974. **2**: p. 556-60.
212. Sun, X., et al., *Suppression of antigen-specific T cell proliferation by measles virus infection: role of a soluble factor in suppression.* Virology, 1998. **246**: p. 24-33.
213. Burstein, D.M. and R.A. Rodby, *Membranoproliferative glomerulonephritis associated with hepatitis C virus infection.* Journal of the American Society of Nephrology : JASN, 1993. **4**: p. 1288-93.
214. Peces, R., et al., *Minimal change nephrotic syndrome associated with Hodgkin's lymphoma.* Nephrology, dialysis, transplantation : official publication of the European Dialysis and Transplant Association - European Renal Association, 1991. **6**: p. 155-8.
215. Maruyama, K., et al., *Effect of supernatants derived from T lymphocyte culture in minimal change nephrotic syndrome on rat kidney capillaries.* Nephron, 1989. **51**: p. 73-6.
216. Meadow, S.R. and J.K. Sarsfield, *Steroid-responsive and nephrotic syndrome and allergy: clinical studies.* Archives of disease in childhood, 1981. **56**: p. 509-16.
217. Lai, K.-W., et al., *Overexpression of interleukin-13 induces minimal-change-like nephropathy in rats.* Journal of the American Society of Nephrology : JASN, 2007. **18**: p. 1476-85.
218. Sellier-Leclerc, A.-L., et al., *A humanized mouse model of idiopathic nephrotic syndrome suggests a pathogenic role for immature cells.* Journal of the American Society of Nephrology : JASN, 2007. **18**: p. 2732-9.
219. Sahali, D., et al., *Transcriptional and post-transcriptional alterations of IkappaBalpha in active minimal-change nephrotic syndrome.* Journal of the American Society of Nephrology : JASN, 2001. **12**: p. 1648-58.

220. Sahali, D., et al., *A novel approach to investigation of the pathogenesis of active minimal-change nephrotic syndrome using subtracted cDNA library screening.* Journal of the American Society of Nephrology : JASN, 2002. **13**: p. 1238-47.
221. Shimada, M., et al., *Minimal change disease: a "two-hit" podocyte immune disorder?* Pediatr Nephrol, 2011. **26**(4): p. 645-9.
222. Reiser, J. and P. Mundel, *Danger signaling by glomerular podocytes defines a novel function of inducible B7-1 in the pathogenesis of nephrotic syndrome.* J Am Soc Nephrol, 2004. **15**(9): p. 2246-8.
223. Reiser, J., et al., *Induction of B7-1 in podocytes is associated with nephrotic syndrome.* The Journal of clinical investigation, 2004. **113**: p. 1390-7.
224. Yu, C.C., et al., *Abatacept in B7-1-positive proteinuric kidney disease.* N Engl J Med, 2013. **369**(25): p. 2416-23.
225. Reiser, J. and N. Alachkar, *Proteinuria: abate or applaud abatacept in proteinuric kidney disease?* Nat Rev Nephrol, 2014. **10**(3): p. 128-30.
226. Delville, M., et al., *A circulating antibody panel for pretransplant prediction of FSGS recurrence after kidney transplantation.* Sci Transl Med, 2014. **6**(256): p. 256ra136.
227. Baricos, W.H., et al., *Evidence suggesting a role for cathepsin L in an experimental model of glomerulonephritis.* Arch Biochem Biophys, 1991. **288**(2): p. 468-72.
228. Sever, S., et al., *Proteolytic processing of dynamin by cytoplasmic cathepsin L is a mechanism for proteinuric kidney disease.* J Clin Invest, 2007. **117**(8): p. 2095-104.
229. Yanagida-Asanuma, E., et al., *Synaptopodin protects against proteinuria by disrupting Cdc42:IRSp53:Mena signaling complexes in kidney podocytes.* The American journal of pathology, 2007. **171**: p. 415-27.
230. Duma, D., C.M. Jewell, and J.A. Cidlowski, *Multiple glucocorticoid receptor isoforms and mechanisms of post-translational modification.* J Steroid Biochem Mol Biol, 2006. **102**(1-5): p. 11-21.
231. Morris, D.J., *Why do humans have two glucocorticoids: A question of intestinal fortitude.* Steroids, 2015. **102**: p. 32-38.
232. Wei, L., T.M. MacDonald, and B.R. Walker, *Taking glucocorticoids by prescription is associated with subsequent cardiovascular disease.* Ann Intern Med, 2004. **141**(10): p. 764-70.
233. Faus, H. and B. Haendler, *Post-translational modifications of steroid receptors.* Biomed Pharmacother, 2006. **60**(9): p. 520-8.
234. Cole, T.J., et al., *Targeted disruption of the glucocorticoid receptor gene blocks adrenergic chromaffin cell development and severely retards lung maturation.* Genes Dev, 1995. **9**(13): p. 1608-21.
235. Cole, T.J., et al., *GRKO mice express an aberrant dexamethasone-binding glucocorticoid receptor, but are profoundly glucocorticoid resistant.* Mol Cell Endocrinol, 2001. **173**(1-2): p. 193-202.
236. Perogamvros, I., D.W. Ray, and P.J. Trainer, *Regulation of cortisol bioavailability--effects on hormone measurement and action.* Nat Rev Endocrinol, 2012. **8**(12): p. 717-27.
237. Oakley, R.H. and J.A. Cidlowski, *The biology of the glucocorticoid receptor: new signaling mechanisms in health and disease.* J Allergy Clin Immunol, 2013. **132**(5): p. 1033-44.
238. Moisan, M.P., *CBG: a cortisol reservoir rather than a transporter.* Nat Rev Endocrinol, 2013. **9**(2): p. 78.
239. Richard, E.M., et al., *Plasma transcortin influences endocrine and behavioral stress responses in mice.* Endocrinology, 2010. **151**(2): p. 649-59.

240. Cameron, A., et al., *Temperature-responsive release of cortisol from its binding globulin: a protein thermocouple.* J Clin Endocrinol Metab, 2010. **95**(10): p. 4689-95.
241. Hammond, G.L., et al., *A role for corticosteroid-binding globulin in delivery of cortisol to activated neutrophils.* J Clin Endocrinol Metab, 1990. **71**(1): p. 34-9.
242. Mendel, C.M., *The free hormone hypothesis. Distinction from the free hormone transport hypothesis.* J Androl, 1992. **13**(2): p. 107-16.
243. Mendel, C.M., et al., *Uptake of cortisol by the perfused rat liver: validity of the free hormone hypothesis applied to cortisol.* Endocrinology, 1989. **124**(1): p. 468-76.
244. Pugeat, M.M., J.F. Dunn, and B.C. Nisula, *Transport of steroid hormones: interaction of 70 drugs with testosterone-binding globulin and corticosteroid-binding globulin in human plasma.* J Clin Endocrinol Metab, 1981. **53**(1): p. 69-75.
245. Rostin, M., et al., *Pharmacokinetics of prednisolone in children with the nephrotic syndrome.* Pediatr Nephrol, 1990. **4**(5): p. 470-3.
246. Frey, F.J. and B.M. Frey, *Altered prednisolone kinetics in patients with the nephrotic syndrome.* Nephron, 1982. **32**(1): p. 45-8.
247. Jenkins, J.S. and P.A. Sampson, *Conversion of cortisone to cortisol and prednisone to prednisolone.* Br Med J, 1967. **2**(5546): p. 205-7.
248. Diederich, S., et al., *11beta-hydroxysteroid dehydrogenase types 1 and 2: an important pharmacokinetic determinant for the activity of synthetic mineralo- and glucocorticoids.* J Clin Endocrinol Metab, 2002. **87**(12): p. 5695-701.
249. Rocci, M.L., Jr., et al., *Effect on nephrotic syndrome on absorption and disposition of prednisolone in children.* Int J Pediatr Nephrol, 1982. **3**(3): p. 159-66.
250. Stimson, R.H. and B.R. Walker, *Glucocorticoids and 11beta-hydroxysteroid dehydrogenase type 1 in obesity and the metabolic syndrome.* Minerva Endocrinol, 2007. **32**(3): p. 141-59.
251. Hult, M., H. Jornvall, and U.C. Oppermann, *Selective inhibition of human type 1 11beta-hydroxysteroid dehydrogenase by synthetic steroids and xenobiotics.* FEBS Lett, 1998. **441**(1): p. 25-8.
252. Tannin, G.M., et al., *The human gene for 11 beta-hydroxysteroid dehydrogenase. Structure, tissue distribution, and chromosomal localization.* J Biol Chem, 1991. **266**(25): p. 16653-8.
253. Roland, B.L., Z.S. Krozowski, and J.W. Funder, *Glucocorticoid receptor, mineralocorticoid receptors, 11 beta-hydroxysteroid dehydrogenase-1 and -2 expression in rat brain and kidney: in situ studies.* Mol Cell Endocrinol, 1995. **111**(1): p. R1-7.
254. Chapman, K., M. Holmes, and J. Seckl, *11beta-hydroxysteroid dehydrogenases: intracellular gate-keepers of tissue glucocorticoid action.* Physiol Rev, 2013. **93**(3): p. 1139-206.
255. Hirasawa, G., et al., *Colocalization of 11 beta-hydroxysteroid dehydrogenase type II and mineralocorticoid receptor in human epithelia.* J Clin Endocrinol Metab, 1997. **82**(11): p. 3859-63.
256. Ferrari, P., E. Lovati, and F.J. Frey, *The role of the 11beta-hydroxysteroid dehydrogenase type 2 in human hypertension.* J Hypertens, 2000. **18**(3): p. 241-8.
257. Kataoka, S., et al., *11beta-hydroxysteroid dehydrogenase type 2 is expressed in the human kidney glomerulus.* J Clin Endocrinol Metab, 2002. **87**(2): p. 877-82.
258. Hellal-Levy, C., et al., *Mechanistic aspects of mineralocorticoid receptor activation.* Kidney Int, 2000. **57**(4): p. 1250-5.

259. Rosenfeld, P., et al., *Ontogeny of corticosteroid receptors in the brain.* Cell Mol Neurobiol, 1993. **13**(4): p. 295-319.
260. Fuller, P.J., S.S. Lim-Tio, and F.E. Brennan, *Specificity in mineralocorticoid versus glucocorticoid action.* Kidney Int, 2000. **57**(4): p. 1256-64.
261. Sasano, H., et al., *Immunolocalization of mineralocorticoid receptor in human kidney, pancreas, salivary, mammary and sweat glands: a light and electron microscopic immunohistochemical study.* J Endocrinol, 1992. **132**(2): p. 305-10.
262. Lombes, M., et al., *The mineralocorticoid receptor discriminates aldosterone from glucocorticoids independently of the 11 beta-hydroxysteroid dehydrogenase.* Endocrinology, 1994. **135**(3): p. 834-40.
263. Grossmann, C., et al., *Transactivation via the human glucocorticoid and mineralocorticoid receptor by therapeutically used steroids in CV-1 cells: a comparison of their glucocorticoid and mineralocorticoid properties.* European journal of endocrinology / European Federation of Endocrine Societies, 2004. **151**: p. 397-406.
264. Encio, I.J. and S.D. Detera-Wadleigh, *The genomic structure of the human glucocorticoid receptor.* J Biol Chem, 1991. **266**(11): p. 7182-8.
265. Pujols, L., et al., *Expression of glucocorticoid receptor alpha- and beta-isoforms in human cells and tissues.* Am J Physiol Cell Physiol, 2002. **283**(4): p. C1324-31.
266. Oakley, R.H., et al., *The dominant negative activity of the human glucocorticoid receptor beta isoform. Specificity and mechanisms of action.* J Biol Chem, 1999. **274**(39): p. 27857-66.
267. Beger, C., et al., *Expression and structural analysis of glucocorticoid receptor isoform gamma in human leukaemia cells using an isoform-specific real-time polymerase chain reaction approach.* Br J Haematol, 2003. **122**(2): p. 245-52.
268. Lu, N.Z. and J.A. Cidlowski, *Translational regulatory mechanisms generate N-terminal glucocorticoid receptor isoforms with unique transcriptional target genes.* Mol Cell, 2005. **18**(3): p. 331-42.
269. Hollenberg, S.M. and R.M. Evans, *Multiple and cooperative trans-activation domains of the human glucocorticoid receptor.* Cell, 1988. **55**(5): p. 899-906.
270. Almlof, T., A.P. Wright, and J.A. Gustafsson, *Role of acidic and phosphorylated residues in gene activation by the glucocorticoid receptor.* J Biol Chem, 1995. **270**(29): p. 17535-40.
271. Umesono, K. and R.M. Evans, *Determinants of target gene specificity for steroid/thyroid hormone receptors.* Cell, 1989. **57**(7): p. 1139-46.
272. Hollenberg, S.M., et al., *Primary structure and expression of a functional human glucocorticoid receptor cDNA.* Nature, 1985. **318**(6047): p. 635-41.
273. Picard, D. and K.R. Yamamoto, *Two signals mediate hormone-dependent nuclear localization of the glucocorticoid receptor.* EMBO J, 1987. **6**(11): p. 3333-40.
274. Pratt, W.B. and D.O. Toft, *Steroid receptor interactions with heat shock protein and immunophilin chaperones.* Endocr Rev, 1997. **18**(3): p. 306-60.
275. Isohashi, F. and K. Okamoto, *ATP-stimulated translocation promoter that enhances the nuclear binding of activated glucocorticoid receptor complex. Biochemical properties and its function (mini-review).* Receptor, 1993. **3**(2): p. 113-24.
276. Barnes, P.J., *How corticosteroids control inflammation: Quintiles Prize Lecture 2005.* British journal of pharmacology, 2006. **148**: p. 245-54.
277. Mittelstadt, P.R. and J.D. Ashwell, *Inhibition of AP-1 by the glucocorticoid-inducible protein GILZ.* J Biol Chem, 2001. **276**(31): p. 29603-10.

278. Smoak, K.A. and J.A. Cidlowski, *Mechanisms of glucocorticoid receptor signaling during inflammation.* Mech Ageing Dev, 2004. **125**(10-11): p. 697-706.
279. Morrison, N. and J. Eisman, *Role of the negative glucocorticoid regulatory element in glucocorticoid repression of the human osteocalcin promoter.* J Bone Miner Res, 1993. **8**(8): p. 969-75.
280. Luecke, H.F. and K.R. Yamamoto, *The glucocorticoid receptor blocks P-TEFb recruitment by NFkappaB to effect promoter-specific transcriptional repression.* Genes Dev, 2005. **19**(9): p. 1116-27.
281. McKay, L.I. and J.A. Cidlowski, *Cross-talk between nuclear factor-kappa B and the steroid hormone receptors: mechanisms of mutual antagonism.* Mol Endocrinol, 1998. **12**(1): p. 45-56.
282. Stoecklin, E., et al., *Specific DNA binding of Stat5, but not of glucocorticoid receptor, is required for their functional cooperation in the regulation of gene transcription.* Mol Cell Biol, 1997. **17**(11): p. 6708-16.
283. Chinenov, Y., et al., *Role of transcriptional coregulator GRIP1 in the anti-inflammatory actions of glucocorticoids.* Proc Natl Acad Sci U S A, 2012. **109**(29): p. 11776-81.
284. Uhlenhaut, N.H., et al., *Insights into negative regulation by the glucocorticoid receptor from genome-wide profiling of inflammatory cistromes.* Mol Cell, 2013. **49**(1): p. 158-71.
285. John, S., et al., *Chromatin accessibility pre-determines glucocorticoid receptor binding patterns.* Nature genetics, 2011. **43**: p. 264-8.
286. McNally, J.G., et al., *The glucocorticoid receptor: rapid exchange with regulatory sites in living cells.* Science, 2000. **287**(5456): p. 1262-5.
287. Stratmann, M. and U. Schibler, *Transcription factor loading: please take my place!* Cell, 2011. **146**(4): p. 497-9.
288. Voss, T.C., et al., *Dynamic exchange at regulatory elements during chromatin remodeling underlies assisted loading mechanism.* Cell, 2011. **146**(4): p. 544-54.
289. Stahn, C. and F. Buttgereit, *Genomic and nongenomic effects of glucocorticoids.* Nat Clin Pract Rheumatol, 2008. **4**(10): p. 525-33.
290. Croxtall, J.D., Q. Choudhury, and R.J. Flower, *Glucocorticoids act within minutes to inhibit recruitment of signalling factors to activated EGF receptors through a receptor-dependent, transcription-independent mechanism.* Br J Pharmacol, 2000. **130**(2): p. 289-98.
291. Solito, E., et al., *Dexamethasone induces rapid serine-phosphorylation and membrane translocation of annexin 1 in a human folliculostellate cell line via a novel nongenomic mechanism involving the glucocorticoid receptor, protein kinase C, phosphatidylinositol 3-kinase, and mitogen-activated protein kinase.* Endocrinology, 2003. **144**(4): p. 1164-74.
292. Samarasinghe, R.A., et al., *Nongenomic glucocorticoid receptor action regulates gap junction intercellular communication and neural progenitor cell proliferation.* Proc Natl Acad Sci U S A, 2011. **108**(40): p. 16657-62.
293. Rogatsky, I., C.L. Waase, and M.J. Garabedian, *Phosphorylation and inhibition of rat glucocorticoid receptor transcriptional activation by glycogen synthase kinase-3 (GSK-3). Species-specific differences between human and rat glucocorticoid receptor signaling as revealed through GSK-3 phosphorylation.* J Biol Chem, 1998. **273**(23): p. 14315-21.
294. Krstic, M.D., et al., *Mitogen-activated and cyclin-dependent protein kinases selectively and differentially modulate transcriptional enhancement by the glucocorticoid receptor.* Mol Cell Biol, 1997. **17**(7): p. 3947-54.

295. Galliher-Beckley, A.J. and J.A. Cidlowski, *Emerging roles of glucocorticoid receptor phosphorylation in modulating glucocorticoid hormone action in health and disease.* IUBMB Life, 2009. **61**(10): p. 979-86.
296. Wang, Z., J. Frederick, and M.J. Garabedian, *Deciphering the phosphorylation "code" of the glucocorticoid receptor in vivo.* J Biol Chem, 2002. **277**(29): p. 26573-80.
297. Chen, W., et al., *Glucocorticoid receptor phosphorylation differentially affects target gene expression.* Mol Endocrinol, 2008. **22**(8): p. 1754-66.
298. Galliher-Beckley, A.J., et al., *Glycogen synthase kinase 3beta-mediated serine phosphorylation of the human glucocorticoid receptor redirects gene expression profiles.* Mol Cell Biol, 2008. **28**(24): p. 7309-22.
299. Webster, J.C., et al., *Mouse glucocorticoid receptor phosphorylation status influences multiple functions of the receptor protein.* J Biol Chem, 1997. **272**(14): p. 9287-93.
300. Deroo, B.J., et al., *Proteasomal inhibition enhances glucocorticoid receptor transactivation and alters its subnuclear trafficking.* Mol Cell Biol, 2002. **22**(12): p. 4113-23.
301. Wallace, A.D. and J.A. Cidlowski, *Proteasome-mediated glucocorticoid receptor degradation restricts transcriptional signaling by glucocorticoids.* J Biol Chem, 2001. **276**(46): p. 42714-21.
302. Tian, S., et al., *Small ubiquitin-related modifier-1 (SUMO-1) modification of the glucocorticoid receptor.* Biochem J, 2002. **367**(Pt 3): p. 907-11.
303. Holmstrom, S., M.E. Van Antwerp, and J.A. Iniguez-Lluhi, *Direct and distinguishable inhibitory roles for SUMO isoforms in the control of transcriptional synergy.* Proc Natl Acad Sci U S A, 2003. **100**(26): p. 15758-63.
304. Charmandari, E., et al., *Peripheral CLOCK regulates target-tissue glucocorticoid receptor transcriptional activity in a circadian fashion in man.* PLoS One, 2011. **6**(9): p. e25612.
305. Barnes, P.J. and I.M. Adcock, *Glucocorticoid resistance in inflammatory diseases.* Lancet, 2009. **373**(9678): p. 1905-17.
306. Barnes, P.J., *Mechanisms and resistance in glucocorticoid control of inflammation.* J Steroid Biochem Mol Biol, 2010. **120**(2-3): p. 76-85.
307. Chikanza, I.C. and D.L. Kozaci, *Corticosteroid resistance in rheumatoid arthritis: molecular and cellular perspectives.* Rheumatology (Oxford), 2004. **43**(11): p. 1337-45.
308. Carmichael, J., et al., *Corticosteroid resistance in chronic asthma.* Br Med J (Clin Res Ed), 1981. **282**(6274): p. 1419-22.
309. Fuchshuber, A. and O. Mehls, *Familial steroid-resistant nephrotic syndromes: recent advances.* Nephrol Dial Transplant, 2000. **15**(12): p. 1897-900.
310. Hakonarson, H., et al., *Profiling of genes expressed in peripheral blood mononuclear cells predicts glucocorticoid sensitivity in asthma patients.* Proc Natl Acad Sci U S A, 2005. **102**(41): p. 14789-94.
311. Donn, R., et al., *Use of gene expression profiling to identify a novel glucocorticoid sensitivity determining gene, BMPRII.* The FASEB journal : official publication of the Federation of American Societies for Experimental Biology, 2007. **21**: p. 402-14.
312. Cheong, H.I., H.G. Kang, and J. Schlondorff, *GLCCI1 single nucleotide polymorphisms in pediatric nephrotic syndrome.* Pediatr Nephrol, 2012. **27**(9): p. 1595-9.
313. Lamberts, S.W., *Hereditary glucocorticoid resistance.* Ann Endocrinol (Paris), 2001. **62**(2): p. 164-7.

314. Lane, S.J., et al., *Chemical mutational analysis of the human glucocorticoid receptor cDNA in glucocorticoid-resistant bronchial asthma.* Am J Respir Cell Mol Biol, 1994. **11**(1): p. 42-8.
315. Han, S.H., et al., *Glomerular glucocorticoid receptor expression is reduced in late responders to steroids in adult-onset minimal change disease.* Nephrology, dialysis, transplantation : official publication of the European Dialysis and Transplant Association - European Renal Association, 2008. **23**: p. 169-75.
316. Hammad, A., et al., *Low expression of glucocorticoid receptors in children with steroid-resistant nephrotic syndrome.* Pediatr Nephrol, 2013. **28**(5): p. 759-63.
317. Koper, J.W., et al., *Lack of association between five polymorphisms in the human glucocorticoid receptor gene and glucocorticoid resistance.* Hum Genet, 1997. **99**(5): p. 663-8.
318. Russcher, H., et al., *Two polymorphisms in the glucocorticoid receptor gene directly affect glucocorticoid-regulated gene expression.* J Clin Endocrinol Metab, 2005. **90**(10): p. 5804-10.
319. van Rossum, E.F., et al., *Association of the ER22/23EK polymorphism in the glucocorticoid receptor gene with survival and C-reactive protein levels in elderly men.* Am J Med, 2004. **117**(3): p. 158-62.
320. Russcher, H., et al., *Increased expression of the glucocorticoid receptor-A translational isoform as a result of the ER22/23EK polymorphism.* Mol Endocrinol, 2005. **19**(7): p. 1687-96.
321. van den Akker, E.L., et al., *Glucocorticoid receptor polymorphism affects transrepression but not transactivation.* J Clin Endocrinol Metab, 2006. **91**(7): p. 2800-3.
322. Hamid, Q.A., et al., *Increased glucocorticoid receptor beta in airway cells of glucocorticoid-insensitive asthma.* Am J Respir Crit Care Med, 1999. **159**(5 Pt 1): p. 1600-4.
323. Kozaci, D.L., Y. Chernajovsky, and I.C. Chikanza, *The differential expression of corticosteroid receptor isoforms in corticosteroid-resistant and -sensitive patients with rheumatoid arthritis.* Rheumatology (Oxford), 2007. **46**(4): p. 579-85.
324. Orii, F., et al., *Quantitative analysis for human glucocorticoid receptor alpha/beta mRNA in IBD.* Biochem Biophys Res Commun, 2002. **296**(5): p. 1286-94.
325. He, X.J., et al., *[Effect of glucocorticoid on glucocorticoid-resistant children with primary nephrotic syndrome].* Zhonghua Er Ke Za Zhi, 2005. **43**(2): p. 109-12.
326. Gagliardo, R., et al., *Glucocorticoid receptor alpha and beta in glucocorticoid dependent asthma.* Am J Respir Crit Care Med, 2000. **162**(1): p. 7-13.
327. Pujols, L., J. Mullol, and C. Picado, *Alpha and beta glucocorticoid receptors: relevance in airway diseases.* Curr Allergy Asthma Rep, 2007. **7**(2): p. 93-9.
328. Ouyang, J., et al., *Abnormal expression and distribution of heat shock protein 90: potential etiologic immunoendocrine mechanism of glucocorticoid resistance in idiopathic nephrotic syndrome.* Clin Vaccine Immunol, 2006. **13**(4): p. 496-500.
329. Ouyang, J., et al., *Nuclear HSP90 regulates the glucocorticoid responsiveness of PBMCs in patients with idiopathic nephrotic syndrome.* Int Immunopharmacol, 2012. **14**(3): p. 334-40.
330. Riebold, M., et al., *A C-terminal HSP90 inhibitor restores glucocorticoid sensitivity and relieves a mouse allograft model of Cushing disease.* Nat Med, 2015. **21**(3): p. 276-80.

331. Jafar, T., et al., *Cytokine gene polymorphism in idiopathic nephrotic syndrome children.* Indian J Clin Biochem, 2011. **26**(3): p. 296-302.
332. Sher, E.R., et al., *Steroid-resistant asthma. Cellular mechanisms contributing to inadequate response to glucocorticoid therapy.* The Journal of clinical investigation, 1994. **93**: p. 33-9.
333. Irusen, E., et al., *p38 Mitogen-activated protein kinase-induced glucocorticoid receptor phosphorylation reduces its activity: role in steroid-insensitive asthma.* J Allergy Clin Immunol, 2002. **109**(4): p. 649-57.
334. Matthews, J.G., et al., *Defective glucocorticoid receptor nuclear translocation and altered histone acetylation patterns in glucocorticoid-resistant patients.* The Journal of allergy and clinical immunology, 2004. **113**: p. 1100-8.
335. Swierczewska, M., et al., *Molecular basis of mechanisms of steroid resistance in children with nephrotic syndrome.* Acta Biochim Pol, 2013. **60**(3): p. 339-44.
336. Santos, L., et al., *Role of macrophage migration inhibitory factor (MIF) in murine antigen-induced arthritis: interaction with glucocorticoids.* Clin Exp Immunol, 2001. **123**(2): p. 309-14.
337. Stosic-Grujicic, S., I. Stojanovic, and F. Nicoletti, *MIF in autoimmunity and novel therapeutic approaches.* Autoimmun Rev, 2009. **8**(3): p. 244-9.
338. Berdeli, A., et al., *Association of macrophage migration inhibitory factor -173C allele polymorphism with steroid resistance in children with nephrotic syndrome.* Pediatr Nephrol, 2005. **20**(11): p. 1566-71.
339. Hew, M., et al., *Relative corticosteroid insensitivity of peripheral blood mononuclear cells in severe asthma.* American journal of respiratory and critical care medicine, 2006. **174**: p. 134-41.
340. Ito, K., et al., *Decreased histone deacetylase activity in chronic obstructive pulmonary disease.* N Engl J Med, 2005. **352**(19): p. 1967-76.
341. Ito, K., et al., *Histone deacetylase 2-mediated deacetylation of the glucocorticoid receptor enables NF-kappaB suppression.* J Exp Med, 2006. **203**(1): p. 7-13.
342. Xystrakis, E., et al., *Reversing the defective induction of IL-10-secreting regulatory T cells in glucocorticoid-resistant asthma patients.* J Clin Invest, 2006. **116**(1): p. 146-55.
343. Farrell, R.J., et al., *High multidrug resistance (P-glycoprotein 170) expression in inflammatory bowel disease patients who fail medical therapy.* Gastroenterology, 2000. **118**(2): p. 279-88.
344. Tsujimura, S., et al., *Overcoming drug resistance induced by P-glycoprotein on lymphocytes in patients with refractory rheumatoid arthritis.* Ann Rheum Dis, 2008. **67**(3): p. 380-8.
345. Jafar, T., et al., *MDR-1 gene polymorphisms in steroid-responsive versus steroid-resistant nephrotic syndrome in children.* Nephrol Dial Transplant, 2011. **26**(12): p. 3968-74.
346. Choi, H.J., et al., *Polymorphisms of the MDR1 and MIF genes in children with nephrotic syndrome.* Pediatr Nephrol, 2011. **26**(11): p. 1981-8.
347. Youssef, D.M., et al., *Soluble interleukine-2 receptor and MDR1 gene expression levels as inflammatory biomarkers for prediction of steroid response in children with nephrotic syndrome.* Iran J Kidney Dis, 2011. **5**(3): p. 154-61.
348. Stachowski, J., et al., *[Resistance to therapy in primary nephrotic syndrome: effect of MDR1 gene activity]*. Pol Merkur Lekarski, 2000. **8**(46): p. 218-21.
349. Chiou, Y.H., et al., *Genetic polymorphisms influence the steroid treatment of children with idiopathic nephrotic syndrome.* Pediatr Nephrol, 2012. **27**(9): p. 1511-7.

350. Yang, N., D.W. Ray, and L.C. Matthews, *Current concepts in glucocorticoid resistance.* Steroids, 2012. **77**(11): p. 1041-9.
351. Ridley, A.J., *Rho GTPases and cell migration.* J Cell Sci, 2001. **114**(Pt 15): p. 2713-22.
352. Maridonneau-Parini, I., *Control of macrophage 3D migration: a therapeutic challenge to limit tissue infiltration.* Immunol Rev, 2014. **262**(1): p. 216-31.
353. Dong, H., et al., *Inhibition of breast cancer cell migration by activation of cAMP signaling.* Breast Cancer Res Treat, 2015. **152**(1): p. 17-28.
354. Coppola, J.M., et al., *A small-molecule furin inhibitor inhibits cancer cell motility and invasiveness.* Neoplasia, 2008. **10**(4): p. 363-70.
355. Kopp, F., et al., *Salinomycin treatment reduces metastatic tumor burden by hampering cancer cell migration.* Mol Cancer, 2014. **13**: p. 16.
356. Juliano, R.L., *Signal transduction by cell adhesion receptors and the cytoskeleton: functions of integrins, cadherins, selectins, and immunoglobulin-superfamily members.* Annu Rev Pharmacol Toxicol, 2002. **42**: p. 283-323.
357. Lock, J.G., B. Wehrle-Haller, and S. Stromblad, *Cell-matrix adhesion complexes: master control machinery of cell migration.* Semin Cancer Biol, 2008. **18**(1): p. 65-76.
358. Ridley, A.J. and A. Hall, *The small GTP-binding protein rho regulates the assembly of focal adhesions and actin stress fibers in response to growth factors.* Cell, 1992. **70**(3): p. 389-99.
359. Ridley, A.J., et al., *Cell migration: integrating signals from front to back.* Science (New York, N.Y.), 2003. **302**: p. 1704-9.
360. Ridley, A.J., *Life at the leading edge.* Cell, 2011. **145**: p. 1012-22.
361. Mattila, P.K. and P. Lappalainen, *Filopodia: molecular architecture and cellular functions.* Nat Rev Mol Cell Biol, 2008. **9**(6): p. 446-54.
362. Buccione, R., G. Caldieri, and I. Ayala, *Invadopodia: specialized tumor cell structures for the focal degradation of the extracellular matrix.* Cancer Metastasis Rev, 2009. **28**(1-2): p. 137-49.
363. Jacquemet, G., M.J. Humphries, and P.T. Caswell, *Role of adhesion receptor trafficking in 3D cell migration.* Curr Opin Cell Biol, 2013. **25**(5): p. 627-32.
364. Dozynkiewicz, M.A., et al., *Rab25 and CLIC3 collaborate to promote integrin recycling from late endosomes/lysosomes and drive cancer progression.* Dev Cell, 2012. **22**(1): p. 131-45.
365. Wennerberg, K., K.L. Rossman, and C.J. Der, *The Ras superfamily at a glance.* J Cell Sci, 2005. **118**(Pt 5): p. 843-6.
366. Spiering, D. and L. Hodgson, *Dynamics of the Rho-family small GTPases in actin regulation and motility.* Cell Adh Migr, 2011. **5**(2): p. 170-80.
367. Schmidt, A. and A. Hall, *Guanine nucleotide exchange factors for Rho GTPases: turning on the switch.* Genes Dev, 2002. **16**(13): p. 1587-609.
368. Bernards, A. and J. Settleman, *GAP control: regulating the regulators of small GTPases.* Trends Cell Biol, 2004. **14**(7): p. 377-85.
369. Takai, Y., T. Sasaki, and T. Matozaki, *Small GTP-binding proteins.* Physiol Rev, 2001. **81**(1): p. 153-208.
370. Repasky, G.A., E.J. Chenette, and C.J. Der, *Renewing the conspiracy theory debate: does Raf function alone to mediate Ras oncogenesis?* Trends Cell Biol, 2004. **14**(11): p. 639-47.
371. Han, J., et al., *Reconstructing and deconstructing agonist-induced activation of integrin alphaIIbbeta3.* Curr Biol, 2006. **16**(18): p. 1796-806.
372. Ohta, Y., et al., *The small GTPase RalA targets filamin to induce filopodia.* Proc Natl Acad Sci U S A, 1999. **96**(5): p. 2122-8.

373. Heasman, S.J. and A.J. Ridley, *Mammalian Rho GTPases: new insights into their functions from in vivo studies.* Nat Rev Mol Cell Biol, 2008. **9**(9): p. 690-701.
374. Ridley, A.J., *Rho family proteins: coordinating cell responses.* Trends Cell Biol, 2001. **11**(12): p. 471-7.
375. Wheeler, A.P. and A.J. Ridley, *Why three Rho proteins? RhoA, RhoB, RhoC, and cell motility.* Exp Cell Res, 2004. **301**(1): p. 43-9.
376. Allen, W.E., et al., *A role for Cdc42 in macrophage chemotaxis.* J Cell Biol, 1998. **141**(5): p. 1147-57.
377. Kozma, R., et al., *The Ras-related protein Cdc42Hs and bradykinin promote formation of peripheral actin microspikes and filopodia in Swiss 3T3 fibroblasts.* Mol Cell Biol, 1995. **15**(4): p. 1942-52.
378. Rothmeier, E., et al., *Activation of Ran GTPase by a Legionella effector promotes microtubule polymerization, pathogen vacuole motility and infection.* PLoS Pathog, 2013. **9**(9): p. e1003598.
379. Nie, Z., D.S. Hirsch, and P.A. Randazzo, *Arf and its many interactors.* Curr Opin Cell Biol, 2003. **15**(4): p. 396-404.
380. Schweitzer, J.K., A.E. Sedgwick, and C. D'Souza-Schorey, *ARF6-mediated endocytic recycling impacts cell movement, cell division and lipid homeostasis.* Semin Cell Dev Biol, 2011. **22**(1): p. 39-47.
381. Small, J.V., *The actin cytoskeleton.* Electron Microsc Rev, 1988. **1**(1): p. 155-74.
382. Paterson, H.F., et al., *Microinjection of recombinant p21rho induces rapid changes in cell morphology.* J Cell Biol, 1990. **111**(3): p. 1001-7.
383. Riento, K. and A.J. Ridley, *Rocks: multifunctional kinases in cell behaviour.* Nat Rev Mol Cell Biol, 2003. **4**(6): p. 446-56.
384. Oser, M. and J. Condeelis, *The cofilin activity cycle in lamellipodia and invadopodia.* J Cell Biochem, 2009. **108**(6): p. 1252-62.
385. Goode, B.L. and M.J. Eck, *Mechanism and function of formins in the control of actin assembly.* Annu Rev Biochem, 2007. **76**: p. 593-627.
386. Pertz, O., *Spatio-temporal Rho GTPase signaling - where are we now?* J Cell Sci, 2010. **123**(Pt 11): p. 1841-50.
387. Vega, F.M., et al., *RhoA and RhoC have distinct roles in migration and invasion by acting through different targets.* J Cell Biol, 2011. **193**(4): p. 655-65.
388. Vega, F.M., et al., *RhoB regulates cell migration through altered focal adhesion dynamics.* Open Biol, 2012. **2**(5): p. 120076.
389. Huang, M., et al., *RhoB regulates PDGFR-beta trafficking and signaling in vascular smooth muscle cells.* Arterioscler Thromb Vasc Biol, 2007. **27**(12): p. 2597-605.
390. Hakem, A., et al., *RhoC is dispensable for embryogenesis and tumor initiation but essential for metastasis.* Genes Dev, 2005. **19**(17): p. 1974-9.
391. Shirsat, N.V., et al., *A member of the ras gene superfamily is expressed specifically in T, B and myeloid hemopoietic cells.* Oncogene, 1990. **5**(5): p. 769-72.
392. Haataja, L., J. Groffen, and N. Heisterkamp, *Characterization of RAC3, a novel member of the Rho family.* J Biol Chem, 1997. **272**(33): p. 20384-8.
393. Uhlen, M., et al., *Towards a knowledge-based Human Protein Atlas.* Nat Biotechnol, 2010. **28**(12): p. 1248-50.
394. Tzima, E., et al., *Activation of Rac1 by shear stress in endothelial cells mediates both cytoskeletal reorganization and effects on gene expression.* EMBO J, 2002. **21**(24): p. 6791-800.

395. Aikawa, R., et al., *Reactive oxygen species in mechanical stress-induced cardiac hypertrophy.* Biochem Biophys Res Commun, 2001. **289**(4): p. 901-7.
396. Nagase, M., et al., *Oxidative stress causes mineralocorticoid receptor activation in rat cardiomyocytes: role of small GTPase Rac1.* Hypertension, 2012. **59**(2): p. 500-6.
397. Papaharalambus, C., et al., *Tumor necrosis factor alpha stimulation of Rac1 activity. Role of isoprenylcysteine carboxylmethyltransferase.* J Biol Chem, 2005. **280**(19): p. 18790-6.
398. Kurokawa, K., et al., *Coactivation of Rac1 and Cdc42 at lamellipodia and membrane ruffles induced by epidermal growth factor.* Mol Biol Cell, 2004. **15**(3): p. 1003-10.
399. Price, L.S., et al., *Activation of Rac and Cdc42 by integrins mediates cell spreading.* Mol Biol Cell, 1998. **9**(7): p. 1863-71.
400. Wei, C., et al., *Modification of kidney barrier function by the urokinase receptor.* Nature medicine, 2008. **14**: p. 55-63.
401. Shen, E., et al., *Rac1 is required for cardiomyocyte apoptosis during hyperglycemia.* Diabetes, 2009. **58**(10): p. 2386-95.
402. Yi, F., et al., *Homocysteine activates NADH/NADPH oxidase through ceramide-stimulated Rac GTPase activity in rat mesangial cells.* Kidney Int, 2004. **66**(5): p. 1977-87.
403. Uhlik, M.T., et al., *Rac-MEKK3-MKK3 scaffolding for p38 MAPK activation during hyperosmotic shock.* Nat Cell Biol, 2003. **5**(12): p. 1104-10.
404. Schmitz, U., et al., *Angiotensin II-induced stimulation of p21-activated kinase and c-Jun NH2-terminal kinase is mediated by Rac1 and Nck.* J Biol Chem, 2001. **276**(25): p. 22003-10.
405. Iwashima, F., et al., *Aldosterone induces superoxide generation via Rac1 activation in endothelial cells.* Endocrinology, 2008. **149**(3): p. 1009-14.
406. Nagase, M. and T. Fujita, *Role of Rac1-mineralocorticoid-receptor signalling in renal and cardiac disease.* Nat Rev Nephrol, 2013. **9**(2): p. 86-98.
407. Ridley, A.J., et al., *The small GTP-binding protein rac regulates growth factor-induced membrane ruffling.* Cell, 1992. **70**(3): p. 401-10.
408. Nobes, C.D. and A. Hall, *Rho GTPases control polarity, protrusion, and adhesion during cell movement.* J Cell Biol, 1999. **144**(6): p. 1235-44.
409. Nodari, A., et al., *Beta1 integrin activates Rac1 in Schwann cells to generate radial lamellae during axonal sorting and myelination.* J Cell Biol, 2007. **177**(6): p. 1063-75.
410. Tan, W., et al., *An essential role for Rac1 in endothelial cell function and vascular development.* FASEB J, 2008. **22**(6): p. 1829-38.
411. McCarty, O.J., et al., *Rac1 is essential for platelet lamellipodia formation and aggregate stability under flow.* J Biol Chem, 2005. **280**(47): p. 39474-84.
412. Wu, Y.I., et al., *A genetically encoded photoactivatable Rac controls the motility of living cells.* Nature, 2009. **461**(7260): p. 104-8.
413. Wang, W., R. Eddy, and J. Condeelis, *The cofilin pathway in breast cancer invasion and metastasis.* Nat Rev Cancer, 2007. **7**(6): p. 429-40.
414. Akhtar, N. and C.H. Streuli, *Rac1 links integrin-mediated adhesion to the control of lactational differentiation in mammary epithelia.* J Cell Biol, 2006. **173**(5): p. 781-93.
415. Nikolova, S., et al., *Rac1-NADPH oxidase-regulated generation of reactive oxygen species mediates glutamate-induced apoptosis in SH-SY5Y human neuroblastoma cells.* Free Radic Res, 2005. **39**(12): p. 1295-304.
416. Jaffe, A.B. and A. Hall, *Rho GTPases: biochemistry and biology.* Annu Rev Cell Dev Biol, 2005. **21**: p. 247-69.

417. Nobes, C.D. and A. Hall, *Rho, rac, and cdc42 GTPases regulate the assembly of multimolecular focal complexes associated with actin stress fibers, lamellipodia, and filopodia.* Cell, 1995. **81**: p. 53-62.
418. Neudauer, C.L., et al., *Distinct cellular effects and interactions of the Rho-family GTPase TC10.* Curr Biol, 1998. **8**(21): p. 1151-60.
419. Tao, W., et al., *Wrch-1, a novel member of the Rho gene family that is regulated by Wnt-1.* Genes Dev, 2001. **15**(14): p. 1796-807.
420. Aspenstrom, P., A. Fransson, and J. Saras, *Rho GTPases have diverse effects on the organization of the actin filament system.* Biochem J, 2004. **377**(Pt 2): p. 327-37.
421. Rottner, K., A. Hall, and J.V. Small, *Interplay between Rac and Rho in the control of substrate contact dynamics.* Curr Biol, 1999. **9**(12): p. 640-8.
422. Machacek, M., et al., *Coordination of Rho GTPase activities during cell protrusion.* Nature, 2009. **461**: p. 99-103.
423. Yu, H., et al., *Rac1 activation in podocytes induces rapid foot process effacement and proteinuria.* Mol Cell Biol, 2013. **33**(23): p. 4755-64.
424. Shibata, S., M. Nagase, and T. Fujita, *Fluvastatin ameliorates podocyte injury in proteinuric rats via modulation of excessive Rho signaling.* Journal of the American Society of Nephrology : JASN, 2006. **17**: p. 754-64.
425. Zhu, L., et al., *Activation of RhoA in podocytes induces focal segmental glomerulosclerosis.* Journal of the American Society of Nephrology : JASN, 2011. **22**: p. 1621-30.
426. Wang, L., et al., *Mechanisms of the proteinuria induced by Rho GTPases.* Kidney international, 2012. **81**: p. 1075-85.
427. Scott, R.P., et al., *Podocyte-specific loss of Cdc42 leads to congenital nephropathy.* Journal of the American Society of Nephrology : JASN, 2012. **23**: p. 1149-54.
428. Blattner, S.M., et al., *Divergent functions of the Rho GTPases Rac1 and Cdc42 in podocyte injury.* Kidney international, 2013.
429. Le Menuet, D., et al., *Alteration of cardiac and renal functions in transgenic mice overexpressing human mineralocorticoid receptor.* J Biol Chem, 2001. **276**(42): p. 38911-20.
430. Ponda, M.P. and T.H. Hostetter, *Aldosterone antagonism in chronic kidney disease.* Clin J Am Soc Nephrol, 2006. **1**(4): p. 668-77.
431. Shibata, S., et al., *Modification of mineralocorticoid receptor function by Rac1 GTPase: implication in proteinuric kidney disease.* Nature medicine, 2008. **14**: p. 1370-6.
432. Gee, H.Y., et al., *ARHGDIA mutations cause nephrotic syndrome via defective RHO GTPase signaling.* The Journal of clinical investigation, 2013. **123**: p. 3243-53.
433. Hsu, H.H., et al., *Mechanisms of angiotensin II signaling on cytoskeleton of podocytes.* J Mol Med (Berl), 2008. **86**(12): p. 1379-94.
434. Babelova, A., et al., *Activation of Rac-1 and RhoA contributes to podocyte injury in chronic kidney disease.* PLoS One, 2013. **8**(11): p. e80328.
435. Ohta, Y., J.H. Hartwig, and T.P. Stossel, *FilGAP, a Rho- and ROCK-regulated GAP for Rac binds filamin A to control actin remodelling.* Nature cell biology, 2006. **8**: p. 803-14.
436. Akilesh, S., et al., *Arhgap24 inactivates Rac1 in mouse podocytes, and a mutant form is associated with familial focal segmental glomerulosclerosis.* The Journal of clinical investigation, 2011. **121**: p. 4127-37.

437. Satchell, S.C., et al., *Conditionally immortalized human glomerular endothelial cells expressing fenestrations in response to VEGF.* Kidney Int, 2006. **69**(9): p. 1633-40.
438. Jangani, M., et al., *The methyltransferase WBSCR22/Merm1 enhances glucocorticoid receptor function and is regulated in lung inflammation and cancer.* J Biol Chem, 2014. **289**(13): p. 8931-46.
439. Byron, A., et al., *Glomerular cell cross-talk influences composition and assembly of extracellular matrix.* J Am Soc Nephrol, 2014. **25**(5): p. 953-66.
440. Welsh, G.I., et al., *Insulin signaling to the glomerular podocyte is critical for normal kidney function.* Cell Metab, 2010. **12**(4): p. 329-40.
441. Saif, Z., et al., *Expression of eight glucocorticoid receptor isoforms in the human preterm placenta vary with fetal sex and birthweight.* Placenta, 2015. **36**(7): p. 723-30.
442. Kim, Y.H., et al., *Podocyte depletion and glomerulosclerosis have a direct relationship in the PAN-treated rat.* Kidney Int, 2001. **60**(3): p. 957-68.
443. Rosewicz, S., et al., *Mechanism of glucocorticoid receptor down-regulation by glucocorticoids.* J Biol Chem, 1988. **263**(6): p. 2581-4.
444. Vedeckis, W.V., M. Ali, and H.R. Allen, *Regulation of glucocorticoid receptor protein and mRNA levels.* Cancer Res, 1989. **49**(8 Suppl): p. 2295s-2302s.
445. Breslin, M.B., C.D. Geng, and W.V. Vedeckis, *Multiple promoters exist in the human GR gene, one of which is activated by glucocorticoids.* Mol Endocrinol, 2001. **15**(8): p. 1381-95.
446. Sathiyaa, R. and M.M. Vijayan, *Autoregulation of glucocorticoid receptor by cortisol in rainbow trout hepatocytes.* Am J Physiol Cell Physiol, 2003. **284**(6): p. C1508-15.
447. Schiller, B.J., et al., *Glucocorticoid receptor binds half sites as a monomer and regulates specific target genes.* Genome Biol, 2014. **15**(7): p. 418.
448. Polman, J.A., et al., *A genome-wide signature of glucocorticoid receptor binding in neuronal PC12 cells.* BMC Neurosci, 2012. **13**: p. 118.
449. Reddy, T.E., et al., *Genomic determination of the glucocorticoid response reveals unexpected mechanisms of gene regulation.* Genome Res, 2009. **19**(12): p. 2163-71.
450. Gibbs, J., et al., *An epithelial circadian clock controls pulmonary inflammation and glucocorticoid action.* Nature medicine, 2014. **20**: p. 919-26.
451. Miller, P.F., et al., *Pharmacokinetics of prednisolone in children with nephrosis.* Arch Dis Child, 1990. **65**(2): p. 196-200.
452. Lu, N.Z. and J.A. Cidlowski, *Glucocorticoid receptor isoforms generate transcription specificity.* Trends Cell Biol, 2006. **16**(6): p. 301-7.
453. Sanchez-Vega, B., et al., *Glucocorticoid receptor transcriptional isoforms and resistance in multiple myeloma cells.* Mol Cancer Ther, 2006. **5**(12): p. 3062-70.
454. Krett, N.L., et al., *A variant glucocorticoid receptor messenger RNA is expressed in multiple myeloma patients.* Cancer Res, 1995. **55**(13): p. 2727-9.
455. de Lange, P., et al., *Expression in hematological malignancies of a glucocorticoid receptor splice variant that augments glucocorticoid receptor-mediated effects in transfected cells.* Cancer Res, 2001. **61**(10): p. 3937-41.
456. Alangari, A.A., *Genomic and non-genomic actions of glucocorticoids in asthma.* Ann Thorac Med, 2010. **5**(3): p. 133-9.
457. Pufall, M.A., *Glucocorticoids and Cancer.* Adv Exp Med Biol, 2015. **872**: p. 315-33.
458. Li, C. and W.H. Wong, *Model-based analysis of oligonucleotide arrays: expression index computation and outlier detection.* Proc Natl Acad Sci U S A, 2001. **98**(1): p. 31-6.

459. Bolstad, B.M., et al., *A comparison of normalization methods for high density oligonucleotide array data based on variance and bias.* Bioinformatics, 2003. **19**(2): p. 185-93.
460. Quackenbush, J., *Computational analysis of microarray data.* Nat Rev Genet, 2001. **2**(6): p. 418-27.
461. Smyth, G.K., *Linear models and empirical bayes methods for assessing differential expression in microarray experiments.* Stat Appl Genet Mol Biol, 2004. **3**: p. Article3.
462. Storey, J.D. and R. Tibshirani, *Statistical significance for genomewide studies.* Proc Natl Acad Sci U S A, 2003. **100**(16): p. 9440-5.
463. Wu, D.Y., et al., *Distinct, genome-wide, gene-specific selectivity patterns of four glucocorticoid receptor coregulators.* Nucl Recept Signal, 2014. **12**: p. e002.
464. Ehrchen, J., et al., *Glucocorticoids induce differentiation of a specifically activated, anti-inflammatory subtype of human monocytes.* Blood, 2007. **109**(3): p. 1265-74.
465. Whirledge, S., X. Xu, and J.A. Cidlowski, *Global gene expression analysis in human uterine epithelial cells defines new targets of glucocorticoid and estradiol antagonism.* Biol Reprod, 2013. **89**(3): p. 66.
466. Gupta, V., et al., *Global gene profiling reveals novel glucocorticoid induced changes in gene expression of human lens epithelial cells.* Mol Vis, 2005. **11**: p. 1018-40.
467. Onesto, C., et al., *Characterization of EHT 1864, a novel small molecule inhibitor of Rac family small GTPases.* Methods Enzymol, 2008. **439**: p. 111-29.
468. Palmer, T.D., et al., *Targeting tumor cell motility to prevent metastasis.* Adv Drug Deliv Rev, 2011. **63**(8): p. 568-81.
469. Kassis, J., et al., *Tumor invasion as dysregulated cell motility.* Semin Cancer Biol, 2001. **11**(2): p. 105-17.
470. Sahai, E. and C.J. Marshall, *Differing modes of tumour cell invasion have distinct requirements for Rho/ROCK signalling and extracellular proteolysis.* Nat Cell Biol, 2003. **5**(8): p. 711-9.
471. Amano, M., et al., *Formation of actin stress fibers and focal adhesions enhanced by Rho-kinase.* Science, 1997. **275**(5304): p. 1308-11.
472. Weiger, M.C., et al., *Real-time motion analysis reveals cell directionality as an indicator of breast cancer progression.* PLoS One, 2013. **8**(3): p. e58859.
473. Dujardin, D.L., et al., *A role for cytoplasmic dynein and LIS1 in directed cell movement.* J Cell Biol, 2003. **163**(6): p. 1205-11.
474. Danen, E.H., et al., *Integrins control motile strategy through a Rho-cofilin pathway.* J Cell Biol, 2005. **169**(3): p. 515-26.
475. Weiner, O.D., *Regulation of cell polarity during eukaryotic chemotaxis: the chemotactic compass.* Curr Opin Cell Biol, 2002. **14**(2): p. 196-202.
476. Duning, K., et al., *KIBRA modulates directional migration of podocytes.* J Am Soc Nephrol, 2008. **19**(10): p. 1891-903.
477. Van Haastert, P.J. and P.N. Devreotes, *Chemotaxis: signalling the way forward.* Nat Rev Mol Cell Biol, 2004. **5**(8): p. 626-34.
478. Srinivasan, S., et al., *Rac and Cdc42 play distinct roles in regulating PI(3,4,5)P3 and polarity during neutrophil chemotaxis.* J Cell Biol, 2003. **160**(3): p. 375-85.
479. Pankov, R., et al., *A Rac switch regulates random versus directionally persistent cell migration.* J Cell Biol, 2005. **170**(5): p. 793-802.
480. Kaneto, N., et al., *RAC1 inhibition as a therapeutic target for gefitinib-resistant non-small-cell lung cancer.* Cancer Sci, 2014. **105**(7): p. 788-94.

481. Kawarazaki, W., et al., *Angiotensin II- and salt-induced kidney injury through Rac1-mediated mineralocorticoid receptor activation.* J Am Soc Nephrol, 2012. **23**(6): p. 997-1007.
482. Zambelli, F., G. Pesole, and G. Pavesi, *PscanChIP: Finding over-represented transcription factor-binding site motifs and their correlations in sequences from ChIP-Seq experiments.* Nucleic Acids Res, 2013. **41**(Web Server issue): p. W535-43.
483. Lee, T.I., S.E. Johnstone, and R.A. Young, *Chromatin immunoprecipitation and microarray-based analysis of protein location.* Nature protocols, 2006. **1**: p. 729-48.
484. Grontved, L., et al., *C/EBP maintains chromatin accessibility in liver and facilitates glucocorticoid receptor recruitment to steroid response elements.* Embo j, 2013. **32**(11): p. 1568-83.
485. O'Geen, H., et al., *A genome-wide analysis of Cas9 binding specificity using ChIP-seq and targeted sequence capture.* Nucleic Acids Res, 2015. **43**(6): p. 3389-404.
486. Bittencourt, D., et al., *G9a functions as a molecular scaffold for assembly of transcriptional coactivators on a subset of glucocorticoid receptor target genes.* Proc Natl Acad Sci U S A, 2012. **109**(48): p. 19673-8.
487. Rada-Iglesias, A., et al., *A unique chromatin signature uncovers early developmental enhancers in humans.* Nature, 2011. **470**(7333): p. 279-83.
488. Hajarnis, S.S., et al., *Transcription Factor HNF-1beta Regulates MicroRNA-200 Expression Through a Long Noncoding RNA.* J Biol Chem, 2015.
489. Diepenbruck, M., et al., *Tead2 expression levels control the subcellular distribution of Yap and Taz, zyxin expression and epithelial-mesenchymal transition.* J Cell Sci, 2014. **127**(Pt 7): p. 1523-36.
490. Rodriguez-Fontenla, C., M. Calaza, and A. Gonzalez, *Genetic distance as an alternative to physical distance for definition of gene units in association studies.* BMC Genomics, 2014. **15**: p. 408.
491. Zhang, K., et al., *i-GSEA4GWAS: a web server for identification of pathways/gene sets associated with traits by applying an improved gene set enrichment analysis to genome-wide association study.* Nucleic Acids Res, 2010. **38**(Web Server issue): p. W90-5.
492. Wang, K., M. Li, and M. Bucan, *Pathway-based approaches for analysis of genomewide association studies.* Am J Hum Genet, 2007. **81**(6): p. 1278-83.
493. Chen, L.S., et al., *Insights into colon cancer etiology via a regularized approach to gene set analysis of GWAS data.* Am J Hum Genet, 2010. **86**(6): p. 860-71.
494. Holmans, P., et al., *Gene ontology analysis of GWA study data sets provides insights into the biology of bipolar disorder.* Am J Hum Genet, 2009. **85**(1): p. 13-24.
495. Eleftherohorinou, H., et al., *Pathway-driven gene stability selection of two rheumatoid arthritis GWAS identifies and validates new susceptibility genes in receptor mediated signalling pathways.* Hum Mol Genet, 2011. **20**(17): p. 3494-506.
496. Liu, J.Z., et al., *A versatile gene-based test for genome-wide association studies.* Am J Hum Genet, 2010. **87**(1): p. 139-45.
497. Nyholt, D.R., et al., *Genome-wide association meta-analysis identifies new endometriosis risk loci.* Nat Genet, 2012. **44**(12): p. 1355-9.
498. Tang, W., et al., *Genetic associations for activated partial thromboplastin time and prothrombin time, their gene expression profiles, and risk of coronary artery disease.* Am J Hum Genet, 2012. **91**(1): p. 152-62.

499. Vijai, J., et al., *Susceptibility loci associated with specific and shared subtypes of lymphoid malignancies.* PLoS Genet, 2013. **9**(1): p. e1003220.
500. Wei, S., et al., *Genome-wide gene-environment interaction analysis for asbestos exposure in lung cancer susceptibility.* Carcinogenesis, 2012. **33**(8): p. 1531-7.
501. Biddie, S.C., et al., *Transcription factor AP1 potentiates chromatin accessibility and glucocorticoid receptor binding.* Molecular cell, 2011. **43**: p. 145-55.
502. Yu, C.Y., et al., *Genome-wide analysis of glucocorticoid receptor binding regions in adipocytes reveal gene network involved in triglyceride homeostasis.* PLoS One, 2010. **5**(12): p. e15188.
503. Jin, F., et al., *A high-resolution map of the three-dimensional chromatin interactome in human cells.* Nature, 2013. **503**(7475): p. 290-4.
504. Perkins, D.N., et al., *Probability-based protein identification by searching sequence databases using mass spectrometry data.* Electrophoresis, 1999. **20**(18): p. 3551-67.
505. Jones, R.C., et al., *Relative quantitative comparisons of the extracellular protein profiles of Staphylococcus aureus UAMS-1 and its sarA, agr, and sarA agr regulatory mutants using one-dimensional polyacrylamide gel electrophoresis and nanocapillary liquid chromatography coupled with tandem mass spectrometry.* J Bacteriol, 2008. **190**(15): p. 5265-78.
506. Huang da, W., B.T. Sherman, and R.A. Lempicki, *Systematic and integrative analysis of large gene lists using DAVID bioinformatics resources.* Nat Protoc, 2009. **4**(1): p. 44-57.
507. Huang da, W., B.T. Sherman, and R.A. Lempicki, *Bioinformatics enrichment tools: paths toward the comprehensive functional analysis of large gene lists.* Nucleic Acids Res, 2009. **37**(1): p. 1-13.
508. Merico, D., et al., *Enrichment map: a network-based method for gene-set enrichment visualization and interpretation.* PLoS One, 2010. **5**(11): p. e13984.
509. Reeves, E.K., et al., *Proteomic profiling of glucocorticoid-exposed myogenic cells: Time series assessment of protein translocation and transcription of inactive mRNAs.* Proteome Sci, 2009. **7**: p. 26.
510. Mundel, P. and S.J. Shankland, *Podocyte biology and response to injury.* J Am Soc Nephrol, 2002. **13**(12): p. 3005-15.
511. Liles, W.C., D.C. Dale, and S.J. Klebanoff, *Glucocorticoids inhibit apoptosis of human neutrophils.* Blood, 1995. **86**(8): p. 3181-8.
512. Zhu, W., J.W. Smith, and C.M. Huang, *Mass spectrometry-based label-free quantitative proteomics.* J Biomed Biotechnol, 2010. **2010**: p. 840518.
513. Issaq, H. and T. Veenstra, *Two-dimensional polyacrylamide gel electrophoresis (2D-PAGE): advances and perspectives.* Biotechniques, 2008. **44**(5): p. 697-8, 700.
514. Nagy, A., *Cre recombinase: the universal reagent for genome tailoring.* Genesis, 2000. **26**(2): p. 99-109.
515. Sauer, B. and N. Henderson, *Site-specific DNA recombination in mammalian cells by the Cre recombinase of bacteriophage P1.* Proc Natl Acad Sci U S A, 1988. **85**(14): p. 5166-70.
516. Laryea, G., G. Schutz, and L.J. Muglia, *Disrupting hypothalamic glucocorticoid receptors causes HPA axis hyperactivity and excess adiposity.* Mol Endocrinol, 2013. **27**(10): p. 1655-65.
517. Comper, W.D., *Is the LPS-mediated proteinuria mouse model relevant to human kidney disease?* Nat Med, 2009. **15**(2): p. 133; author reply 133-4.
518. Finlayson, J.S. and C.A. Baumann, *Mouse proteinuria.* Am J Physiol, 1958. **192**(1): p. 69-72.

519. Cheetham, S.A., et al., *Limited variation in the major urinary proteins of laboratory mice.* Physiol Behav, 2009. **96**(2): p. 253-61.
520. Tronche, F., et al., *Disruption of the glucocorticoid receptor gene in the nervous system results in reduced anxiety.* Nat Genet, 1999. **23**(1): p. 99-103.
521. Vettorazzi, S., et al., *Glucocorticoids limit acute lung inflammation in concert with inflammatory stimuli by induction of SphK1.* Nat Commun, 2015. **6**: p. 7796.
522. Schulz-Baldes, A., et al., *Induction of the epithelial Na+ channel via glucocorticoids in mineralocorticoid receptor knockout mice.* Pflugers Arch, 2001. **443**(2): p. 297-305.
523. Naray-Fejes-Toth, A. and G. Fejes-Toth, *Glucocorticoid receptors mediate mineralocorticoid-like effects in cultured collecting duct cells.* Am J Physiol, 1990. **259**(4 Pt 2): p. F672-8.
524. Goodwin, J.E., et al., *The glucocorticoid receptor in the distal nephron is not necessary for the development or maintenance of dexamethasone-induced hypertension.* Biochem Biophys Res Commun, 2010. **394**(2): p. 266-71.
525. Greenbaum, L.A., R. Benndorf, and W.E. Smoyer, *Childhood nephrotic syndrome--current and future therapies.* Nat Rev Nephrol, 2012. **8**(8): p. 445-58.
526. Fornoni, A., et al., *Rituximab targets podocytes in recurrent focal segmental glomerulosclerosis.* Sci Transl Med, 2011. **3**(85): p. 85ra46.
527. Patrakka, J. and K. Tryggvason, *New insights into the role of podocytes in proteinuria.* Nat Rev Nephrol, 2009. **5**(8): p. 463-8.
528. Chugh, S.S., et al., *Angiopoietin-like 4 based therapeutics for proteinuria and kidney disease.* Front Pharmacol, 2014. **5**: p. 23.
529. Koshikawa, M., et al., *Role of p38 mitogen-activated protein kinase activation in podocyte injury and proteinuria in experimental nephrotic syndrome.* J Am Soc Nephrol, 2005. **16**(9): p. 2690-701.
530. Schiffer, M., et al., *Apoptosis in podocytes induced by TGF-beta and Smad7.* J Clin Invest, 2001. **108**(6): p. 807-16.
531. Menne, J., et al., *Diminished loss of proteoglycans and lack of albuminuria in protein kinase C-alpha-deficient diabetic mice.* Diabetes, 2004. **53**(8): p. 2101-9.
532. Kitamura, M., *Endoplasmic reticulum stress and unfolded protein response in renal pathophysiology: Janus faces.* Am J Physiol Renal Physiol, 2008. **295**(2): p. F323-34.
533. Henderson, J.M., M.P. Alexander, and M.R. Pollak, *Patients with ACTN4 mutations demonstrate distinctive features of glomerular injury.* J Am Soc Nephrol, 2009. **20**(5): p. 961-8.
534. Bensman, A. and P. Niaudet, *Non-immunologic mechanisms of calcineurin inhibitors explain its antiproteinuric effects in genetic glomerulopathies.* Pediatr Nephrol, 2010. **25**(7): p. 1197-9.
535. Mathieson, P.W., *The podocyte as a target for therapies--new and old.* Nat Rev Nephrol, 2012. **8**(1): p. 52-6.
536. Yang, H.C., et al., *Peroxisome proliferator-activated receptor-gamma agonist is protective in podocyte injury-associated sclerosis.* Kidney Int, 2006. **69**(10): p. 1756-64.
537. Agrawal, S., et al., *Comparison of direct action of thiazolidinediones and glucocorticoids on renal podocytes: protection from injury and molecular effects.* Mol Pharmacol, 2011. **80**(3): p. 389-99.
538. Lee, H.S. and C.Y. Song, *Effects of TGF-beta on podocyte growth and disease progression in proliferative podocytopathies.* Kidney Blood Press Res, 2010. **33**(1): p. 24-9.

539. Wells, A., et al., *Targeting tumor cell motility as a strategy against invasion and metastasis.* Trends Pharmacol Sci, 2013. **34**(5): p. 283-9.
540. Schacke, H., et al., *Dissociation of transactivation from transrepression by a selective glucocorticoid receptor agonist leads to separation of therapeutic effects from side effects.* Proc Natl Acad Sci U S A, 2004. **101**(1): p. 227-32.